Identification of genes regulated during neuronal apoptosis using oligonucleotide microarrays

Jennefer Lindsay

A thesis submitted for the Degree of Doctor of Philosophy

2005

Molecular Haematology and Cancer Biology Unit,
Institute of Child Heath,
University College London.

ProQuest LLC
789 East Eisenhower Parkway
P.O. Box 1346
Ann Arbor, MI 48106-1346

Abstract

Neuronal apoptosis occurs extensively during the normal development of the mammalian nervous system and ensures that appropriate connections are made between neurons and their target cells. Developing sympathetic neurons and the PC6-3 cell line, a PC12 sub-clone, are useful *in vitro* systems for studying neuronal apoptosis. Both sympathetic neurons and neuronally differentiated PC6-3 cells depend on nerve growth factor (NGF) for survival and die by apoptosis after NGF withdrawal in a transcription and translation-dependent manner. The c-Jun protein is known to be required for neuronal cell death following survival factor withdrawal, however the direct targets of this basic/leucine zipper transcription factor are unknown. The aim of this thesis was to identify and study c-Jun target genes involved in neuronal apoptosis.

In experiments using Affymetrix GeneChip® oligonucleotide microarrays, 78 genes were identified that had an altered pattern of expression after NGF withdrawal from neuronal PC6-3 cells. One of the induced genes, ATF-3, a basic/leucine zipper transcription factor that can dimerise with c-Jun, was confirmed as an up-regulated transcript during PC6-3 cell apoptosis and this occurred after the induction of c-Jun. In sympathetic neurons, *atf-3* RNA and protein levels increase between 8 and 16 hours after NGF withdrawal and remain elevated at 24 hours. This protein induction occurs after that of c-Jun and is inhibited by the c-Jun N-terminal kinase inhibitor SP600125 and the mixed-lineage kinase (MLK) inhibitor CEP-11004. This suggests that induction of ATF-3 may require JNK activity in neurons and that the *atf-3* gene might be a target of c-Jun.

The function of ATF-3 in sympathetic neurons was investigated in microinjection experiments. Injection of expression vectors for c-Jun and ATF-3 decreased the survival of sympathetic neurons in the presence of NGF, as measured at 72 hours after injection. In contrast, overexpression of ATF-3 or the ATF-3 basic/leucine zipper domain in the absence of NGF increased the survival of sympathetic neurons. In addition, when ATF-3 expression was knocked down, using a pSUPER ATF-3 RNAi expression vector, the amount of cell death observed after 48 hours of NGF deprivation in neurons was increased.

Acknowledgements

I would like to thank Jonathan Ham, my supervisor, for his help and support to produce this thesis. Thank you to my friends at work for keeping me sane and especially to Jonathan Gilley for always answering my questions. I'd like to thank my friends and family for believing in me and for all their encouragement over the years – you know who you are!

Table of contents

Table of Figures

Tables and Appendices

Abbreviations

AIF	apoptosis inducing factor
AP-1	activator protein-1
Apaf-1	apoptotic protease activating factor-1
ASK-1	apoptosis signal-regulated kinase 1
ATF	activating transcription factor
ATP	adenosine triphosphate
BDNF	brain derived neurotrophic factor
BH3	Bcl-2 homology domain 3
CAT	chloramphenicol acetyl transferase
CRE	cAMP response element
CREB	CRE binding protein
DISC	death inducing signalling complex
eIF2α	eukaryotic initiation factor 2-alpha
ERK	extracellular signal-regulated kinase
FADD	Fas/APO-1-associated death domain protein
GADD	growth arrest and DNA-damage-inducible
6-OHDA	6-hydroxydopamine
IAP	inhibitor-of-apoptosis protein
ICE	interleukin-1β-converting enzyme
IL-3	interleukin-3
JNK	c-Jun N-terminal kinase
MAPK	mitogen-activated protein kinase
MCAO	middle cerebral artery occlusion
MEKK1	MAPK/ERK kinase kinase 1
MKK4/7	MAPK kinase
MLK	mixed-lineage kinase
MPTP	1-methyl-4-phenyl-1,2,3,6-tetrahydropyridine
NF-M	neurofilament-M
NF-κB	nuclear factor-κB
NGF	nerve growth factor
PC6-3/PC12	pheochromocytoma cell line 6-3/12

PI3K	phosphatidylinositol-3-kinase
PIP_2	phosphatidylinositol 4,5-bisphosphate
PIP_3	phosphatidylinositol 3,4,5-trisphosphate
PTP	permeability transition pore
SAPK	stress activated protein kinase
SCG	superior cervical ganglion
SOD1	superoxide dismutase-1
TNF	tumour necrosis factor
TPA	12-O-tetradecanoylphorbol-13-acetate
TRE	TPA-responsive element
TUNEL	terminal deoxynucleotidyl transferase-mediated dUTP nick-end labelling
SEK1	SAPK/ERK kinase 1
SMAC	second mitochondrial-derived activator of apoptosis
zVADfmk	N-benzyloxycarbonyl-Val-Ala-Asp(OMe)-fluoromethylketone

Chapter 1: Introduction

1.1 Apoptosis

1.1.1 History of apoptosis

The process of cell death was first recognised in the middle of the nineteenth century during amphibian metamorphosis (Vogt, 1842). Other examples of cell death soon followed: chromatolytic cell death in ovarian follicles, loss of an entire neuron population in fish embryos and loss of motor and sensory neurons in chick embryos (reviewed in Clarke and Clarke, 1996). The importance of cell death during development was not established until the early 1950s when Glucksmann summarised all of the published work on cell death and stated that naturally occurring cell death was observed at certain developmental stages during all normal vertebrate embryogenesis (Glucksmann, 1951). The term 'programmed cell death' was introduced to describe a type of cell death that occurred at predictable places and at predictable times during development (Lockshin and Williams, 1965). Inhibitors of RNA and protein synthesis were later found to inhibit cell death during amphibian and insect metamorphosis, indicating that macromolecular synthesis was required (Lockshin, 1969; Tata, 1966). One further key finding was made by John Saunders, who recognized that there were reproducible patterns of cell death in chick embryos and that death was primed by time-dependent intrinsic stimuli, which could be influenced by the environment (Saunders, 1966). In other words, signals from one cell could apparently suppress the cell death observed in another.

However, it was not until 1972 that the term apoptosis was defined. In a landmark paper by Kerr, Wyllie and Currie (Kerr *et al.*, 1972), they suggested that certain cells can undergo an active form of cell death involving the cell's own biochemical mechanisms. Using classical ultrastructural studies, Kerr provided evidence that cells undergo two very different types of cell death. Necrosis, which had already been described, occurs when a cell swells, organelles are destroyed, the cell ruptures releasing its contents and this leads to an inflammatory response. In contrast, Kerr also observed cells with intact organelles that had shrunken bodies, showed plasma membrane blebbing and had condensed chromatin (Kerr *et al.*, 1972). These cells, initially described as "shrunken necrosis" were then rapidly phagocytosed by

neighbouring cells or macrophages and destroyed, thus preventing an immune response. It was during this time that Kerr and colleagues concluded that the many forms of developmental cell death observed by Glucksmann in the 1950s had the same features as the cell death they were observing in normal untreated liver and in liver cells treated with hepatotoxins (Kerr, 1969; Kerr, 1970), as well as basal cell carcinomas of the skin (Kerr and Searle, 1972). The term "apoptosis" is used in Greek to describe the falling of leaves from a tree or petals from a flower and was chosen to emphasise the importance of the process during natural development and as a complementary but opposite role to mitosis.

The idea that a cell has its own built-in death program was not widely accepted for almost another 20 years. Kerr and colleagues continued to publish many examples of cell death that they now classified as apoptosis, for example, the regression of the tadpole tail during metamorphosis (Kerr *et al.*, 1974), the death of proliferating normal and neoplastic cells killed by cancer chemotherapeutics (Searle *et al.*, 1975) and the mechanism of T-cell killing (Don *et al.*, 1977). In 1980, Wyllie reported that thymocytes treated with glucocorticoid undergo apoptosis and that the chromosomal DNA was cleaved between nucleosomes by an endonuclease, giving a characteristic DNA ladder on an ethidium bromide-stained agarose gel (Wyllie, 1980). This is in contrast to cells undergoing necrosis, in which the DNA breakdown is random and results in a diffuse smear. After these findings, another research group published the observation that radiation caused the DNA in lymphocytes to break down into multiples of approximately 180 - 200 base pairs (Yamada *et al.*, 1981). Wyllie incorporated these findings and realised that the DNA ladder formation was indeed a hallmark of apoptosis (Wyllie *et al.*, 1984). This was the first biochemical marker for apoptosis and the development of a molecular mechanism to study apoptosis led to a rapid expansion of apoptosis research.

Further interest in the apoptosis field was stimulated by work with the nematode worm *Caenorhabditis elegans*. Sulston and Horvitz showed that precisely 131 of the 1090 somatic cells that make up a *C. elegans* worm, die by apoptosis at a precise time during development (Sulston and Horvitz, 1977). Genetic studies identified genes involved in cell death and its control (Ellis and Horvitz, 1986; Horvitz *et al.*, 1983). Two of these genes, *ced-3* and *ced-4* (where ced means 'cell death abnormal') are involved in cell killing, whereas *ced-9* is involved in survival. This,

and the identification of mammalian homologues of these cell death genes (Hengartner and Horvitz, 1994; Yuan *et al.*, 1993) lead to a greater acceptance of an inherited intracellular programme of death within cells. In 1988, David Vaux, Suzanne Cory and Jerry Adams observed that the principal function of the proto-oncogene *bcl-2* is to prevent death, and they coined the term 'survival factor' (Vaux *et al.*, 1988). *Bcl-2*, the mammalian homologue of *ced-9,* is the prototype of a family of genes that influence cell survival by regulating the activity of cell death effectors. The mammalian homologues of CED-3, the caspases, cleave cellular substrates at specific aspartic acid residues (Alnemri *et al.*, 1996; Thornberry *et al.*, 1997) and ultimately cause the destruction of the cell.

1.1.2 Apoptosis during development

Programmed cell death is an important mechanism in both development and homeostasis in adult tissues for the removal of either superfluous, infected, transformed or damaged cells and the elimination of self-reactive clones from the immune system (Ellis *et al.*, 1991b; Jacobson *et al.*, 1997; Raff, 1992). During embryogenesis, cell death is involved in sculpting different parts of the body. The removal of the interdigital web between developing digits involves apoptosis and inhibition of this cell death blocks digit formation (Jacobsen *et al.*, 1996). Cell death is also involved in the formation of hollow structures such as the preamniotic cavity, which is formed by ectodermal cell death (Coucouvanis and Martin, 1995) and in the formation of vertebrate neural tube and lens (Weil *et al.*, 1997).

Physiological apoptosis occurs during development to remove transitory organs and tissues, those required by an ancestral species and not the descendent or those needed at one stage in development but not another. For example, the pronephric tubules that form kidneys in fish and amphibian larvae, but which are not used by mammals (Saxen and Sariola, 1987), and during insect and amphibian metamorphosis, apoptosis removes cells no longer required such as muscles and neurons involved in larval locomotion in insects or the amphibian tadpole tail. This provides greater flexibility as structures are adapted for different functions at different stages of life or in different sexes. The Müllerian duct forms the uterus and oviduct in female mammals, but is not needed in males and is thought to be removed by programmed cell death (Price *et al.*, 1977). Conversely, the Wolffian duct forms the vas deferens,

epididymis and seminal vesicle in males, but is not required in females, and is deleted by apoptosis (Smith and Mackay, 1991). In addition, many cells are made in excess and later removed by apoptosis when they receive insufficient survival signals. During the normal development of the mammalian nervous system, apoptosis ensures that appropriate connections are made between neurons and their target cells (Oppenheim, 1991). It is thought that neurons compete for limiting amounts of survival factors produced by their target cells and neurons that fail to obtain sufficient neurotrophic support die by apoptosis (Barde, 1989). This would provide a system for eliminating cells that are in the wrong place (Raff, 1992).

Finally, apoptosis functions as part of a quality control process during development to ensure that any abnormal, misplaced, non-functional or potentially dangerous cells are eliminated. In the developing immune system, apoptosis eliminates self reactive T and B cells to induce self tolerance (Opferman and Korsmeyer, 2003). This negative selection of lymphocytes by apoptosis is also used to remove any lymphocytes that lack useful antigen receptors. This is again a further example of a situation in which cells are produced in vast excess and the numbers are reduced by apoptosis when only appropriate signals are available. During development, when a cell becomes damaged, for example the DNA, it undergoes apoptosis if unable to repair the damage (Clarke *et al.*, 1993; Lowe *et al.*, 1993). This serves as an anti-cancer mechanism and prevents any defects in DNA being passed onto offspring. Apoptosis may also be involved in the production of specialised differentiated cells. Cells such as skin keratinocytes and red blood cells, lose their nucleus and other organelles in the process of differentiation and it has been suggested that these processes may be modified forms of programmed cell death (Testa, 2004; Weil *et al.*, 1999).

The regulation of cells by apoptosis continues into the adult organism and is required for homeostasis to maintain stability and to survive. The maintenance of tissues such as bone and gastric epithelium as well as the removal of excess immune cells after infection require apoptosis. Harmful cells, for example, those infected with virus, cells in which the DNA has become damaged, or inappropriately generated autoreactive T-cells, are also eliminated by apoptosis.

1.1.3 Apoptosis and disease

In the adult organism, the number of cells within an organ or tissue has to be constant within a certain range. Blood and skin cells for instance, are constantly renewed by their respective progenitor cells, but proliferation has to be compensated by cell death. Lymphocytes and cells within reproductive organs undergo cyclic expansions and contraction as they take part in host defence and reproduction, respectively. In contrast, neural cells have a limited capacity for self-renewal, and most neurons survive for the life of the organism. This balancing process is part of the homeostasis required by living organisms. Homeostasis is achieved when the rate of mitosis in the tissue is balanced by cell death. If this equilibrium is disturbed, either of two things happens: 1) The cells are dividing faster than they die, effectively developing a tumour, or 2) The cells are dividing slower than they die, which results in a disorder of cell loss. Both states can be fatal or highly damaging. Failure of cells to undergo apoptosis may be involved in the pathogenesis of a variety of human diseases, including cancer, autoimmune disorders and viral infections (Hoffman and Liebermann, 1994; Thompson, 1995). In addition diseases that can arise from cell loss, such as neurodegenerative disorders, AIDS (acquired immunodeficiency syndrome) and ischaemic injury, have been suggested to involve accelerated rates of apoptosis (Akhtar *et al.*, 2004; Estus *et al.*, 1997; Meyaard *et al.*, 1992; Namura *et al.*, 1998; Rasola *et al.*, 2001; Thompson, 1995; Vila and Przedborski, 2003).

Cell proliferation is highly regulated, with growth factors and proto-oncogenes as positive regulators and tumour suppressors acting to oppose uncontrolled cell proliferation (Levine, 1993; Rozengurt, 1992). Normal cells depend on environmental stimuli to maintain their viability and prevent their survival in inappropriate locations (Boudreau *et al.*, 1995; Cyster *et al.*, 1994; Raff, 1992; Williams *et al.*, 1990). Metastatic tumour cells, however, are able to overcome these limitations and survive at sites distinct from the tissue in which they arose. This is accomplished by alterations in the level of expression or function of genes controlling both survival and apoptotic signaling pathways. The *bcl-2* proto-oncogene was initially identified in B-cell lymphoma at the t(14;18) translocation (Cleary and Sklar, 1985; Tsujimoto *et al.*, 1985). This translocation results in inappropriate *bcl-2* activation and cell survival. It was discovered that Bcl-2 acts as a survival factor in cells by preventing apoptosis induced by various stimuli (Hockenbery *et al.*, 1990; Hockenbery *et al.*, 1993; Nunez

et al., 1990; Vaux *et al.*, 1988). Genes that inhibit Bcl-2 can induce apoptosis in tumour cells and Bcl-2 expression has been linked to poor prognosis in prostate and colon cancers and neuroblastoma (Castle *et al.*, 1993; Hague *et al.*, 1994; McDonnell *et al.*, 1992). The tumour suppressor p53 is the most frequently mutated gene in human tumours. It plays a key role in DNA damage repair, cell cycle regulation and cellular apoptosis (Vogelstein *et al.*, 2000). Thus, cells with aberrant p53 can no longer initiate apoptosis in response to damaging signals, such as genotoxic stress (Lee and Bernstein, 1993; Lowe *et al.*, 1993). Failure to die in response to DNA damage would result in cells with translocations or mutations in their DNA surviving and developing into tumours. In addition, the proapoptotic Bcl-2 family members Noxa and Puma have been shown to be direct targets of p53 in some cells (Nakano and Vousden, 2001; Oda *et al.*, 2000; Yu *et al.*, 2001). The apoptotic protease activating factor-1 (Apaf-1) has been reported as a transcriptional target of p53 during DNA damage induced apoptosis in lymphoblastoid cell lines and in neurons (Fortin *et al.*, 2001; Robles *et al.*, 2001).

Physiological apoptosis is essential for the removal of potentially autoreactive lymphocytes during development and for the removal of excess cells following an immune response. Failure to remove these cells can lead to autoimmune disease. Stimulation of lymphocytes with Fas can induce apoptosis (Dhein et al., 1994; Krammer et al., 1994; Trauth et al., 1989) and at least two forms of inherited autoimmune disease had been attributed to alterations in Fas-mediated apoptosis (Drappa *et al.*, 1996; Fisher *et al.*, 1995; Rieux-Laucat *et al.*, 1995).

Excessive apoptosis can cause unwarranted cell death and may lead to diseases such as immunodeficiency and neurodegeneration. Virus-induced lymphocyte depletion occurs with AIDS, induced by the human immunodeficiency virus (HIV). The development of AIDS is associated with depletion of CD4+ T cells. CD4 acts as the receptor for viral attachment, facilitating infection. CD4 receptor stimulation has been proposed to enhance susceptibility to apoptosis (Banda *et al.*, 1992; Meyaard *et al.*, 1992). Viral genes have been proposed to induce apoptosis. The HIV protein nef causes an increased apoptotic response and down-modulation of Bcl-2 and Bcl-x_L in T cell lines (Rasola *et al.*, 2001). In addition, levels of TNF-related apoptosis-inducing ligand (TRAIL) are elevated in plasma of HIV-1-infected patients and may contribute to the death of CD4+ T cells (Herbeuval *et al.*, 2004). A variety of neurological

disorders are characterized by gradual loss of specific sets of neurons, which in many instances involves apoptosis (see section 1.3.2).

1.2 The molecular mechanisms of apoptosis

1.2.1 Programmed cell death in *Caenorhabditis elegans*

One of the best characterised developmental models of apoptosis is in the nematode *C. elegans* and much of the knowledge about the molecular genetics of programmed cell death comes from work performed on these worms. In the hermaphrodite, 131 of the 1090 original somatic cells formed are destined to die by apoptosis, the majority of which are neuronal cells (Sulston and Horvitz, 1977). Genes involved in the death process were identified through genetic screens for mutants defective in cell death, leading to the identification of a core apoptotic pathway that is evolutionarily conserved (Metzstein *et al.*, 1998). The first gene discovered in the programmed cell death system, was *egl-1* (egg laying defective). This gain-of-function mutation caused death of two neurons innervating the vulva, and hence the egg laying defect. A number of *ced* genes (cell death abnormal) were identified as regulators of the death process. Loss-of-function mutations in two of the genes, *ced-3* and *ced-4*, were shown to allow survival of the 131 somatic cells that normally die during development (Ellis and Horvitz, 1986; Yuan and Horvitz, 1990). *Egl-1* loss-of-function mutations also lead to survival of all of the 131 doomed cells (Conradt and Horvitz, 1998). These gene products are required for the killing process, whereas, another *ced* gene, *ced-9* protects cells from undergoing apoptosis. *C. elegans* lacking functional *ced-9* die early in development due to massive ectopic cell death, whereas a gain-of-function mutation in *ced-9* blocks all cell death (Hengartner *et al.*, 1992). Interestingly mutant nematodes that have a block in cell death have a normal life span, even though they have about 15% more cells and function less well than wild-type worms (Ellis *et al.*, 1991b). *Ced-3* encodes a caspase (section 1.2.2.1), part of a family of cysteine proteases that are responsible for the cleavage of critical cellular substrates at aspartate residues, and are key components of the cell death machinery (Thornberry and Lazebnik, 1998). CED-4 is a positive regulator of CED-3 (Yang *et al.*, 1998b). This adaptor protein encoded by *ced-4* is homologous to the mammalian Apaf-1 involved in apoptosome formation (section 1.2.2.4). *Ced-9* encodes an antiapoptotic

protein that promotes survival by inhibiting the functions of CED-3 and CED-4. This gene product has homology with the Bcl-2 family of proteins and binds CED-4, maintaining it in an inactive state, in which it cannot activate CED-3 (Chinnaiyan *et al.*, 1997; Hengartner and Horvitz, 1994). In addition, CED-9 is negatively regulated by EGL-1 (Conradt and Horvitz, 1998), a protein homologous to the mammalian BH3-only Bcl-2 family members (section 1.2.2.2), forming a cascade of cell death proteins. Only when CED-4 is displaced from CED-9 by EGL-1, is the lethal proteolytic activity of CED-3 released in the dying cells. These proteins form the core regulators of *C. elegans* programmed cell death and are evolutionarily conserved in both *Drosophila melanogaster* and mammals.

Additional genetic screens identified many other genes – *ced-1, ced-2, ced-5, ced-6, ced-7, ced-10* and *ced-12* – that are required for the efficient clearance of apoptotic cells (Chung *et al.*, 2000; Ellis *et al.*, 1991a; Hedgecock *et al.*, 1983). Genes involved in the death of specific cells, for example neurosecretory motoneurons (NSM) sister cells, have been identified. *Ces-1* gain-of-function and *ces-2* loss-of-function mutations allow survival of the NSM sister cells that are normally destined to die (Ellis and Horvitz, 1991). *Ces-1* and *ces-2* encode transcription factors that regulate *egl-1* expression in specific cells (Metzstein *et al.*, 1996; Thellmann *et al.*, 2003).

1.2.2 Caspase mediated apoptotic cell death

Apoptosis can be triggered by many different stimuli, both intrinsic and extrinsic. These signals feed into an evolutionary conserved intracellular machinery of execution (Green, 2000; Hengartner, 2000), which mainly involves the activation of caspases. Cell death can be classified into three major pathways according to the initiator caspase involved: the death receptor pathway involving caspase-8, the mitochondrial pathway, in which proapoptotic proteins are released from the mitochondria and which leads to the activation of caspase-9 and effector caspase-3, -6 or -7, and the ER stress pathway, which involves caspase-12 activation.

1.2.2.1 Caspases

The key effector enzymes of apoptosis are caspases, a distinct family of cysteine proteases that share the ability to cleave their substrates on the carboxyl side

of aspartate residues (Alnemri *et al.*, 1996). The first caspase discovered (caspase-1) was originally designated interleukin-1β-converting enzyme, ICE (Cerretti *et al.*, 1992; Thornberry *et al.*, 1992), and found to be homologous to the *C. elegans* gene product *ced-3* (Xue *et al.*, 1996; Yuan *et al.*, 1993). Since then at least 14 mammalian caspases have been discovered that exist in cells as inactive zymogens, about two thirds of which are implicated in apoptosis. These can be grouped according to function. Caspases-1, -4, -5, -11, -13 and -14 are thought to mainly be involved in cytokine processing. In particular, caspase-1 and caspase-11 process the proinflammatory cytokines IL-1 and IL-8 (Kuida *et al.*, 1995; Li *et al.*, 1995a; Wang *et al.*, 1998b). Caspase-12 has been shown to be involved in the ER stress pathway in mice (section 1.2.2.5). Caspases-2, -3, -6, -7, -8, -9 and -10 are implicated in apoptosis (Bergeron *et al.*, 1998; Hakem *et al.*, 1998; Kuida *et al.*, 1996; Nicholson, 1999; Varfolomeev *et al.*, 1998).

Although caspases differ in their primary sequence and substrate specificity, they share several features. Each caspase is made up of a tetramer, $\alpha_2\beta_2$, of two identical large (17-22 kDa) subunits and two identical small (10-12 kDa) subunits. In addition, each caspase is synthesised as an inactive zymogen that contains an N-terminal prodomain, a large subunit and a small subunit, and each is activated by cleavage into the mature caspase protein. On the basis of structural studies of caspases associated with inhibitors and more recently the structure of free caspase-7, a general mechanism for caspase activation has emerged (Piana *et al.*, 2003). The proteolytic cleavage of a caspase occurs either by autocatalysis or by an upstream protease and induces a dramatic conformational change that exposes the catalytic pocket of the enzyme. A caspase that cleaves and activates itself is called an initiator caspase and can go on to trigger downstream signalling cascades that lead to the activation of executioner caspases. The executioner caspases go on to cleave numerous cellular targets to destroy normal cellular functions, activate other apoptotic factors, inactivate antiapoptotic proteins and eventually lead to the death of the cell (Nicholson, 1999).

The initiator caspases, caspase-2, -8, -9 and -10 have long prodomains with motifs that facilitate protein-protein interaction, such as the death effector domain (DED) and the caspase activation and recruitment domain (CARD). These caspases are regulated mainly through autoproteolytic cleavage, which has been proposed to occur through an induced proximity model (Muzio *et al.*, 1998; Salvesen and Dixit,

1999). For example, caspase-8 is the key initiator caspase in the death receptor pathway, in which binding of ligand to receptor, recruits procaspase-8 via adaptor proteins to the intracellular side of the plasma membrane. This results in a high local concentration of zymogen molecules, which mutually cleave and activate one another. The initiator caspase-9 has a more complex activation mechanism. Proteolytic processing of caspase-9 has only a minor effect on the enzyme's activity (Rodriguez and Lazebnik, 1999; Stennicke *et al.*, 1999) The key requirement for caspase-9 activation is association with Apaf-1. Cytochrome c is released from the mitochondria during apoptosis and binds Apaf-1, ATP and caspase-9 to from a holoenzyme complex, the apoptosome (Cain *et al.*, 2000; Li *et al.*, 1997a; Rodriguez and Lazebnik, 1999; Zou *et al.*, 1997). This complex contains active caspase-9, which cleaves downstream effector caspases, such as caspase-3.

Caspases-3, -6 and -7 are effector caspases. Their inactive zymogens have short prodomains that lack any intrinsic enzymatic activity. Proteolytic cleavage between the large and small subunits leads to their activation. In addition, these caspases may be regulated by transcription in certain circumstances. Procaspase-3, for example, is present at high levels in many lymphoid and mature myeloid cells but present at low levels in breast epithelium and normal neurons (Krajewska *et al.*, 1997). Studies have shown elevated procaspase-3 in neurons following apoptotic insult (de Bilbao *et al.*, 1999; Ginham *et al.*, 2001; Ni *et al.*, 1998).

Effector caspases selectively cleave a restricted set of target polypeptides (possibly fewer than 200), usually at one, or at most a few positions in the primary sequence (Nicholson, 1999). This most commonly leads to inactivation of the target protein, but has also been reported to activate proteins, either by cleaving off a negative regulatory domain or inactivating a regulatory subunit. One of the hallmark events of apoptosis is the breakdown of chromosomal DNA into oligonucleosomal fragments. Caspase-3 activates CAD (caspase-activated DNase), by cleaving its inhibitory subunit (ICAD), allowing it to cut the genomic DNA (Nagata, 2000). In addition, caspases can disable normal DNA repair processes by inactivating poly(ADP-ribose) polymerase (PARP) and DNA-PK, further contributing to the changes in DNA integrity. Other targets of the caspases include nuclear lamins, leading to nuclear shrinkage and budding, and cytoskeletal proteins such as fodrin and gelsolin, causing an overall loss of cell shape (Buendia *et al.*, 1999; Kothakota *et al.*,

1997; Rao *et al.*, 1996). Bcl-2 family proteins can also be cleaved by caspases. For example, caspase-8 cleaves Bid to generate active tBid, which activates the mitochondrial pathway as described in section 1.2.2.3. The antiapoptotic proteins Bcl-2 and Bcl-x_L can be cleaved by caspases, converting them into proapoptotic proteins (Cheng *et al.*, 1997; Clem *et al.*, 1998; Grandgirard *et al.*, 1998). It has been suggested that cleavage removes the protective function of these proteins.

Caspases are regulated by inhibitor-of-apoptosis proteins (IAPs). This family includes cIAP1, cIAP2, XIAP, NAIP, survivin and livin in humans. These proteins inhibit caspases by directly binding to the active enzymes via a BIR (baculovirus IAP repeat) domain (Deveraux *et al.*, 1997; Salvesen and Duckett, 2002; Takahashi *et al.*, 1998). IAP proteins contain one or more N-terminal BIR domains and a C-terminal RING domain (Deveraux and Reed, 1999; Miller, 1999). The RING domains can act as ubiquitin ligases, facilitating ubiquitination and proteosomal degradation of the bound caspases (Huang *et al.*, 2000; Yang *et al.*, 2000). Some IAP proteins are aberrantly up-regulated in certain cancer tissues (Dierlamm *et al.*, 1999; Imoto *et al.*, 2001; Vucic *et al.*, 2000). The IAP proteins are in turn regulated through inhibition by mammalian SMAC / DIABLO (second mitochondrial-derived activator of apoptosis / direct IAP-binding protein with low pI), which is released from the mitochondria along with other proteins following activation of the mitochondrial death pathway (section 1.2.2.4). Caspases also appear to be regulated by post-translational modifications. For example, in TPA or EGF-treated HeLa cells, ERK-mediated phosphorylation of caspase-9 at Thr 125 blocks the processing of caspase-9 and subsequent caspase-3 activation (Allan *et al.*, 2003).

1.2.2.2 Bcl-2 family

The Bcl-2 family of proteins are critical regulators of apoptosis, which can act as either proapoptotic or antiapoptotic molecules, based on their ability to kill or protect cells *in vitro* and the effect of gene knockout on cell death and tissue homeostasis in mice. The *Bcl-2* proto-oncogene was initially identified in B-cell lymphoma at the t(14;18) translocation (Cleary and Sklar, 1985; Tsujimoto *et al.*, 1985). Bcl-2 is an integral membrane protein mainly localised to the mitochondria, but also found in the ER (Akao *et al.*, 1994; Lithgow *et al.*, 1994). At the mitochondria, Bcl-2 family members function to control the release of cytochrome c and other

apoptosis-promoting factors from the mitochondria. Members of the family are characterised by the presence of up to four alpha-helical Bcl-2 homology (BH) domains, designated BH1-4. Most antiapoptotic proteins contain all four domains, whereas the proapoptotic proteins contain either BH1-3 or BH3 only. These proteins have the ability to form homo- or heterodimers, altering their function within the cell.

The antiapoptotic members prevent the release of mitochondrial proteins involved in apoptosis, by interacting with and inhibiting proapoptotic family members, such as Bax (Antonsson *et al.*, 2001; Cheng *et al.*, 2001). In mammals, members of this sub group include Bcl-2, Bcl-x_L, Bcl-W, Mcl-1, A1/BFL-1, BOO/DIVA and NF-13. The BH4 domain of these proteins is required for antiapoptotic activity (Huang *et al.*, 1998; Sugioka *et al.*, 2003). The proapoptotic Bcl-2 family members can be spilt into two subfamilies according to their homology with Bcl-2. Bax, Bak and Bok/Mtd contain BH1-3 and resemble Bcl-2 fairly closely. In contrast, the other proapoptotic members contain only the short (9-16 residue) BH3 domain of Bcl-2 and are otherwise unrelated to any known protein. These BH3-only proteins are potent cell killers and include, Bid, Bad, Bim, Blk, Bik, Bmf, Hrk/DP5, Bnip3, Nix, Noxa and Puma. The BH3 domain of these proteins and of the other proapoptotic members has been shown to be essential for their proapoptotic activity (Chittenden *et al.*, 1995; O'Connor *et al.*, 1998; Wang *et al.*, 1998a; Zha *et al.*, 1997). Replacement of the BH3 region of Bcl-2 by the BH3 region of Bax converts Bcl-2 from a death antagonist to a death agonist (Hunter and Parslow, 1996), suggesting that there is a critical sequence difference which distinguishes the BH3 domain of the antiapoptotic and proapoptotic members of the family. Proapoptotic and antiapoptotic members can heterodimerise and influence each other's function, suggesting that their relative concentrations within a cell may act as a rheostat for the suicide program (Oltvai *et al.*, 1993).

When cells are exposed to apoptotic stimuli, proapoptotic proteins are activated through post-translational modifications or changes in their conformation, as well as transcriptional controls. Activation of Bax and Bak involves the translocation of cytosolic monomeric proteins to the mitochondrial membrane, the formation of oligomers within the membrane and the release of cytochrome c (Gross *et al.*, 1998; Korsmeyer *et al.*, 2000; Wolter *et al.*, 1997). The antiapoptotic proteins Bcl-2 and Bcl-x_L localise to the outer mitochondrial membrane and inactivate Bax by heterodimerising with the proapoptotic protein, preventing the formation of Bax

homodimers in the membrane (Antonsson *et al.*, 2001; Cheng *et al.*, 2001). The BH3-only protein Bim is transcriptionally controlled and also translocates to the mitochondria following certain apoptotic stimuli, such as after NGF withdrawal from sympathetic neurons (Putcha *et al.*, 2001; Whitfield *et al.*, 2001). The cleavage of proapoptotic Bcl-2 family members is another mechanism of regulation. The BH3-only protein Bid is cleaved into tBid by caspase-8 during death receptor-mediated apoptosis. This truncated protein then translocates to the mitochondria, where it can oligomerise with Bax and Bak to form pores in the membrane (Korsmeyer *et al.*, 2000; Li *et al.*, 1998; Luo *et al.*, 1998a). In contrast, Bad is regulated by phosphorylation. In haematopoietic cells for example, IL-3 stimulation leads to Bad phosphorylation and its sequestration in the cytosol by binding to 14-3-3 proteins which prevents it from binding to and inhibiting Bcl-x_L (del Peso *et al.*, 1997; Zha *et al.*, 1996). Following a death signal, such as IL-3 deprivation, Bad becomes dephosphorylated and is found associated with Bcl-x_L-Bcl-2 and this interaction requires the BH3 domain of Bad (Kelekar *et al.*, 1997; Ottilie *et al.*, 1997; Zha *et al.*, 1997). In addition, survival signals such as the P-I3K/Akt pathway can directly phosphorylate Bad and inhibit its ability to induce apoptosis (Datta *et al.*, 1997; del Peso *et al.*, 1997). Some proapoptotic members are transcriptionally controlled, for example, Noxa and Puma are under p53 mediated transcriptional control in response to DNA damage (Nakano and Vousden, 2001; Oda *et al.*, 2000; Yu *et al.*, 2001). NGF-withdrawal from sympathetic neurons leads to increased expression of the BH3-only protein DP5 (Imaizumi *et al.*, 1997).

The pro-survival members of the Bcl-2 family, such as Bcl-2 or Bcl-x_L, serve a principal, although perhaps not an exclusive role of binding and sequestering BH3-only molecules, preventing Bax or Bak activation (Cheng *et al.*, 2001). Post-translational modification of the Bcl-2 protein has been described in a variety of cell models with effects varying from enhanced to abrogated function. Bcl-2 may be activated by phosphorylation at Ser70, but inactivated when phosphorylated perhaps by JNK at loop sites in the protein which may initiate a conformational change (Brichese *et al.*, 2004; Haldar *et al.*, 1997; Ito *et al.*, 1997; Maundrell *et al.*, 1997). Bcl-x_L can also undergo phosphorylation, which is thought to negatively regulate its activity (Basu and Haldar, 2003; Chang *et al.*, 1997). Transcriptional regulation can also play a part in controlling the activity of antiapoptotic members of the Bcl-2 family

under selective conditions, for example, IL-3 induces the expression of *mcl-1* in myeloid progenitor cells (Boise *et al.*, 1995; Catz and Johnson, 2001; Karlsson *et al.*, 2003; Lin *et al.*, 1993; Yang *et al.*, 1996).

Bax-deficient mice are viable demonstrating it is not essential for development, however, these animals have abnormalities in haematopoietic, neuronal and gametogenic development (Knudson and Korsmeyer, 1997; Knudson *et al.*, 1995). For example, neuronal cell death in the peripheral and central nervous system is decreased, in particular sympathetic neurons absolutely require endogenous Bax expression and translocation for apoptosis (Deckwerth *et al.*, 1996; Deshmukh and Johnson, 1998; Putcha *et al.*, 1999; White *et al.*, 1998). Bak knockout mice are viable without obvious age-related abnormalities, however $bax^{-/-}bak^{-/-}$ mice have a dramatic phenotype with 90% perinatal lethality (Lindsten *et al.*, 2000). These animals have interdigital webs, an accumulation of neurons within the central nervous system and splenomegaly. Embryonic fibroblasts from the double knockouts show resistance to many apoptotic stimuli such as UV radiation and serum withdrawal.

Bcl-2-deficient mice are viable despite the widespread expression of Bcl-2 during development (Merry *et al.*, 1994; Novack and Korsmeyer, 1994). The mice are runted and die a few months after birth due to renal failure. In addition, a lack of Bcl-2 causes premature loss of lymphoid cells and melanocytes, resulting in immunodeficiency and loss of hair pigmentation, respectively (Nakayama *et al.*, 1993; Veis *et al.*, 1993). Bcl-x_L deficient mice die at E13 with extensive apoptosis of postmitotic differentiating neurons in the developing brain, spinal cord and dorsal root ganglia (Motoyama *et al.*, 1995).

Mouse models of the BH3-only family members also exist. The majority of Bim-deficient mice die during embryonic development around E9.5 (Bouillet *et al.*, 1999). Survivors have abnormal homeostasis within the haematopoietic compartment. The absence of Bim increases the survival of resting lymphocytes and protects activated T and B cells against cytokine withdrawal. With age, Bim-deficient animals demonstrate progressive lymphadenopathy and splenomegaly with a dramatic increase in plasma cell numbers and corresponding immunoglobulin levels (Bouillet *et al.*, 1999; O'Reilly *et al.*, 2000). Neurons from $bim^{-/-}$ mice show delayed developmental and induced apoptosis (Putcha *et al.*, 2001). Mice deficient in DP5 are fertile, show no gross abnormalities, and appear normal (Imaizumi *et al.*, 2004). Analysis of neuronal

populations indicated a delay in sympathetic neuron death *in vitro* and an inhibition of axotomy-induced motoneuron death *in vivo*.

1.2.2.3 The death receptor pathway

Receptor-mediated apoptosis has been demonstrated for numerous growth factors, including transforming growth factor β and cytokines, such as tumour necrosis factor (TNF) (Oberhammer *et al.*, 1992; Shinagawa *et al.*, 1991). This extrinsic pathway is recruited through activation of cell-surface receptors, such as Fas/CD95, TRAIL receptors, and the tumour necrosis factor receptor 1 (TNFR1). This large family of death receptors are transmembrane proteins expressed on the surface of target cells. Fas ligand (FasL) binds to the Fas receptor, TRAIL binds the TRAIL receptors, DR4 and DR5, and TNF and lymphotoxin α bind to TNFR1 (Ashkenazi and Dixit, 1998). The N-terminus on the extracellular side of the membrane contains between one and six ligand binding domains. Within the cell, the C-terminus consists of a 60-70 residue region, known as the death domain (DD). Upon activation by ligand, the receptors form a cluster, bringing together the death domains. This leads to the recruitment of adaptor proteins FADD (Fas/APO-1-associated death domain protein), TRADD (TNFR1-associated protein with death domain), RIP (receptor interacting protein), RAIDD (RIP-associated ICH-1 homologous protein with a death domain) or MADD (MAP kinase-activating death domain protein) depending on the receptor (Boldin *et al.*, 1995; Chinnaiyan *et al.*, 1995; Duan and Dixit, 1997; Hsu *et al.*, 1995; Schievella *et al.*, 1997; Stanger *et al.*, 1995). The binding of these adaptor proteins with death effector domains (DEDs) leads to the formation of the death-inducing signalling complex (DISC), and it is this DISC that recruits the precursor enzymes, procaspase-8 or procaspase-10, leading to their activation by proximity-induced self cleavage and/or dimerisation (Muzio *et al.*, 1998; Salvesen and Dixit, 1999; Shi, 2004).

At this point, death receptor signalling diverges in different cells (see Figure 1.1). In type I cells formation of the DISC leads to recruitment of procaspase-8, its cleavage and therefore activation of caspase-8 (Muzio *et al.*, 1998), which then directly cleaves and activates procaspase-3. In type II cells, caspase-8 activation is much less efficient and generally insufficient to activate caspase-3. However, in these cells activated caspase-8 activates other caspases indirectly by cleaving the Bcl-2

family member Bid. Truncated Bid (tBid) subsequently goes on to activate the mitochondrial pathway by translocating to the mitochondria and triggering Bax oligomerisation (Wei *et al.*, 2000). This leads to the release of multiple polypeptides from the mitochondria, including cytochrome c. This binds to Apaf-1 and causes an ATP-dependent conformational change that results in Apaf-1 oligomerisation, and binding to procaspase-9 (Li *et al.*, 1997a). The formation of this complex, the apoptosome, results in procaspase-9 cleavage to caspase-9, which in turn proteolytically activates caspase-3 (section 1.2.2.4). This provides a means of cross-talk and integration between the death-receptor and mitochondrial pathways, however, under most conditions cross-talk is minimal. The existence of these distinct pathways is supported by genetic and biochemical experiments. Targeted disruption of the genes for FADD and procaspase-8 renders cells resistant to death receptor ligands, but not to ionizing radiation or anti-cancer drugs *in vitro*. Also, disruption of Bid prevents FasL-induced hepatic damage *in vivo*, but not immune cell death (Gross *et al.*, 1999; Yin *et al.*, 1999). Bid-deficient mice undergo developmental cell death relatively normally, which contrasts sharply with the embryonic lethality of FADD or caspase-8 deficiency (Varfolomeev *et al.*, 1998; Yeh *et al.*, 1998).

There are three distinct mechanisms involved in the regulation of death receptor activity. Inhibitors of procaspase recruitment and/or activation of the DISC have been identified (Hu *et al.*, 1997; Inohara *et al.*, 1997), such as cFLIP (FLICE inhibitory protein). FLIP has two isoforms FLIP-long and FLIP-short, which bind to FADD, procaspase-8 and procaspase-10, via their DED domains (Irmler *et al.*, 1997). This interaction blocks procaspase processing at the DISC. Cells transfected with FLIP are resistant to death receptor-induced stimuli, but not other apoptotic stimuli, such as UV-irradiation. Another mechanism of regulation is through the expression of decoy receptors closely related to the TRAIL receptors DR4 and DR5 (Golstein, 1997). These either lack the cytoplasmic domain (DcR1) or have a truncated death domain in the cytoplasmic region (DcR2) and thus are unable to activate downstream signalling. These receptors sequester TRAIL ligand away from the DR4 and DR5 receptors (Marsters *et al.*, 1997). Another decoy receptor (DcR3) has been described, that can bind to FasL and thus prevent FasL from binding to Fas (Pitti *et al.*, 1998). The third mechanism of regulation is through direct inhibition of the proteolytic activity of the initiator procaspases, such as procaspase-8 and -10. For example, the viral protein

Figure 1.1 The death receptor pathway

The extrinsic death receptor pathway is activated when death ligands bind to their specific cell surface death receptors. For example, the binding of Fas ligand (FasL) binds to the Fas receptor, leads to its activation. The cytoplasmic domain of the receptor contains a death domain (DD). Upon activation by ligand, the receptors form a cluster, bringing together the death domains and leading to the recruitment of adaptor proteins, such as FADD (Fas/APO-1-associated death domain protein). The binding of these adaptor proteins with death effector domains (DEDs) leads to the formation of the death-inducing signalling complex (DISC), and it is this DISC that recruits the precursor enzymes, procaspase-8 or procaspase-10, leading to their activation. At this point, death receptor signalling diverges in different cells. In type I cells, the activated caspase-8 directly cleaves and activates procaspase-3. In type II cells, activated caspase-8 cleaves the Bcl-2 family member Bid to form truncated Bid (tBid). This activates the mitochondrial pathway by translocating to the mitochondria and triggering Bax oligomerisation. This leads to the release of multiple proapoptotic polypeptides from the mitochondria, including cytochrome c. This binds to Apaf-1 and procaspase-9, forming the apoptosome. The formation of this complex results in procaspase-9 cleavage to caspase-9, which in turn proteolytically activates caspase3. This provides a means of cross-talk and integration between the death-receptor and mitochondrial pathways.

Taken from (Kaufmann and Hengartner, 2001).

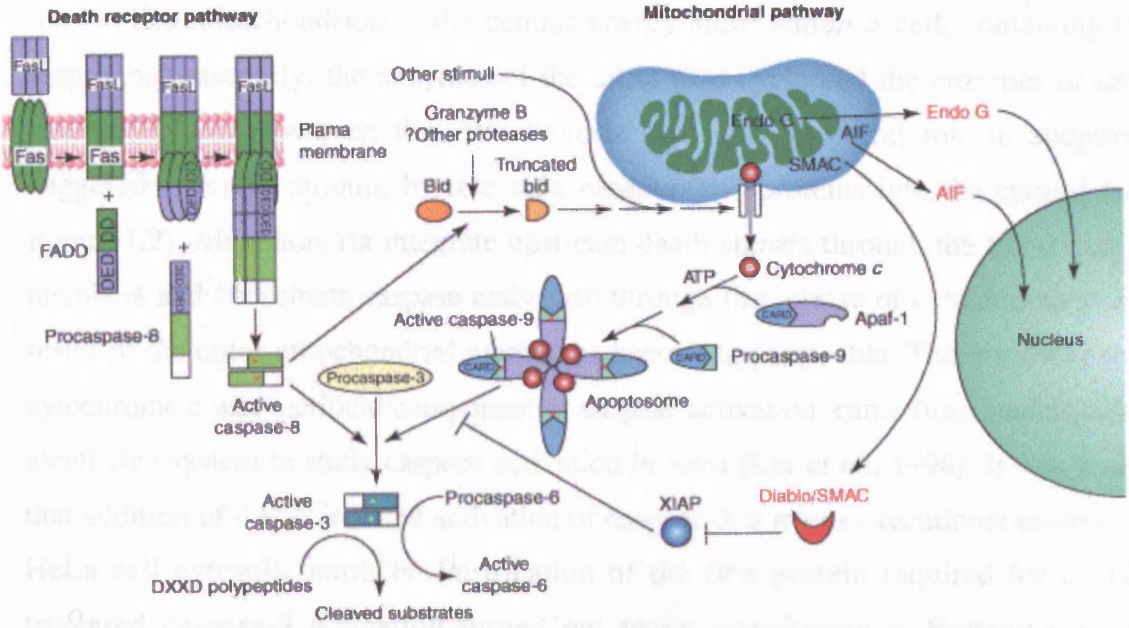
Death receptor pathway
Mitochondrial pathway
FasL
Fas
FADD
DED
Procaspase-8
Plama membrane
Other stimuli
Granzyme B
?Other proteases
Truncated bid
Bid
Endo G
AIF
SMAC
Cytochrome c
ATP
Apaf-1
CARD
Procaspase-9
Active caspase-9
Apoptosome
Nucleus
Procaspase-3
Active caspase-8
Active caspase-3
Procaspase-6
XIAP
Diablo/SMAC
DXXD polypeptides
Active caspase-6
Cleaved substrates

crmA can inhibit both the autoproteolytic activation of procaspase-8 as well as the ability of caspase-8 to cleave Bid (Komiyama *et al.*, 1994; Ray *et al.*, 1992). The silencer of death domains (SODD) is associated with the death domain of the TNFR1 in the absence of TNF treatment, preventing spontaneous activation (Jiang *et al.*, 1999).

1.2.2.4 Mitochondrial pathway

The mitochondrion is the central energy store within a cell, containing the respiratory assembly, the enzymes of the citric acid cycle and the enzymes of fatty acid oxidation. However, the mitochondria also play a central role in apoptosis triggered by many stimuli, by releasing proapoptotic proteins into the cytosol (see Figure 1.2). Mitochondria integrate upstream death signals through the Bcl-2 family members and coordinate caspase activation through the release of cytochrome c as a result of the outer mitochondrial membrane becoming permeable. The discovery that cytochrome c was a critical component of caspase activation, came from studies using a cell-free system to study caspase activation *in vitro* (Liu *et al.*, 1996). It was found that addition of dATP induced activation of caspase-3, a major executioner caspase in HeLa cell cytosolic extracts. Purification of the first protein required for dATP-triggered caspase-3 activation turned out to be cytochrome c. Further analysis identified two other components, Apaf-1 and caspase-9, as being required for the activation of downstream caspases (Li *et al.*, 1997a; Zou *et al.*, 1997). When cytochrome c is released from the mitochondria, it accumulates in the cytoplasm where it binds to Apaf-1 forming the oligomeric Apaf-1/cytochrome c apoptosome in the presence of ATP. This complex then recruits procaspase-9 and induces its activation. Unlike conventional caspase activation, in which complete proteolytic cleavage of the caspase is both necessary and sufficient for its activation, caspase-9 activation requires constant association of the enzyme with the apoptosome (Jiang and Wang, 2000; Rodriguez and Lazebnik, 1999). The apoptosome consists of seven molecules of Apaf-1, arranged in a symmetrical wheel-like structure. Each Apaf-1 molecule interacts with the adjacent Apaf-1 molecule via their N-terminal CARD domain in the centre of the structure (Acehan *et al.*, 2002). This region recruits procaspase-9 through CARD domain interaction and induces a conformational change

in the enzyme, leading to an active holoenzyme complex that activates downstream effector caspases, such as caspase-3 and caspase-7.

Mice deficient in caspase-3, caspase-9 or Apaf-1 have a similar phenotype (Cecconi *et al.*, 1998; Hakem *et al.*, 1998; Kuida *et al.*, 1998; Kuida *et al.*, 1996; Yoshida *et al.*, 1998). A lack of any one of these proteins leads to embryonic or perinatal death due to deficits in the central nervous system, reflecting the failure of apoptosis during neural development. In *caspase-9*$^{-/-}$ knockout mice, caspase-3 was not activated, supporting the proposal that caspase-9 is upstream of caspase-3. Caspase-9-deficient thymocytes are resistant to radiation and dexamethasone-induced death, but remain sensitive to TNFα or ligation of Fas (Hakem *et al.*, 1998; Kuida *et al.*, 1998), supporting the presence of distinct cell death-receptor and mitochondrial pathways. Similarly, *apaf-1*$^{-/-}$ thymocytes are sensitive to Fas-induced killing, whereas Apaf-1-deficient embryonic fibroblasts resemble cells overexpressing Bcl-2, as they are resistant to other cell death stimuli known to activate the mitochondrial pathway (Cecconi *et al.*, 1998; Yoshida *et al.*, 1998). Caspase-3 deficient thymocytes and hepatocytes do not display all of the typical apoptotic features of membrane blebbing and nuclear fragmentation, which indicates its substrates are essential for the features of apoptotic morphology (Zheng *et al.*, 1998).

Upstream of the mitochondria, Bcl-2 family members regulate apoptosis by controlling the release of cytochrome c. In particular, overexpression of Bcl-2 and Bcl-x_L inhibits cell death by preventing cytochrome c release, whereas Bax overexpression triggers cytochrome c release from the mitochondria in the absence of any apoptotic stimuli (Finucane *et al.*, 1999; Jurgensmeier *et al.*, 1998; Pastorino *et al.*, 1998; Yang *et al.*, 1997c). Based on the structural similarity of Bcl-x_L to the pore-forming subunit of diphtheria toxin (Muchmore *et al.*, 1996), it had been suggested that Bcl-2 proteins may act by inserting, following a conformational change, into the outer mitochondrial membrane, where they could form channels or pores. Bax/Bak oligomerisation on the mitochondrial membrane is essential for release of cytochrome c (Wei *et al.*, 2001; Zong *et al.*, 2001). Bax and tBid can decrease the stability of planar phospholipid bilayers, and so may directly act on the outer mitochondrial membrane allowing intermembrane proteins to simply diffuse out into the cytsol (Basanez *et al.*, 1999; Kudla *et al.*, 2000).

Figure 1.2 The mitochondrial pathway

The intrinsic cell death pathway, through the mitochondria, integrates upstream death signals through the Bcl-2 family members and coordinates caspase activation through the release of cytochrome c as a result of the outer mitochondrial membrane becoming permeable. Upstream of the mitochondria, Bcl-2 family members regulate apoptosis by controlling the release of cytochrome c. Overexpression of Bcl-2 and Bcl-x_L inhibits cell death by preventing cytochrome c release, whereas Bax overexpression triggers cytochrome c release. Bcl-2 family proteins, such as Bax and Bak may act by inserting into the outer mitochondrial membrane, where they could form channels or pores. It has been proposed that Bcl-2 family proteins may associate with other mitochondrial membrane proteins, such as VDAC and PTP, and regulate channel activity. Apoptotic signals may alter mitochondrial physiology, leading to swelling of the organelle and rupture of the outer mitochondrial membrane.

When cytochrome c is released from the mitochondria, it accumulates in the cytoplasm where it binds to Apaf-1 forming the oligomeric Apaf-1/cytochrome c apoptosome in the presence of ATP. This complex then recruits procaspase-9 and induces its activation. Recruitment of procaspase-9 induces a conformational change in the enzyme, leading to an active holoenzyme complex to activate downstream effector caspases, such as caspase-3 and caspase-7. These executioner caspases go on to cleave numerous cellular targets to destroy normal cellular functions, activate other apoptotic factors, inactivate antiapoptotic proteins and eventually lead to the death of the cell. Other important proapoptotic polypeptides are released from the mitochondria. SMAC and Omi/HtrA2 inactivate IAP proteins, a group of polypeptides that inhibit caspase activation, thus allowing caspases to execute apoptosis. AIF is a mitochondrial oxidoreductase with potent apoptotic activity, which induces chromatin condensation and DNA fragmentation in isolated nuclei.

Taken from (Zimmermann *et al.*, 2001).

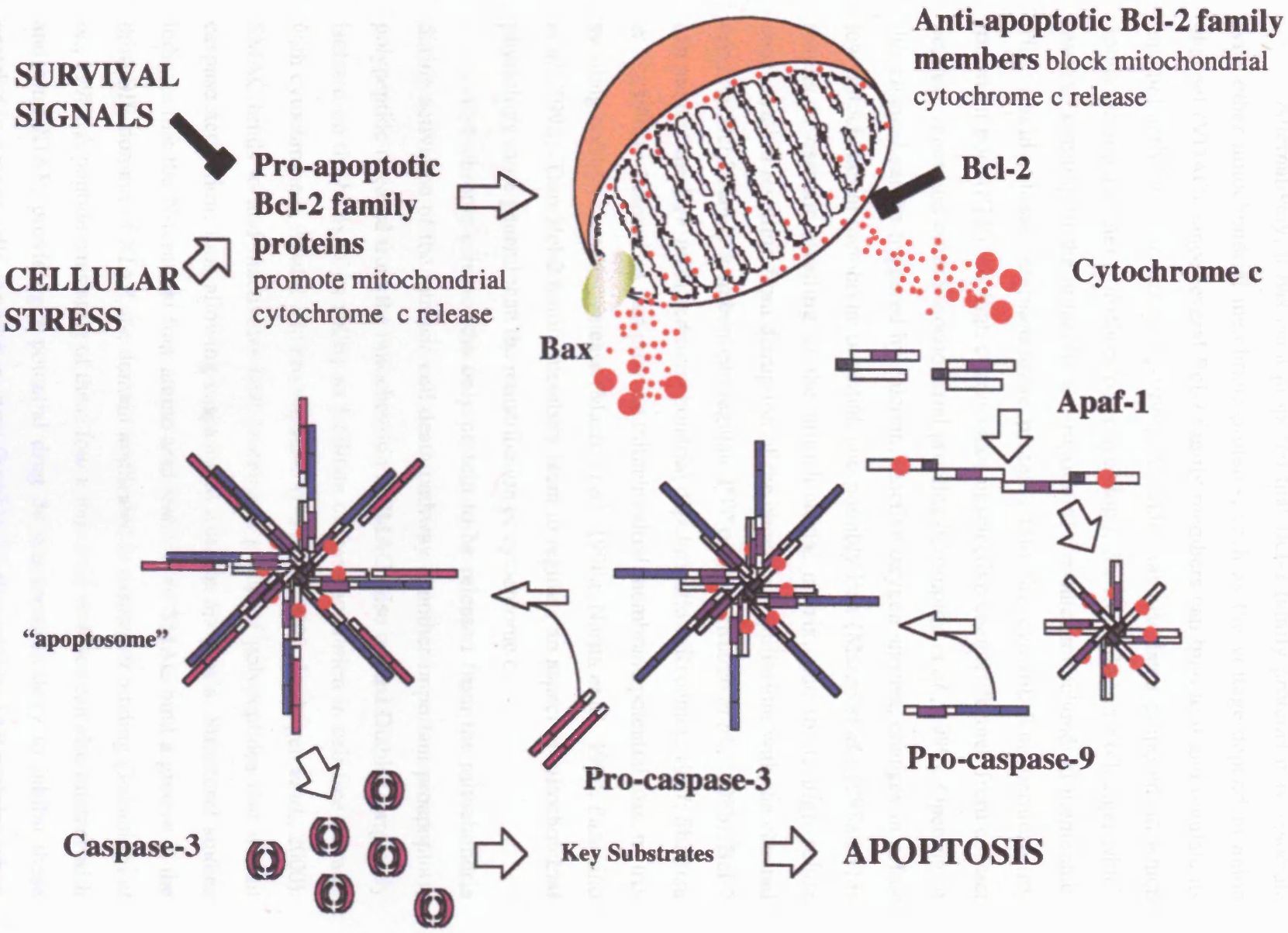
SURVIVAL SIGNALS
CELLULAR STRESS
Pro-apoptotic Bcl-2 family proteins promote mitochondrial cytochrome c release
Anti-apoptotic Bcl-2 family members block mitochondrial cytochrome c release
Bcl-2
Cytochrome c
Bax
Apaf-1
"apoptosome"
Pro-caspase-3
Pro-caspase-9
Caspase-3
Key Substrates
APOPTOSIS

Alternatively, it has been proposed that Bcl-2 family proteins may associate with other mitochondrial membrane proteins, such as the voltage-dependent anion channel (VDAC), since several Bcl-2 family members can bind to it and regulate its channel activity (Shimizu *et al.*, 1999). A model has also been proposed, in which apoptotic signals alter mitochondrial physiology, for example ion exchange, which leads to swelling of the organelle and rupture of the outer mitochondrial membrane. This would release intermembrane proteins into the cytosol. The permeability transition pore (PTP) is a high conductance unselective channel formed from contact between inner and outer mitochondrial proteins (Crompton *et al.*, 1999). Opening of this channel can be triggered by calcium, reactive oxygen species, changes in pH or low mitochondrial membrane potential, and possibly Bax (Marzo *et al.*, 1998a). This results in osmotic swelling of the mitochondrial matrix, due to its high solute concentration resulting from disruption of the chemical equilibrium with the channel opening. Bcl-2 family members can regulate PTP opening (Marzo *et al.*, 1998b). Bcl-2 can prevent the PTP-mediated mitochondrial depolarization (Kroemer, 1997; Shimizu *et al.*, 1998) whereas Bax can provoke mitochondrial membrane potential loss, matrix swelling and cytochrome c release (Marzo *et al.*, 1998a; Narita *et al.*, 1998; Pastorino *et al.*, 1998). Thus Bcl-2 family members seem to regulate an aspect of mitochondrial physiology more general than the redistribution of cytochrome c.

Cytochrome c is not the only protein to be released from the mitochondria during activation of the intrinsic cell death pathway. Another important proapoptotic polypeptide released from the mitochondria is SMAC (also termed Diablo), originally isolated on the basis of its ability to facilitate caspase activation in cell-free extracts with cytochrome c, Apaf-1 and procaspase-9 (Du *et al.*, 2000; Verhagen *et al.*, 2000). SMAC binds to and inactivates IAP proteins, a group of polypeptides that inhibit caspase activation, thus allowing caspases to execute apoptosis. Structural studies indicate that the N-terminal four amino acid residues of SMAC bind a groove in the third BIR domain of XIAP, the domain implicated in caspase-9 binding (Takahashi *et al.*, 1998). A peptide consisting of these four amino acid residues can also interact with and bind XIAP, providing a potential drug development strategy to inhibit these proteins in cancer cells. Another protein Omi/HtrA2 also inhibits IAP proteins when released from the mitochondria. This is a serine protease that can cleave and inactivate

IAP proteins (Jin *et al.*, 2003; Yang *et al.*, 2003) and could therefore be a more efficient IAP suppressor.

Apoptosis-inducing factor (AIF) is a mitochondrial oxidoreductase with potent apoptotic activity and was isolated through its ability to induce caspase-independent chromatin condensation and DNA fragmentation in isolated nuclei (Susin *et al.*, 1999). However, the exact mechanism of this remains unclear, and it has been suggested from *AIF* gene knockout experiments that it may have a role in embryonic development (Joza *et al.*, 2001). In addition to AIF, mitochondria release endonuclease G, which is also implicated in DNA degradation during apoptosis (Li *et al.*, 2001; Parrish *et al.*, 2001). AIF and endonuclease G have mainly been implicated in caspase-independent cell death mechanisms, although endonuclease G may work in parallel with caspases in some cells.

1.2.2.5 ER stress pathway

The endoplasmic reticulum (ER) is a highly dynamic organelle, which in addition to synthesizing and packaging proteins also plays a central role in many signalling processes. Input signals to the ER are extensive and include calcium, inositol 1,4,5-trisphosphate and reactive oxygen species (Berridge, 2002). The main output signal is calcium. The release of calcium from the ER controls the levels of cytoplasmic free calcium and thus many cellular functions. The release of calcium through, for example, calcium sensitive receptors (calcium-induced calcium release) spreads signals throughout the cell and is particularly important in the control of muscle cells and neurons.

The function of the ER is intimately connected to the mitochondria, with the mitochondria taking up calcium to assist in the recovery phase of the calcium signal (Csordas and Hajnoczky, 2001; Rizzuto *et al.*, 1998). If the normal equilibrium is altered, with calcium accumulating in the mitochondria, a number of stress signals are induced, such as the formation of the PTP, collapse of the mitochondrial membrane potential and release of cytochrome c and AIF, that activate caspases and induce apoptosis, as discussed in section 1.2.2.4.

Disruption of calcium homeostasis affects protein synthesis and conversely accumulation of misfolded proteins can alter the ER calcium balance. Chaperone proteins within the ER lumen, such as GRP78, are responsible for folding newly

synthesised proteins into their tertiary structure. However, stress factors, such as decreased calcium levels in the ER lumen, results in dysfunctional chaperones and accumulation of misfolded proteins (Ferri and Kroemer, 2001; Kaufman, 1999). This unfolded protein response pathway shuts down general protein synthesis, while upregulating ER resident chaperone proteins and other regulatory components. This gives the cell sufficient time to correct the folding problem incurred by the ER stress prior to synthesizing additional proteins (Ma *et al.*, 2002). The protein kinase PERK phosphorylates the alpha subunit of the translation initiation factor 2 (eIF2α) causing its inactivation and impaired initiation of protein synthesis (Harding *et al.*, 1999; Ron, 2002). In addition, this pathway of ER stress response results in the activation of ATF-6, which is released from the ER to enter the nucleus, where it can activate the transcription of the *GADD153/CHOP* gene (Gotoh *et al.*, 2002). If the damage to the ER is extensive and homeostasis cannot be resumed, then apoptosis is initiated.

The ER can play a direct role in activating a number of caspases in murine cells (Ferri and Kroemer, 2001; Morishima *et al.*, 2002; Nakagawa *et al.*, 2000). Caspase-12 is associated with the ER membrane and is released by proteolytic cleavage following ER stress. Caspase-12 can activate caspase-9 without cytochrome c release in C2C12 myoblast cells under ER stress (Morishima *et al.*, 2002), leading to effector caspase activation and apoptosis. The Bcl-2 family of proteins has also been implicated in the regulation of the apoptotic ER pathway. Bcl-2 can be found localised to the ER in addition to the mitochondria (Lithgow *et al.*, 1994). This association with the ER may stabilise calcium homeostasis and suppress oxidative stress (He *et al.*, 1997). When Bcl-2 is overexpressed in cells, there is a decrease in calcium stored in the ER. Bcl-2 may act by increasing the leak of calcium from the ER lumen, leading to reduced receptor-induced calcium release and reduced levels of calcium within the mitochondria (Foyouzi-Youssefi *et al.*, 2000; Pinton *et al.*, 2000). Bcl-x_L can suppress ER stress-induced apoptosis and caspase-12 activation, perhaps by preventing proapoptotic proteins from translocating to the ER and activating caspase-12 (Morishima *et al.*, 2004). The proapoptotic protein Bim was found to translocate to the ER in cells under ER stress, possibly causing the indirect activation of caspase-12, and this leads to apoptosis (Morishima *et al.*, 2004). Bax and Bak can increase the permeability of the ER membrane to calcium, which would increase mitochondrial calcium levels, and oligomerisation of Bax/Bak has been proposed to activate caspase-

12 (McConkey and Orrenius, 1997; Scorrano *et al.*, 2003; Zong *et al.*, 2003). Therefore, the levels of Bcl-2 family members in the ER and mitochondria may determine whether either or both of the ER and mitochondrial pathways are activated during ER stress.

1.2.3 Caspase-independent cell death

The process of apoptosis is characterised by morphological features distinct from that of necrosis. Features of apoptotic cells are shrinkage, plasma membrane blebbing, mostly intact organelles, extensive condensation and fragmentation of the DNA and finally the ordered removal of the cell by phagocytosis (Kerr *et al.*, 1972). Necrotic cells undergo a violent and quick form of degeneration affecting extensive cell populations, characterised by cytoplasm swelling, destruction of organelles and plasma membrane, leading to the release of the cell contents, and an inflammatory response.

It is likely that all nucleated animal cells constitutively express all the proteins required for apoptosis as evidenced by the use of the drug staurosporine. This inhibits protein kinases and causes cells to undergo apoptosis, even in the presence of cycloheximide to inhibit new protein synthesis (Ishizaki *et al.*, 1995; Weil *et al.*, 1996). This is also true for *Drosophila melanogaster* and *C. elegans* (Shaham and Horvitz, 1996; Steller, 1995). The only reported exception is human red blood cells (Weil *et al.*, 1996), which do not contain a nucleus or other organelles. However, it had also been shown that the nucleus is not required for cell death in cells that normally have one, since anucleated cytoplasts are capable of undergoing STS-induced apoptosis (Jacobson *et al.*, 1994). Thus the cell death machinery lies in the cytoplasm of nucleated cells. Although all of the proteins required to execute the programme of cell death seem to be constitutively expressed in animal cells, apoptosis can often be inhibited by inhibitors of transcription and translation indicating that new macromolecular synthesis is required to activate the pre-existing cell death programme (Martin *et al.*, 1988).

The division of cell death into necrosis or apoptosis can be viewed as an oversimplification. In general, necrosis has been attributed to accidental and uncontrolled death, whereas apoptosis presents features of a controlled death programme. Evidence is now available for multiple alternative death pathways, as well

as cross-talk between different intracellular pathways involved in each form of cell death. Recently caspase-independent apoptotic cell deaths have been described, where caspase inhibition fails to block programmed cell death, but apoptotic morphology is still observed (Carmody and Cotter, 2000; Lorenzo et al., 1999; Mathiasen et al., 1999). DNA damage or Bax overexpression can kill cells in the presence of a broad-spectrum caspase inhibitor zVADfmk (McCarthy *et al.*, 1997b; Xiang *et al.*, 1996). The insertion of Bax into the mitochondrial membrane facilitates cytochrome c release (Jurgensmeier *et al.*, 1998), but may also provoke mitochondrial membrane potential loss and matrix swelling, leading to the release of the mitochondrial contents (Marzo *et al.*, 1998b; Narita *et al.*, 1998; Pastorino *et al.*, 1998). Mitochondria release other apoptotic molecules such as the caspase-independent endonuclease G and AIF. Endonuclease G has been implicated in the cleavage of DNA during apoptosis (Li *et al.*, 2001; Parrish *et al.*, 2001). Following apoptotic stimuli, AIF is released from the mitochondria and migrates to the nucleus and participates in the induction of chromatin condensation in a zVADfmk-insensitive manner (Susin *et al.*, 1999).

Certain hallmarks of apoptosis may be triggered by enzymes other than caspases. Cell deaths involving the activation of other proteases, such as calpains (Squier *et al.*, 1994), the proteasome (Hirsch *et al.*, 1998) and serine proteases (Hughes *et al.*, 1998) have been described. The calpains participate in apoptosis in response to hypoxia in hepatocytes (Bronk and Gores, 1993) and in neuronal degeneration (Saito *et al.*, 1993). These are calcium-requiring enzymes and so may be activated in response to increased cytoplasmic calcium levels, for example during mitochondrial damage or ER stress. Calpains have also been reported to cleave the cytoskeletal protein fodrin upstream of caspases, causing the membrane blebbing seen in caspase-independent apoptosis (Waterhouse *et al.*, 1998). The serine proteases have a role in early chromatin cleavage and are activated during apoptosis of thymocytes induced by glucocorticoids (Mann *et al.*, 2000). These proteases participate in a pathway involving the activation of the endonuclease leucocyte elastase inhibitor DNase II, which is also involved in cell death of retinal cells during development (Torriglia *et al.*, 2001). The serine protease Omi/HtrA2 is released from the mitochondria during apoptosis and directly inhibits XIAP function (van Loo *et al.*, 2002), suggesting co-operation between serine proteases and caspases under certain circumstances.

1.3 Neuronal Apoptosis

1.3.1 Neuronal apoptosis during development

Neuronal apoptosis occurs extensively during the normal development of the mammalian nervous system, ensuring that neuronal populations of the correct size are established and inappropriate connections are eliminated. It is estimated that at least half of the original cell population is eliminated by apoptosis during embryonic and early postnatal development (Oppenheim, 1991). Neurons are produced in excess and compete for limiting amounts of survival factors produced by their target cells and those neurons that fail to obtain sufficient neurotrophic support die by apoptosis (Barde, 1989; Cowan *et al.*, 1984; Levi-Montalcini, 1987). Neurons also receive support from glial cells, pre-synaptic cells and steroid hormones (Linden, 1994; Lindsay, 1979; Nordeen *et al.*, 1985; Okado and Oppenheim, 1984). The trophic dependence of the developing neurons also eliminates unwanted or unnecessary neurons, such as in the creation of sexually dimorphic structures during both invertebrate and vertebrate development (Bottjer and Arnold, 1997).

The neurotrophins, NGF, BDNF, NT-3 and NT-4/5 are essential for the development of the vertebrate nervous system, and can promote survival, differentiation, and maintenance of neuronal function in the CNS and in PNS neurons (Lewin and Barde, 1996; Snider, 1994). These proteins bind to the Trk family of receptor tyrosine kinases and the p75 receptor (p75NTR), a TNF receptor superfamily member. For example, NGF acts through TrkA, BDNF and NT-4 through TrkB and NT-3 via TrkC (Chao, 1992). The p75 receptor can bind each of the neurotrophins, but with lower affinity, and can regulate the binding affinity of the Trk receptor for its ligand (Bibel *et al.*, 1999; Dechant and Barde, 1997). For example, NGF and NT-3 can both bind to TrkA, however p75NTR restricts the signalling of TrkA to NGF (Benedetti *et al.*, 1993). The p75NTR forms heteromultimeric complexes with the different Trk receptors and this association increases the affinity of Trks for their ligands. In TrkA-expressing cells, p75NTR enhances NGF signalling through TrkA at non-saturating NGF levels and increases TrkA phosphorylation (Lee *et al.*, 1994; Ryden *et al.*, 1997). However, recent studies also indicate that the binding of NGF to p75NTR in the absence of TrkA may promote cell death rather than prevent it. The p75NTR can mediate cell death in a ligand-dependent manner, as does the structurally

related Fas receptor (Bamji *et al.*, 1998; Casaccia-Bonnefil *et al.*, 1996; Davey and Davies, 1998; Frade and Barde, 1999).

Binding of neurotrophins to Trk receptors results in receptor dimerisation and activation. This kinase activation initially occurs through phosphorylation of conserved tyrosine residues in the autoregulatory loop, leading to further activation of the kinase and subsequent phosphorylation of other tyrosine residues (Barbacid, 1995). Receptor autophosphorylation leads to the recruitment of adaptor proteins, such as SHC, FRS-2 (Kouhara *et al.*, 1997) and SH2B/rAPS (Qian *et al.*, 1998), and triggers the activation of downstream survival signalling cascades, such as the PI3K/Akt and MAPK pathways (section 1.3.4).

1.3.2 Neuronal apoptosis and disease

Neuronal apoptosis has been implicated in a number of diseases, including neurodegeneration and stroke. The study of programmed cell death in neurodegeneration initially focused on *post-mortem* tissues and tended to give conflicting results, probably due to detection difficulty due to a low rate of neuronal loss and the rapid engulfment of apoptotic cells. Also *post-mortem* specimens typically come from advanced stages of the disease when most affected neurons would be lost. More research is now being carried out to assess the molecular components of the apoptosis machinery involved in neurodegeneration and animal models of human neurodegenerative disease have been useful.

Parkinson's disease (PD) is a common neurodegenerative disorder characterised by resting tremor, slowness of movement, rigidity and postural instability. As the disease progresses, many patients develop cognitive dysfunction, including anxiety, depression and dementia (Lang and Lozano, 1998a; Lang and Lozano, 1998b). Symptoms arise due to the loss of dopaminergic neurons in the substantia nigra pars compacta (SNPC). The etiology of PD is not fully understood, but animal models, human *post-mortem* material and genetic analyses have provided important clues (Dawson *et al.*, 2002; Mizuno *et al.*, 2001; Polymeropoulos, 2000). Initial experiments showed TUNEL-positive neurons in the brains of PD patients, supporting the occurrence of apoptosis in the disease (Mochizuki *et al.*, 1996). However, subsequent studies using a greater variety of morphological tools, have either succeeded (Anglade *et al.*, 1997; Tatton *et al.*, 1998; Tompkins *et al.*, 1997) or

failed (Banati *et al.*, 1998; Kosel *et al.*, 1997; Wullner *et al.*, 1999) to find apoptotic neurons in *post-mortem* tissue. Studies using neuronal cell culture systems have shown that oxidative stress generated by toxic metabolites of dopamine or dopamine itself induces apoptosis (Junn and Mouradian, 2001; Masserano *et al.*, 1996; Ziv *et al.*, 1994) and this can be partially inhibited by overexpression of Bcl-2 (Offen *et al.*, 1997; Ziv *et al.*, 1997). In particular, caspase-3 and caspase-9 are activated through p38 MAPK and cytochrome c in SH-SY5Y neuroblastoma cells and JNK activity is increased in striatal cultures following dopamine treatment (Junn and Mouradian, 2001; Luo *et al.*, 1998b).

Significant insights into the pathogenesis of PD have been achieved by the use of the neurotoxin MPTP (1-methyl-4-phenyl-1,2,3,6-tetrahydropyridine). Administration of MPTP reproduces most of the hallmarks of PD, including dramatic degeneration of dopaminergic neurons in mice (Petroske *et al.*, 2001; Przedborski and Jackson-Lewis, 1998). DNA fragmentation is observed in the substantia nigra (SN) and increased c-Jun expression in the nigrostriatum (Nishi, 1997; Tatton and Kish, 1997). The dopaminergic neuron loss and c-Jun activation observed after MPTP treatment can be inhibited by JNK inhibition (Saporito *et al.*, 1999; Xia *et al.*, 2001). In addition, the level of Bax mRNA and protein increases in MPTP-treated mice (Hassouna *et al.*, 1996; Vila *et al.*, 2001) and this may be mediated by p53 (Duan *et al.*, 2002; Trimmer *et al.*, 1996). Bcl-2 levels have also been shown to decrease in the SN following MPTP treatment (Vila *et al.*, 2001). In cell culture models, for example SH-SY5Y cells, MPTP-induced apoptosis may involve p53, *bcl-2* family genes, JNK activation, caspase activity and DNA fragmentation (Kitamura *et al.*, 1998; Xia *et al.*, 2001). Other *in vivo* animal models of PD exist. Hemiparkinsonian rats have been produced by injection of 6-OHDA, a dopamine metabolite, into one side of the ventrotegmental bundle. This leads to apoptotic death of dopaminergic neurons of the SN (He *et al.*, 2000; Zuch *et al.*, 2000), with increased neuronal survival observed if Bcl-2 is overexpressed one week prior to injection (Yamada *et al.*, 1999). Finally, the molecule α-synuclein has been linked to PD, due to its accumulation in Lewy bodies and neurites, and mutations in this gene are associated with familial PD (Olanow and Tatton, 1999; Polymeropoulos *et al.*, 1997). In MPTP-treated animals, α-synuclein accumulates in the cytosol of dopaminergic neurons of the SNPC (Vila *et al.*, 2000). Expression of mutant α-synuclein in cell culture promotes apoptosis and cytochrome c

stimulates the aggregation of α-synuclein *in vitro* (El-Agnaf *et al.*, 1998; Kakimura *et al.*, 2001).

Amyotrophic lateral sclerosis (ALS) is a neurodegenerative disease affecting upper motor neurons in the cerebral cortex and lower motor neurons in the spinal chord. This leads to progressive loss of voluntary muscle function and paralysis, speech and swallowing difficulties and ultimately respiratory failure and death within 2-5 years after onset. Familial cases of the disease are linked to mutations in the superoxide dismutase-1 (SOD1) gene that lead to a decrease in the enzyme activity (Deng *et al.*, 1993; Przedborski *et al.*, 1996). Mice deficient in SOD1 do not develop motor neuron disease (Reaume *et al.*, 1996), however, transgenic expression of different human SOD1 mutations in mice and rats replicates the clinical and pathological hallmarks of ALS (Gurney *et al.*, 1994; Nagai *et al.*, 2001; Wong *et al.*, 1995). This indicates that the cytotoxicity of mutant SOD1 is a gain-of-function effect (Brown, 1995). Transfected neuronal cells expressing mutant SOD1 undergo apoptosis (Ghadge *et al.*, 1997; Rabizadeh *et al.*, 1995), as do primary neurons from transgenic mice expressing mutant SOD1 (Mena *et al.*, 1997). Biochemical studies have implicated the Bcl-2 family in ALS. Decreased expression of *bcl-2* mRNA and increased *dp5* and *bax* mRNA have been reported in *post-mortem* ALS patients and transgenic mice (Ekegren *et al.*, 1999; Martin, 1999; Mena *et al.*, 1997; Shinoe *et al.*, 2001; Vukosavic *et al.*, 1999). In addition, Bax dimerises and translocates to the mitochondria, cytochrome c is released and caspase-9 is activated in transgenic mice expressing mutant SOD1 (Guegan *et al.*, 2001; Martin, 1999) and overexpression of Bcl-2 mitigates neurodegeneration and prolongs survival of these mice (Vukosavic *et al.*, 1999). Inhibition of cytochrome c release delays onset of the disease and increases survival of SOD1 transgenic mice (Zhu *et al.*, 2002) and caspase-3 activation has been reported in the spinal chords of patients with ALS (Martin, 1999), giving further evidence for activation of the mitochondrial pathway during ALS.

Cerebrovascular disease is one of the leading causes of human morbidity and mortality worldwide. The brain is particularly vulnerable to hypoxic-ischaemic injury, for example, that seen focally in stroke or globally after cardiac arrest. Historically cell death after ischaemic injury was considered to be a rapid, necrotic form of death, resulting from excitotoxicity caused by overstimulation of neuronal glutamate receptors (Choi, 1992). Indeed neurons in the most severely affected areas do die

rapidly, however there is also a more gradual loss of neurons outside the stroke's core where the oxygen supply is reduced but not eliminated, or in cases where the ischaemic injury is mild, perhaps during cardiac surgery (Arrowsmith *et al.*, 2000; Barinaga, 1998; Du *et al.*, 1996; Hossmann, 2001; Pulsinelli *et al.*, 1982). The observation that cycloheximide reduced this delayed neuronal death in rats (Goto *et al.*, 1990; Shigeno *et al.*, 1990) and that some cell deaths after ischaemia show DNA fragmentation, TUNEL-labelling and activation of caspases indicated a role for apoptosis in these neurons (Choi, 1996; Li *et al.*, 1995b). Caspase activation has been observed in three different models of ischaemic injury: the middle cerebral artery occlusion (MCAO) model of focal cerebral ischaemia in rats and mice (Friedlander *et al.*, 1997; Hara *et al.*, 1997; Loddick *et al.*, 1996; Namura *et al.*, 1998), the carotid artery occlusion model of transient global ischaemia in adult rats (Chen *et al.*, 1998) and in the model of hypoxic-ischaemic brain injury (H-I) in neonatal rats (Cheng *et al.*, 1998). In the MCAO model of stroke, down-regulation of antiapoptotic Bcl-2 family members, and upregulation of p53, Bax and Fas have all been reported (Hossmann, 2001; Li *et al.*, 1997b; Love, 2003; Matsuyama *et al.*, 1995; Waldmeier, 2003). Bcl-2 overexpression can lead to diminished neuronal cell death and infarct reduction (Howard *et al.*, 2002; Lawrence *et al.*, 1997; Martinou *et al.*, 1994). Bcl-2 deficient mice show increased infarct size and more severe neurological deficits following transient MCAO, compared with heterozygote and wild-type littermates (Hata *et al.*, 1999). Bax deficient animals exhibit significantly decreased caspase-3 activation and infarct volume as compared to wild-type littermates in the neonatal hypoxic-ischaemic model (Gibson *et al.*, 2001). The JNK signalling pathway has been implicated in ischaemic apoptosis (Irving and Bamford, 2002) and targeted deletion of the JNK isoform *Jnk3*, which is selectively expressed in the nervous system and heart (Gupta *et al.*, 1996; Kuan *et al.*, 1999), reduces the stress-induced JNK activity and protects mice from brain injury after cerebral ischaemia-hypoxia (Kuan *et al.*, 2003).

1.3.3 *In vitro* models of neuronal apoptosis

1.3.3.1 Sympathetic neurons

Sympathetic neurons, which form part of the peripheral nervous system, have proved to be a useful *in vitro* model for studying neuronal apoptosis mechanisms. During development these neurons depend on NGF from approximately embryonic

day 16 to 1 week postnatally and deprivation of NGF during this time causes apoptosis both *in vivo* and *in vitro* (Coughlin and Collins, 1985; Levi-Montalcini, 1987; Wright *et al.*, 1983). Deletion of the gene for NGF or its receptor TrkA results in extensive neuron loss *in vivo* (Crowley *et al.*, 1994; Smeyne *et al.*, 1994). Sympathetic neurons can be isolated from the superior cervical ganglia of one-day-old rats and cultured *in vitro* in the presence of NGF. Removal of NGF from the growth medium results in a cell death with the classic features of apoptosis. This cell death in culture is representative of the physiological cell death in which neurons are deprived of NGF *in vivo*. The period between postnatal days 3 and 7 is the major time of developmental death for sympathetic neurons, when approximately one third of these neurons die 24-48 hours later (Wright *et al.*, 1983). The NGF withdrawal-induced death of sympathetic neurons requires *de novo* transcription and translation (Martin *et al.*, 1988) that ultimately leads to cytochrome c release from the mitochondria and caspase activation (Deshmukh and Johnson, 1998; Neame *et al.*, 1998).

Sympathetic neurons undergoing apoptosis following NGF withdrawal, do not exhibit any morphological changes until 12 hours after NGF deprivation *in vitro*. After this time, neurites begin to degenerate, the plasma membrane loses its smooth appearance and cells begin to shrink, with half the neurons atrophied by 24-36 hours. After 48 hours of NGF withdrawal, at least 95% of the neurons are dead (Deckwerth and Johnson, 1993; Edwards and Tolkovsky, 1994; Martin *et al.*, 1988). Neurons can be rescued from cell death by the re-addition of NGF to cultured cells, before they are irreversibly committed to die. The cell death commitment point for sympathetic neurons is defined as, the time after NGF deprivation when half the neuron population can no longer be rescued by NGF re-addition. This is around 22 hours for sympathetic neurons (Deckwerth and Johnson, 1993).

1.3.3.2 PC12/PC6-3 cell line

Clonal cell lines that express neuronal properties are useful *in vitro* model systems for studying the nervous system. The PC12 cell line was derived from a transplantable rat adrenal pheochromocytoma (Greene and Tischler, 1976). Chromaffin granule-containing cells from this tumour were found to respond to NGF by exiting the cell cycle and extending long, branching neurite-like processes (Tischler and Greene, 1975). These cells develop a phenotype similar to that of sympathetic

neurons if differentiated in the presence of NGF, and then die by apoptosis after NGF withdrawal (Mesner *et al.*, 1992; Rukenstein *et al.*, 1991). In addition, PC12 cells display many of the biochemical changes characteristic of sympathetic neurons after NGF withdrawal and this NGF withdrawal-induced death of PC12 cells requires *de novo* transcription and translation (Mesner *et al.*, 1992). PC6-3 cells are a sub-clone of PC12 cells, isolated due to their increased sensitivity to NGF removal (Pittman *et al.*, 1993). After 14 days in the presence of NGF, PC6-3 cells have a very well developed neuronal morphology. Following the removal of NGF, the first morphological signs of cell death at the light microscopic level occur after about 16 hours and involve the thinning and beading of the neurites. By 20 hr after removal of NGF, a number of neurites have been lost and some of the cell bodies are beginning to degenerate. After 24-30 hours of NGF withdrawal, extensive loss of neurites occurs and cellular degeneration is obvious. Apoptosis of this PC6-3 sub-clone also requires *de novo* transcription and translation.

1.3.4 Survival pathways

The binding of trophic factors to their receptors elicits a variety of signalling responses, depending on the receptor and the cell type (Kaplan and Miller, 1997). The two pathways that have been implicated the most in neuronal survival are the phosphatidylinositol-3-OH kinase (PI3K) and mitogen-activated protein kinase (MAPK) pathways.

1.3.4.1 PI3K pathway

The PI3K signalling pathway is activated by many types of cellular stimuli or toxic insults and regulates fundamental cellular functions such as transcription, translation, proliferation, growth, and survival (Datta *et al.*, 1999; Vivanco and Sawyers, 2002). Survival signals generally activate intracellular signalling pathways by binding to transmembrane receptors which posses intrinsic tyrosine kinase activity, or that are indirectly coupled to tyrosine kinases, or to G-protein coupled receptors (Clark and Brugge, 1995; Segal and Greenberg, 1996; Weiner and Chun, 1999).

In neurons, trophic factors bind to Trk receptors causing their dimerisation and activation through autophosphorylation, leading to the recruitment of adaptor molecules at the plasma membrane. Trk receptors can activate PI3K through at least

two distinct pathways, which are different in different neurons. PI3K enzymes are normally present in the cytosol and can be directly activated by either recruitment to an activated Trk receptor, or indirectly through activated Ras. These active PI3K enzymes catalyse the formation of the lipid 3'-phosphorylated phosphoinositides, for example PIP_2 and PIP_3, which regulate the localisation and activity of key components in cell survival, including Akt/protein kinase B and 3-phosphoinositide-dependent kinases (PDKs). Akt is recruited to the plasma membrane through the interaction of its pleckstrin-homology domain with the phospholipid products of PI3K. Akt is activated through phosphorylation by PDKs and then in turn it phosphorylates substrates involved in promoting survival of the cells. Signalling through Ras can also activate the PI3K-Akt pathway. Recruitment of the adaptor Grb-2 via Shc recruitment and phosphorylation leads to activation of the Ras exchange factor SOS. This in turn activates Ras which then activates PI3K.

PI3K was first implicated in the suppression of apoptosis in a study by Yao and Cooper (Yao and Cooper, 1995) in which the signal transduction pathways that control growth factor-mediated survival of the PC12 cell line were investigated. This study demonstrated that inhibition of PI3K activity abrogated the ability of NGF to promote cell survival. Since then, the PI3K pathway has been implicated in the survival of many neuronal cell types, including sympathetic neurons (Crowder and Freeman, 1998; Miller *et al.*, 1997; Philpott *et al.*, 1997). Active Akt protein supports the survival of neurons in the absence of trophic factor support, whereas dominant-negative mutants of Akt inhibit neuronal survival even in the presence of survival factors (Datta *et al.*, 1999).

Akt targets several key proteins to keep neurons alive. Activation of Akt induces the phosphorylation of the proapoptotic BH3-only protein Bad and promotes its interaction with the chaperone protein 14-3-3. This sequesters Bad in the cytoplasm thus preventing its proapoptotic activity, the binding and inhibition of Bcl-x_L (Datta *et al.*, 1997; Yang *et al.*, 1995). The Forkhead box transcription factor, class O (FOXO) subfamily of Forkhead transcriptional regulators (FKHR, FKHRL1 and AFX), are directly controlled by phosphorylation by Akt (Biggs *et al.*, 1999; Brunet *et al.*, 1999; Kops *et al.*, 1999). The phosphorylated FOXO transcription factors are bound by 14-3-3 and retained in the cytoplasm, away from their target genes. The gene encoding the BH3-only protein Bim is a direct target of FKHRL1 in sympathetic neurons deprived

of NGF, and inhibition of FOXO activity can protect against this death (Gilley *et al.*, 2003). Akt has also been reported to regulate CREB and NF-κB transcription through phosphorylation of CREB or IκB kinase, resulting in the stimulation of survival pathways (Du and Montminy, 1998; Kane *et al.*, 1999; Riccio *et al.*, 1999). In sympathetic neurons, CREB mutants block NGF-induced survival and CREB may act through transcriptional activation of *bcl-2* (Riccio *et al.*, 1999).

1.3.4.2 MAPK pathway

Neurotrophins stimulate the docking of the adaptor protein Shc to activated Trk receptors at the plasma membrane, triggering the recruitment and activation of the small GTP-binding protein Ras, and the activation of the downstream mitogen-activated protein kinase (MAPK) signalling cascade, the Raf/ERK pathway or PI3K (Bonni *et al.*, 1999). Ras regulates neuronal differentiation, but also promotes survival. In PC12 cells, addition of NGF leads to activation of the Ras-Raf pathway and phosphorylation of extracellular signal-regulated kinase (ERK), leading to differentiation and prevents apoptosis induced by NGF withdrawal (Kaplan and Miller, 1997; Xia *et al.*, 1995). However, ERK activation is not necessary for the survival-promoting effects of NGF on sympathetic neurons (Creedon *et al.*, 1996; Virdee *et al.*, 1997). The effect of the MAP kinase pathway on survival of cerebellar granule neurons is mediated at least in part by the activation of the pp90 ribosomal S6 kinase (RSK) family members. These phosphorylate the BH3-only protein Bad and can activate the transcription factor CREB and thereby increase expression of Bcl-2 (Bonni *et al.*, 1999; Riccio *et al.*, 1999).

1.3.5 Apoptosis of sympathetic neurons

Removal of NGF from its receptors on the plasma membrane triggers a downstream signalling cascade (see Figure 1.3) involving the JNK/c-Jun pathway that leads to Bax translocation, cytochrome c release from the mitochondria and caspase activation (Deshmukh and Johnson, 1998; Neame *et al.*, 1998; Putcha *et al.*, 1999).

1.3.5.1 JNK/c-Jun pathway

The involvement of the c-Jun N-terminal kinase (JNK) / stress activated protein kinase (SAPK) pathway in apoptosis has been much studied. JNK proteins are

phosphorylated and activated in response to apoptotic stimuli such as TNF, DNA damage, heat shock, ischaemia-reperfusion, oxidative stress, axonal injury and loss of trophic support (Herdegen and Waetzig, 2001; Ip and Davis, 1998; Kyriakis and Avruch, 1996; Maroney *et al.*, 1999; Raingeaud *et al.*, 1995; Xia *et al.*, 1995). These kinases are activated by exposure of cells to stress, with the specific roles dependent upon the cellular context. Indeed, the JNK pathway has been implicated in both apoptosis and survival signalling (Davis, 2000; Ip and Davis, 1998).

The removal of NGF from sympathetic neurons leads to a slow and sustained increase in JNK activity (Eilers *et al.*, 1998; Virdee *et al.*, 1997). This JNK activity is necessary for c-Jun phosphorylation, *c-jun* promoter activation and NGF withdrawal-induced death (Eilers *et al.*, 2001). There are three mammalian *Jnk* genes, *Jnk1*, *Jnk2* and *Jnk3*, which encode different JNK isoforms with different substrate specificities and activities in response to different stimuli (Gupta *et al.*, 1996). JNK1 and JNK2 are ubiquitously expressed, whereas JNK3 is selectively expressed in the brain, and to a lesser extent in the heart and testes (Kuan *et al.*, 1999; Martin *et al.*, 1996). Mice deficient in *Jnk3* do not have any obvious abnormal phenotype and these animals are born normally. Hippocampal neurons from these animals are protected from kainate-induced excitotoxicity, consistent with an involvement of c-Jun induction and transcriptional activity in this neurotoxic response (Yang *et al.*, 1997b). A similar result was observed in mice with mutations in the c-*jun* gene that replaced the JNK phosphorylation sites at serines 63 and 73 with alanine residues (Behrens *et al.*, 1999). Sympathetic neurons from *Jnk3*$^{-/-}$ mice are more resistant to NGF withdrawal induced death than heterozygous littermate controls (Bruckner *et al.*, 2001). In these neurons, *Jnk3* deficiency leads to decreased *c-jun* induction and c-Jun phosphorylation following NGF deprivation. *Jnk1*$^{-/-}$ and *Jnk2*$^{-/-}$ mice are viable, but are immunodeficient due to altered T-cell differentiation (Constant *et al.*, 2000; Dong *et al.*, 1998; Yang *et al.*, 1998a). *Jnk1*$^{-/-}$ mice have compromised neuronal microtubule assembly (Chang *et al.*, 2003) and are protected from obesity-induced insulin resistance (Hirosumi *et al.*, 2002). *Jnk2*$^{-/-}$ mice have decreased induction of interferon-α1 and -β transcription following infection (Chu *et al.*, 1999) and show moderately decreased joint damage in a model of passive collagen-induced arthritis (Han *et al.*, 2002). Double knockout mice for both *Jnk1* and *Jnk2* die during embryogenesis due to increased apoptosis in the forebrain and decreased apoptosis in the lateral edges of the hindbrain prior to

neural tube closure (Kuan *et al.*, 1999). This would indicate both proapoptotic and antiapoptotic roles for JNK1 and JNK2 during development of the brain. Embryonic fibroblasts from *Jnk1*$^{-/-}$ *Jnk2*$^{-/-}$ double knockout mice lack expression of all JNK protein and JNK activity, reflecting the neuronal-specific expression pattern of the *Jnk3* gene (Tournier *et al.*, 2000). These cells show profound defects in stress-induced apoptosis, for example in response to UV radiation, but showed no defects in Fas-induced apoptosis. The absence of JNK caused a defect in the mitochondrial death signaling pathway, including the failure to release cytochrome c and activate caspase-3, indicating that mitochondria are influenced by proapoptotic signal transduction through the JNK pathway (section 1.3.5.3).

Several upstream components of the JNK/c-Jun pathway have been identified in sympathetic neurons (see Figure 1.3). The most distal of these are the Rho small GTPase family members Rac1 and Cdc42. Activated mutants of Cdc42 and Rac1 induce apoptosis of sympathetic neurons, by activating the c-Jun transcriptional pathway, and Cdc42 is required for NGF withdrawal-induced death (Bazenet *et al.*, 1998). Conversely, dominant negative mutants of these GTPases prevent elevation of c-Jun and death by NGF-withdrawal in sympathetic neurons. Cdc42-induced death and *c-jun* activation were blocked by inhibition of apoptosis signal-regulated kinase 1 (ASK1), suggesting that ASK1 is downstream of Cdc42 in the signalling pathway (Kanamoto *et al.*, 2000). ASK1 is activated after NGF withdrawal in sympathetic neurons. In sympathetic neurons, JNK and c-Jun activation and NGF withdrawal-induced death, can be inhibited by a kinase-inactive mutant of ASK1. Overexpression of ASK1-ΔN, a constitutively active mutant of ASK1, activated JNK, and induced apoptosis in both neuronally differentiated PC12 cells and sympathetic neurons.

Several other MAPKKK have been reported to activate the JNK signalling cascade, such as the MEKK proteins and the mixed-lineage kinases (MLKs). MEKK1 activates SEK1/MKK4 which in turn can phosphorylate JNK (Yan *et al.*, 1994). Overexpression of MEKK1 in sympathetic neurons increases c-Jun levels and c-Jun phosphorylation and induces apoptosis in the presence of NGF (Eilers *et al.*, 1998). These effects were prevented by co-expression of SEK*AL*, a SEK1/MKK4 dominant negative mutant, indicating that MEKK1 acts by activating MKK4 to induce apoptosis in these cells. However, overexpression of SEK*AL* in sympathetic neurons did not block induction of c-Jun protein, c-Jun phosphorylation or apoptosis after

Figure 1.3 Signalling events upstream of cytochrome c release in sympathetic neurons undergoing NGF withdrawal-induced apoptosis

Several components of the JNK/c-Jun pathway have been identified in sympathetic neurons. The Rho small GTPase family members Rac1 and Cdc42 activate the c-Jun transcriptional pathway, and Cdc42 is required for NGF withdrawal-induced death. Cdc42-induced death and *c-jun* activation were blocked by inhibition of ASK1, and ASK1 is activated after NGF withdrawal in sympathetic neurons. This suggests that ASK1 is downstream of Cdc42 in the signalling pathway. In sympathetic neurons, overexpression of MEKK1 increases c-Jun levels and c-Jun phosphorylation and induces apoptosis in the presence of NGF. These effects were prevented by co-expression of SEK*AL*, a SEK1/MKK4 dominant negative mutant, suggesting that MEKK1 acts by activating MKK4 to induce apoptosis in these cells. However, overexpression of SEK*AL* in sympathetic neurons did not block induction of c-Jun protein, c-Jun phosphorylation or apoptosis after NGF withdrawal, which suggests the presence of an MKK4-independent pathway. MLK proteins can function as MAPKKKs and lead to the activation of JNKs via activation of MAPK kinases, such as MKK4/MKK7. In sympathetic neurons, overexpression of MLK family members induced cell death via the JNK pathway and expression of dominant negative MLKs protected these cells from NGF-withdrawal induced death. MLKs been shown to act downstream of Cdc42 and upstream of MKK4 and MKK7 in the JNK pathway. JNK proteins are activated by MKK4 and MKK7, which phosphorylate JNK on specific threonine and tyrosine residues. The removal of NGF from sympathetic neurons leads to a slow and sustained increase in JNK activity. This JNK activity is necessary for c-Jun phosphorylation, *c-jun* promoter activation and NGF withdrawal-induced death. JNKs bind to the transactivation domain and phosphorylate c-Jun on serines 63 and 73, increasing the transcriptional activity of the protein. c-Jun activates transcription via AP-1 DNA binding sites present in the promoters of target genes and also in *c-jun* itself. In sympathetic neurons, expression of dominant negative c-Jun (FLAGΔ169) protects the neurons from NGF withdrawal-induced death by preventing cytochrome c release from the mitochondria, indicating that c-Jun functions upstream of the mitochondria in sympathetic neurons.

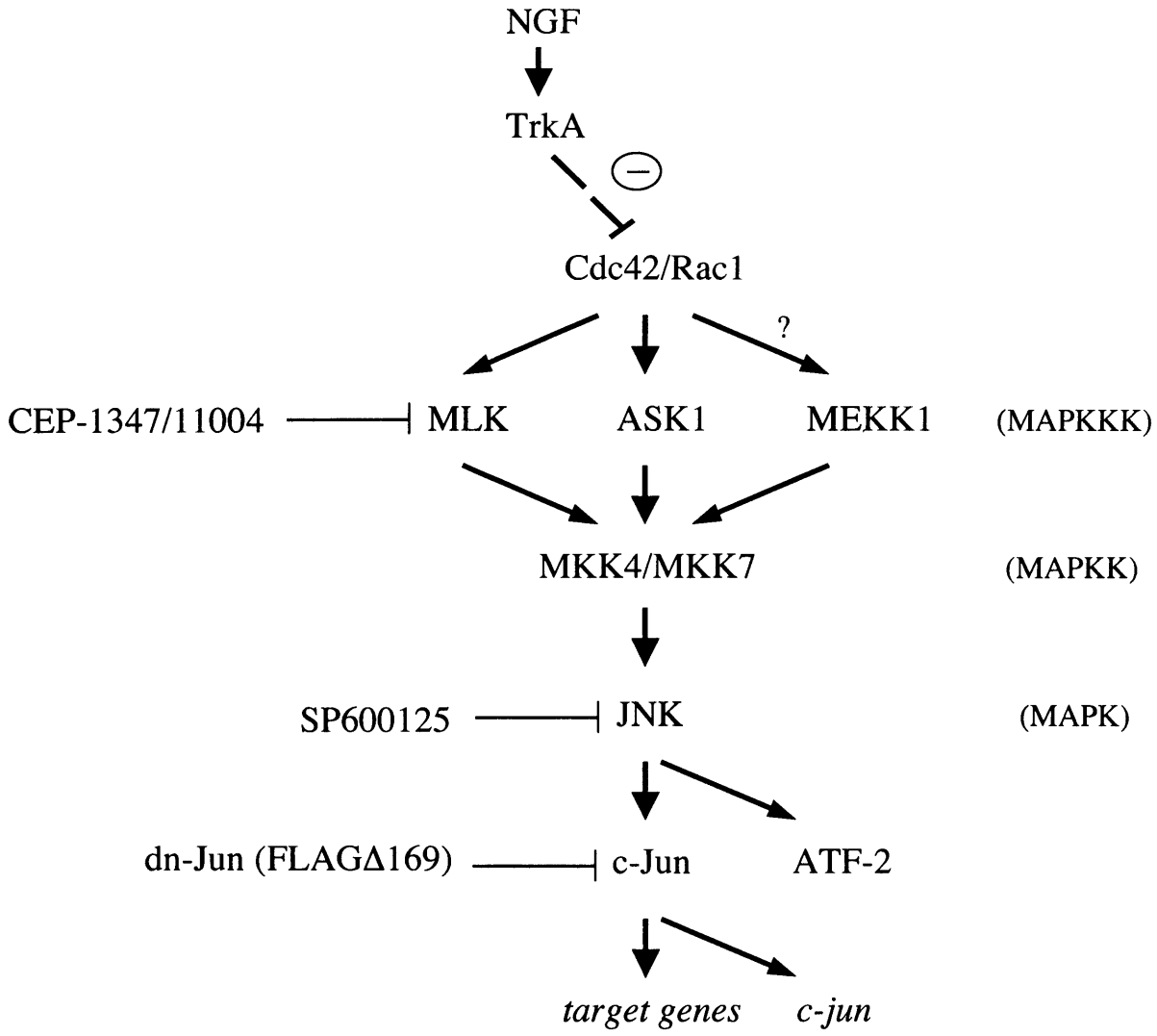
NGF
TrkA
Cdc42/Rac1
?
CEP-1347/11004
MLK
ASK1
MEKK1
(MAPKKK)
MKK4/MKK7
(MAPKK)
SP600125
JNK
(MAPK)
dn-Jun (FLAGΔ169)
c-Jun
ATF-2
target genes
c-jun

NGF withdrawal, which suggests the presence of a SEK1-independent pathway, perhaps through ASK1 or the MLKs.

The MLK proteins represent an additional protein kinase family with the potential to be involved in the JNK activation pathway. These proteins can function as MAPKKKs and lead to the activation of JNKs via activation of MAPK kinases, such as MKK4 (Bock *et al.*, 2000; Cuenda and Dorow, 1998; Hirai *et al.*, 1997; Tibbles *et al.*, 1996). In sympathetic neurons and neuronally differentiated PC12 cells, overexpression of MLK family members induced cell death via the JNK pathway and expression of dominant negative MLKs protected these cells from NGF-withdrawal induced death (Xu *et al.*, 2001). MLKs been shown to act downstream of Cdc42 and upstream of MKK4 and MKK7 in the JNK pathway and are thought to be the direct targets of the semisynthetic JNK pathway inhibitor CEP-1347 (Maroney *et al.*, 2001). This inhibitor protects sympathetic neurons and neuronally differentiated PC12 cells against death induced by NGF-withdrawal, exposure to UV radiation or oxidative stress (Maroney *et al.*, 1999). In NGF-deprived sympathetic neurons, CEP-1347 blocks the release of cytochrome c and maintains the metabolic function and growth of the neurons (Harris *et al.*, 2002). The trophic effects of CEP-1347 might be mediated through the PI3K survival pathway. Recent studies have shown that CEP-1347 activates Akt and ERK and a blockade of PI3K or MEK activity ablates the effect of CEP-1347 on cell survival (Roux *et al.*, 2002). In addition, the CEP-1347 related compound, CEP-11004, has been found to induce an increase in the mRNA and protein levels of TrkA, the NGF receptor, resulting in ligand-independent activation of the TrkA receptor and the downstream PI3K pathway, in sympathetic neurons (Wang *et al.*, 2005). Therefore the neuroprotective and neurotrophic effects of CEP-1347 may involve the activation of several signaling pathways. The JNK/c-Jun pathway can also be inhibited with the JNK inhibitor SP600125. This acts as a reversible ATP-competitive inhibitor against JNK1, JNK2 and JNK3 (Bennett *et al.*, 2001).

The JNKs are activated by the dual specificity MAPK kinases, MKK4 and MKK7, which phosphorylate JNK on specific threonine and tyrosine residues (Derijard *et al.*, 1995; Lawler *et al.*, 1998; Lin *et al.*, 1995; Tournier *et al.*, 1997). Disruption of the genes for MKK4 and MKK7 results in embryonic death (Dong et al., 2000; Ganiatsas et al., 1998; Nishina et al., 1999; Swat et al., 1998; Yang et al.,

1997a). The death of *Mkk4*$^{-/-}$ embryos appears to be due to liver apoptosis and this phenotype is similar to that observed for *c-jun*$^{-/-}$ embryos (Hilberg *et al.*, 1993).

JNK proteins bind to the transactivation domain and phosphorylate c-Jun on serines 63 and 73 (Hibi *et al.*, 1993; Ip and Davis, 1998; Karin *et al.*, 1997). This increases the transcriptional activity of the protein. The c-Jun transcription factor acts via AP-1 DNA binding sites present in the promoters of target genes and also in *c-jun* itself (Angel *et al.*, 1988). c-Jun binds to DNA as homodimers or as heterodimers with other basic/leucine zipper transcription factors, such as Jun D and activating transcription factor 2 (ATF-2), to regulate gene expression (Deng and Karin, 1993; Hai and Curran, 1991). ATF-2 is also a target for JNK phosphorylation (Gupta *et al.*, 1995; van Dam *et al.*, 1995).

1.3.5.2 c-Jun

The transcription factor c-Jun is a member of the AP-1 family. AP-1 was one of the first transcription factors to be identified and controls a wide range of cellular processes, including cell proliferation, death, survival and differentiation (Angel and Karin, 1991; Maki *et al.*, 1987; Vogt and Bos, 1990). AP-1 is a dimer made up of basic/leucine zipper (bZIP) proteins of the Jun, Fos and ATF subfamilies, which recognise either TPA response elements (TRE) or cAMP response elements (CRE) in DNA (Karin *et al.*, 1997). c-Jun is a potent activator of transcription and its level of expression and transcriptional activity are controlled by the MAPK family of proteins, in particular JNK (Karin, 1995). Phosphorylation of c-Jun increases its ability to activate target genes, such as *cyclin D1, FasL* and *c-jun* itself (Angel *et al.*, 1988; Schreiber *et al.*, 1999; Shaulian and Karin, 2001; Whitfield *et al.*, 2001).

Sympathetic neurons express several members of the AP-1 family: c-Jun, JunB, JunD, Fra-1 and ATF-2 (Ham *et al.*, 1995). The levels of c-Jun protein, c-Jun N-terminal phosphorylation and *c-jun* promoter activity increase after NGF withdrawal and this requires JNK activity (Eilers *et al.*, 2001; Estus *et al.*, 1994; Ham *et al.*, 1995). *c-jun* promoter activation following NGF withdrawal requires the jun1 and jun2 TRE elements, which are DNA binding sites for c-Jun/ATF-2 heterodimers (Eilers *et al.*, 1998). *c-jun* knockout mice die during embryonic development at day 12.5 due to hepatic failure (Hilberg *et al.*, 1993). To study the role of c-Jun in neurons, a floxed *c-jun* gene has been successfully knocked out in sympathetic neurons *in vitro* (infected

with a CRE adenovirus) and this inhibited NGF withdrawal-induced death (Palmada *et al*, 2002). Microinjection of sympathetic neurons with a dominant negative c-Jun (FLAGΔ169) or antibodies specific for c-Jun, protects sympathetic neurons from NGF withdrawal-induced death (Ham *et al.*, 1995). FLAGΔ169 lacks the N-terminal 168 amino acids encoding the transactivation domain, but can still dimerise and bind DNA via the bZIP domain (Hirai *et al.*, 1989) and acts as a dominant negative mutant against AP-1 family members (Brown *et al.*, 1994; Castellazzi *et al.*, 1991). Expression of dominant negative c-Jun also inhibits apoptosis in differentiated PC12 cells and cerebellar granule neurons following survival factor withdrawal (Watson *et al.*, 1998; Xia *et al.*, 1995).

c-Jun has also been implicated in axonal regeneration in adult peripheral and central nervous system neurons that have been axotomised (Dragunow, 1992; Herdegen *et al.*, 1998; Herdegen and Waetzig, 2001). A recent study using mice with a conditional knockout of c-Jun in neural cells (*c-Jun*$^{\Delta N}$), showed that CNS-specific inactivation of *c-jun* caused severe defects in the axonal response, leading to impaired target reinnervation (Raivich *et al.*, 2004). These c-Jun-deficient motoneurons were resistant to axotomy-induced cell death, supporting a role for c-Jun in both neuronal apoptosis and axonal regeneration. The transcription factor ATF-3 is also up-regulated in response to axotomy with a similar expression pattern to c-Jun (Takeda *et al.*, 2000; Tsujino *et al.*, 2000). Expression of ATF-3 enhances c-Jun-mediated neurite sprouting in PC12 cells (Pearson *et al.*, 2003) and suggests that expression of these proteins following axotomy represents an attempt by an injured cell to activate an axonal regeneration response.

1.3.5.3 Mechanism of JNK-dependent neuronal apoptosis

JNK activation is known to be required for the stress-induced mitochondrial death pathway (Tournier *et al.*, 2000). In sympathetic neurons, expression of dominant negative c-Jun (FLAGΔ169) protects the neurons from NGF withdrawal-induced death by preventing cytochrome c release from the mitochondria, suggesting that c-Jun functions upstream of the mitochondria in sympathetic neurons (Whitfield *et al.*, 2001). Cytochrome c release is required for this NGF-withdrawal-induced death (Neame *et al.*, 1998). The release of cytochrome c occurs before caspase function and requires Bax translocation and new protein synthesis (Deshmukh and Johnson, 1998;

Putcha *et al.*, 1999). However, microinjection of purified cytochrome c on its own is insufficient to induce cell death in NGF-maintained sympathetic neurons, but does induce death in Bax deficient or cycloheximide-treated neurons deprived of NGF. This suggests that these neurons require the induction of other simultaneous events that occur after NGF withdrawal, to become competent-to-die in response to cytochrome c injection. This is now thought to be a decrease in the level of XIAP after NGF withdrawal (see later).

Bax is essential for sympathetic neuron apoptosis (Deckwerth *et al.*, 1996). *Bax*$^{-/-}$ sympathetic neurons are independent of NGF for survival and do not die after NGF withdrawal. Overexpression of Bax kills sympathetic neurons in the presence of NGF and increases the rate of cell death following NGF withdrawal, an effect that was blocked by co-expression of Bcl-x_L or caspase inhibition (Vekrellis *et al.*, 1997). Bcl-x_L can inhibit sympathetic neuronal apoptosis after NGF withdrawal (Gonzalez-Garcia *et al.*, 1995), although levels of Bcl-x_L remain relatively constant during sympathetic neuron apoptosis (Aloyz *et al.*, 1998; Whitfield *et al.*, 2001). The targeted disruption of the *bax* gene protected against Bcl-x_L deficiency-induced neuronal death, suggesting that these proteins act within the same cell death pathway in neurons (Shindler *et al.*, 1997).

In sympathetic neurons, overexpression of the antiapoptotic protein Bcl-2 inhibits apoptosis and sympathetic neurons from one-day-old *bcl-2*$^{-/-}$ mice undergo apoptosis more rapidly than neurons from control littermates after NGF deprivation in culture (Garcia *et al.*, 1992; Greenlund *et al.*, 1995). Bcl-2 protects against NGF-withdrawal induced death by preventing cytochrome c release from the mitochondria and caspase activation (Putcha *et al.*, 1999). However, overexpression of Bcl-2 does not block the increase in c-Jun protein level that occurs after NGF withdrawal, suggesting that c-Jun acts upstream of Bcl-2 (Ham *et al.*, 1995).

BH3-only proteins such as Bad, Bim, Bid and DP5 are proapoptotic and may directly dimerise with Bcl-2 or Bcl-x_L to inhibit their action (O'Connor *et al.*, 1998; Ottilie *et al.*, 1997; Yang *et al.*, 1995). In sympathetic neurons, Bim is induced by NGF withdrawal and experiments with neurons isolated from *bim*$^{-/-}$ mice indicate that Bim is required for normal NGF withdrawal-induced death (Putcha *et al.*, 2001; Whitfield *et al.*, 2001). On the other hand the levels of the Bid and Bad proteins do not change and these proteins are not essential for death after NGF deprivation (Putcha *et*

al., 2002). DP5 RNA and protein levels also increase in sympathetic neurons following NGF withdrawal and overexpression of DP5 leads to increased neuronal apoptosis in the presence of NGF (Imaizumi *et al.*, 1997). This cell death induced by DP5 is inhibited by co-expression of Bcl-2. DP5 can interact with Bcl-x_L during cortical neuronal apoptosis following exposure to amyloid beta protein and may inhibit the survival activity of Bcl-x_L (Imaizumi *et al.*, 1999). Sympathetic neurons from *dp5*$^{-/-}$ mice show a small delay in NGF withdrawal induced death *in vitro* (Imaizumi *et al.*, 2004). However, motoneurons from *dp5*$^{-/-}$ mice were resistant to cell death induced by axotomy, indicating that DP5 plays an important role in this form of neuronal cell death.

The induction of DP5 and Bim in sympathetic neurons is partially dependent on JNK signalling. The MLK inhibitor CEP-1347, which inhibits JNK activation, reduced the induction of DP5 and Bim in sympathetic neurons following NGF withdrawal (Harris and Johnson, 2001). This is consistent with the findings of Whitfield *et al.* (2001) who reported that Bim induction is decreased in NGF-deprived sympathetic neurons that express dominant negative c-Jun (Whitfield *et al.*, 2001). *Bim*$^{-/-}$ neurons deprived of NGF still show increased c-Jun phosphorylation but have delayed cytochrome c release, again indicating that Bim acts somewhere between c-Jun activation and mitochondrial cytochrome c release (Putcha *et al.*, 2001).

The *bim* gene is a target for FKHRL1 in sympathetic neurons deprived of NGF, and inhibition of FOXO activity can protect against this death (Gilley *et al.*, 2003). In the presence of NGF, FKHRL1 is phosphorylated in a PI3K-Akt dependent manner and localised in the cytoplasm. However, in the absence of NGF, FKHRL1 is dephosphorylated, becomes localised to the nucleus and activates *bim* gene expression. Inhibition of the PI3K pathway and activation of the JNK pathway seem to both contribute to the induction of Bim in sympathetic neurons. Bim can also be regulated by phosphorylation. NGF reduces Bim protein levels and increases Bim phosphorylation in an ERK-dependent manner in neuronally differentiated PC12 cells, leading to a suppression of its proapoptotic activity (Biswas and Greene, 2002). In serum-stimulated fibroblasts, ERK-mediated phosphorylation of Bim at serine 65 leads to a substantial increase in the turnover of the protein via the ubiquitin-proteasome pathway (Ley et al., 2003; Ley et al., 2004). However, in the case of sympathetic and cerebellar granule neurons it has been reported that, following

survival factor withdrawal, Bim is phosphorylated by JNK at serine 65 and this potentiates the proapoptotic activity of Bim in these cells by an as yet unknown mechanism (Becker *et al.*, 2004; Putcha *et al.*, 2003).

Neuronal cells undergoing apoptosis release cytochrome c, which leads to apoptosome formation and caspase activation. Treatment of sympathetic neurons with caspase inhibitors, such as the cell-permeable, pan-caspase inhibitor BOC-aspartyl(OMe)-fluoromethylketone (BAF), or expression of the baculovirus p35 protein, reduces the death of these cells *in vitro* (Deshmukh *et al.*, 1996; Martinou *et al.*, 1995; McCarthy *et al.*, 1997a). Caspase activity increases in neuronal PC12 cells (Stefanis *et al.*, 1996) and sympathetic neurons (Deshmukh *et al.*, 1996), deprived of NGF. The effector caspases in PC12 cells appear to be caspase-2 and -3, whereas in sympathetic neurons only caspase-2 has been reported to be activated (Deshmukh *et al.*, 1996; Haviv *et al.*, 1998; Stefanis *et al.*, 1997; Troy *et al.*, 1997). Sympathetic neurons cultured from caspase-2 null mice, however, still retain their sensitivity to NGF deprivation (Bergeron *et al.*, 1998), perhaps due to a developmental compensation by other caspases (Troy et al., 2001). Caspase-9 knockout mice die due to deficits in the central nervous system, reflecting the failure of apoptosis during neural development (Hakem *et al.*, 1998; Kuida *et al.*, 1998) and sympathetic neurons isolated from caspase-9-null embryos have a delay in NGF withdrawal-induced death (Deshmukh *et al.*, 2000). The importance of the mitochondria and caspase activation in sympathetic neuron apoptosis is also supported by the involvement of SMAC and IAP. SMAC binds to and inactivates IAP proteins, a group of polypeptides that inhibit caspase activation. Expression of exogenous SMAC induces apoptosis in sympathetic neurons (Deshmukh *et al.*, 2002), whereas the overexpression of IAPs block apoptosis in sympathetic neurons deprived of NGF (Wiese *et al.*, 1999; Yu *et al.*, 2003). A decrease in XIAP expression seems to be a critical event that induces competence-to-die in these cells. Sympathetic neurons maintained in NGF are resistant to injection of cytochrome c, in contrast to XIAP-deficient neurons, which die rapidly with cytosolic cytochrome c alone (Potts *et al.*, 2003). In addition, XIAP levels decrease after NGF withdrawal in competent neurons. This indicates that the removal of XIAP inhibition is both necessary and sufficient for cytochrome c to activate caspases in sympathetic neurons.

1.4 Aims of the thesis

The JNK/c-Jun pathway promotes apoptosis in sympathetic neurons deprived of NGF, but little is known about the transcriptional targets of this pathway. The aim of this study was to use Affymetrix GeneChip® arrays to identify genes involved in neuronal apoptosis after NGF withdrawal. Differentiated PC6-3 cells deprived of NGF were used as a model of neuronal apoptosis, to generate sufficient RNA for the Affymetrix analysis.

One of the regulated genes identified by microarray analysis, ATF-3, was studied further in PC6-3 cells and sympathetic neurons. ATF-3 RNA and protein levels were found to increase after NGF withdrawal in both PC6-3 cells and sympathetic neurons. Regulation of ATF-3 expression by the MLK/JNK pathway was investigated using chemical inhibitors of MLK and JNK activity and the role of ATF-3 in sympathetic neurons was studied in microinjection experiments.

Chapter 2: Materials and Methods

2.1 Materials

2.1.1 Chemicals and equipment

A.G. Scientific Incorporated

SP600125

Ambion Incorporated

glycogen, phenol:chloroform:isoamyl alcohol (25:24:1, saturated with 10 mM Tris-HCl pH 8.0/1 mM EDTA), RNA 6000 ladder, RNaseZAP

Affymetrix

Rat Genome U34A GeneChip® arrays, GeneChip® Fluidics Station 400

Agilent Technologies

Agilent 2100 Bioanalyzer, Agilent RNA 6000 Nano LabChip kit

Amersham Biosciences

Hybond™-C Extra nitrocellulose, ECL/ECL+ western blotting detection system, HEPES, ProbeQuant™ G-50 Microcolumns, Typhoon™ phosphorimager 8600 and phosphorimager screens, ImageMaster VDS-CL, ImageMaster Total Lab software, MOPS

Amresco

formamide, 10 x SSC

Applied Biosystems

ABI PRISM® BigDye™ Terminator Cycle Sequencing Ready Reaction Kit

Becton-Dickinson and Company

Bacto™ tryptone, Bacto™ yeast extract, Bacto™ agar

BDH

chloroform, isopropyl alcohol, methanol, glass slides, ethylenediamine tetra-acetic acid (EDTA), NaCl, NaOH, polyvinylpyrrolidone, Tris, HCl, $MgCl_2$

Bio-Rad Laboratories

N,N,N'N'-tetramethylethylenediamine (TEMED), GS Gene Linker™ UV chamber, Kaleidoscope Prestained molecular weight marker, Bradford assay reagent, Mini-PROTEAN 3 protein gel and electrophoresis equipment, GS-800 Calibrated Densitometer

BMA

agarose

Carl Zeiss

Axiovert 200 and S100 inverted fluorescence microscopes, Axiocam digital camera

Cedarlane Laboratories Ltd

nerve growth factor (NGF) for sympathetic neuron cultures

Cephalon Incorporated

CEP-11004

Citifluor Ltd

Citifluor AF1 glycerol/PBS solution

Clontech

rat brain cDNA library, Advantage-GC 2 PCR kit

Corning Incorporated

Costar 0.22 μM Spin-X centrifuge tube filters

Eppendorf

Micro Centrifuge Model 5415C, microloaders, microinjection equipment: micromanipulator (5171), transjector (5246)

Enzo Diagnostics, Incorporated

Enzo BioArray™ HighYield™ RNA transcript labeling kit

GlobePharm

foetal calf serum

Hayman Ltd

ethanol

Hewlett-Packard

GeneArray™ scanner

Invitrogen

RPMI 1640 medium, L-glutamine, penicillin/streptomycin, L-15 medium, Dulbecco's Minimal Essential Medium (DMEM), 0.24 kb – 9.5 kb RNA ladder, 1 kb DNA ladder, dithiothreitol (DTT), First strand cDNA buffer, SSII Reverse Transcriptase, Second strand cDNA buffer, DNA ligase, DNA polymerase I, RNase H, T4 DNA polymerase, SuperScript™ RNase H$^-$ reverse transcriptase, DH5α competent cells, Lipofectamine 2000, TRIzol® reagent, Opti-MEM® I reduced serum medium, pcDNA1

Intracel

1.2 mm od x 0.8 mm id x 10 cm glass capillaries

John Weiss

dissection scissors and forceps

Kodak

X-OMAT scientific imaging film

Kopf Instruments

Vertical pipette puller model 720

Marvel

non-fat milk powder

National diagnostics

37.5:1 acrylamide to bisacrylamide Protogel® solution (30% w/v), 10 x TBE

NEN™ Life Science

Genescreen Plus hybridisation transfer membrane

New England Biolabs

T4 polynucleotide kinase, T4 polynucleotide kinase buffer

Oligoengine™

Oligoengine™ software, pSUPER RNAi vector

PAA laboratories

horse serum

Perkin Elmer Life Sciences Incorporated

[α-^{32}P]dCTP

Pharmacia

hexadeoxynucleotides pd$(N)_6$

Promega

2.5S NGF (for PC6-3 cells), RNasin, T4 DNA Ligase, T4 DNA Ligase buffer, T4 DNA Polymerase, T4 DNA Polymerase buffer, deoxyribonucleotide triphosphates (dNTPs), restriction endonucleases, restriction endonuclease digestion buffers, bovine serum albumin (BSA), Klenow enzyme, PCR reagents: $MgCl_2$, Taq DNA Polymerase, PCR buffer

Qiagen

RNeasy mini kit, mRNA isolation kit, gel extraction kit, HiSpeed plasmid maxi kit, PCR purification kit, QIAprep spin miniprep kit, Oligotex mRNA mini kit

Roche

calf intestine alkaline phosphatase

Sigma-Aldrich Chemical Company

trypsin, poly-L-lysine, 5-fluoro-2-deoxyuridine, uridine, laminin, diethyl pyrocarbonate (DEPC), formaldehyde, sterile phosphate-buffered saline ($\pm Ca^{2+}$, Mg^{2+}), trypsin/EDTA, ethidium bromide, bovine serum albumin (BSA), sodium dodecyl sulphate (SDS), triton X-100, 2-mercaptoethanol, Tween 20, bromophenol blue, xylene cyanol, Ponceau S solution, REDTaq DNA Polymerase, REDTaq PCR buffer, ampicillin, guinea pig IgG, paraformaldehyde, dimethyl sulphoxide (DMSO), ethylene glycol-bis (β-aminoethyl ether)-N,N,N'N',-tetraacetic acid (EGTA), goat serum, protein inhibitor cocktail, Hoechst 33342, chloramphenicol, sodium acetate, ammonium persulphate

Sigma Genosys

T7-$(dT)_{24}$ primer, PCR primers, T7 primer, SP6 primer, siRNA oligonucleotides

Silicon Genetics

GeneSpring 6 data analysis software

Sorvall

Sorvall Discovery 90 ultracentrifuge, ultracentrifuge tubes, RC-5B Plus Superspeed refrigerated centrifuge

Techne Touchgene

PCR machine

Upstate Biotechnology

Collagen type 1

VWR International

13 mm coverslips

Whatman Scientific

3MM paper

Worthington Biochemical Corporation

collagenase type 2

Wolf laboratories

Uvi tec UV transilluminator

2.1.2 Antibodies

Amersham Biosciences

Donkey anti-rabbit horse radish peroxidase-conjugated Ig (Cat # NA934V)

Sheep anti-mouse horse radish peroxidase-conjugated Ig (Cat # NA931V)

BD Transduction Laboratories

Mouse monoclonal anti-Bcl-x_L antibody (Cat # B22620)

Mouse monoclonal anti-c-Jun antibody (Cat # J31920)

Chemicon

Mouse anti-NGF antibody (Cat # MAB5260-60UG)

Jackson Immunoresearch Laboratories

Donkey anti-mouse IgG, FITC-conjugated (Cat # 715-095-150)

Donkey anti-rabbit IgG, FITC-conjugated (Cat # 711-095-152)

Donkey anti-guinea pig IgG, TRITC-conjugated (Cat # 706-025-148)

Santa Cruz Biotechnology, Incorporated

Rabbit polyclonal anti-ATF-3 antibody (C-19, Cat # SC-188)

Goat anti-Rat IgG-horse radish peroxidase conjugated (Cat # SC-2032)

Serotec

Rat monoclonal anti-alpha-tubulin antibody (Cat # MCAP77)

Sigma

Mouse monoclonal M2 anti-FLAG® epitope antibody (Cat # F3165)

Promega

Mouse monoclonal anti-β-galactosidase antibody (Cat # Z3783)

2.1.3 Plasmids

CMVlacZ was described by Alberts *et al.* (1993)

pcDNA1 was purchased from Invitrogen

pCDFLAGBcl-x_L was described by Vekrellis *et al.* (1997)

pCDc-Jun and pCDFLAGΔ169 were described by Ham *et al.* (1995)

2.1.4 Primers

DP5

forward 5'-GTTGGATCCATGTGCCCGTGTCCCCGGC-3'

reverse 5'-ATTGGATCCCTACGCGCTCCGCCTGCCG-3'

ATF-3

forward 5'-CATGGATCCATGATGCTTCAACATCCAGGC-3'

reverse 5'-CTTGAATTCTTAGCTCTGCAATGTTCCTTC-3'

ATF-3bZIP

forward 5'-GTTGGATCCCCTGAAGAAGATGAGAGAAAAAG-3'

reverse 5'-CGAGAATTCTTGAGCATGT AAATCAGATGCTG-3'

NF-M

forward 5'-ACGCTGGACTCGCTGGGCAA-3'

reverse 5'-GCGAGCGCGCTGCGCTTGTA-3'

T7-Oligo$(dT)_{24}$

5'-GGCCAGTGAATTGTAATACGACTCACTATAGGGAGGCGG$(dT)_{24}$-3'

T7

5'-TAATACGACTCACTATAGGG-3'

SP6

5'-GATTTAGGTGACACTATAG-3'

2.1.5 Stock Solutions

TE	10 mM Tris-Cl pH 8.0 1 mM EDTA
TNE	10 mM Tris-Cl pH 8.0 1 mM EDTA 100 mM NaCl
2 x protein loading buffer	0.1 M Tris-HCl pH 6.8 4% SDS 20% glycerol 0.2% bromophenol blue 200 mM DTT

SDS lysis buffer	10 mM Tris-Cl, pH 7.6
	150 mM sodium chloride
	0.5 mM EDTA
	1 mM EGTA
	1% SDS
	30 μM pepstatin A
	80 μM bestatin
	40 μM leupeptin
	1.6 μM aprotinin
	28 μM E-64
	2.08 mM AEBSF
SDS polyacrylamide gels	<u>15%</u>
	15% acrylamide
	0.375 M Tris-Cl, pH 8.8
	0.1% SDS
	0.05% APS
	0.1 % TEMED
	<u>stacking gel</u>
	4% acrylamide
	0.375 M Tris-Cl, pH 6.8
	0.1% SDS
	0.05% APS
	0.1% TEMED
SDS electrophoresis buffer	25 mM Tris
	192 mM glycine
	0.1% SDS
Tris Buffered Saline (TBS)/	10 mM Tris-Cl, pH 8.0
0.1% Tween 20 (TBS-T)	150 mM NaCl
	0.1% Tween-20

5% milk/TBS-T	5% Marvel 10 mM Tris-Cl, pH 8.0 150 mM NaCl 0.1% Tween-20
GeneChip® non-stringent wash buffer	6 x SSPE 0.01% Tween 20 0.005% Antifoam 0-30
GeneChip® array hybridisation buffer	100 mM MES 1 M [Na^+] 20 mM EDTA 0.01% Tween 20
GeneChip® fragmentation buffer	40 mM Tris-acetate, pH 8.1 100 mM potassium acetate 30 mM magnesium acetate
Denhardt's solution	0.1% BSA 0.1% Ficoll™400 0.1% polyvinylpyrrolidone
SSPE	0.15 M sodium chloride 10 mM sodium phosphate 1 mM EDTA
northern blot hybridisation solution	5 x SSPE 5 x Denhardt's solution 10% dextran sulphate 0.5% SDS
DEPC-treated water	0.1% diethyl pyrocarbonate

1 x OLB	solutions A:B:C in the ratio 10:25:15 Solution A: 52 mM Tris-HCl 0.125 M $MgCl_2$ 75% 2-mercaptoethanol 20 mM dGTP, dTTP, dATP Solution B: 2 M HEPES, pH 6.6 Solution C: hexadeoxynucleotides $pd(N)_6$ in TE (90 OD units/ml)
1 x MOPS buffer	20 mM MOPS 8 mM sodium acetate 1 mM EDTA
RNA sample buffer	1 x MOPS buffer 8% formaldehyde 65% formamide
RNA loading buffer	50% glycerol 1 mM EDTA 0.4% bromophenol blue
LB	1% Bacto™ tryptone 0.5% Bacto™ yeast extract 17 mM NaCl
LB-agar	LB containing 1.5% Bacto™ agar
6 x DNA loading buffer	0.24% bromophenol blue 0.24% xylene cyanol 30% glycerol 60 mM EDTA, pH 8.0

Chloramphenicol	34 mg/ml in ethanol
Western blot transfer buffer	25 mM Tris 0.2 M glycine 20% methanol
NaCl-saturated isopropanol:water	50% isopropanol 50% sterile water NaCl added until 2 phases appear

2.2 Methods

2.2.1 Tissue Culture

2.2.1.1 PC6-3 cell culture

Undifferentiated PC6-3 cells were cultured in dishes coated with 1 x poly-L-lysine and collagen at 10 mg/ml in RPMI 1640 medium supplemented with 10% horse serum, 5% foetal calf serum (FCS), 2 mM glutamine and penicillin-streptomycin. Cells were kept in 5% CO_2 at 37°C. PC6-3 cells were subcultured every 7 days by removing the growth medium, rinsing the cells with PBS, incubating for 5 minutes with 1 x trypsin/EDTA and harvesting the cells by centrifugation. The cell pellet was resuspended in RPMI 1640 medium supplemented as above and plated at a density of 1 x 10^6 cells per 9 cm dish.

PC6-3 cells were differentiated by plating 1 x 10^6 cells per 9 cm dish in differentiation medium, which consisted of RPMI 1640 medium supplemented with 2% horse serum, 1% FCS, 2 mM glutamine, penicillin-streptomycin and NGF at 100 ng/ml. The cells were differentiated for 7 days before being used for experiments. In NGF withdrawal experiments, cells were cultured without NGF by carefully rinsing the cells once in differentiation medium lacking NGF and refeeding with differentiation medium supplemented with 100 ng/ml of anti-NGF antibody.

2.2.1.2 Sympathetic neuron culture

Sympathetic neurons from the superior cervical ganglia (SCG) of one-day-old Sprague Dawley rats (supplied by the Biological Services Unit, University College London) were isolated and cultured as described (Whitfield *et al.*, 2004). Briefly, after dissection, the ganglia were desheathed in L15 medium supplemented with 0.1% FCS and penicillin-streptomycin. Ganglia were digested in 0.025% trypsin in PBS followed by 0.2% collagenase type 2 in PBS (containing Mg^{2+} and Ca^{2+}) for 30 minutes each at 37°C. Dissociated ganglia were triturated gently, centrifuged for 10 minutes at 1000 rpm and resuspended in SCG medium. SCG medium consisted of Dulbecco's Minimal Essential Medium (DMEM) supplemented with 10% FCS, 2 mM glutamine, penicillin-streptomycin and NGF (50 ng/ml). The antimitotic agents

fluorodeoxyuridine and uridine were added to a final concentration of 20 μM to limit the proliferation of non-neuronal cells. Neurons were pre-plated for 2 hours in an uncoated 9cm dish to remove non-neuronal cells. The supernatant enriched in sympathetic neurons was centrifuged at 1000 rpm for 10 minutes and the pelleted neurons resuspended in SCG medium. Neurons were plated on poly-L-lysine and laminin coated coverslips at a density of 8,000-10,000 neurons per coverslip. Coverslips, placed in 3.5 cm dishes, were incubated at 37°C in 10% CO_2 for 2 hours prior to the addition of 2 ml of SCG medium. Neurons were incubated in 10% CO_2 at 37°C and grown for 6-7 days in the presence of NGF before use in experiments. In NGF withdrawal experiments neurons were cultured without NGF by carefully rinsing the cells twice in SCG medium lacking NGF and then refeeding with SCG medium supplemented with anti-NGF antibody at 100 ng/ml.

2.2.1.3 Treatment of sympathetic neurons with chemical inhibitors CEP-11004 and SP600125

Sympathetic neurons were grown in the presence of NGF for 6-7 days before treatment. Neurons were then cultured in the presence or absence of NGF for 24 hours and in the presence or absence of each inhibitor or DMSO as control. CEP-11004 and SP600125 stock solutions were 4 mM and 20 mM respectively in DMSO and were stored at -20°C. CEP-11004 was added to neurons at 400 nM and SP600125 was used at 20 μM. Protein was extracted and samples analysed by western blotting experiments (section 2.2.5).

2.2.1.4 Cos-7 cell culture

Cos-7 cells were cultured in dishes coated with 1 x poly-L-lysine in DMEM medium supplemented with 10% FCS, 2 mM glutamine and penicillin-streptomycin in 5% CO_2 at 37°C. Cos-7 cells were passaged when approximately 70-80% confluent by rinsing the cells with PBS, incubating for 5 minutes with 1 x trypsin/EDTA and harvesting the cells by centrifugation. Cells were resuspended in DMEM medium supplemented as above and plated on 1 x poly-L-lysine coated dishes.

2.2.1.5 Transient transfections

Cos-7 or PC6-3 cells were grown in 9 cm or 6 cm dishes respectively, until 90-95% confluent at the time of transfection. One day prior to transfection, the medium was changed to growth medium without antibiotics. Lipofectamine™ 2000 was used to transfect cells with plasmid DNA. DNA (5-8 μg) was added to 273 μl (6 cm dish) or 821 μl (9 cm dish) Opti-MEM® I reduced serum medium. Lipofectamine™ 2000 (20-40 μl) was added to 273 μl (6 cm dish) or 821 μl (9 cm dish) Opti-MEM® I reduced serum medium and incubated at room temperature for 5 minutes. The diluted DNA and lipofectamine solutions were mixed together gently and incubated at room temperature for 20 minutes. The DNA/lipofectamine mix was added to the cells by gentle pipetting and mixed by slowly rocking the dishes. Cells were then incubated for 48 hours prior to protein extraction.

2.2.2 RNA manipulations

2.2.2.1 RNA Extraction

2.2.2.1.1 PC6-3 cells

Total RNA was prepared from PC6-3 cells using TRIzol®. Cells were placed on ice, the medium removed and 2 ml of TRIzol was added per dish to lyse the cells. Cell lysates were passed through a pipette several times and stored on ice. Homogenised samples were incubated at 15 - 30°C for 5 minutes and 0.2 ml of chloroform was added per ml of TRIzol. Samples were vigorously shaken for 15 seconds and incubated at 15 - 30°C for 2 minutes. Centrifugation of the samples at 1,780 x g for 15 minutes at 4°C was performed and the upper aqueous phase removed and stored on ice. Addition of 0.5 ml of isopropyl alcohol per ml of TRIzol, followed by incubation at 15 - 30°C for 10 minutes and centrifugation at 1,780 x g for 10 minutes precipitated the RNA. The pellets were washed once in 75% ethanol (1 ml per ml of TRIzol), vortexed and centrifuged at 1,780 x g for 5 minutes at 4°C. RNA pellets were air dried briefly and dissolved in DEPC-treated water containing 1 unit/μl of RNasin.

2.2.2.1.2 Sympathetic neurons

RNA was extracted from sympathetic neurons by rinsing the cells from coverslips using ice-cold PBS and spinning the cells at 16,000 x g for 5 minutes at 4°C. Pelleted cells were lysed in 350 µl of buffer RLT and RNA was extracted as described in the Qiagen RNeasy mini kit handbook. RNA was eluted from the RNeasy columns in 30 µl of RNase-free water.

2.2.2.2 mRNA purification

This method is a modification of the protocol supplied with the Qiagen Oligotex mRNA mini kit. Oligotex resin consists of polystyrene–latex particles of uniform size with $dC_{10}T_{30}$ oligonucleotides covalently linked to the surface, which bind mRNA. Total RNA was made up to 100 µl with DEPC-treated water. 100 µl of 2 x binding buffer and 30-50 µl of Oligotex suspension were added to each sample, mixed well and incubated at 65°C for 3 minutes. Samples were incubated at room temperature for 15 minutes, mixed every 3 minutes, and then centrifuged at 16,000 x g for 3 minutes. Oligotex pellets were washed twice in 300 µl of wash buffer. The mRNA was eluted from the Oligotex beads with two 100 µl volumes of pre-heated elution buffer, by pipetting several times and vortexing, and then incubating at 75°C for 2 minutes. Samples were centrifuged at 16,000 x g for 3 minutes and the supernatant stored on ice. mRNA samples were prepared by precipitating overnight with 0.1 volumes of 3 M sodium acetate and 2.5 volumes of 100% ethanol at -70°C. Samples were centrifuged at 16,000 x g for 30 minutes at 4°C, washed in 70% ethanol, centrifuged for a further 15 minutes at 4°C and resuspended in DEPC-treated water.

2.2.2.3 Assessing RNA quality using the Agilent 2100 Bioanalyzer

mRNA (100-200 ng) was analysed using the Agilent RNA 6000 Nano LabChip kit. Initially electrodes were decontaminated using RNaseZAP reagent as instructed. RNA 6000 Nano gel matrix was prepared by centrifugation for 10 minutes at 1,500 x g through a spin filter. The gel was stored at 4°C in 65 µl aliquots. RNA 6000 Nano dye concentrate was vortexed for 10 seconds and centrifuged briefly to collect the sample at the bottom of the tube. 1 µl dye was added to 65 µl filtered gel, vortexed to mix thoroughly and centrifuged at 16,000 x g for 10 minutes at room temperature. An RNA 6000 Nano LabChip was placed on the Chip Priming Station. The gel-dye mix

(9 µl) was added to the corresponding well on the chip and loaded by pressing the 1 ml plunger of the Chip Primer Station. After 30 seconds the plunger was released. Additional gel-dye mix (9 µl) was added to each of the wells marked 'G'. RNA 6000 Nano Marker (5 µl) was added to the well corresponding to the ladder and each of the 12 sample wells on the chip. RNA 6000 ladder (1 µl) and the RNA samples (1 µl) to be analysed were heat denatured at 70°C for 2 minutes before being added to the appropriate wells on the chip. When less than 12 RNA samples were used, the remaining wells were made up to the same volume with RNA 6000 Nano Marker (1 µl). The chip was placed in the adaptor of the vortex mixer and vortexed for 1 minute at the IKA vortexer set-point (2400 rpm). The RNA 6000 Nano LabChip was inserted into the Agilent 2100 Bioanalyzer, ensuring the electrodes in the cartridge were inserted into the wells of the chip. The mRNA Nano Assay was performed. Once the run was complete the chip was removed immediately from the bioanalyzer and electrodes cleaned with RNase-free water as instructed.

2.2.2.4 Northern Blot Analysis

mRNA samples (3-6 µg) were electrophoresed on a 1% agarose-formaldehyde gel consisting of 1% agarose, 6% formaldehyde and 1 x MOPS buffer at 100 V for 3 hours. RNA samples and 0.24 kb - 9.5 kb RNA ladder were heated to 65°C in 2 volumes of RNA sample buffer and placed on ice for 2 minutes. RNA loading buffer (0.5 volumes) was added to the samples. In addition, ethidium bromide (0.5 µg) was added to the RNA ladder sample for visualisation under UV light. Following electrophoresis, gels were rinsed with DEPC-treated water for 10 minutes and then twice with 10 x SSC for 15 minutes with shaking. Blotting onto Genescreen Plus hybridisation transfer membrane was performed overnight using 10 x SSC (Sambrook *et al.*, 1989).

The RNA was covalently linked to the membrane by UV irradiation using a GS Gene Linker™ UV chamber. The nitrocellulose membrane was rehydrated in 5 x SSC for 10 minutes with shaking and then incubated in hybridisation solution for 1-2 hours at 65°C. Salmon sperm DNA (50 µg/ml) was added during this prehybridisation stage to block non-specific binding of radioactive DNA probes to the membrane. Salmon sperm DNA was prepared by boiling for 10 minutes and then cooling on ice for 5 minutes prior to addition to the hybridisation solution. DNA probes were labelled with

[α-^{32}P]dCTP (3000 Ci/mmol) by boiling the DNA in 1 x Oligo-Labelling Buffer (OLB) for 5 minutes and then incubating on ice for 2 minutes before addition of 5 units of Klenow enzyme, 10 μg of BSA and 30 μCi of [α-^{32}P]dCTP. Labelling reactions were performed at room temperature for a minimum of 4 hours. DNA probes were denatured and the unincorporated deoxyribonucleotide triphosphates (dNTPs) removed from the probe DNA using ProbeQuant™ G-50 microcolumns. Each column was centrifuged for 2 minutes at 400 x g into a microfuge tube and the flow-through discarded. The column was placed into a fresh tube containing 33 μl of 1 M NaOH. 80 μl of 0.1% SDS in TE was added to the DNA probe and this was then added to the column. Samples were centrifuged for 2 minutes at 400 x g. Columns containing unincorporated nucleotides were discarded and the DNA was neutralised with an equal volume of 1 M Tris-Cl (pH 8.5). Probes were added to the hybridisation bottle and incubated at 65°C overnight.

Membranes were washed in 2 x SSC, 0.1% SDS at room temperature for 10 minutes and then twice in 1 x SSC, 0.1% SDS for 15 minutes. Membranes were wrapped in Saran Wrap and exposed to a phosphorimager screen for 1-4 nights at room temperature. Screens were scanned using a Typhoon™ 8600 phosphorimager and the RNA bands quantitated using Image Quant analysis software.

2.2.2.5 RT-PCR

Total RNA from PC6-3 cells (1 μg) or SCG neurons (10 μl) was reverse transcribed using SuperScript™ RNase H$^-$ reverse transcriptase as described by the manufacturer. Reactions were inactivated by heating at 70°C for 15 minutes. RNase H (2 units) was added, and the samples were incubated for 20 minutes at 37°C, to remove RNA complementary to the cDNA. The final reaction volume of 20 μl was diluted 1 in 10 to give 200 μl and 10 μl was used in each PCR reaction.

PCR reactions (50 μl) were prepared using 10 μl of cDNA in 1 x REDTaq PCR buffer with each dNTP (0.2 mM), 100 pmoles of each primer and 2.5 units of REDTaq DNA Polymerase. PCR was performed for the minimum number of cycles required to detect a product with cDNA prepared at time 0. Reaction conditions were 94°C for 1 minute, 60°C for 1 minute and 72°C for 1 minute for typically 18-35 cycles and a final extension at 72°C for 5 minutes.

The primers used were as follows: *NF-M*, forward 5'-A CGCTGGACTCGCTG GGCAA-3' and reverse 5'-GCGAGCGCGCTGCGCTTGTA-3', *ATF-3*, forward 5'-CA TGGATCCATGATGCTTCAACATCCAGGC-3' and reverse 5'-CTTGAATTCTTAG CTCTGCAATGTTCCTTC-3' and *DP5*, forward 5'-GTTGGATCCATGTGCCCGT GTCCCCGGC-3' and reverse 5'-ATTGGATCCCTACGCGCTCCGCCTGCCG-3'.

After amplification, the cDNAs were separated on 1.5% agarose gels, visualised by staining with ethidium bromide, and images were captured using an ImageMaster VDS-CL and quantitated using ImageMaster Total Lab software.

2.2.3 Affymetrix GeneChip® analysis

2.2.3.1 RNA extraction from PC6-3 cells

PC6-3 cells were differentiated in the presence of NGF for 7 days and then cultured in the presence or absence of NGF for 16 hours. At this time, total RNA was extracted and mRNA purified, as described previously, for use in Affymetrix GeneChip® analysis.

2.2.3.2 cDNA synthesis

mRNA (3-5 μg) was hybridised to 100 pmoles of T7-Oligo$(dT)_{24}$ primer at 70°C for 10 minutes. Samples were centrifuged briefly and incubated on ice. First strand cDNA buffer, 10 mM dithiothreitol (DTT) and 0.5 mM dNTPs were added and the temperature of the reactions adjusted to 37°C for 2 minutes. First strand synthesis was initiated by addition of 600-1000 units of SSII Reverse Transcriptase and incubation at 37°C for 1 hour. Reactions were placed on ice and centrifuged briefly to bring down condensation. Second strand buffer, 0.2 mM dNTPs, 10 units of DNA Ligase, 40 units of DNA polymerase I and 2 units of RNase H were added to the first strand reactions and incubated at 16°C for 2 hours. Reactions were incubated with 10 units of T4 DNA polymerase at 16°C for 5 minutes and then EDTA was added to 30 μM.

An equal volume of phenol:chloroform:isoamyl alcohol (25:24:1, saturated with 10 mM Tris-HCl pH 8.0/1 mM EDTA) was added to cDNA samples, which were vortexed and centrifuged at 16,000 x g for 5 minutes. The top aqueous layer was

transferred to a fresh microfuge tube and an equal volume of chloroform:isoamyl alcohol (24:1) was added. The samples were vortexed and centrifuged at 16,000 x g for a further 5 minutes. 0.5 volumes of 7.5 M ammonium acetate and 2.5 volumes of 100% ethanol were added and the DNA was precipitated on ice for 1 hour. 5 μg of glycogen was added to aid visualisation of the pellet. Samples were centrifuged at 16,000 x g for 20 minutes at 4°C, washed in 75% ethanol and centrifuged for a further 10 minutes at 4°C. DNA pellets were air dried and resuspended in 12 μl of DEPC-treated water.

2.2.3.3 Synthesis of biotin-labelled cRNA (*in vitro* transcription)

Biotin-labelled cRNA was prepared from 1 μg of cDNA using the ENZO BioArray™ HighYield™ RNA transcript labeling kit as instructed. Qiagen RNeasy columns were used to clean up the cRNA. Samples were precipitated for 1 hour at -20°C using 0.5 volumes of 7.5 M ammonium acetate and 2.5 volumes of 100% ethanol. Glycogen (5 μg) was added to aid visualisation of the pellet. RNA was centrifuged at 16,000 x g for 30 minutes at 4°C, washed twice in 80% ethanol (stored at -20°C) and air dried at room temperature for 5 minutes. Pellets were resuspended in 20 μl of DEPC-treated water. Labelled RNA (20 μg) was fragmented in fragmentation buffer at 94°C for 35 minutes to prepare target RNA for hybridisation to the Affymetrix GeneChip® arrays.

2.2.3.4 Affymetrix GeneChip® array hybridisation

Rat Genome U34A GeneChip® arrays were filled with GeneChip® array hybridisation buffer and incubated at 45°C with rotation for 10 minutes. During this time hybridisation cocktails for each target were prepared. Fragmented RNA (15 μg) was mixed with control oligonucleotide B2 (50 pM), Eukaryotic hybridisation controls - BioB, BioC, BioD and cre (1.5, 5, 25 and 100 pM respectively), herring sperm DNA (0.1 mg/ml), acetylated BSA (0.5 mg/ml), hybridisation buffer (as above) and made up to the appropriate volume with DEPC-treated water. Each hybridisation cocktail was heated to 99°C for 5 minutes and then incubated at 45°C for 5 minutes. Samples were centrifuged at 16,000 x g for 5 minutes to remove any insoluble material. Hybridisation buffer was removed from the GeneChip® arrays and replaced with the

hybridisation cocktail for each RNA sample. GeneChip® arrays were rotated at 45°C for 16 hours.

2.2.3.5 Washing, staining and scanning of Affymetrix GeneChip® arrays

After 16 hours of hybridisation, the hybridisation cocktail was removed from the arrays and replaced with Non-Stringent wash buffer. The GeneChip® Fluidics Station 400 was used with the Affymetrix antibody amplification procedure to wash and stain the arrays as instructed in the user's manual. The GeneChip® arrays were scanned by the Hewlett-Packard GeneArray™ scanner at the excitation wavelength of 488 nm. The amount of light emitted at 570 nm is proportional to the amount of bound target at each location on the array.

2.2.3.6 Analysis of Affymetrix GeneChip® array data

Data was collected using MAS 5.0 with the U34A gene set. This was analysed using GeneSpring 6 data analysis software (Silicon Genetics). Samples in the presence of NGF were set at a value of one. Data from samples in the absence of NGF were normalised to the data from samples in the presence of NGF for each of the GeneChip® experiments (normalisation to individual samples). Further filtering of the data was performed. Genes that changed more than 1.5 fold and which were present in either 2 of 3 or 3 of 3 experiments were selected. Additional analysis was performed on these lists to generate statistically significant gene changes.

2.2.4 DNA manipulations

2.2.4.1 Polymerase Chain Reaction (PCR)

2.2.4.1.1 DP5

DP5 cDNA was amplified from a rat brain cDNA library. The primers used to amplify DP5 were, forward 5'-GTTGGATCCATGTGCCCGTGTCCCCGGC-3' and reverse 5'-ATTGGATCCCTACGCGCTCCGCCTGCCG-3'. The cDNA was amplified using the Advantage-GC 2 PCR kit for GC rich sequences. Reactions (25 µl) were prepared using 2.5 µl of cDNA library in 1 x advantage PCR buffer with each dNTP (0.2 mM), 100 pmoles of each primer, 1 M advantage GC melt solution and 1 x

advantage polymerase mix. Reaction conditions were 94°C for 3 minutes followed by 40 cycles of 94°C for 1 minute and 68°C for 1 minute then a final extension at 68°C for 5 minutes.

2.2.4.1.2 ATF-3

ATF-3 cDNA was amplified from a rat brain cDNA library. The primers used to amplify ATF-3 were, forward 5'-CATGGATCCATGATGCTTCAACATCCAG GC-3' and reverse 5'-CTTGAATTCTTAGCTCTGCAATGTTCCTTC-3'. PCR reactions (25 µl) were prepared using 2.5 µl of cDNA library in 1 x PCR buffer with each dNTP (0.2 mM), 50 pmoles of each primer, 1.5 mM $MgCl_2$ and 2.5 units of Taq DNA Polymerase. Reaction conditions were 94°C for 5 minutes followed by 40 cycles of 94°C for 30 seconds, 60°C for 30 seconds and 72°C for 1 minute then a final extension at 72°C for 5 minutes.

2.2.4.1.3 ATF-3bZIP

The ATF-3bZIP domain of ATF-3 was amplified from the ATF-3 cDNA. The primers used to amplify the ATF-3bZIP domain were, forward 5'-GTTGGATCCCCT GAAGAAGATGAGAGAAAAAG-3' and reverse 5'-CGAGAATTCTTGAGCATGT AAATCAGATGCTG-3'. PCR reactions (25 µl) were prepared using approximately 100 ng of ATF-3 cDNA in 1 x PCR buffer with each dNTP (0.2 mM), 100 pmoles of each primer and 2.5 units of REDTaq DNA Polymerase. Reactions were initially incubated at 94°C for 2 minutes and then 94°C for 1 minute, 58°C for 1 minute and 72°C for 1 minute for 30 cycles and then a final extension at 72°C for 5 minutes.

2.2.4.2 Restriction endonuclease digestion

Plasmid DNA (1 µg) was digested by mixing with an excess of restriction enzyme, typically 10 units/µg DNA, in the appropriate 1 x restriction enzyme buffer with BSA at 0.5-1 µg/µl. Reactions were performed for 2-3 hours at 37°C. When plasmid DNA was subsequently to be used in ligation reactions, enzymes were heat inactivated at 68°C for 15 minutes followed by the addition of calf intestine alkaline phosphatase (1 unit) in 1 x calf intestine alkaline phosphatase buffer for 30 minutes at 37°C. Reactions were inactivated by addition of 20 mM EGTA and heating to 65°C for 10 minutes. Digested DNA was electrophoresed on a 1% agarose gel, visualized by staining with ethidium bromide and purified using a Qiagen gel extraction kit as instructed.

2.2.4.3 Ligation of DNA

Digested plasmid DNA (approximately 200 ng) and insert cDNA (approximately 50 ng) were ligated using 10 units of T4 DNA Ligase in 1 x T4 DNA Ligase buffer at 16°C overnight.

2.2.4.4 Bacterial transformation

DH5α cells (50 µl) were transformed with ligation mixtures or plasmids by incubating together on ice for 30 minutes, followed by heat shock at 37°C for 1 minute and incubation on ice for 2 minutes. LB medium (950 µl) was added to the cells and incubation at 37°C with shaking was performed for 1 hour. Cells were pelleted by centrifugation at 16,000 x g for 2 minutes and resuspended in approximately 100 µl of the supernatant. Cells were spread on LB-agar plates containing ampicillin at 50 µg/ml and grown overnight at 37°C.

2.2.4.5 Plasmid preparations

2.2.4.5.1 Small scale plasmid preparations (minipreps)

Single colonies were inoculated into 5 ml of LB medium containing ampicillin (50 µg/ml) and grown overnight at 37°C with shaking. Plasmid DNA was purified from 4 ml liquid cultures using the QIAprep Spin miniprep kit as instructed in the manufacturer's handbook. This protocol involves the alkaline lysis of the cells followed by absorption of the DNA onto a silica gel membrane that binds up to 20 µg of DNA in the presence of a high concentration of chaotropic salt. Endonucleases and salts are removed by subsequent wash steps and DNA samples are eluted in a small volume of low-salt Tris buffer or water.

2.2.4.5.2 Large scale plasmid preparations (maxipreps)

Single colonies were inoculated into 5 ml of LB medium containing ampicillin (50 µg/ml) and grown overnight at 37°C with shaking. An aliquot of 4 ml was used to inoculate 400 ml of LB medium containing ampicillin (50 µg/ml) and cultures were grown at 37°C with shaking until an optical density at 600 nm of 1. At this stage chloramphenicol was added to a final concentration of 170 µg/ml for amplification of the plasmid DNA and cultures incubated for a further 16 hours overnight.

Bacterial cultures were harvested by centrifugation at 6,000 x g for 15 minutes at 4°C in a Sorvall RC-5B PLUS Superspeed refrigerated centrifuge and plasmid DNA purified using the Qiagen HiSpeed plasmid maxi kit as instructed. This purification protocol is based on an alkaline lysis procedure, followed by binding of plasmid DNA to an anion-exchange resin under appropriate low-salt and pH conditions. RNA, proteins, dyes, and low-molecular-weight impurities are removed by a medium-salt wash. Plasmid DNA is eluted in a high-salt buffer and then concentrated and desalted by isopropanol precipitation.

Plasmid DNA was further purified by centrifugation through a CsCl-ethidium bromide gradient. DNA samples were mixed with 11 ml of CsCl/TE (0.95 g of CsCl/ml TE) and 400 µl of ethidium bromide (10 mg/ml) and transferred to ultracentrifuge tubes using a 19 G needle and syringe. Tubes and lids were balanced to within 0.01 g and sealed using an ultracentrifuge tube crimper machine. Samples were centrifuged at 57,000 rpm for at least 16 hours in a Sorvall Discovery 90 ultracentrifuge at 20°C with slow deceleration at the end of the run. The lower ethidium bromide stained band containing supercoiled DNA was extracted from the tubes using a 19 G needle and syringe, with a second needle used to release the air from the top of the tube. DNA was transferred to a 15 ml centrifuge tube and extracted with NaCl-saturated isopropanol:water. An equal volume of saturated isopropanol was added to the DNA solution and mixed vigorously. After allowing the two phases to separate, the upper phase was discarded. This was repeated until the DNA solution was colourless. The DNA was transferred to a 50 ml polypropylene tube with 3 volumes of water and precipitated by adding 2 volumes of ethanol and incubating at 4°C for 15 minutes. The tube was then centrifuged for 30 minutes at 1,780 x g. The DNA pellet was washed with 70% ethanol, centrifuged for a further 15 minutes at 1,780 x g, air dried and redissolved in TE.

2.2.4.6 Agarose gel electrophoresis of DNA

To analyse DNA by agarose gel electrophoresis, 6 x DNA loading buffer was added to the samples. The DNA was then resolved on 1-1.5% agarose gels, prepared in 1 x TBE with 0.5 µg/ml of ethidium bromide. In addition a 1 kb DNA ladder was also loaded onto gels to determine the size of DNA fragments separated on the gel. DNA was visualised using a Uvi tec UV transilluminator.

2.2.4.7 Construction of pSUPERATF-3 vectors

RNAi sequences were designed using the Oligoengine™ design tool on the Oligoengine website (oligoengine.com). Three 19-nucleotide sequences were selected at positions 158 (5'-CCTTTGCCATCGGATGTCC-3'), 268 (5'-GGAGGCGGCGGGA AAGAAA-3') and 484 (5'-CGCCGGAAGACGAGAGGAA-3') of the ATF-3 coding sequence. These were incorporated into two 64-nucleotide sequences containing a hairpin sequence and BglII and HindIII restriction enzyme sites, as illustrated below for sequence 158.

(BglII) target sequence 158: sense Hairpin target sequence158: antisense

5'-GATCCCC**CCTTTGCCATCGGATGTCC**TTCAAGAGA**GGACATCCGATGGCAAAGG**TTTTTGGAA- 3'

3'-GGG**GGAAACGGTAGCCTACAGG**AAGTTCTCT**CCTGTAGGCTACCGTTTCC**AAAAACCTTTTCGA-5'

(HindIII)

Each pair of 64 base oligonucleotides (500 ng) was phosphorylated by addition of T4 polynucleotide kinase (10 units), 1 x T4 polynucleotide kinase buffer and 1 mM ATP and incubating at 37°C for 1 hour. The phosphorylated oligonucleotides (100 ng) were annealed together in TNE buffer at 65°C for 30 minutes and then allowed to cool slowly to room temperature.

pSUPER vector (2 μg) was digested with BglII (10 units) and HindIII (10 units) restriction enzymes in 1 x Buffer B at 37°C for 2 hours. Calf intestine alkaline phosphatase (1 unit) in 1 x calf intestine alkaline phosphatase buffer was added for 30 minutes at 37°C. Reactions were stopped by adding EGTA to 20 mM and heating to 65°C for 10 minutes. Digested DNA was electrophoresed on a 1% agarose gel, visualized by staining with ethidium bromide and purified using a Qiagen gel extraction kit as instructed. Vector and oligonucleotide insert were ligated and used to transform DH5α cells as described previously.

2.2.4.8 DNA Sequencing

Sequencing was performed using the ABI PRISM® BigDye™ Terminator Cycle Sequencing Ready Reaction kit. Reactions (15 μl) were prepared using approximately 500 ng of DNA with 6 μl of BigDye and 50 pmoles of either T7 or SP6 primers. PCR reactions were at 96°C for 30 seconds, 50°C for 30 seconds and 60°C for 4 minutes for 25 cycles. DNA was precipitated on ice for 30 minutes using 0.1 volumes of 3 M ammonium acetate and 2.5 volumes of 100% ethanol. Samples were

centrifuged at 16,000 x g for 30 minutes at 4°C, washed in 70% ethanol, vortexed and incubated at room temperature for 10 minutes. Samples were centrifuged for a further 15 minutes at 4°C and the DNA pellets air dried. Samples were run on an ABI Prism 377 DNA sequencer by Mr. Martin Woodward and DNA sequences analysed using MacVector software.

2.2.5 Protein Analysis

2.2.5.1 Preparation of protein extracts

2.2.5.1.1 PC6-3 and Cos-7 cells

Medium was removed from the cells and kept on ice. Ice cold PBS was added to each plate, the cells were scraped off and added to the removed medium on ice. Plates were rinsed with an additional 1 ml of PBS to collect any remaining cells. Cells were pelleted by centrifugation at 400 x g for 5 minutes at 4°C and then resuspended in 500 µl of PBS. At this stage, samples were transferred into 1.5 ml microfuge tubes and the cells re-pelleted by centrifugation at 16,000 x g for 5 minutes at 4°C. Cell pellets were resuspended in 200 µl of SDS lysis buffer supplemented with a protease inhibitor cocktail and mixed. Samples were incubated at 90°C for 20 minutes, mixed and then centrifuged at 16,000 x g for 20 minutes at 4°C. The supernatant was removed, snap frozen on dry ice and stored at -80°C.

2.2.5.1.2 Sympathetic neurons

Neurons grown on glass coverslips were rinsed twice with PBS. Cells were rinsed off the coverslips using ice cold PBS supplemented with a protease inhibitor cocktail and cells pelleted by centrifugation at 16,000 x g for 5 minutes. Cells were lysed directly in 2 x protein loading buffer by vortexing for 1 minute and boiling for 5 minutes. Samples were run on an SDS-polyacrylamide gel (see section 2.2.5.3).

2.2.5.2 Protein concentration

The concentration of proteins was determined by the Bradford method using a Bio-Rad kit as instructed by the manufacturer, with γ-globulin as a standard. A standard curve was prepared by plotting the OD_{595} against amount of γ-globulin (µg).

2.2.5.3 Western Blot Analysis

Protein samples and Kaleidoscope Prestained molecular weight marker were mixed with 2 x protein loading buffer and boiled for 5 minutes. Samples were run on 15% SDS-polyacrylamide gels in SDS electrophoresis buffer at 80-100 V for 2-3 hours using the Mini-PROTEAN 3 electrophoresis system from Bio-Rad. Gels were transferred to Hybond-C nitrocellulose as described (Sambrook *et al.*, 1989) at 100 V for 1 hour at room temperature or 20 V overnight at 4°C with constant stirring. Membranes were stained with Ponceau S solution for 5 minutes, to establish transfer efficiency.

Membranes were blocked overnight at 4°C or for 1 hour at room temperature, with shaking, in 5% milk/TBS-T. Primary antibodies were added in 5% milk/TBS-T at the appropriate dilution for 1-2 hours at room temperature with rotation. Blots were washed three times in 5% milk/TBS-T. HRP-linked secondary antibodies were diluted 1 in 2000 in 5% milk/TBS-T and added to membranes for 1 hour with rotation. Blots were washed three times in 5% milk/TBS-T followed by a final wash in TBS-T. Antibodies were detected using an ECL or ECL+ reagent kit as instructed by the manufacturer and membranes were exposed to X-ray film, usually X-OMAT imaging film from Kodak. Western blots were scanned on a Bio-Rad GS800 densitometer and the protein bands quantitated using Bio-Rad Quantity One® software.

2.2.6 Microinjection of sympathetic neurons

Sympathetic neurons were grown in the presence of NGF for 5-7 days before microinjection. DNA mixtures were injected directly into the nucleus of 150-250 neurons per coverslip. Injection mixes contained 0.001-0.4 μg/μl of DNA constructs in 0.5 x PBS with guinea pig IgG (2.5 μg/μl) as the injection marker. Mixes were filtered through Costar Spin-X columns by centrifugation at 16,000 x g for 30 minutes at 4°C.

Microinjection needles were pulled from glass capillary tubes using a Kopf Instruments gravity puller (model 720) and loaded using Eppendorf microloaders. Microinjection was performed using a Zeiss Axiovert 200 microscope fitted with a heated stage and CO_2 chamber, with Eppendorf transjector (5246) and micromanipulator (5171).

2.2.7 Immunocytochemistry

Neurons grown on glass coverslips were rinsed in PBS and fixed in 4% paraformaldehyde at room temperature for 30 minutes, rinsed in PBS and permeabilized with 0.5% Triton X-100 in PBS for 5 minutes at room temperature. After permeablization, coverslips were rinsed in PBS and non-specific binding blocked using 50% horse serum in 1% BSA in PBS for 30 minutes at room temperature. Coverslips were rinsed in PBS and incubated with primary antibody at the appropriate dilution in 1% BSA in PBS for 1 hour at room temperature. Cells were rinsed again in PBS and incubated with TRITC-conjugated anti-guinea pig antibody and the appropriate FITC-conjugated secondary antibody in 1% BSA in PBS for 1 hour at room temperature. Cells were rinsed for a final time in PBS and nuclei were stained with Hoechst dye at 10 μg/ml in water for 5-10 minutes. The coverslips were finally rinsed in water, air dried and mounted on glass slides using Citifluor glycerol/PBS solution and sealed using clear nail varnish.

Chapter 3: Affymetrix GeneChip® Analysis

3.1 Introduction

PC12 cells are a useful *in vitro* model for studying neuronal apoptosis mechanisms because many of the events that are characteristic of sympathetic neuron apoptosis also occur in PC12 cells. These cells are a clonal cell line derived from a rat adrenal pheochromocytoma, which respond to NGF by exiting the cell cycle and forming long, branching neurite-like processes (Greene and Tischler, 1976). Removal of NGF from neuronally differentiated PC12 cells leads to apoptosis, which is promoted by the JNK/c- Jun pathway (Xia *et al.*, 1995). PC6-3 cells are a sub-clone of PC12 cells that have increased sensitivity to NGF removal, and apoptosis of this sub-clone requires *de novo* transcription and translation (Pittman *et al.*, 1993). These cells are therefore a useful tool for studying changes in transcription involved in programmed neuronal cell death.

To date only a small number of genes have been reported to be induced by NGF withdrawal. It is likely that there are many others to be discovered, some of which may be c-Jun targets with important functions in the neuronal death pathway. A useful technique for studying changes in the transcription of large numbers of cellular genes is microarray analysis. There are many different types of this technology that analyse the expression levels of thousands of genes in a cell population. Affymetrix GeneChip® expression arrays have 10,000-100,000 different oligonucleotide probes synthesized on each array to represent thousands of genes and EST sequences from a particular genome. The GeneChip® Rat Genome U34 Set provides gene expression data for more than 24,000 known genes and EST clusters. This includes all rat sequence clusters from Build 34 of the UniGene database supplemented with additional annotated sequences from Genbank 110. The U34A array contains probe sets of 7,000 full length or annotated genes and thousands of EST clusters. Figure 3.1 shows an outline of the Affymetrix GeneChip® experiment. Briefly, RNA extracted from the different populations of cells to be studied is converted into cDNA, which is transcribed to form biotin-labelled cRNA. These cRNA samples are then fragmented and hybridised to the DNA on the chip. This is stained with streptavidin phycoerythrin conjugate and scanned at 488 nm. The amount of light emitted at 570 nm is

Figure 3.1 GeneChip® eukaryotic target labelling assay for expression analysis

Outline of the Affymetrix GeneChip® experiment (reproduced from www.affymetrix.com). RNA is extracted from the different populations of cells to be studied and reverse transcribed into cDNA using Oligo(dT) primer. Samples are then converted into biotin-labelled cRNA using an *in vitro* transcription labelling kit. The cRNA is purified and subsequently fragmented for hybridisation to the DNA on the chip. The chip is then stained with streptavidin phycoerythrin conjugate and scanned at 488 nm. The amount of light emitted at 570 nm is proportional to the bound target at each location on the array and therefore to the level of the mRNA species in the RNA sample being tested. Comparison of the levels of fluorescence produced by each chip indicates differential gene expression between cell populations.

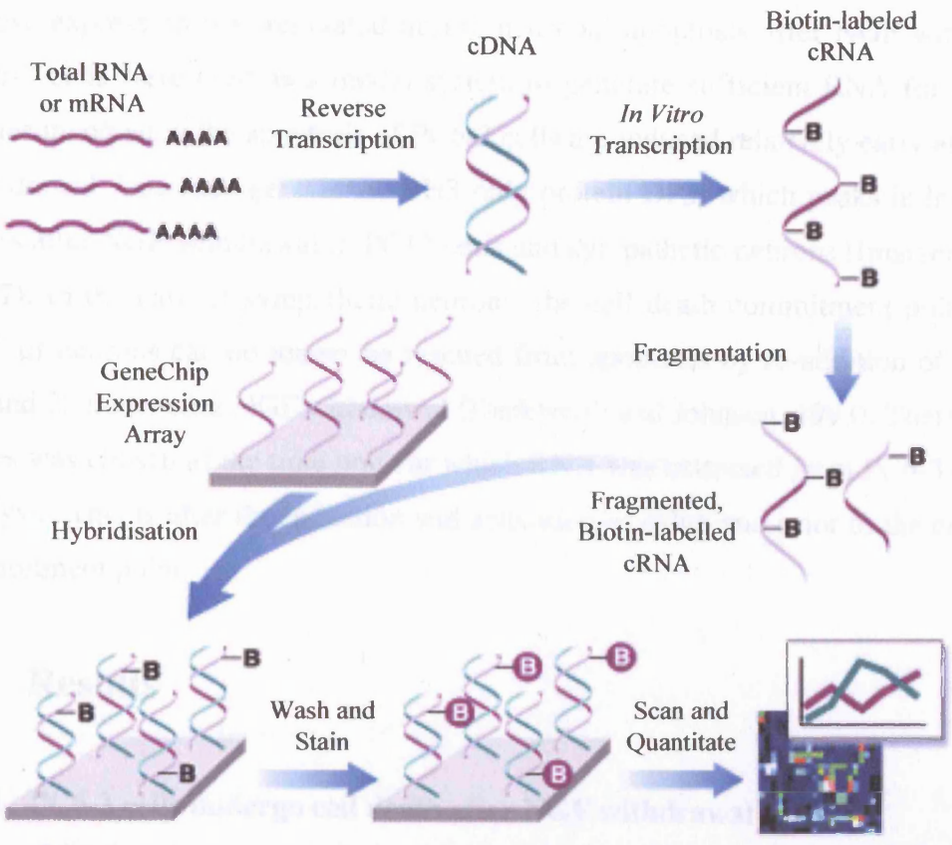
Total RNA
or mRNA
AAAA
AAAA
AAAA
Reverse
Transcription
cDNA
In Vitro
Transcription
Biotin-labeled
cRNA
B
Fragmentation
GeneChip
Expression
Array
Hybridisation
Fragmented,
Biotin-labelled
cRNA
Wash and
Stain
Scan and
Quantitate

proportional to the amount of bound target at each location on the array and therefore to the level of the mRNA species in the RNA sample being tested. Comparison of the levels of fluorescence produced by each chip can identify differential gene expression between cell populations.

Affymetrix GeneChip® Rat Genome U34A arrays were used to identify genes whose expression was regulated during neuronal apoptosis after NGF withdrawal. PC6-3 cells were used as a model system to generate sufficient RNA for analysis. Genes involved in the apoptosis of PC6-3 cells are induced relatively early after NGF withdrawal. One such gene is the BH3-only protein DP5, which peaks in level at 16 hours after NGF withdrawal in PC12 cells and sympathetic neurons (Imaizumi *et al.*, 1997). In the case of sympathetic neurons, the cell death commitment point, when 50% of neurons can no longer be rescued from apoptosis by re-addition of NGF, is around 22 hours after NGF withdrawal (Deckwerth and Johnson, 1993). Therefore, 16 hours was chosen as the time point at which RNA was extracted from PC6-3 cells for analysis. This is after the induction and activation of c-Jun and prior to the cell death commitment point.

3.2 Results

3.2.1 PC6-3 cells undergo cell death after NGF withdrawal

PC6-3 cells were differentiated in the presence of NGF for 7 days, and then cultured in the presence or absence of NGF for 16 hours. After NGF withdrawal, the cells display the classic morphological changes associated with programmed cell death, such as shrunken cell bodies, membrane blebbing and neurite fragmentation. Figure 3.2 shows PC6-3 cells at different stages of differentiation and during cell death after NGF withdrawal.

3.2.2 Isolation of RNA for Affymetrix GeneChip® analysis

RNA was extracted from neuronally differentiated PC6-3 cells that had been cultured in the presence or absence of NGF for 16 hours. Initially, samples of total RNA (15-20 μg) were electrophoresed on an agarose-formaldehyde gel in the presence of ethidium bromide to determine RNA integrity (Figure 3.3A). The presence of intact 28S and 18S ribosomal RNA bands indicated that the RNA had not become degraded

during purification. The *dp5* RNA is known to be induced in PC12 cells after NGF withdrawal (Imaizumi *et al.*, 1997). To further examine the integrity of RNA samples, northern blot analysis of *dp5* levels in PC6-3 cells cultured in the presence and absence of NGF was performed. mRNA was purified from total RNA and samples (5 μg) electrophoresed on an agarose-formaldehyde gel. *Dp5* probe DNA was amplified from a rat brain cDNA library by PCR and *bcl-x_L* probe DNA was generated by digesting the pCDFLAGBcl-x_L vector with BglII and EcoRI restriction enzymes. In the northern blot shown, *dp5* was up-regulated 3.2 fold after 16 hours of NGF deprivation (Figure 3.3B). This induction of *dp5* following NGF withdrawal in PC6-3 cells established that the RNA samples were of an appropriate quality for Affymetrix GeneChip analysis.

The quality of mRNA was also assessed using the Agilent 2100 Bioanalyzer with the Agilent RNA 6000 Nano LabChip kit. This assay produced an mRNA trace that had standard features, including a broad peak indicating the range of mRNA species size isolated, two ribosomal RNA peaks and a marker peak.

3.2.3 Preparation of samples for Affymetrix GeneChip® hybridisation

Three independent Affymetrix GeneChip® array experiments were performed using RNA from differentiated PC6-3 cells cultured for 16 hours in the presence or absence of NGF. In each experiment, the RNA quality was assessed as described above and each set of two populations of RNA was prepared for chip hybridisation (Figure 3.4). Initially, cDNA was prepared from mRNA samples isolated from PC6-3 cells in the presence or absence of NGF (Figure 3.4A). The intense bands correspond to cDNA generated from the 28S and 18S ribosomal RNA bands. The DNA smear indicates cDNA in the range of 400 to 2,000 base pairs. Biotin-labelled cRNA was prepared from the cDNA and purified using Qiagen RNeasy columns (Figure 3.4B). This is observed as a smear on the gel indicating the presence of different sized RNA fragments. Some sample was lost during purification, with less labelled cRNA present in the -NGF sample. Approximately equal amounts of labelled RNA were fragmented to prepare target RNA for hybridisation to the Affymetrix GeneChip® arrays, with the appropriate control samples as described previously (Figure 3.4C).

Figure 3.2 PC6-3 cells at different stages of differentiation and cell death

PC6-3 cells were maintained undifferentiated (i) in normal growth medium. In experiments, cells were differentiated by the addition of NGF. After 3 days in the presence of NGF (ii) cells begin to form neurites and after 7 days in NGF-containing medium (iii) the cells have exited from the cell cycle and become fully differentiated with long neurite-like projections. PC6-3 cells cultured in the presence of NGF for 7 days and then in the absence of NGF for 16 hours (iv) and 24 hours (v) have begun to display signs of cell death. White arrows indicate dead cells. Cells become rounded and shrunken in appearance, neurites fragment and the cells detach from the cell culture dish. Cells were examined on a Zeiss Axiovert 200 microscope and photographed using an Axiocam digital camera and Axiovision software. Images were exported as TIFFs and processed in Adobe photoshop. The bar represents 40 μM.

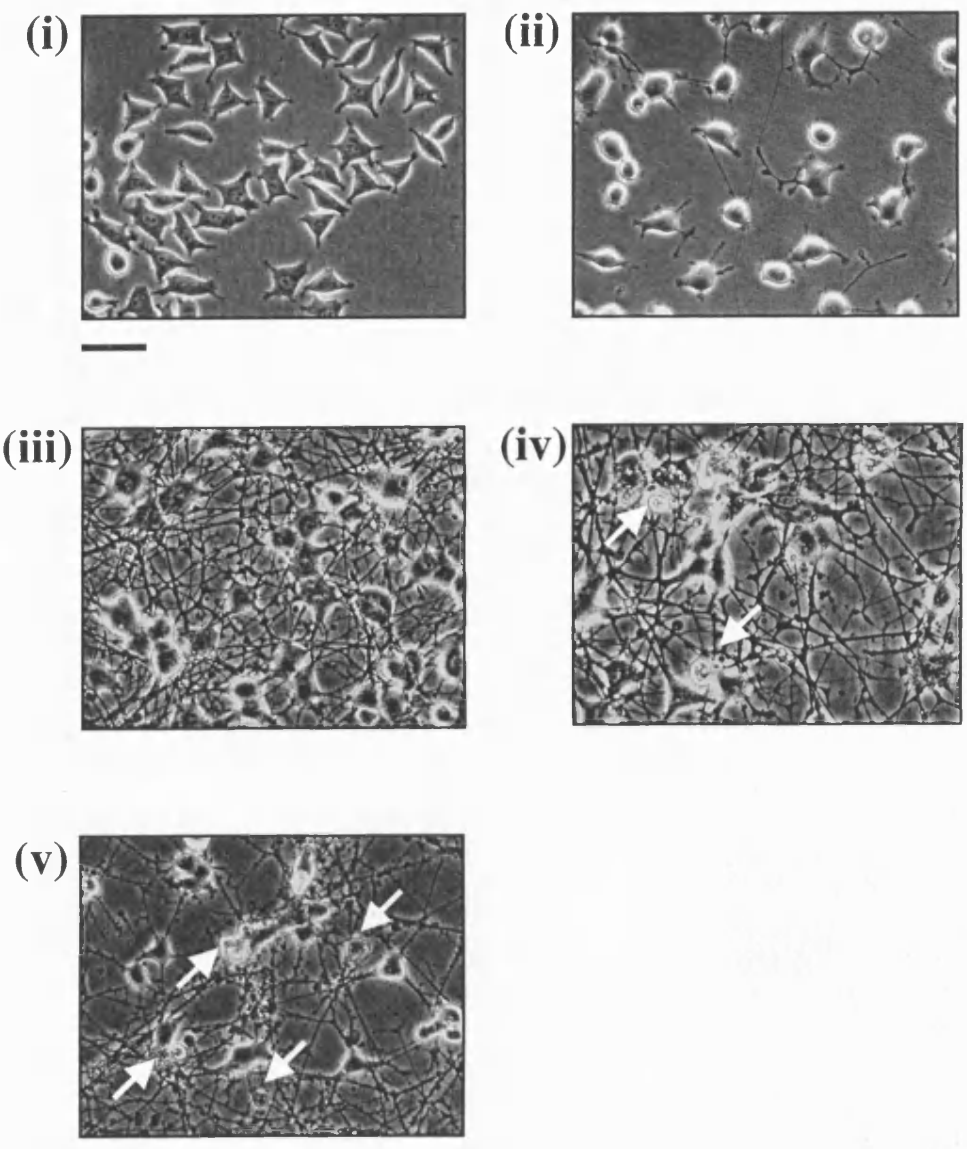
(i)
(ii)
(iii)
(iv)
(v)

Figure 3.3 *DP5* is up-regulated in PC6-3 cells deprived of NGF for 16 hours

(A) PC6-3 cells were differentiated for 7 days in the presence of NGF and then cultured for 16 hours in the presence or absence of NGF. Total RNA was isolated and electrophoresed on a 1% agarose-formaldehyde gel in the presence of ethidium bromide for visualisation of the 28S and 18S ribosomal RNA bands. The molecular weight marker (M) used was the 0.24 kb - 9.5 kb RNA ladder from Invitrogen.

(B) mRNA was purified from total RNA and mRNA samples (5 μg) were electrophoresed on a 1% agarose-formaldehyde gel and transferred to nitrocellulose. Northern blotting was performed using ^{32}P-labelled *dp5* and *bcl-x$_L$* probe DNAs. Membranes were exposed to a phosphorimager screen for 1-4 nights at room temperature and the screens were scanned using a Typhoon™ 8600 phosphorimager to quantitate the levels of *dp5* and *bcl-x$_L$* mRNA. RNA bands were quantitated using the ImageQuant analysis program and the ratio of *dp5* to *bcl-x$_L$* was calculated. *Bcl-x$_L$* RNA levels remain relatively constant for the first 24 hours after NGF withdrawal and were used as a control for gel loading. In the northern blot shown, *dp5* is up-regulated 3.2 fold after 16 hours of NGF deprivation. The size of the *dp5* and *bcl-x$_L$* mRNAs is indicated.

A

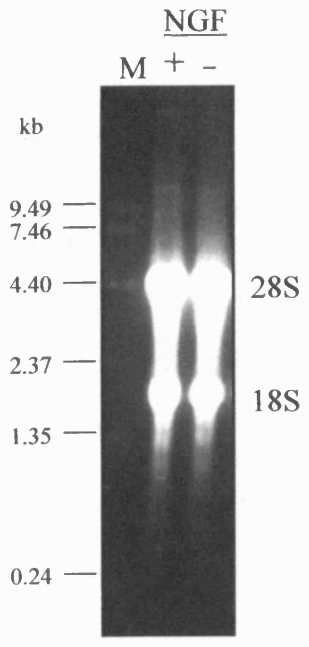

B

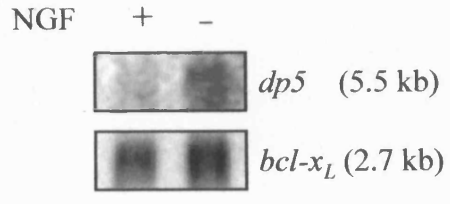

Figure 3.4 Preparation of samples for Affymetrix GeneChip® hybridisation

(A) RNA was isolated from differentiated PC6-3 cells cultured for 16 hours in the presence (+) or absence (-) of NGF. mRNA samples were reverse transcribed into cDNA and 1/12th volume (1 µl) of each cDNA sample was electrophoresed on a 1% agarose gel.

(B) Biotin-labelled cRNA was prepared from the cDNA using the ENZO BioArray™ HighYield™ RNA transcript labeling kit and purified using Qiagen RNeasy columns. 1 µl samples before (pre) and after (post) purification were removed and analysed on a 1% agarose gel.

(C) Labelled RNA was fragmented to prepare target RNA for hybridisation to Affymetrix GeneChip® arrays and 2 µl samples were electrophoresed on a 1% agarose gel for quantification. The marker (M) was the 1 kb ladder from Invitrogen.

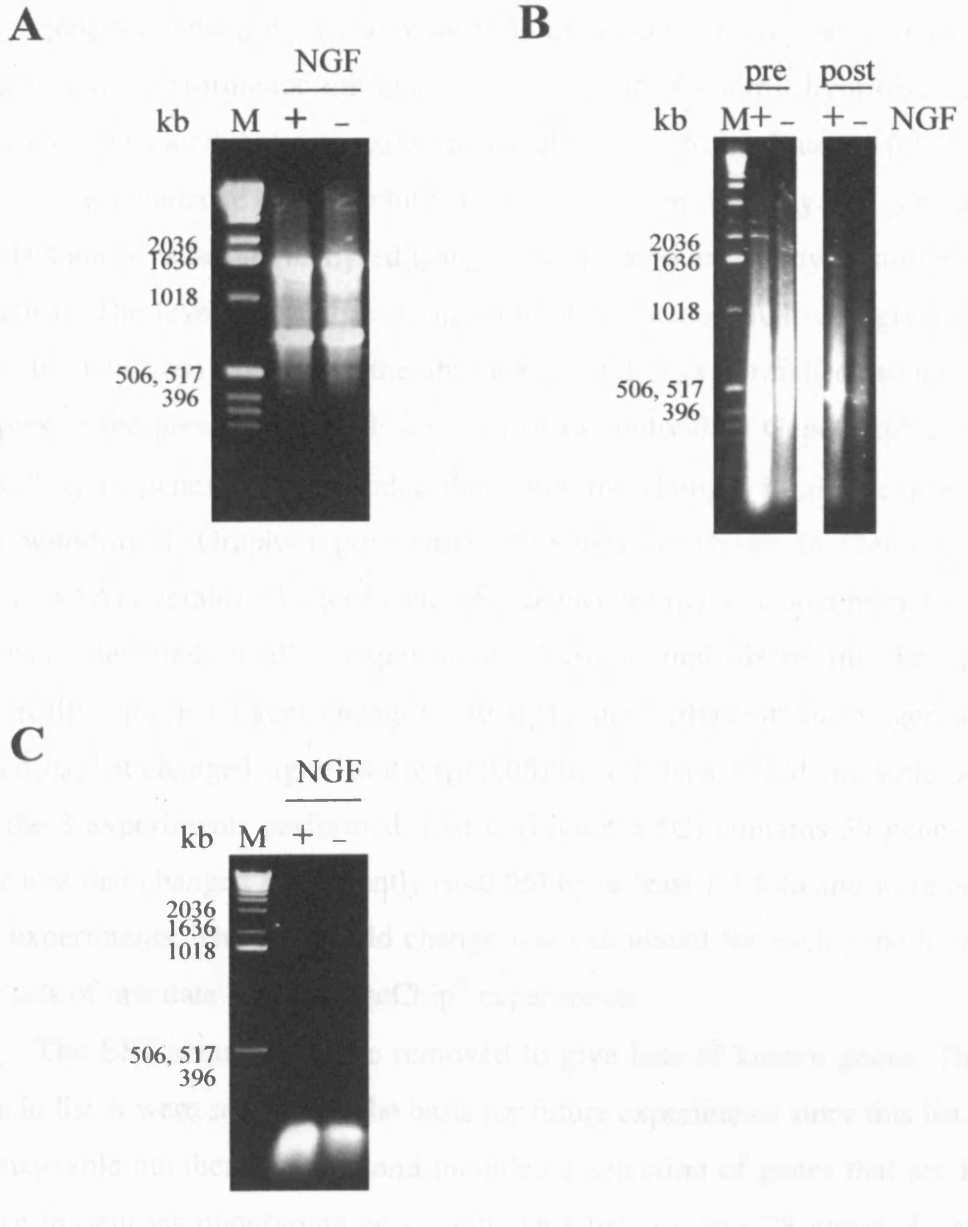
A
NGF
kb M + -
2036
1636
1018
506, 517
396
B
pre post
kb M+ - + - NGF
2036
1636
1018
506, 517
396
C
NGF
kb M + -
2036
1636
1018
506, 517
396

3.2.4 78 genes were induced or repressed in PC6-3 cells after NGF withdrawal

Data was collected using Affymetrix Microarray Suite 5.0 software with the U34A gene set. This provides an indication of sample integrity, assay execution, and hybridization performance through the assessment of control hybridizations. These parameters indicated that each experiment had been performed successfully.

The abundance of each transcript represented on the array was generated as the raw data and was further analysed using GeneSpring 6 data analysis software (Silicon Genetics). The level of each transcript in the presence of NGF was given a value of one. The data from samples in the absence of NGF was normalised to the data from samples in the presence of NGF for each of the individual GeneChip® experiments. Three lists of genes were compiled that show the changes in gene expression after NGF withdrawal. Graphs representing these lists are shown in Figure 3.5. List A (Figure 3.5A) contains 134 genes and EST sequences that changed more than 1.5 fold and were detected in all 3 experiments. Further analysis of the data generated statistically significant gene changes. List B (Figure 3.5B) contains 57 genes and EST sequences that changed significantly ($p<0.05$) by at least 1.5 fold and were detected in 2 of the 3 experiments performed. List C (Figure 3.5C) contains 39 genes and EST sequences that changed significantly ($p<0.05$) by at least 1.5 fold and were detected in all 3 experiments. The mean fold change was calculated for each gene based on the three sets of raw data for the GeneChip® experiments.

The EST sequences were removed to give lists of known genes. The known genes in list A were selected as the basis for future experiments since this list provided a manageable number of genes and included a selection of genes that are known to change in neurons undergoing cell death. This list contains 78 genes, 41 genes that increased and 37 genes that decreased, after 16 hours of NGF withdrawal. These genes were classified into tables according to their proposed function and include, transcription factors, cell growth/apoptosis regulators, signalling molecules, protein regulators, receptors, ion transporters, electron transporters and genes involved in various types of metabolism. These results are shown on the following pages in Tables 1 – 11. Gene lists B and C are represented in the form of tables in Appendix A and B.

Figure 3.5 Graphical representation of the lists showing changes in gene expression after NGF withdrawal

Data was analysed using GeneSpring 6 data analysis software (Silicon Genetics). The level of each transcript in the presence of NGF was given a value of one. Data from samples in the absence of NGF were normalised to the data from samples in the presence of NGF, for each of the individual GeneChip® experiments. Three lists of genes were compiled that show the changes in gene expression after NGF withdrawal. Graphs representing these lists are shown. (A) List A contains 134 genes and EST sequences that changed more than 1.5 fold and were detected all 3 experiments. (B) List B contains 57 genes and EST sequences that changed significantly ($p<0.05$) by at least 1.5 fold and were detected in 2 of the 3 experiments. (C) List C contains 39 genes and EST sequences that changed significantly ($p<0.05$) by at least 1.5 fold and were detected in all 3 experiments. The average fold change was calculated for each gene based on the 3 GeneChip® experiments. The y-axis on the graphs is a log scale. Increases in gene expression are shown in purple and decreases in blue. The level of expression in the presence of NGF (+) is shown as 1 on the left of the graph. Expression levels in the absence of NGF (-) are shown on the right of the graph.

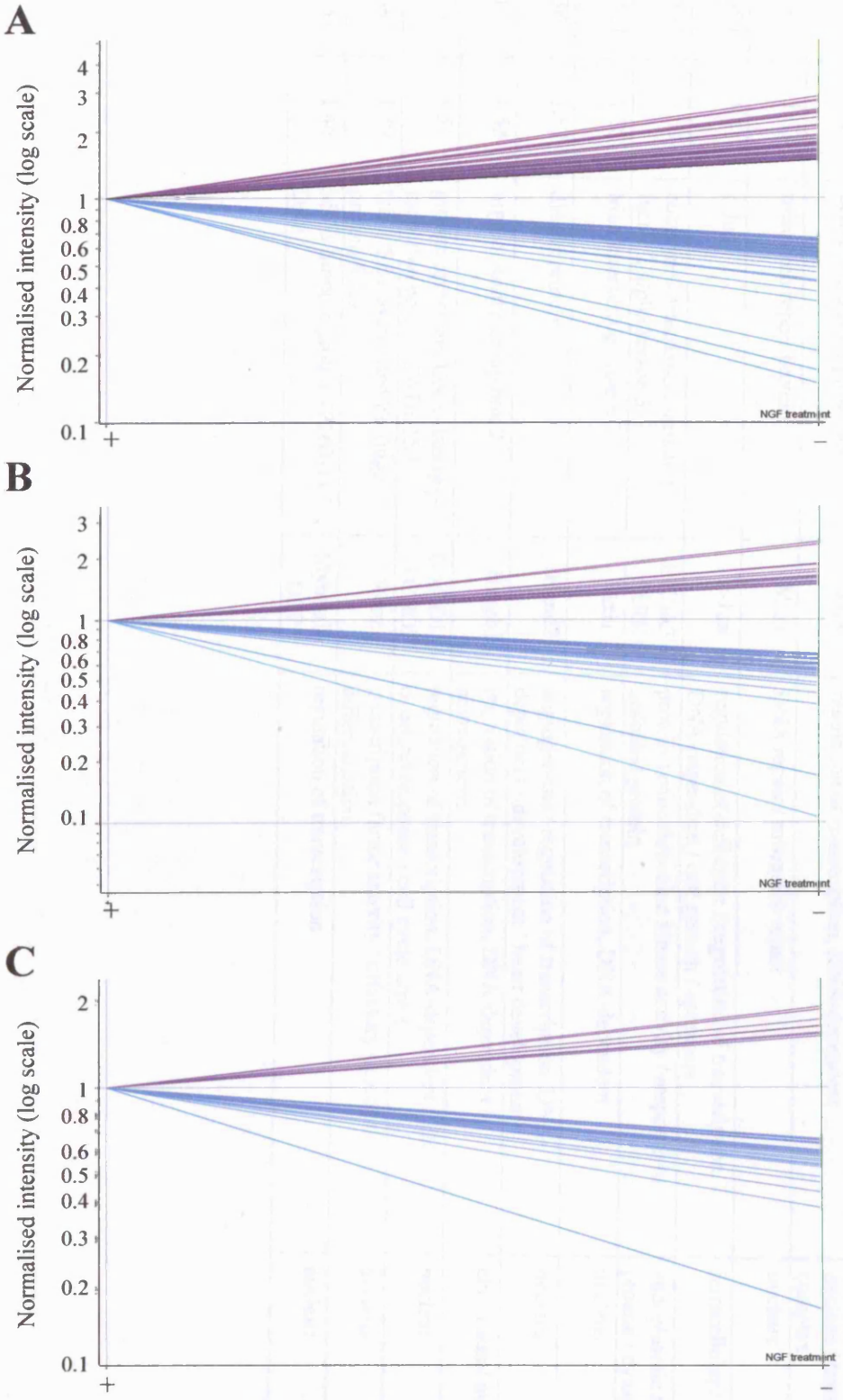
A
Normalised intensity (log scale)
4
3
2
1
0.8
0.6
0.5
0.4
0.3
0.2
0.1
+
NGF treatment
−
B
Normalised intensity (log scale)
3
2
1
0.8
0.6
0.5
0.4
0.3
0.2
0.1
+
NGF treatment
−
C
Normalised intensity (log scale)
2
1
0.8
0.6
0.5
0.4
0.3
0.2
0.1
+
NGF treatment
−

Table 1 Increased genes Transcription/Translation/DNA repair

Accession number	Fold Increase	Gene	Gene Symbol	Function	Cellular component
M63282	2.68	activating transcription factor 3	Atf3	regulation of transcription, DNA-dependent	nucleus / transcription factor complex
U80054	1.63	mismatch repair protein	Mlh1	DNA repair / mismatch repair	nucleus
AI175959	1.61	c-Jun	c-Jun	regulation of cell cycle / regulation of transcription, DNA-dependent / cell growth / apoptosis	intracellular / nucleus
AF096835	1.59	eukaryotic translation initiation factor 2 alpha kinase 3	Eif2ak3 / PERK	protein serine/threonine kinase activity / response to unfolded protein	endoplasmic reticulum / membrane protein / cytoplasm
AA893611	1.58	Max interacting protein 1	Mxi1	regulation of transcription, DNA-dependent	nucleus
Y08138	1.57	dHand protein	Hand2	angiogenesis / regulation of transcription, DNA-dependent / development / heart development	nucleus
D84418	1.53	high mobility group box 2	Hmgb2	regulation of transcription, DNA-dependent / neurogenesis	chromatin / nucleus / chromosome
U30186	1.51	growth arrest and DNA-damage-inducible protein GADD153	GADD153 / CHOP	regulation of transcription, DNA-dependent / ER-overload response / cell cycle arrest	nucleus
U92564	1.49	Olf-1/EBF associated Zn finger protein Roaz	Roaz	transcription factor activity / olfactory neuronal differentiation	nucleus
AI229637	1.46	MYB binding protein (P160)1a / DBP	Mybbp1a / DBP	regulation of transcription	nucleus

Table 2 Increased genes Apoptosis/Cell cycle/Cell growth/differentiation

Accession number	Fold Increase	Gene	Gene Symbol	Function	Cellular component
AI014169	1.78	up-regulated by 1,25-dihydroxyvitamin D-3	Vdup1 / Txnip	regulation of cell proliferation / inhibition of thioredoxin	cytoplasm
AF020618	1.6	myeloid differentiation primary response gene 116/GADD34	Myd116 / GADD34	regulation of cell growth / apoptosis	endoplasmic reticulum / ribosome
M60921	1.57	B-cell translocation gene 2	Btg2	anti-proliferative / signal transduction / cellular differentiation / transcription factor activity / DNA repair	nucleus
L26268	1.51	B-cell translocation gene 1	Btg1	anti-proliferative / t(8;12)(q24;q22) chromosomal translocation in a B-cell chronic lymphocytic leukemia	nucleus / cytoplasm

Table 3 Increased genes Receptor/signalling/ion transport

Accession number	Fold Increase	Gene	Gene Symbol	Function	Cellular component
J03754	1.9	ATPase, Ca++ transporting, plasma membrane 2	Atp2b2	cation transport / calcium ion transport / perception of sound / metabolism	plasma membrane / integral to membrane
L33869	1.86	Ceruloplasmin	Cp	iron ion homeostasis / plasma membrane copper ion transport	extracellular / extrinsic to plasma membrane, GPI-anchored
J05087	1.76	ATPase, Ca++ transporting, plasma membrane 3 / PMCA3	Atp2b3 / PMCA3	ATPase / calcium ion transport	plasma membrane
S75359	1.74	bone morphogenetic protein receptor, type 1A	Bmpr1a	serine/threonine kinase receptor / bone formation	membrane
AI236721	1.58	14-3-3 protein gamma-subtype	Ywhag	intracellular signaling cascade / enzyme activator activity / protein kinase C binding / protein targeting / cell cycle	cytoplasm
D17352	1.57	low Mr GTP-binding protein	Rab27a	GTP binding / GTPase activity / intracellular membrane trafficking	cytoplasm
AJ000556	1.56	Janus kinase 1	Jak1	protein amino acid phosphorylation / intracellular signaling cascade	cytoskeleton
U03120	1.52	solute carrier family 5 (sodium /glucose cotransporter), member 1	Slc5a1	sodium ion transport / glucose transport / metanephros development	membrane / integral to membrane / apical plasma membrane

Table 4 Increased genes Protein modification/ Metabolism / Synthesis

Accession number	Fold Increase	Gene	Gene Symbol	Function	Cellular component
AF102854	2.58	membrane-associated guanylate kinase-interacting protein	Cnksr2 / MAGUIN	protein binding	postsynaptic membrane / synaptosome
AA893357	2.58	Membrane associated guanylate kinase interacting protein-like 1	Magi1	kinase activity	integral to membrane
E03344	2.48	peroxisomal membrane protein 3	Pxmp3	peroxisome organization and biogenesis	peroxisomal membrane / integral to membrane
M26686	2.3	protein-L-isoaspartate (D-aspartate) O-methyltransferase 1	Pcmt1 / PIMT	S-adenosylmethionine-dependent methyltransferase activity / protein modification	cytoplasmic
Y09333	1.94	mitochondrial acyl-CoA thioesterase 1	Mte1	catalytic activity / hydrolase / palmitoyl-CoA hydrolase activity / serine esterase activity / lipid metabolism	mitochondrion
E04239	1.86	choline kinase alpha	Chka	Acetylcholine synthesis / choline kinase activity / kinase activity / transferase activity / cell growth	cytoplasm
M64755	1.55	cysteine-sulfinate decarboxylase	Csad	amino acid metabolism / taurine biosynthesis	cytoplasm (?)
S85184	1.5	cathepsin L	Ctsl	proteolysis and peptidolysis	extracellular space / lysosome
U38379	1.59	gamma-glutamyl hydrolase	Ggh	gamma-glutamyl hydrolase activity / hydrolase activity / peptidase	extracellular space / lysosome
AI145502	1.57	prostaglandin F2 receptor negative regulator	Ptgfrn	negative regulation of protein biosynthesis	integral to membrane
AA892897	1.49	procollagen lysine, 2-oxoglutarate 5-dioxygenase 2	Plod2	hydroxylation of lysine residues in procollagen / collagen formation	endoplasmic reticulum / integral to membrane
M62388	1.47	ubiquitin conjugating enzyme	LOC81816	ubiquitin-dependent proteolysis	nucleus
AB000199	1.46	CCA2 protein	Hsd3b7	steroid biosynthesis / oxidoreductase activity / regulation of cell growth	endoplasmic reticulum / integral to membrane

Table 5 Increased genes Cell-cell interaction/cell migration/Structural

Accession number	Fold Increase	Gene	Gene Symbol	Function	Cellular component
U75928 AA891204 Y13714	1.78 1.75 1.65	secreted acidic cysteine rich glycoprotein	Sparc	calcium ion binding / structural protein	basement membrane / extracellular / extracellular matrix (sensu Metazoa)
D85183	1.55	protein tyrosine phosphatase, non-receptor type substrate 1	Ptpns1	cell motility / actin filament organization / cell-matrix adhesion / cell migration	extracellular space / integral to membrane
S61868	1.53	syndecan 4	Sdc4	cell adhesion / cell-cell signaling	extracellular space / membrane / integral to membrane

Table 6 Increased genes Other genes

Accession number	Fold Increase	Gene	Gene Symbol	Function	Cellular component
AJ131888	2.01	sperm autoantigenic protein 17	Spa17	protein binding / fertilisation	sperm acrosome
M13100	2.01	LINE retrotransposable element 3	L1Rn/Lre3	retrotransposon / genome diversification	DNA / nucleus
AF018261	1.54	Epsin 1	Epn1	endocytosis	cytoplasm / peripheral membrane

Table 7 Decreased genes Transcription/Translation/DNA repair

Accession number	Fold Decrease	Gene	Gene Symbol	Function	Cellular component
AF030089	1.87	activity and neurotransmitter-induced early gene protein 4	Ania4	regulation of transcription, DNA dependent	nucleus
S69329	1.64	ISL1 transcription factor, LIM/homeodomain 1	Isl1	energy pathways / regulation of transcription, DNA-dependent / development	nucleus
Y00396	1.62	c-myc / v-myc myelocytomatosis viral oncogene homolog (avian)	Myc	regulation of cell cycle / transcription initiation / regulation of transcription, DNA-dependent / cell growth and/or maintenance / pathogenesis	nucleus
U75397	1.61	early growth response 1 / nerve growth factor-induced gene	Egr1	regulation of transcription, DNA-dependent / learning and/or memory / positive regulation of transcription from Pol II promoter / thymocyte differentiation	nucleus
M19651	1.52	Fra-1 / fos-like antigen 1	Fra-1	regulation of transcription, DNA-dependent / positive regulation of transcription from Pol II promoter, mitotic / Wnt signaling	nucleus
AA891041	1.51	Jun-B oncogene	Junb	regulation of transcription, DNA-dependent / positive regulation of transcription from Pol II promoter, mitotic	nucleus
Y09507	1.51	hypoxia inducible factor 1, alpha subunit	Hif1a	response to hypoxia / regulation of transcription, DNA-dependent / signal transduction	nucleus

Table 8 Decreased genes Apoptosis/Cell cycle/Cell growth/differentiation

Accession number	Fold Decrease	Gene	Gene Symbol	Function	Cellular component
U42627 X94185	5.46 5.33	dual specificity phosphatase 6 / MAPkinase phosphatase-3	Dusp6 / MKP-3	protein amino acid dephosphorylation / cell differentiation / MAP kinase phosphatase activity	cytoplasm
AI639318 AA859878 AF042830	2.44 2.19 1.56	ret proto-oncogene	Ret	regulation of cell cycle / protein phosphorylation / cell adhesion / transmembrane receptor protein tyrosine kinase ligand binding / cell growth / morphogenesis	extracellular space / membrane / integral to membrane
AI030286 D10938	2.06 1.48	brain derived neurotrophic factor	Bdnf	neurogenesis / neuron differentiation / regulation of long-term and short-term neuronal synaptic plasticity	extracellular space
S63521	1.78	glucose-regulated protein GRP78	GRP78	Heat shock protein family / antiapoptotic ER chaperone-glucose-regulated protein / inhibit PERK phosphorylation / ER stress	endoplasmic reticulum

Table 9 Decreased genes Receptor/signalling/ion transport

Accession number	Fold Decrease	Gene	Gene Symbol	Function	Cellular component
U36895	1.8	putative vomeronasal receptor 3	Vnr3/VN3	olfactory receptor / putative transmembrane receptor	putative membrane protein
X80187	1.75	bradykinin receptor b2	Bdkrb2	G-protein coupled receptor protein signaling pathway / perception of pain	integral to membrane
AA998446	1.72	phosphatidylinositol transfer protein, beta	Pitpnb	transport	intracellular
S74141	1.75	hemopoietic cell kinase	Hck	protein amino acid phosphorylation / intracellular signaling cascade	cytoplasm / membrane
U01227 U59672	1.62 1.49	5-hydroxytryptamine (serotonin) receptor 3a	Htr3a	synaptic transmission / transport / ion transport	extracellular space / integral to plasma membrane
U93306	1.59	kinase insert domain protein receptor	Kdr	angiogenesis / protein amino acid phosphorylation / transmembrane receptor protein tyrosine kinase signaling pathway / cell fate commitment	extracellular space / membrane / integral to membrane
X05137	1.56	nerve growth factor receptor (TNFR superfamily, member 16)	Ngfr	lipid metabolism / apoptosis / induction of apoptosis / signal transduction / neurogenesis / axon guidance / central nervous system development	extracellular space / integral to membrane
AF061266	1.52	transient receptor protein 1	Trp1	cation channels / receptor-dependent activation / Store-operated calcium entry	membrane
L35558	1.47	solute carrier family 1 (neuronal/epithelial high affinity glutamate transporter), member 1	Slc1a1	transport / dicarboxylic acid transport	integral to plasma membrane / membrane

Table 10 Decreased genes Protein modification / Metabolism / Synthesis / electron transport

Accession number	Fold Decrease	Gene	Gene Symbol	Function	Cellular component
M29249 X55286	3.28 2.01	3-hydroxy-3-methylglutaryl-Coenzyme A reductase	Hmgcr	lipid metabolism / cholesterol biosynthesis / biosynthesis	endoplasmic reticulum / endoplasmic reticulum membrane / integral to membrane
AI177004 X52625	2.53 2.15	3-hydroxy-3-methylglutaryl-Coenzyme A synthase 1	Hmgcs1	acetyl-CoA metabolism / cholesterol biosynthesis	cytoplasm
E12625 AI172293	2.1 1.74	sterol-C4-methyl oxidase-like	Sc4mol	metabolism / sterol biosynthesis	endoplasmic reticulum / integral to membrane
D37920	1.85	squalene epoxidase	Sqle	electron transport / aromatic compound metabolism / metabolism / Cholesterol biosynthesis	integral to membrane
M89945 AI180442	1.81 1.62 1.56	farensyl diphosphate synthase	Fdps	cholesterol biosynthesis / isoprenoid biosynthesis	cytoplasm
AF003835	1.71	isopentenyl-diphosphate delta isomerase	Idi1	cholesterol biosynthesis / isoprenoid biosynthesis / carotenoid biosynthesis / sterol biosynthesis	peroxisome
U67995 AF036761 M15114	1.67 1.58 1.45	stearoyl-Coenzyme A desaturase 2	Scd2	fatty acid synthesis	integral to membrane
M95591	1.65	farnesyl diphosphate farnesyl transferase 1	Fdft1	cholesterol biosynthesis / isoprenoid biosynthesis / lipid biosynthesis	endoplasmic reticulum / farnesyl-diphosphate farnesyl transferase complex / integral to membrane
AA963449 AB004096 U17697	1.59 1.55 1.54	cytochrome P450, subfamily 51 (Cyp51)	Cyp51	electron transport / proteolysis and peptidolysis / cholesterol biosynthesis	extracellular space / integral to membrane

Table 10 continued

Accession number	Fold Decrease	Gene	Gene Symbol	Function	Cellular component
AA963839	1.54	diaphorase 1	Dia1	electron transport	soluble fraction / endoplasmic reticulum / membrane
J02585	1.51	stearoyl-Coenzyme A desaturase 1	Scd1	fatty acid synthesis	integral to membrane
U53706	1.49	mevalonate (diphospho) decarboxylase	Mvd	cholesterol biosynthesis / isoprenoid biosynthesis / sterol biosynthesis / phosphorylation	Peroxisome / cytoplasm
U22424	1.49	hydroxysteroid 11-beta dehydrogenase 2	Hsd11b2	Glucocorticoid/mineralocorticoid metabolism	extracellular space / microsome

Table 11 Decreased genes Cell-cell interaction/cell migration/Structural

Accession number	Fold Decrease	Gene	Gene Symbol	Function	Cellular component
AA892506	1.78	coronin, actin binding protein 1A	Coro1a	cytoskeletal protein	actin cytoskeleton / lysosomal membrane
X05834	1.72	fibronectin 1	Fn1	acute-phase response / cell adhesion / metabolism / wound healing / inflammatory response pathway	extracellular / extracellular matrix (sensu Metazoa) / extracellular space
U81037	1.6	neuron-glia-CAM-related cell adhesion molecule	Nrcam	cell adhesion molecule / control of axonal growth / cell growth and motility	integral to membrane
X02412	1.47	tropomyosin 1, alpha	Tpm1	actin-binding protein / muscle contraction / development / cytoskeleton	cytoskeleton

3.3 Discussion

Three Affymetrix GeneChip® experiments were performed using RNA from neuronally differentiated PC6-3 cells cultured either in the presence or absence of NGF for 16 hours. The RNA prepared was carefully checked for integrity using the Agilent 2100 Bioanalyzer with the Agilent RNA 6000 Nano LabChip kit and by northern analysis of *dp5* levels in PC6-3 cells maintained in the presence and absence of NGF. Both methods indicated that the RNA was intact and not degraded.

Analysis of the data produced by the GeneChip® experiments gave three lists of genes that showed a change in expression after NGF withdrawal from PC6-3 cells. List A contains 78 genes whose transcripts changed in level by at least 1.5 fold and which could be detected in all three experiments. Further filtering of the data generated statistically significant gene changes. List B contains 34 genes whose level of expression changed significantly ($p<0.05$) by at least 1.5 fold and for which transcripts were detected in 2 of the 3 experiments performed. List C contains 26 genes whose expression changed significantly ($p<0.05$) by at least 1.5 fold in and detected in all 3 experiments.

List A contains 78 genes, 41 genes that increased and 37 genes that decreased in expression level, after 16 hours of NGF withdrawal. These genes were sorted into tables according to their proposed function. Some of the genes have previously been described as being NGF regulated, or induced in neurons undergoing apoptosis.

The AP-1 family member c-Jun is up-regulated on average 1.61 fold in the three GeneChip® experiments. Induction of this transcription factor was previously observed in PC12 cells deprived of NGF (Mesner *et al.*, 1995) and c-Jun plays an important role in neuronal apoptosis. When sympathetic neurons and PC12 cells are deprived of NGF, the JNK protein kinase cascade is activated and this leads to an increase in the level of c-Jun and increased c-Jun N-terminal phosphorylation. Overexpression of c-Jun kills sympathetic neurons in the presence of NGF and inhibition of the function of c-Jun, either by microinjection of antibodies against c-Jun or by expression of a c-Jun dominant negative mutant, protected sympathetic neurons from NGF withdrawal-induced death (Estus *et al.*, 1994; Ham *et al.*, 1995). In addition, a floxed *c-jun* gene has been successfully knocked out in sympathetic neurons *in vitro* (infected with a CRE adenovirus) and this inhibited NGF withdrawal-induced death (Palmada *et al.*, 2002).

The transcription factor Activating Transcription Factor-3 (ATF-3) was up-regulated 2.68 fold following NGF withdrawal in PC6-3 cells. ATF-3 is a stress-inducible gene that is up-regulated following myocardial ischemia, DNA damage and neuronal axotomy (Chen *et al.*, 1996; Hai *et al.*, 1999; Mashima *et al.*, 2001; Tsujino *et al.*, 2000). It has also been reported that *atf-3* RNA is induced in PC6-3 cells and sympathetic neurons following NGF withdrawal (Mayumi-Matsuda *et al.*, 1999). ATF-3 is a member of the ATF/CREB family of basic/leucine zipper proteins and can repress or activate transcription as a homodimer or heterodimer, respectively. It can heterodimerise with c-Jun to activate transcription (Hai and Curran, 1991; Hsu *et al.*, 1992) and ATF-3 expression correlates with that of c-Jun after nerve injury (Takeda *et al.*, 2000; Tsujino *et al.*, 2000).

ATF-3 is also induced in response to endoplasmic reticulum (ER) stress by a mechanism requiring eIF2 kinases, such as PERK/EIF2AK3, in mouse embryonic fibroblasts (Jiang *et al.*, 2004). PERK phosphorylates eIF2 leading to the inhibition of translation initiation. In the absence of stress, PERK associates with the ER chaperone GRP78 (BiP). This ER chaperone serves to repress PERK activity and thus translation is allowed to proceed. Release of ER chaperones from PERK (when misfolded proteins accumulate in the ER) results in the increased phosphorylation of eIF2α, which impedes translation initiation in the cell. This allows the cell sufficient time to correct the folding problem incurred by the ER stress prior to synthesizing additional proteins (Ma *et al.*, 2002). Although PERK-mediated eIF2α phosphorylation leads to a general suppression of translation, it promotes the preferential translation of certain mRNAs, for example those encoding ATF-3 and ATF-4. Induction of ATF-3 and eIF2 phosphorylation has also been reported following exposure to ethanol, homocysteine, and oxidizing conditions (Cai *et al.*, 2000; Clemens, 1996; Hai and Hartman, 2001; Hai *et al.*, 1999). Increased expression of *PERK* and decreased expression of *GRP78* were observed in my GeneChip® experiments suggesting that ER stress may be involved in PC6-3 cell apoptosis following NGF withdrawal. Up-regulation of *GADD153/CHOP*, a transcription factor involved in the ER-overload response would support this idea. It has been reported that this gene is up-regulated in mouse cerebral cortical neurons exposed to hypoxia for 24 hours (Jin *et al.*, 2002) and induction can be mediated by PERK (Jiang *et al.*, 2004).

GADD153/CHOP was induced 1.51 fold in these GeneChip® experiments. This is a member of the CCAAT/enhancer-binding protein (C/EBP) transcription factor family and is transcriptionally activated by cellular stress signals. It has been demonstrated that arsenite treatment of PC12 cells results in the induction of *GADD153* mRNA expression. There is enhanced binding of ATF4 to a C/EBP-ATF site in the *GADD153* promoter after 2 hours of arsenite treatment, as the *GADD153* mRNA levels increase. Subsequently, there is enhanced binding of ATF3 complexes after 6 hours of arsenite treatment, as *GADD153* expression declines. ATF4 activates, while ATF3 represses, *GADD153* promoter activity through the C/EBP-ATF site (Fawcett *et al.*, 1999). In addition, ATF-3 can interact with the bZIP protein GADD153 to regulate transcription and forms a nonfunctional heterodimer that does not bind to the ATF/CRE consensus site and does not repress transcription (Chen *et al.*, 1996). There seems to be mutual negative regulation between ATF-3 and GADD153, which could allow fine-tuning of the levels of these proteins within the cell (Wolfgang *et al.*, 1997). Ectopic expression of GADD153 induces apoptosis in M1 myeloblastic leukaemia cells and this is accompanied by a down-regulation of *bcl-2* (Matsumoto *et al.*, 1996). Oxidative stress leads to increased binding of Fos and Jun proteins to the AP-1 site in the *GADD153* promoter when transfected into HeLa cells (Guyton *et al.*, 1996). Thus, GADD153 expression may be regulated by the ATF/AP-1 family during apoptosis.

Increased expression of GADD34 correlates with apoptosis (Hollander *et al.*, 1997), and forced overexpression of the protein leads to apoptosis. GADD34 protein modulates protein phosphatase type 1 activity through both direct binding to the protein, as well as through binding to other proteins that also modulate phosphatase activity (Connor *et al.*, 2001). Expression of GADD34 has also been linked to eIF2 dephosphorylation (Novoa *et al.*, 2001) and mRNA levels increase following activation of PERK. In addition, GADD34 is induced by ATF-3. In mouse embryonic fibroblasts lacking ATF-3, reduced GADD34 expression is observed following ER stress (Jiang *et al.*, 2004). In my GeneChip® experiments *GADD34* was induced 1.6 fold following NGF withdrawal from PC6-3 cells. It has been reported that *GADD34* mRNA is induced following transient forebrain ischemia in mice (Doutheil *et al.*, 1999).

Vdup1/Txnip (Vitamin D3 up-regulated protein 1/thioredoxin inhibitor protein) mRNA is induced rapidly in cerebellar granule neurons undergoing apoptosis during removal of high potassium and in sympathetic neurons deprived of NGF (Saitoh *et al.*, 2001). Txnip inhibits the antioxidant protein thioredoxin. Thioredoxin can inhibit the apoptosis signal-regulating kinase 1 (ASK1). In sympathetic neurons and PC12 cells, ASK1 activates the JNK pathway and thus promotes apoptosis (Kanamoto *et al.*, 2000). Inhibition of thioredoxin by Txnip would remove the inhibition on ASK1 and thus facilitate activation of the JNK pathway. This transcript is up-regulated 1.78 fold in my microarray experiment.

Dual specificity phosphatase 6/MAP kinase phosphatase-3 (Dusp6/MKP-3) is a protein tyrosine phosphatase that dephosphorylates the extracellular signal-regulated protein kinase (ERK). Expression of this phosphatase is induced by NGF in PC12 cells (Camps *et al.*, 1998) and levels decrease following NGF withdrawal. This was found to decrease ~ 5.4 fold in my microarray experiments.

JunB and Fra-1 (Fos-related antigen 1) are members of the Jun/AP-1 family of transcription factors. In contrast to *c-jun*, the expression of these genes decreased 1.5 fold after NGF withdrawal from PC6-3 cells. JunB can antagonise the DNA binding and function of c-Jun (Chiu *et al.*, 1989; Deng and Karin, 1993; Schlingensiepen *et al.*, 1993). It has weak DNA binding activity and so is thought to act as transcriptional repressor. It has been reported to form dimers with both c-Jun and ATF-3, and so would thus repress their activity. Fra-1 can also form dimers with c-Jun and is thought to function as a negative regulator since it lacks transactivation domains and fails to activate transcription when fused to the DNA-binding domain of Gal4 (Metz *et al.*, 1994). NGF induces Fra-1 and JunB expression in PC12 cells (Boss *et al.*, 2001; Ham *et al.*, 1995) and therefore levels may drop after NGF withdrawal. Decreased levels of these transcription factors could therefore lead to increased c-Jun or ATF-3 activity within a cell.

The mRNA encoding the BH3-only protein DP5 increases in level in PC12 cells and sympathetic neurons after NGF withdrawal (Imaizumi *et al.*, 1997) and this was confirmed in my northern blotting experiments (Figure 3.3). However, *dp5* was not one of the up-regulated genes in my GeneChip® experiments. The *dp5* oligonucleotide probes on the arrays were designed to be complementary to the mRNA at the 5' end of the sequence. The *dp5* mRNA is 5.5 kb in length and therefore

it is unlikely that the IVT reaction, during the target preparation, produced cRNA sequences of sufficient length to include the very 5' end. This would result in an inaccurate assessment of *dp5* levels within the different RNA populations.

The statistically significant lists B and C reduced the number of genes that were found to change after NGF withdrawal from differentiated PC6-3 cells. Many of the genes previously reported to change after NGF withdrawal were no longer on the lists, for example *c-jun* and *atf-3*. This is possibly due to the nature of the experiment performed. The RNA samples were extracted 16 hours after NGF withdrawal, and thus the kinetics of induction of a gene will determine whether it is detected at a higher level or not. For example, c-Jun is induced by 6 hours after NGF withdrawal in PC12 cells (Mesner *et al.*, 1995). By 24 hours, levels are comparable to those in the presence of NGF. If all cells are not synchronous in their kinetics of induction some may take longer to induce *c-jun* and thus a higher level could be detected at 16 hours and in other experiments levels of *c-jun* may have decreased again by 16 hours. This could also be true for the expression level of *aft-3*. ATF-3 is not present in the statistically significant lists of genes, even though its level of expression was increased on average 2.68 fold in 3 experiments. Looking at the raw data for this gene shows that *atf-3* expression levels did not change in one of the experiments and changed by 4.99 fold in another. This therefore cannot be classified as a statistically significant change in expression.

However, ATF-3 was selected for more detailed analysis because it was the most highly up-regulated gene in the Affymetrix GeneChip® experiments and is a potential c-Jun dimerisation partner and c-Jun target gene, whose role in neuronal apoptosis had not been investigated in detail previously.

Chapter 4: ATF-3 is induced during neuronal apoptosis

4.1 Introduction

Sympathetic neuron apoptosis following NGF withdrawal, is blocked by inhibitors of RNA and protein synthesis (Martin *et al.*, 1988). This suggests that this cell death requires new gene expression and therefore that transcription factors play a critical role in the death process. The AP-1 family member c-Jun has been shown to be an important component of this process. When sympathetic neurons are deprived of NGF an intracellular signalling cascade is activated that induces the basic/leucine zipper transcription factor c-Jun. Removal of NGF from its receptors on the cell surface leads to the activation of c-Jun N-terminal kinase (JNK). JNK activity is necessary for c-Jun phosphorylation, *c-jun* promoter activation and the NGF withdrawal-induced death of sympathetic neurons (Eilers *et al.*, 2001; Harding *et al.*, 2001). This phosphorylation of c-Jun increases the transcriptional activity of the protein. The c-Jun transcription factor acts via AP-1 DNA binding sites present in the promoters of target genes and also in *c-jun* itself (Angel *et al.*, 1988). c-Jun binds to DNA as a homodimer or heterodimer with other basic/leucine zipper transcription factors, such as c-Fos, Jun D, ATF-2 and ATF-3, to regulate gene expression (Deng and Karin, 1993; Hai and Curran, 1991; Hsu *et al.*, 1992).

The transcription factor ATF-3 is a member of the ATF/CREB family of basic leucine zipper proteins originally defined by their ability to bind the consensus ATF/CRE site (5'-TGACGTCA-3'). These proteins bind DNA via the basic leucine zipper (bZIP) region, where there is most homology between different family members. ATF-3 acts as a transcriptional repressor when a homodimer (Hai *et al.*, 1999), but has been reported to act as a transactivator when a heterodimer with other proteins, such as c-Jun (Hai and Curran, 1991; Hsu *et al.*, 1992). ATF-3 is a stress-inducible gene that is up-regulated following myocardial ischemia, DNA damage, neuronal axotomy and excitotoxic insult (Chen *et al.*, 1996; Hai *et al.*, 1999; Mashima *et al.*, 2001; Tsujino *et al.*, 2000). The injury specific expression of ATF-3 in axotomised dorsal root ganglia and spinal cord following sciatic nerve cut (Tsujino *et al.*, 2000) and retinal ganglion cells after optic nerve injury (Takeda *et al.*, 2000)

correlates with expression of c-Jun in these cells. The *aft-3* promoter contains a number of AP-1 binding sites and can be activated by overexpression of c-Jun and ATF-2 in HeLa cells (Liang *et al.*, 1996) and by MEKK1, an upstream activator of JNK, in HCT116 colorectal carcinoma cells (Fan *et al.*, 2002). ATF-3 therefore has the potential to be a dimerisation partner of c-Jun and/or a c-Jun target gene in sympathetic neurons undergoing apoptosis.

My Affymetrix GeneChip® results showed that ATF-3 expression was up-regulated 2.68 fold following NGF withdrawal in differentiated PC6-3 cells. In addition it has previously been reported that *atf-3* RNA is induced in PC6-3 cells and sympathetic neurons following NGF withdrawal (Mayumi-Matsuda *et al.*, 1999). ATF-3 was selected for more detailed analysis because it is a potential c-Jun dimerisation partner and c-Jun target gene, whose role in neuronal apoptosis had not been investigated in detail previously. In the following experiments, ATF-3 protein and RNA levels were examined in PC6-3 cells and sympathetic neurons following NGF withdrawal and the potential involvement of the JNK/c-Jun pathway in the induction of ATF-3 expression was studied using chemical inhibitors.

4.2 Results

4.2.1 ATF-3 is up-regulated in PC6-3 cells after NGF withdrawal

To confirm the GeneChip® result, *atf-3* RNA levels in PC6-3 cells cultured in the presence and absence of NGF were examined. Northern blot analysis was performed. mRNA was purified from total RNA and samples (5 μg) electrophoresed on an agarose-formaldehyde gel. *Aft-3* probe DNA was amplified from a rat brain cDNA library by PCR and *bcl-x_L* probe DNA was generated by digesting the pCDFLAGBcl-x_L vector with BglII and EcoRI restriction enzymes. Northern analysis of RNA isolated from differentiated PC6-3 cells cultured in the presence or absence of NGF for 16 hours showed that the *atf-3* mRNA increases in level by 2.6 fold after NGF deprivation (Figure 4.1A). This correlates with the GeneChip® result of an average induction of 2.68 fold and that of previously published results, which show enhanced levels of *atf-3* RNA after 6 hours of NGF withdrawal in PC6-3 cells (Mayumi-Matsuda *et al.*, 1999).

Figure 4.1 The *aft-3* mRNA increases in level in differentiated PC6-3 cells following NGF withdrawal

(A) PC6-3 cells were differentiated for 7 days in the presence of NGF and then cultured in the presence or absence of NGF for 16 hours. Total RNA was isolated, mRNA was purified from the total RNA, and mRNA samples (5 μg) were electrophoresed on a 1% agarose-formaldehyde gel and transferred to nitrocellulose. Northern blotting was performed using ^{32}P-labelled *atf-3* and *bcl-x_L* probe DNAs. Membranes were exposed to a phosphorimager screen for 1-4 nights at room temperature and the screens were scanned using a Typhoon™ 8600 phosphorimager to quantitate the levels of *atf-3* and *bcl-x_L* mRNA. RNA bands were quantitated using the ImageQuant analysis program and the ratio of *atf-3* to *bcl-x_L* was calculated. *Bcl-x_L* RNA levels remain relatively constant for the first 24 hours after NGF withdrawal and were used as a control for gel loading. In the northern blot shown, the level of *atf-3* mRNA is 2.6 fold higher after 16 hours of NGF deprivation. The size of the *aft-3* and *bcl-x_L* mRNAs is indicated.

(B) PC6-3 cells were differentiated for 7 days in the presence of NGF and then cultured for various times in the absence of NGF. RNA was extracted and converted into cDNA before being analysed by PCR. The PCR products were separated on 1.5% agarose gels. Representative gels for *dp5*, *aft-3* and *nf-m* are shown.

(C) Images of bands for *atf-3*, *dp5* and *nf-m* were captured using ImageMaster VDS-CL and quantitated using ImageMaster Total Lab. Levels of *atf-3* and *dp5* relative to *nf-m* were calculated and displayed on the graphs as relative level of RNA. The data shown represents the average of two independent experiments. The bars indicate range. *Atf-3* levels increased 3.2 fold over 16 hours.

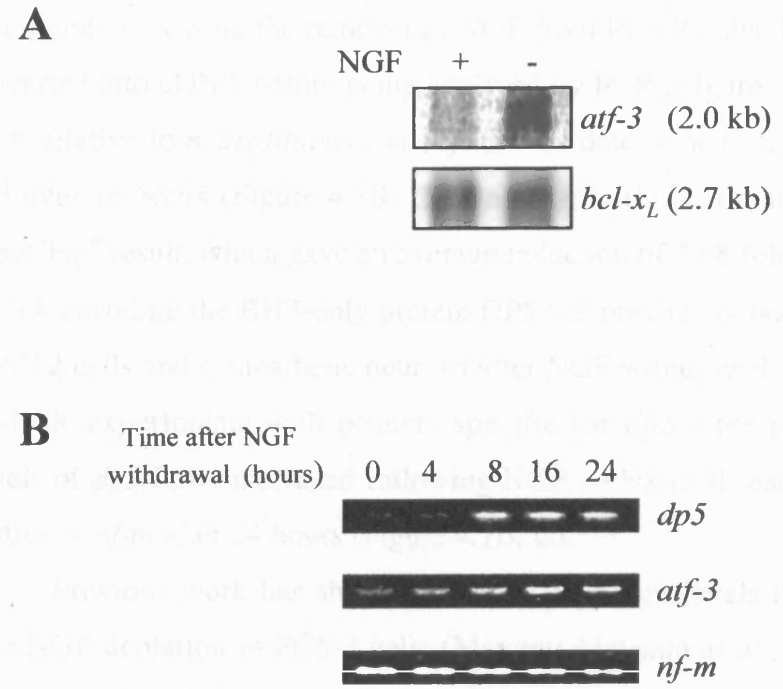
A
NGF + -
atf-3 (2.0 kb)
bcl-x$_L$ (2.7 kb)
B
Time after NGF withdrawal (hours) 0 4 8 16 24
dp5
atf-3
nf-m
C
dp5 expression
Relative level of RNA
Time after NGF withdrawal (hours)
atf-3 expression
Relative level of RNA
Time after NGF withdrawal (hours)

To get a better idea of the kinetics of gene induction following NGF withdrawal, semi-quantitative RT-PCR was performed on RNA extracted at various time-points following the removal of NGF from PC6-3 cells. RNA was extracted and converted into cDNA before being analysed by PCR (Figure 4.1B). The level of *atf-3* RNA relative to *neurofilament-m (nf-m)* was determined. *Atf-3* levels increased 3.2 fold over 16 hours (Figure 4.1B, C). Once again this correlates with the Affymetrix GeneChip® result, which gave an average induction of 2.68 fold at this time-point. The mRNA encoding the BH3-only protein DP5 has previously been shown to be induced in PC12 cells and sympathetic neurons after NGF withdrawal (Imaizumi *et al.*, 1997). RT-PCR experiments with primers specific for *dp5* were performed as a control. Levels of *dp5* RNA increased following NGF withdrawal reaching a maximum level relative to *nf-m* after 24 hours (Figure 4.1B, C).

Previous work has shown that ATF-3 protein levels increase within 9 hours after NGF depletion in PC6-3 cells (Mayumi-Matsuda *et al.*, 1999). In addition it is known that the c-Jun protein is induced and phosphorylated in PC12 cells at 4-8 hours after NGF withdrawal (Ham *et al.*, 1995; Mesner *et al.*, 1995). ATF-3 can heterodimerise with Jun proteins (Hai and Curran, 1991; Hsu *et al.*, 1992) and the *aft-3* promoter can be activated by overexpression of c-Jun in HeLa cells (Liang *et al.*, 1996). It was therefore of interest to examine the levels of ATF-3 and c-Jun in differentiated PC6-3 cells during a timecourse of NGF withdrawal to establish the time of induction of these proteins relative to each other (Figure 4.2). Figure 4.2A shows a western blot for ATF-3, c-Jun and Bcl-x_L. Levels of ATF-3 and c-Jun were normalised to the levels of Bcl-x_L to control for any differences in protein loading (Figure 4.2B). ATF-3 protein levels started to increase between 8 and 16 hours after NGF withdrawal and remained elevated at 24 hours. However, c-Jun levels started to increase between 4 and 8 hours after NGF withdrawal and reached a peak at 8 hours. The c-Jun protein had decreased again to minimum levels after 16 hours of NGF deprivation. In the case of this one experiment, the induction of c-Jun occurs prior to the induction of ATF-3 in PC6-3 cells, which suggests that ATF-3 might be a potential target of c-Jun in this cell system and thus perhaps also in sympathetic neurons.

Figure 4.2 ATF-3 and c-Jun protein levels increase in differentiated PC6-3 cells after NGF withdrawal

(A) PC6-3 cells were differentiated for 7 days in the presence of NGF and then cultured for various times in the presence or absence of NGF. Protein was isolated and 15 μg samples were run on a 15% SDS-polyacrylamide gel and western blot analysis performed. Blots were incubated with antibodies for ATF-3, c-Jun and Bcl-x_L. ATF-3 and c-Jun are present at low levels in undifferentiated (UD) PC6-3 cells. The results of a single experiment are shown.

(B) Western blots were scanned on a Bio-Rad GS800 densitometer to quantitate levels of protein. Images of bands were captured and quantitated using Bio-Rad Quantity One® software. The graph represents the levels of c-Jun and ATF-3 protein relative to that of Bcl-x_L. Bcl-x_L protein levels remain relatively constant for the first 24 hours after NGF withdrawal and were used as a control for any differences in protein loading. The data shown represents one experiment. In neuronally-differentiated PC6-3 cells, ATF-3 protein levels peaked at 16 hours after NGF withdrawal. c-Jun protein increases in level between 4 and 8 hours after NGF withdrawal, reaching a peak at 8 hours.

A

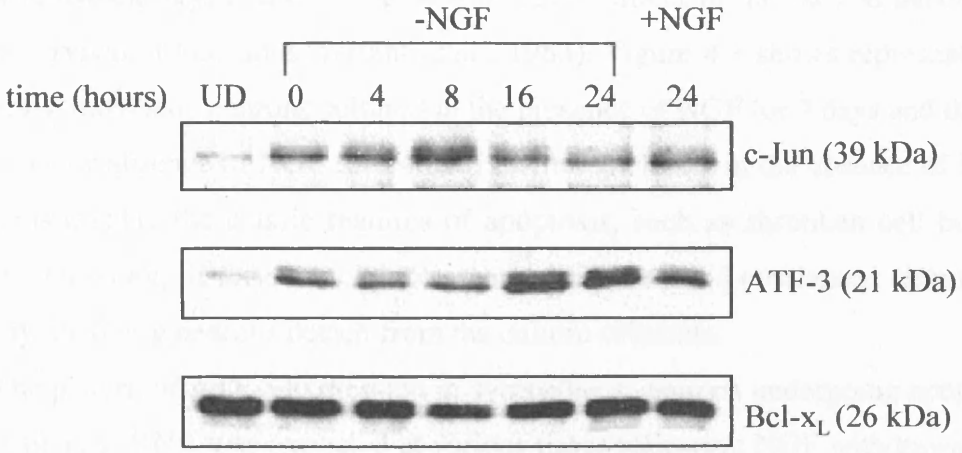
-NGF
+NGF
time (hours) UD 0 4 8 16 24 24
c-Jun (39 kDa)
ATF-3 (21 kDa)
Bcl-x$_L$ (26 kDa)

B

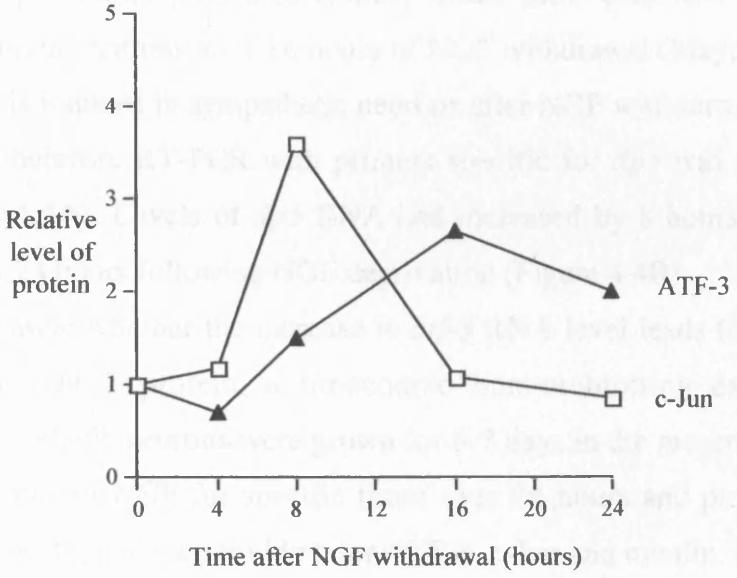
Relative level of protein
0
1
2
3
4
5
0 4 8 12 16 20 24
Time after NGF withdrawal (hours)
ATF-3
c-Jun

4.2.2 ATF-3 RNA and protein levels increase in sympathetic neurons after NGF withdrawal

Sympathetic neurons have proved to be a useful *in vitro* model for studying neuronal apoptosis mechanisms (Deshmukh and Johnson, 1997). These cells die by apoptosis between days 3 and 7 of postnatal development in the rat and depend on NGF for survival at that time (Wright *et al.*, 1983). Figure 4.3 shows representative pictures of sympathetic neurons cultured in the presence of NGF for 7 days and then in the presence or absence of NGF for 24 hours. After 24 hours in the absence of NGF, the neurons display the classic features of apoptosis, such as shrunken cell bodies, membrane blebbing, distorted nuclei, fragmented neurites and condensed chromatin. Eventually the dying neurons detach from the culture substrate.

The pattern of ATF-3 expression in sympathetic neurons undergoing apoptosis was investigated. RNA was extracted at various times following NGF withdrawal and converted into cDNA for semi-quantitative RT-PCR analysis (Figure 4.4A). *Atf-3* RNA levels, relative to *nf-m* RNA levels, were determined (Figure 4.4B). On average, the *atf-3* RNA had increased 2.1 fold at 16 hours after NGF withdrawal. This correlates with previously published results, which show enhanced levels of *atf-3* RNA in sympathetic neurons after 18 hours of NGF withdrawal (Mayumi-Matsuda *et al.*, 1999). *Dp5* is induced in sympathetic neurons after NGF withdrawal (Imaizumi *et al.*, 1997) and therefore RT-PCR with primers specific for *dp5* was performed as a control (Figure 4.4A). Levels of *dp5* RNA had increased by 8 hours and reached a maximum at 16-24 hours following NGF deprivation (Figure 4.4B).

To determine whether the increase in *atf-3* RNA level leads to an increase in the amount of ATF-3 protein, a timecourse immunoblotting experiment was performed. Sympathetic neurons were grown for 6-7 days in the presence of NGF and then in the absence of NGF for specific times over 24 hours and protein extracted. Figure 4.5A shows typical western blots for ATF-3, c-Jun and tubulin. Levels of ATF-3 and c-Jun were normalised to the levels of tubulin to control for any differences in protein loading (Figure 4.5B). The level of c-Jun protein and c-Jun N-terminal phosphorylation (manifested as a mobility shift) began to increase between 4 and 8 hours after NGF withdrawal and remained elevated at 16 and 24 hours. This correlates with previously published results that showed that c-Jun increases between 8 and 24 hours after NGF withdrawal (Ham *et al*, 1995). The ATF-3 protein started to increase

Figure 4.3 Morphology of sympathetic neurons cultured in the presence or absence of NGF

Sympathetic neurons were cultured for 7 days in the presence of NGF. In NGF withdrawal experiments (-NGF) neurons were cultured without NGF by carefully rinsing the cells twice in SCG medium lacking NGF and then refeeding with SCG medium supplemented with anti-NGF antibody at 100 ng/ml. Cells in the presence of NGF (+NGF) were also rinsed twice in SCG medium and refed with medium containing NGF (+NGF) and left for 24 hours. Cells were then examined on a Zeiss Axiovert 200 microscope and photographed using an Axiocam digital camera. Images were exported as TIFFs and processed in Adobe photoshop. After 24 hours in the absence of NGF, the neurons have begun to display signs of cell death. Cells become rounded and smaller in appearance, nuclei become shrunken and have an irregular shape, neurites fragment and the neurons detach from the coverslip. The bar represents 10 μM.

+NGF

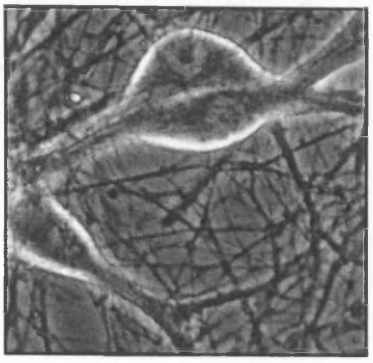

-NGF

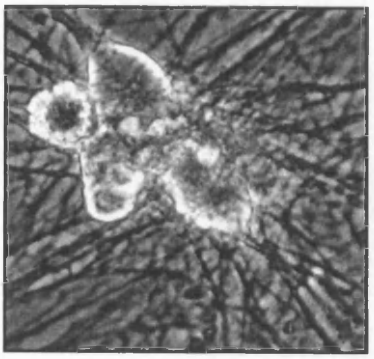

Figure 4.4 *Atf-3* RNA levels increase in sympathetic neurons deprived of NGF

(A) Sympathetic neurons were grown in the presence of NGF for 6-7 days and then cultured for various times in the absence of NGF. RNA was extracted and converted into cDNA before being analysed by PCR. The PCR products were separated on 1.5% agarose gels and representative images are shown.

(B) Images of bands for *atf-3*, *dp5* and *nf-m* were captured using ImageMaster VDS-CL and quantitated using ImageMaster Total Lab software. Levels of *atf-3* and *dp5* relative to *nf-m* were calculated and displayed on the graphs as relative level of RNA. The data shown represents the average of three independent experiments. Error bars indicate SEM. There was a 2.1 fold increase in *atf-3* RNA at 16 hours after NGF withdrawal.

A

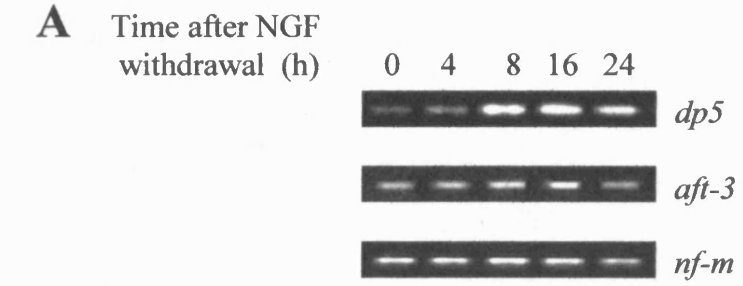
Time after NGF withdrawal (h)
0 4 8 16 24
dp5
aft-3
nf-m

B

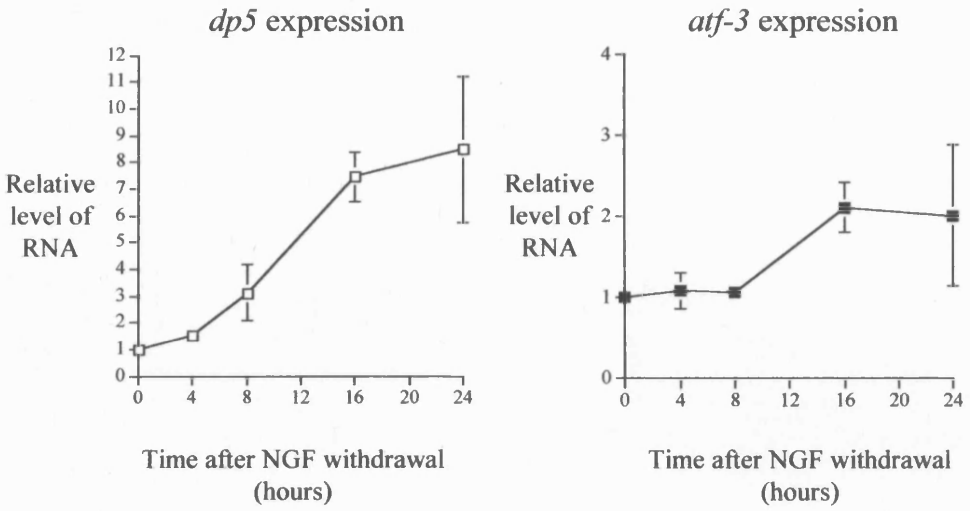
dp5 expression
Relative level of RNA
Time after NGF withdrawal (hours)
atf-3 expression
Relative level of RNA
Time after NGF withdrawal (hours)

Figure 4.5 ATF-3 protein levels increase in sympathetic neurons deprived of NGF

(A) Sympathetic neurons were grown in the presence of NGF for 6-7 days and then cultured in the absence of NGF. Protein was extracted at various times over the course of 24 hours. Protein isolated from two coverslips of neurons (approximately 16,000 cells) was loaded per lane of a 15% SDS-polyacrylamide gel and western blot analysis performed. Blots were incubated with antibodies specific for c-Jun, ATF-3 and tubulin. Representative western blots are shown.

(B) Western blots were scanned on a Bio-Rad GS800 densitometer to quantitate levels of protein. Images of bands were captured and quantitated using Bio-Rad Quantity One® software. The graph represents the levels of c-Jun and ATF-3 protein relative to that of tubulin (to normalise for any differences in protein loading). The data shown represents the average of three independent experiments. Error bars indicate SEM. c-Jun protein levels start to increase within the first 8 hours after NGF withdrawal, whereas ATF-3 levels start to increase between 8 and 16 hours.

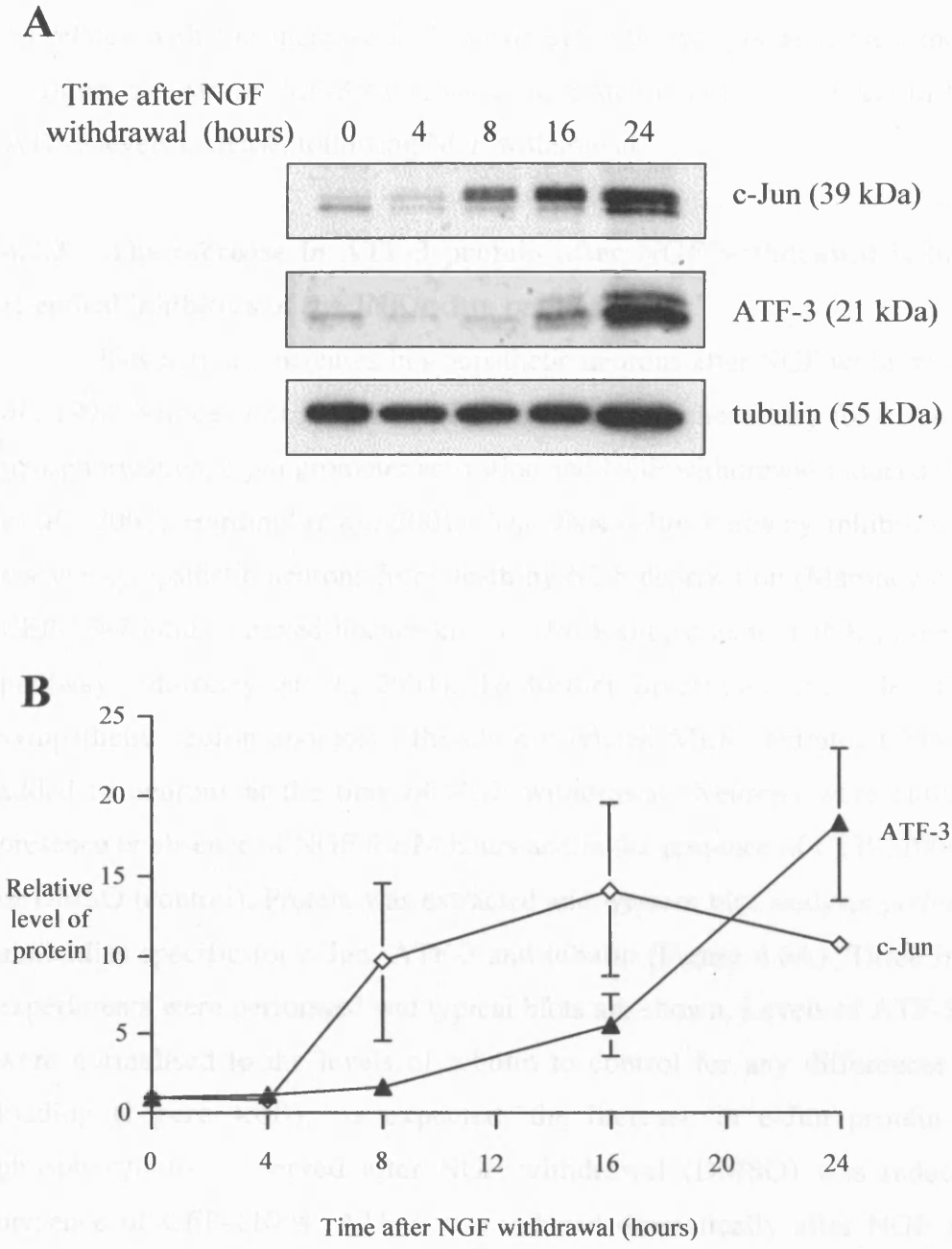
A
Time after NGF withdrawal (hours)
0
4
8
16
24
c-Jun (39 kDa)
ATF-3 (21 kDa)
tubulin (55 kDa)
B
Relative level of protein
25
20
15
10
5
0
0
4
8
12
16
20
24
ATF-3
c-Jun
Time after NGF withdrawal (hours)

between 8 and 16 hours after NGF withdrawal and continued to increase between 16 and 24 hours in the absence of NGF. Thus the increase in level of ATF-3 protein correlates with the increase in level of *atf-3* transcripts at these time-points. In addition, as seen in PC6-3 cells, the c-Jun protein starts to increase in level before ATF-3 levels increase, following NGF withdrawal.

4.2.3 The increase in ATF-3 protein after NGF withdrawal is inhibited by chemical inhibitors of the JNK/c-Jun pathway

JNK activity increases in sympathetic neurons after NGF withdrawal (Eilers *et al.*, 1998; Virdee *et al.*, 1997). This kinase activity is necessary for c-Jun N-terminal phosphorylation, *c-jun* promoter activation and NGF withdrawal-induced death (Eilers *et al.*, 2001; Harding *et al.*, 2001). The JNK/c-Jun pathway inhibitor, CEP-1347 rescues sympathetic neurons from death by NGF deprivation (Maroney *et al.*, 1999). CEP-1347 inhibits mixed-lineage kinases (MLKs) upstream of JNK in the JNK/c-Jun pathway (Maroney *et al.*, 2001). To further investigate the role of ATF-3 in sympathetic neuron apoptosis, the closely related MLK inhibitor CEP-11004 was added to neurons at the time of NGF withdrawal. Neurons were cultured in the presence or absence of NGF for 24 hours and in the presence of CEP-11004 (400 nM) or DMSO (control). Protein was extracted and western blot analysis performed using antibodies specific for c-Jun, ATF-3 and tubulin (Figure 4.6A). Three independent experiments were performed and typical blots are shown. Levels of ATF-3 and c-Jun were normalised to the levels of tubulin to control for any differences in protein loading (Figure 4.6B). As expected, the increase in c-Jun protein level and phosphorylation observed after NGF withdrawal (DMSO) was reduced by the presence of CEP-11004. ATF-3 was induced dramatically after NGF withdrawal (DMSO) and this was completely inhibited by CEP-11004.

The JNK inhibitor SP600125 was also used to investigate the involvement of the JNK/c-Jun pathway in ATF-3 protein induction after NGF withdrawal. Neurons were cultured in the presence or absence of NGF for 24 hours and in the presence of SP600125 (20 μM) or DMSO (control). Protein was extracted and western blot analysis performed for c-Jun, ATF-3 and tubulin (Figure 4.7A). Three independent experiments were performed and typical blots are shown. Levels of ATF-3 and c-Jun were normalised to the levels of tubulin to control for any differences in protein

loading (Figure 4.7B). As expected, the increase in c-Jun protein level and phosphorylation observed after NGF withdrawal (DMSO) was completed inhibited by the presence of SP600125. ATF-3 induction after NGF withdrawal (DMSO) was also completely prevented by SP600125.

These results suggest that ATF-3 is regulated by the JNK/c-Jun pathway in sympathetic neurons. A hypothetical model of the regulation of ATF-3 by the JNK/c-Jun pathway in neurons is shown in Figure 4.8.

Figure 4.6 The increase in the level of the ATF-3 and c-Jun proteins following NGF withdrawal is reduced by the MLK inhibitor CEP-11004

(A) Sympathetic neurons were grown in the presence of NGF for 6-7 days and then cultured in the presence or absence of NGF for 24 hours. At this time, neurons were also treated with DMSO (control) or CEP-11004 (400 nM) for 24 hours. Protein was extracted from two coverslips of neurons (approximately 16,000 cells) for each treatment. Samples were electrophoresed on a 15% SDS-polyacrylamide gel and western blot analysis performed. Blots were incubated with antibodies specific for c-Jun, ATF-3 and tubulin. Typical western blots are shown.

(B) Western blots were scanned on a Bio-Rad GS800 densitometer to quantitate levels of protein. Images of bands were captured and quantitated using Bio-Rad Quantity One® software. The graph represents the levels of c-Jun and ATF-3 protein relative to that of tubulin (to normalise for any differences in protein loading). The data shown represents the average of three independent experiments. Error bars indicate SEM. The increase in the level of c-Jun and ATF-3 following NGF withdrawal is reduced by CEP-11004.

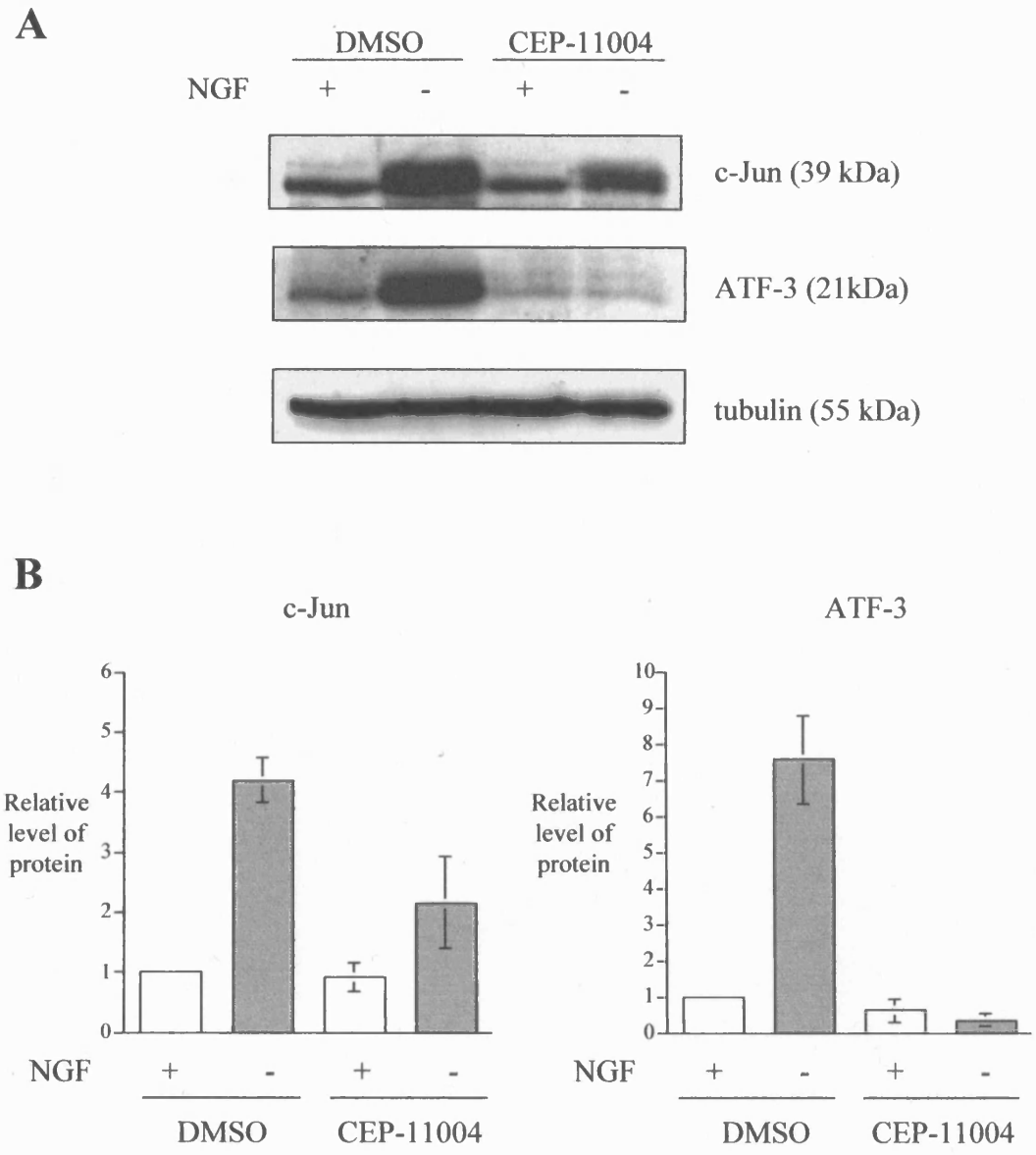
A
DMSO
CEP-11004
NGF
+
-
+
-
c-Jun (39 kDa)
ATF-3 (21kDa)
tubulin (55 kDa)
B
c-Jun
ATF-3
Relative level of protein
0
1
2
3
4
5
6
7
8
9
10
NGF
+
-
+
-
DMSO
CEP-11004

Figure 4.7 The increase in the level of the ATF-3 and c-Jun proteins following NGF withdrawal is inhibited by the JNK inhibitor SP600125

(A) Sympathetic neurons were grown in the presence of NGF for 6-7 days and then cultured in the presence or absence of NGF for 24 hours. At this time, neurons were also treated with DMSO (control) or SP600125 (20 μM) for 24 hours. Protein was extracted from two coverslips of neurons (approximately 16,000 cells) for each treatment. Samples were electrophoresed on a 15% SDS-polyacrylamide gel and western blot analysis performed. Blots were incubated with antibodies specific for c-Jun, ATF-3 and tubulin. Typical western blots are shown.

(B) Western blots were scanned on a Bio-Rad GS800 densitometer to quantitate levels of protein. Images of bands were captured and quantitated using Bio-Rad Quantity One® software. The graph represents the levels of c-Jun and ATF-3 protein relative to that of tubulin (to normalise for any differences in protein loading). The data shown represents the average of three independent experiments. Error bars indicate SEM. The increase in the level of c-Jun and ATF-3 following NGF withdrawal is completely reduced by SP600125.

A

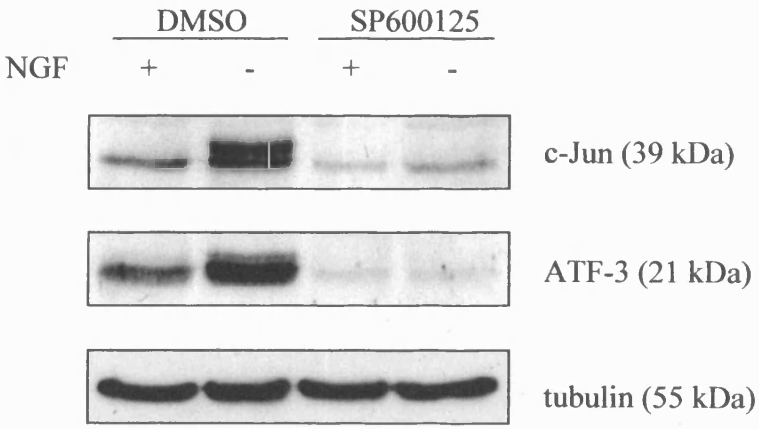
DMSO
SP600125
NGF + - + -
c-Jun (39 kDa)
ATF-3 (21 kDa)
tubulin (55 kDa)

B

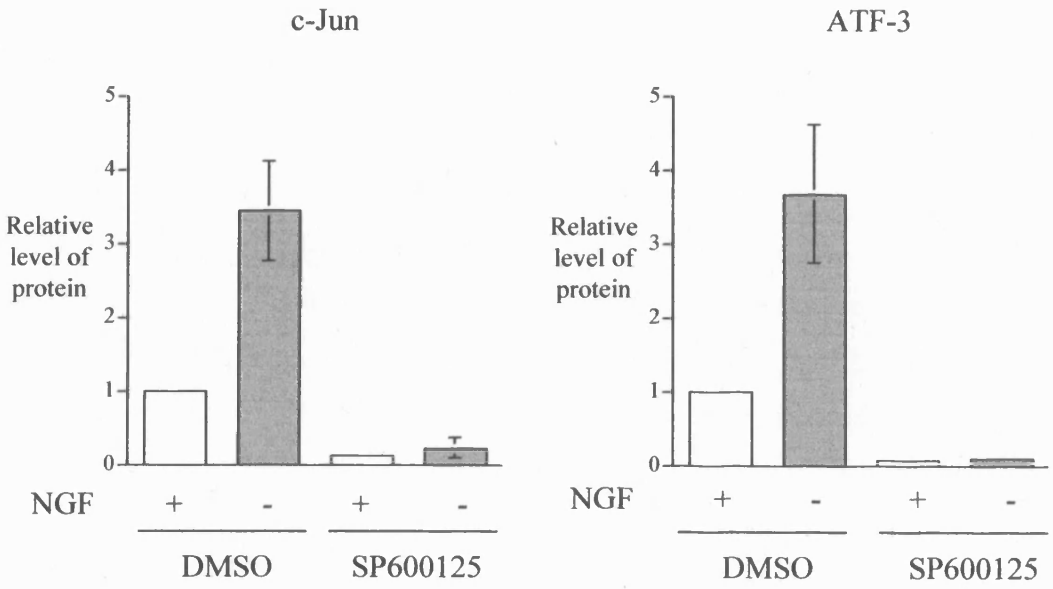
c-Jun
ATF-3
Relative level of protein
0
1
2
3
4
5
NGF + - + -
DMSO
SP600125

Figure 4.8 Hypothetical model of how ATF-3 expression is regulated in sympathetic neurons deprived of NGF

NGF withdrawal leads to a decrease in signalling from TrkA receptors on the cell surface and activation of mixed-lineage kinases (MLK), which activates a cascade of kinases including c-Jun N-terminal kinase (JNK) kinases (JNKK) and JNK. The chemical inhibitors of the pathway used in this study are indicated. c-Jun levels and c-Jun N-terminal phosphorylation increase after NGF withdrawal and expression of a dominant negative c-Jun mutant, FLAGΔ169, blocks NGF withdrawal-induced apoptosis (Ham *et al.*, 1995). In sympathetic neurons, ATF-3 is induced following NGF withdrawal and this is observed after the initial induction and phosphorylation of c-Jun. The *atf-3* promoter can be activated by overexpression of c-Jun and ATF-2 (Cai *et al.*, 2000, Liang *et al.*, 1996), thus implicating it as a potential c-Jun target gene. ATF-3 and c-Jun can dimerise to regulate transcription (Hai and Curran, 1991, Hsu *et al.*, 1992) and may do so during neuronal apoptosis. The increase in the level of ATF-3 after NGF withdrawal, is inhibited by the MLK inhibitor CEP-11004 and the JNK inhibitor SP600125, suggesting that ATF-3 is regulated by the JNK/c-Jun pathway in sympathetic neurons. The induction of DP5 and Bim is partially dependent on JNK signalling. The MLK inhibitor CEP-1347 reduced the induction of DP5 and Bim in sympathetic neurons following NGF withdrawal (Harris and Johnson, 2001). This is consistent with the findings of Whitfield *et al.* (2001), who reported that Bim induction is decreased in NGF-deprived sympathetic neurons that express dominant negative c-Jun (Whitfield *et al.*, 2001). These BH3-only proteins may directly dimerise with Bcl-2 or Bcl-x_L to inhibit their action (Yang *et al*, 1995; O'Connor *et al.*, 1998). The cell death induced by DP5 is inhibited by Bcl-2 (Imaizumi *et al.*, 1999).

During NGF withdrawal-induced sympathetic neuron apoptosis, cytochrome c is released from the mitochondria (Deshmukh and Johnson, 1998; Neame *et al.*, 1998). Cytochrome c is required for this cell death because microinjection of blocking antibodies increases cell survival (Neame *et al.*, 1998). When released into the cytosol, cytochrome c binds procaspase-9 and Apaf-1, which leads to activation of caspase-9 in the presence of ATP. This cleaves executioner caspases, such as procaspase-3, into their active forms, which cleave the protein substrates that lead to the cellular changes that are characteristic of apoptosis. These events occur downstream of c-Jun activation, because expression of FLAGΔ169 blocks cytochrome c release from the mitochondria (Whitfield *et al.*, 2001).

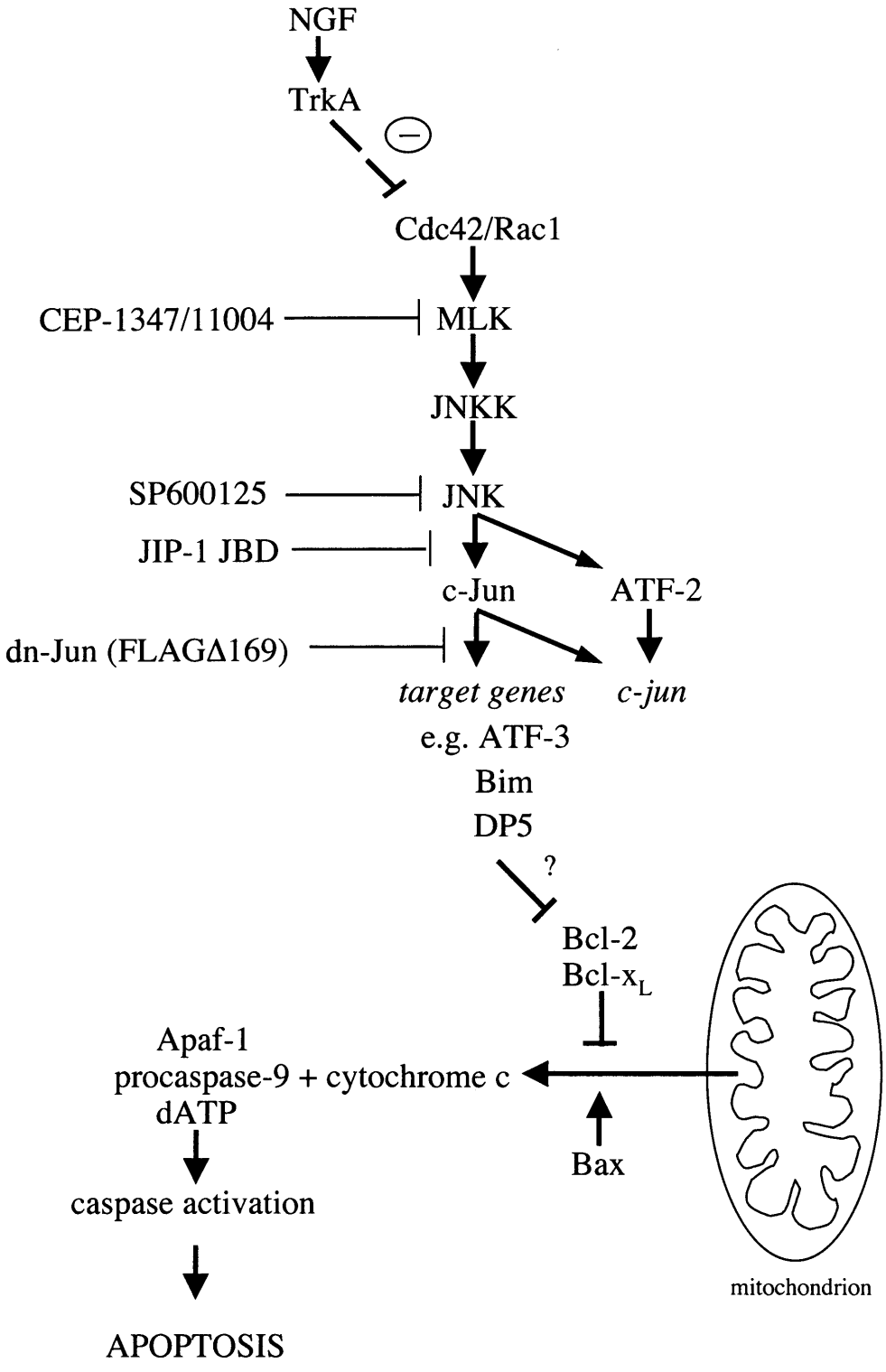
NGF
TrkA
Cdc42/Rac1
CEP-1347/11004
MLK
JNKK
SP600125
JNK
JIP-1 JBD
c-Jun
ATF-2
dn-Jun (FLAGΔ169)
target genes
c-jun
e.g. ATF-3
Bim
DP5
?
Bcl-2
Bcl-x$_L$
Apaf-1
procaspase-9 + cytochrome c
dATP
Bax
caspase activation
APOPTOSIS
mitochondrion

4.3 Discussion

In the experiments described in this chapter I have confirmed my Affymetrix GeneChip® result that ATF-3 is induced in neuronal cells following NGF withdrawal. The *atf-3* RNA increased in neuronally differentiated PC6-3 cells after NGF deprivation. This induction peaked at 16 hours after NGF withdrawal. This correlates with the GeneChip® result of an average induction of 2.68 fold and with previously published results, which showed enhanced levels of *atf-3* RNA after 6 hours of NGF withdrawal in PC6-3 cells (Mayumi-Matsuda *et al.*, 1999). The increase in RNA led to an increase in the level of ATF-3 protein. ATF-3 protein levels had increased by 16 hours after NGF withdrawal and remained elevated after 24 hours. Following NGF withdrawal from PC6-3 cells, c-Jun is induced and phosphorylated prior to the induction of ATF-3. The expression of ATF-3 in sympathetic neurons undergoing apoptosis was also investigated. There was a 2.1 fold increase in *atf-3* RNA at 16 hours after NGF withdrawal. This agrees with previously published results, which show enhanced levels of *atf-3* RNA after 18 hours of NGF withdrawal in sympathetic neurons (Mayumi-Matsuda *et al.*, 1999). I also observed that the ATF-3 protein increased in level between 8 and 16 hours after NGF withdrawal and continued to increase in level after 24 hours in the absence of NGF. This increase in expression was observed after the induction and phosphorylation of c-Jun protein, which began to increase between 4 and 8 hours after NGF withdrawal and remained elevated at 16 and 24 hours.

The induction of ATF-3 after NGF withdrawal, was completely inhibited by the MLK inhibitor CEP-11004 and the JNK inhibitor SP600125, suggesting that ATF-3 is a component of the JNK/c-Jun pathway. However, the induction of c-Jun was not completely inhibited by CEP-11004. At the concentration of CEP-11004 used (400 nM), there are low levels of phospho-JNK (Thr 183/Tyr 185) present in NGF-deprived sympathetic neurons (Wang *et al.*, 2005). This may be sufficient to activate c-Jun and/or ATF-2 and induce c-Jun expression, but insufficient to initiate ATF-3 induction. The effect of these chemical inhibitors is not definitive proof of ATF-3 regulation by the JNK/c-Jun pathway. Cephalon have found that in *in vitro* kinase assays for CEP-11004 the IC_{50} for MLKs and other kinases is: MLK1, 45 nM; MLK2, 89 nM; MLK3, 31 nM; DLK, 160 nM; MLK6, >10,000 nM; PKC (brain α, β, γ), 930 nM; TrkA, >1000 nM (datasheet supplied by Cephalon, Inc). However, CEP-11004

has been found to induce an increase in TrkA mRNA and protein levels, resulting in NGF-independent activation of the TrkA receptor and the downstream PI3K pathway, in sympathetic neurons (Wang *et al.*, 2005). In contrast to CEP-11004, SP600125 has been shown to directly inhibit JNKs (Bennett *et al.*, 2001; Bogoyevitch *et al.*, 2004), but this compound is not as selective as the original reports suggested (Bain *et al.*, 2003).

Further evidence for an involvement of the JNK/c-Jun pathway in ATF-3 regulation is reported by Cai *et al.* (2000). Homocysteine-induced vascular endothelial cell injury leads to increased *atf-3* gene expression and this induction involves the activation of JNK. A complex containing ATF-2 and c-Jun activated the *atf-3* promoter, whereas ATF-3 repressed its own promoter. In addition, the induction of ATF-3 by ionizing radiation in primary human fibroblasts is mediated by signalling through JNKs and ATF-2 (Kool *et al.*, 2003). In sympathetic neurons, the phosphorylation of c-Jun and ATF-2 increases after NGF withdrawal. However, the increase in ATF-2 phosphorylation is more transient than the increase in c-Jun N-terminal phosphorylation after NGF withdrawal (Eilers *et al.*, 2001). In addition, c-Jun protein levels increase but ATF-2 protein levels fall after NGF withdrawal. Since ATF-3 protein induction after NGF deprivation in sympathetic neurons follows that of c-Jun and since ATF-3 can dimerise with c-Jun, it is possible that ATF-3 may dimerise with c-Jun in neurons undergoing apoptosis. ATF-3 contains a putative phosphoacceptor site for JNK at Thr-148, however no change in protein migration was observed after treatment of HEK293 cells with anisomycin, a JNK activator, suggesting that ATF-3 is not a direct target of JNKs (Katz and Aronheim, 2002). It has been reported that ATF3 migrates as a 21 and 23 kDa doublet band due to an alternative ATG usage and not due to phosphorylation (Hagmeyer *et al.*, 1996).

ATF-3 and c-Jun have been found to co-localise in many types of neurons following injury. The expression of ATF-3 correlates with expression of c-Jun in the dorsal root ganglia and spinal cord following sciatic nerve cut (Tsujino *et al.*, 2000) and retinal ganglion cells after optic nerve injury (Takeda *et al.*, 2000). In addition, c-Jun is phosphorylated at these sites of injury. In PC12 cells, overexpressed c-Jun and ATF-3 can co-immunoprecipitate and there is increased neurite formation in cells transfected with c-Jun as well as c-Jun and ATF-3 together (Pearson *et al.*, 2003). Thus, c-Jun activation has been implicated in nerve regeneration after injury as well as

in neuronal cell death. The role of c-Jun and ATF-3 in sympathetic neurons may depend on the relative levels of each transcription factor present within dying neurons.

In conclusion, the results described in this chapter suggest a potential involvement of the JNK/c-Jun pathway in ATF-3 up-regulation after NGF withdrawal from differentiated PC6-3 cells and sympathetic neurons. The increase in ATF-3 level follows that of c-Jun and these transcription factors may physically and functionally interact to regulate neuronal death and survival.

Chapter 5: The function of ATF-3 in sympathetic neurons

5.1 Introduction

The stress-inducible ATF-3 transcription factor can activate or repress transcription. The induction of ATF-3 correlates with cellular damage and signals that do not induce ATF-3 do not induce damage (Hai *et al.*, 1999). However, the actual function of ATF-3 is not clear, with both protective and detrimental roles proposed. ATF-3 is induced in beta cells of the pancreas undergoing apoptosis via the NF-κB and JNK pathways (Hartman *et al.*, 2004). Overexpression of ATF-3 in these cells in transgenic mice, leads to abnormal development and dysfunction, whereas inactivation of the *atf-3* gene partially protected the cells from apoptosis induced by cytokines or nitric oxide. ATF-3 has also been implicated in the acceleration of caspase activation during DNA damage-induced apoptosis (Mashima *et al.*, 2001). On the other hand, overexpression of ATF-3 can protect rat hippocampal neurons *in vivo* against kainic acid-induced death (Francis *et al.*, 2004) and can promote the survival of PC12 cells and sympathetic neurons following JNK activation by MEKK1 or in the absence of NGF respectively (Nakagomi *et al.*, 2003). A protective role for ATF-3 in cardiomyocytes has also been described (Nobori *et al.*, 2002). In these rat neonatal cardiomyocytes, doxorubicin rapidly activated JNK, c-Jun and ATF-3 and overexpression of ATF-3 protected the cells from apoptosis.

ATF-3 is thought to repress transcription by stabilizing inhibitory co-factors on the promoters of target genes (Chen *et al.*, 1994). Alternatively spliced isoforms of ATF-3 have been described that lack the leucine zipper domain and which therefore do not bind to DNA. The human isoforms ATF-3ΔZIP, ATF-3ΔZIP2a, ATF-3ΔZIP2b, ATF-3ΔZIP2c and ATF-3ΔZIP3 are induced along with ATF-3 by various stress signals and may modulate the activity of full length ATF-3 (Hashimoto *et al.*, 2002; Pan *et al.*, 2003). It has been proposed that these isoforms antagonise the action of ATF-3 by binding inhibitory co-factors, sequestering them away from the transcription machinery and thus stimulating transcription. Another ATF-3 isoform ATF-3b was identified in mouse pancreatic αTC1.6 cells (Wang *et al.*, 2003). This lacks 106 base pairs in exon 2 of the full length ATF-3 coding sequence but retains the bZIP domain.

In these cells, both ATF-3 and ATF-3b are down-regulated by glucose. ATF-3 and ATF-3b bind to CRE/ATF binding sites in the proglucagon gene promoter as homodimers and heterodimers with each other to activate transcription. This describes a novel mechanism of transcriptional activation by ATF-3 binding at the CRE/ATF site in the promoter.

Several ATF-3 target genes have been identified. ATF-3 has been shown to regulate its own transcription by binding to a non-consensus ATF-3 site immediately downstream of the TATA box in the *atf-3* promoter (Wolfgang *et al.*, 2000). This site is necessary for efficient autorepression by ATF-3. ATF-3 homodimers have been reported to repress the transcription of TNF-α-induced E-selectin gene expression (Nawa *et al.*, 2000) and arsenite-induced GADD153 expression (Fawcett *et al.*, 1999; Wolfgang *et al.*, 1997). In addition, ATF-3 can interact with the GADD153 to regulate transcription and forms a nonfunctional heterodimer that does not bind to the ATF/CRE element consensus site and which does not repress transcription (Chen *et al.*, 1996). ATF-3 can also activate transcription when dimerised with other bZIP proteins, such as c-Jun (Hai and Curran, 1991; Hsu *et al.*, 1992). In sympathetic neurons, overexpressed ATF-3 promotes heat shock protein 27 (Hsp27) expression by binding to an atypical CRE site in the gene promoter, and this may involve c-Jun (Nakagomi *et al.*, 2003).

ATF-3 is induced in many examples of nerve injury. The injury specific expression of ATF-3 in axotomised dorsal root ganglia and spinal cord following sciatic nerve cut (Tsujino *et al.*, 2000) and in retinal ganglion cells after optic nerve injury (Takeda *et al.*, 2000) correlates with expression of c-Jun in these surviving cells. The induction of c-Jun has been associated with neurite sprouting in undifferentiated PC12 cells (Dragunow *et al.*, 2000) and ATF-3 has been shown to enhance this process in both PC12 cells and mouse Neuro-2a cells (Pearson *et al.*, 2003).

The study of c-Jun in the nervous system *in vivo* has been limited because *c-jun* knockout mice die during embryonic development at day 12.5 due to hepatic failure (Hilberg *et al.*, 1993). However, a floxed *c-jun* gene has been successfully knocked out in sympathetic neurons *in vitro* (infected with a CRE adenovirus) and this inhibited NGF withdrawal-induced death (Palmada *et al.*, 2002). Overexpression of c-Jun kills sympathetic neurons in the presence of NGF and a dominant negative c-Jun

protein (FLAGΔ169) protects sympathetic neurons from NGF withdrawal-induced death (Ham *et al.*, 1995). This mutant lacks the N-terminal 168 amino acids encoding the transactivation domain, but can still dimerise and bind DNA via the bZIP domain (Hirai *et al.*, 1989) and acts as a dominant negative mutant against all AP-1 family members (Brown *et al.*, 1994; Castellazzi *et al.*, 1991). ATF-3 also contains a bZIP domain and can dimerise with c-Jun to activate transcription (Hai and Curran, 1991; Hsu *et al.*, 1992). A protein containing only the bZIP domain of ATF-3 could potentially regulate ATF-3 function by binding the full length transcription factor and preventing transactivation or repression of target genes. Alternatively the ATF-3bZIP domain could potentiate the role of ATF-3 in a similar manner to the ATF-3b isoform found in mice (Wang *et al.*, 2003). Another way of inhibiting ATF-3 function in neurons would be to use the pSUPER RNAi system to knock down the expression of ATF-3. This vector system ensures efficient expression of small interfering RNA (siRNA) under the control of an RNA polymerase-III dependent promoter (Brummelkamp *et al.*, 2002). The RNA transcript forms a short hairpin structure with a 19 base-pair double-stranded region and a short loop formed by a spacer region and has been designed to be an optimal substrate for the enzyme Dicer, which cleaves the hairpins to generate short double stranded RNA. These RNA species bind to newly synthesised RNA in the cell and cause sequence-specific mRNA degradation (Brummelkamp *et al.*, 2002; Elbashir *et al.*, 2001).

In the following experiments, the function of ATF-3 in sympathetic neurons undergoing apoptosis was investigated using both the truncated ATF-3bZIP domain and RNAi specific for ATF-3.

5.2 Results

5.2.1 Construction of ATF-3 and ATF-3bZIP expression vectors

To investigate the function of ATF-3 in sympathetic neurons, expression vectors encoding the full length ATF-3 protein or the basic/leucine zipper (bZIP) domain of ATF-3, were constructed. The ATF-3 coding sequence was amplified by PCR from a rat brain cDNA library. The forward and reverse primers used contained a BamHI site (GGATCC) and an EcoRI site (GAATTC) respectively, for cloning into the pCDFLAG expression vector. This vector is the pcDNA1 expression vector with

the FLAG epitope inserted between the HindIII and BamHI sites (Vekrellis *et al.*, 1997). The bZIP domain of ATF-3 was amplified by PCR using the ATF-3 cDNA as template. The forward and reverse primers used for this also contained a BamHI and an EcoRI site respectively, for cloning into the pCDFLAG vector (Figure 5.1A). The PCR products were purified by gel extraction and digested with BamHI and EcoRI (Figure 5.1B) and the inserts encoding ATF-3 or the ATF-3bZIP domain were cloned into pCDFLAG (Figure 5.1C) to generate pCDFLAGATF-3 and pCDFLAGATF-3bZIP respectively. The constructs were sequenced to verify that the insert DNAs did not contain any mutations and had the correct structure.

5.2.2 The ATF-3 and ATF-3bZIP proteins are expressed in transfected Cos-7 cells and microinjected sympathetic neurons

To verify that proteins of the correct size were expressed, Cos-7 cells were transiently transfected with the pCDFLAGATF-3 and pCDFLAGATF-3bZIP expression vectors. Cos-7 cells were plated in 9 cm dishes and 5 μg of pCDFLAG, pCDFLAGATF-3, pCDFLAGATF-3bZIP or pCDFLAGΔ169 (dominant negative c-Jun) were transfected into the cells using Lipofectamine 2000. 48 hours after transfection, protein was extracted and western blot analysis performed with the anti-FLAG M2 antibody (Figure 5.2A). pCDFLAGΔ169 was used as a positive control for the expression of FLAG-tagged proteins. All constructs expressed proteins of the expected sizes, although the level of expression of the FLAG-tagged ATF-3bZIP protein appeared to be much lower than that of the full length ATF-3 or dominant negative c-Jun proteins. This small protein (7.2 kDa) may be less stable than full length ATF-3. Alternatively, it might be less efficiently retained by the membranes used in western blots.

To confirm that the FLAG-tagged proteins were expressed in sympathetic neurons, the expression vectors were microinjected into neurons cultured in the presence of NGF. Sympathetic neurons were injected with guinea pig IgG (2.5 μg/μl) and 0.1 μg/μl of either pCDFLAGATF-3 or pCDFLAGATF-3bZIP. 24 hours after injection, the cells were fixed and stained for the injection marker and FLAG-tagged proteins. In these immunocytochemistry experiments, injected cells were detected using a rhodamine-conjugated anti-guinea pig IgG antibody and the FLAG-tagged proteins were detected using the M2 monoclonal antibody and then a FITC-conjugated

Figure 5.1 Construction of ATF-3 and ATF-3bZIP expression vectors

(A) Sequence of the primers used to amplify the ATF-3 and ATF-3bZIP coding sequences by PCR. Restriction enzymes sites for BamHI (GGATCC) and EcoRI (GAATTC) are shown in bold type.

(B) The ATF-3 and ATF-3bZIP PCR products were digested with BamHI and EcoRI to generate DNA inserts suitable for ligation into the pCDFLAG vector. The codons amplified are indicated in brackets after the insert name. The full length ATF-3 (1-541) and the bZIP domain of ATF-3, ATF-3bZIP (247-440) were cloned into the BamHI and EcoRI sites of pCDFLAG.

(C) Structure of pCDFLAG. This vector contains the following features: Col E1 origin, bases 1-587; M13 origin, bases 588-1180; Ampicillin gene, bases 1360-2303; CMV promoter, bases 2304-2954; T7 primer sequence, bases 2938-2957; Polylinker, bases 2956-3074; Sp6 primer, bases 3075-3093; Splice and poly A, bases 3094-3792; Polyoma origin, bases 3798-4693 and SV40 origin, bases 4634-4797. The FLAG epitope is cloned between the HindIII and BamHI sites of the multiple cloning site. The ATF-3 and ATF-3bZIP inserts were cloned between the BamHI and EcoRI restriction sites.

A

ATF-3 primers

Forward 5'-CAT**GGATCC**ATGATGCTTCAACATCCAGGC-3'

BamHI

Reverse 5'-CTT**GAATTC**TTAGCTCTGCAATGTTCCTTC-3'

EcoRI

ATF-3bZIP primers

Forward 5'-GTT**GGATCC**CCTGAAGAAGATGAGAGAAAAAG-3'

BamHI

Reverse 5'-CGA**GAATTC**TTGAGCATGTAAATCAGATGCTG-3'

EcoRI

B

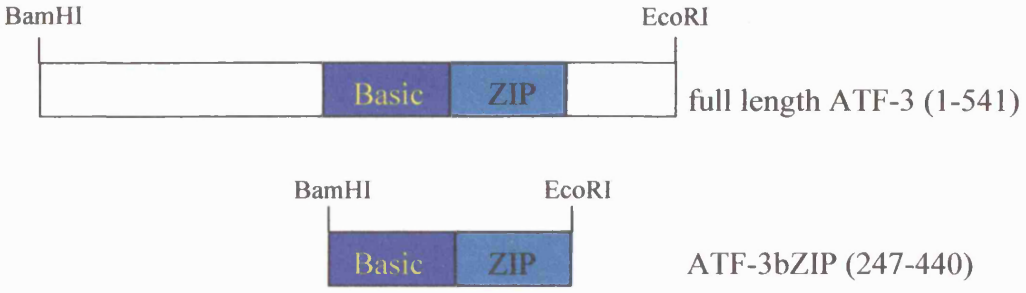

C

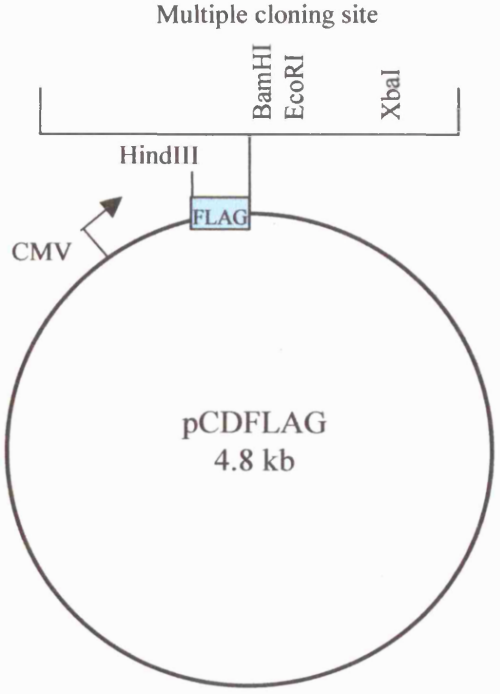

Figure 5.2 Expression of FLAG-tagged ATF-3 and ATF-3bZIP in Cos-7 cells and sympathetic neurons

(A) The expression vectors pCDFLAG, pCDFLAGATF-3, pCDFLAGATF-3bZIP and pCDFLAGΔ169 (a dominant negative c-Jun construct) were transfected into Cos-7 cells using Lipofectamine 2000. Cos-7 cells (approximately 1.8 x 10^6 cells) were plated in 9 cm dishes. The DNA (5 μg) and Lipofectamine (40 μl) were both mixed with 821 μl of Opti-MEM® I reduced serum medium as instructed and gently added to the cells. Protein was extracted after 48 hours. Samples were run on a 15% SDS polyacrylamide gel and western blot analysis performed. Blots were hybridised with the anti-FLAG M2 antibody. All constructs expressed proteins of the expected sizes. pCDFLAGΔ169 was used as a positive control for the expression of FLAG-tagged proteins. A representative western blot is shown. The position of molecular weight markers run in parallel is indicated. A non-specific band recognised by the anti-FLAG M2 monoclonal antibody is indicated. This band was detected in the extract prepared from cells transfected with empty vector (pCDFLAG) and is present at a similar level in all four lanes, suggesting that the protein loadings were equal.

(B) Sympathetic neurons were microinjected with guinea pig IgG (2.5 μg/μl) and 0.1 μg/μl of either pCDFLAGATF-3 or pCDFLAGATF-3bZIP. 24 hours after injection, cells were fixed and stained for the injection marker and the FLAG-tagged proteins. Injected cells were detected using a rhodamine-conjugated anti-guinea pig IgG antibody (diluted 1-100). FLAG-tagged proteins were detected using the M2 monoclonal antibody (1-200) and then a FITC-conjugated anti-mouse IgG antibody (1-100). Nuclei were stained using Hoechst dye (10 μg/ml). Representative images of ATF-3 and ATF-3bZIP expression in microinjected sympathetic neurons are shown. The bar represents 10 μM.

A

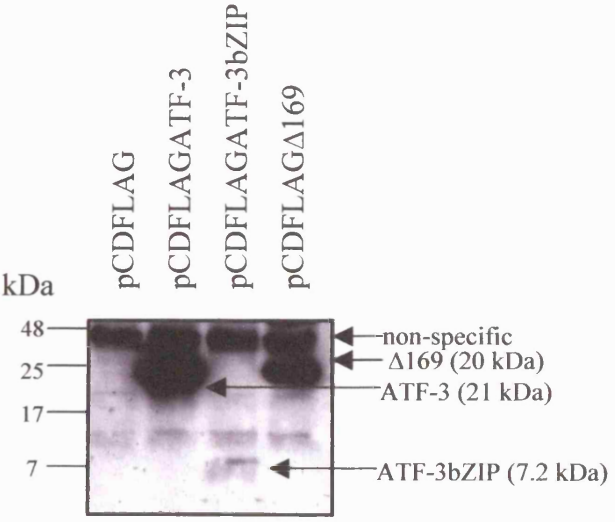
pCDFLAG
pCDFLAGATF-3
pCDFLAGATF-3bZIP
pCDFLAGΔ169
kDa
48
25
17
7
non-specific
Δ169 (20 kDa)
ATF-3 (21 kDa)
ATF-3bZIP (7.2 kDa)

B

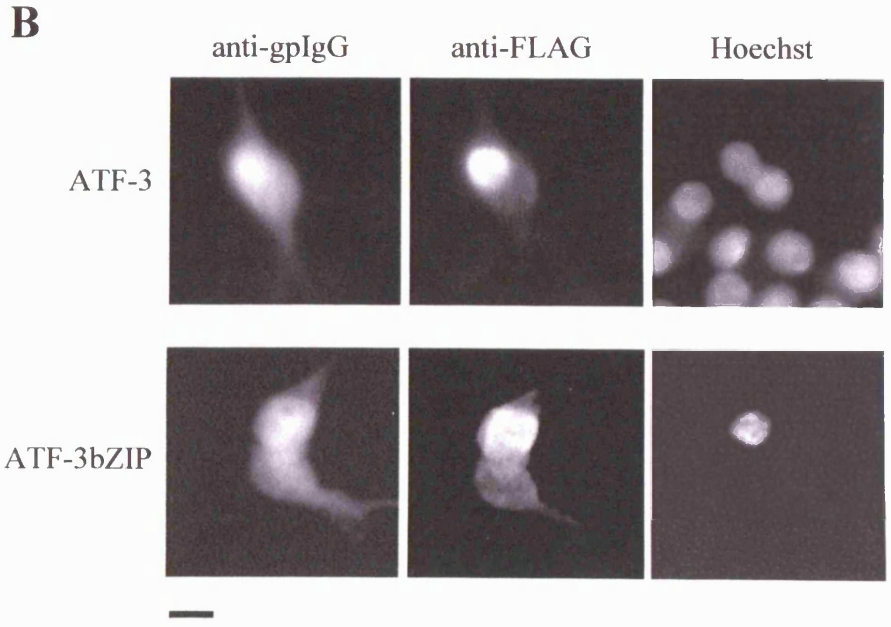
anti-gpIgG
anti-FLAG
Hoechst
ATF-3
ATF-3bZIP

anti-mouse IgG antibody. Both FLAG-tagged proteins were expressed in the injected cells (Figure 5.2B). FLAGATF-3 mainly localised to the nucleus whereas FLAGATF-3bZIP was distributed throughout the whole cell. The truncated ATF-3bZIP protein may lack the appropriate nuclear localisation signal to localise all of the protein in the nucleus. Alternatively, the bZIP protein may be small enough to move freely in and out of the nucleus, whereas the full length ATF-3 protein is retained within the nucleus once it has crossed the nuclear membrane.

5.2.3 Overexpression of ATF-3 kills sympathetic neurons in the presence of NGF, but can protect against death induced by NGF withdrawal

The role of ATF-3 in sympathetic neurons was investigated in microinjection experiments. Sympathetic neurons were injected with guinea pig IgG (2.5 μg/μl) and 0.1 μg/μl of each expression vector, CMVlacZ (as a negative control), pCDc-Jun, pCDFLAGATF-3 or pCDc-Jun and pCDFLAGATF-3 together. Neurons were maintained in medium containing NGF and at 72 hours after injection, the cells were fixed and stained for the injection marker and overexpressed proteins. Injected cells were detected using a rhodamine-conjugated anti-guinea pig IgG antibody. Overexpressed proteins were detected using anti-β-galactosidase, anti-c-Jun or anti-ATF-3 antibodies and then FITC-conjugated anti-mouse IgG antibody or FITC-conjugated anti-rabbit IgG antibody. All of the overexpressed proteins were detected in the injected cells (Figure 5.3A). Injected neurons were scored for nuclear morphology (visualised by Hoechst staining). Cells with normal nuclei were counted for each of the four injection mixes tested (Figure 5.3B). 71.7% of neurons injected with CMVlacZ had normal nuclei. In contrast, 39.1% of the neurons overexpressing ATF-3 had normal nuclei, in the presence of NGF. c-Jun killed neurons to a similar extent with only 39.3% of nuclei having a normal morphology. This is in agreement with previously published results that showed that overexpression of c-Jun can kill the neurons in the presence of NGF (Ham *et al.*, 1995). A significant reduction in the percentage of normal nuclei was also observed when ATF-3 and c-Jun were co-expressed. Injection of both of the expression vectors for ATF-3 and c-Jun together lead to 46.8% of injected neurons with normal nuclei. Thus, co-expression of c-Jun and ATF-3 did not have an additive effect.

Figure 5.3 Overexpression of ATF-3 and c-Jun kills sympathetic neurons in the presence of NGF

(A) Sympathetic neurons were microinjected with guinea pig IgG (2.5 μg/μl) and 0.1 μg/μl of each expression vector, CMVlacZ, pCDc-Jun, pCDFLAGATF-3 or pCDc-Jun and pCDFLAGATF-3 together. Where necessary, injection mixes were made up to a concentration of 0.2 μg/μl with pcDNA1. 72 hours after injection the cells were fixed and stained for the injection marker and overexpressed proteins. Injected cells were detected using rhodamine-conjugated anti-guinea pig IgG antibody (1-100). Overexpressed proteins were detected using anti-β-galactosidase (1-400), anti-c-Jun (1-200) or anti-ATF-3 (1-200) antibodies and then a FITC-conjugated anti-mouse IgG antibody (1-100) or FITC-conjugated anti-rabbit IgG antibody (1-100). Nuclei were stained using Hoechst (10 μg/ml). Coverslips were mounted on glass slides using Citifluor. Representative images of sympathetic neurons expressing β-galactosidase, c-Jun or ATF-3 are shown. Pyknotic nuclei are indicated by the white arrowheads. The bar represents 10 μM.

(B) Injected neurons were scored for nuclear morphology. Cells with normal nuclei were counted for each of the four injection mixes tested. The graph shows the percentage of injected cells, expressing the proteins, that have normal nuclei. The data shown represents the average of six independent experiments. Error bars indicate SEM. The decrease in the percentage of normal nuclei observed for cells expressing ATF-3, c-Jun or ATF-3 and c-Jun together, was significantly different to that of β-galactosidase (Student's t-test: $*p<0.005$, $**p<0.001$).

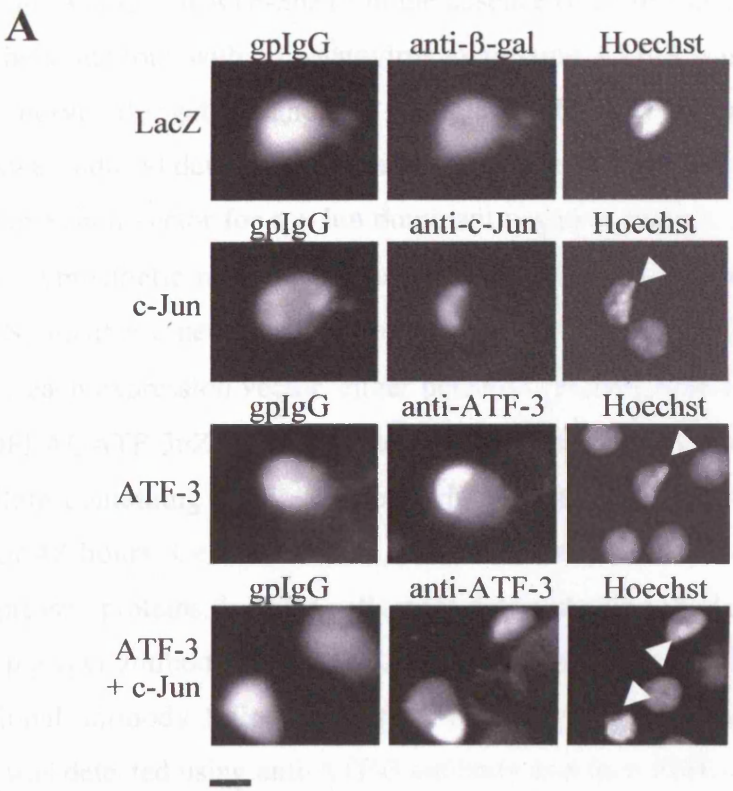
A
gpIgG
anti-β-gal
Hoechst
LacZ
gpIgG
anti-c-Jun
Hoechst
c-Jun
gpIgG
anti-ATF-3
Hoechst
ATF-3
gpIgG
anti-ATF-3
Hoechst
ATF-3
+ c-Jun
B
Percentage of injected neurons with normal nuclei
100
90
80
70
60
50
40
30
20
10
0
**
*
**
LacZ
c-Jun
ATF-3
ATF-3
+ c-Jun
+ NGF 72 hours

To further characterise the role of ATF-3 in sympathetic neurons, the effect of expressing ATF-3 and ATF-3bZIP in the absence of NGF was examined. Infection of sympathetic neurons with an adenovirus expressing ATF-3 was previously shown to induce nerve elongation and the infected cells were protected against NGF withdrawal-induced death to a certain extent (Nakagomi *et al.*, 2003). Microinjection of an expression vector for a c-Jun dominant negative mutant, pCDFLAGΔ169, also protects sympathetic neurons against NGF withdrawal-induced death (Ham *et al.*, 1995). Sympathetic neurons were injected with guinea pig IgG (2.5 μg/μl) and 0.1 μg/μl of each expression vector, either pcDNA1, pCDFLAGΔ169, pCDFLAGATF-3 or pCDFLAGATF-3bZIP. Neurons were allowed to recover from injection overnight in medium containing NGF. The following day the neurons were withdrawn from NGF for 48 hours. Cells were then fixed and stained for the injection marker and overexpressed proteins. Injected cells were detected using rhodamine-conjugated anti-guinea pig IgG antibody and the FLAG-tagged proteins were detected using the M2 monoclonal antibody followed by the FITC-conjugated anti-mouse IgG antibody. ATF-3 was detected using anti-ATF-3 antibody and then FITC-conjugated anti-rabbit IgG antibody, since this worked better than the anti-FLAG antibody for this protein. Injected neurons were scored for nuclear morphology (Figure 5.4). In control experiments with the empty vector pcDNA1, 45.85% of the injected neurons had normal nuclei after 48 hours of NGF withdrawal. Expression of FLAGΔ169 increased the percentage of neurons with normal nuclei to 62.45%. Overexpression of ATF-3 also lead to increased survival of the neurons after NGF withdrawal. 65.55% of the injected cells had normal nuclei. This is similar to the results obtained with adenovirus-infected sympathetic neurons, which showed 60% survival in the case of the ATF-3 virus after 48 hours of NGF withdrawal (Nakagomi *et al.*, 2003). Interestingly the bZIP domain of ATF-3 alone inhibited cell death to an even greater extent than full length ATF-3. 79.68% of the neurons had normal nuclear morphology after 48 hours in the absence of NGF. The ATF-3bZIP protein lacks any transcriptional activation or repression domains. The bZIP domain, by binding to full length transcription factors, such as c-Jun, may prevent them from activating the transcription of target genes. This would suggest that overexpressed ATF-3 may be acting as a transcriptional repressor after NGF withdrawal in sympathetic neurons, since it has the same effect as the bZIP domain alone.

Figure 5.4 Overexpression of ATF-3 or the ATF-3bZIP domain protects sympathetic neurons against NGF withdrawal-induced death

Sympathetic neurons were injected with guinea pig IgG (2.5 μg/μl) and 0.1 μg/μl of each expression vector, either pcDNA1, pCDFLAGΔ169, pCDFLAGATF-3 or pCDFLAGATF-3bZIP. Neurons were allowed to recover overnight in medium containing NGF. The following day the neurons were withdrawn from NGF for 48 hours. Cells were fixed and stained for the injection marker and overexpressed proteins. Injected cells were detected using rhodamine-conjugated anti-guinea pig IgG antibody (1-100). FLAG-tagged proteins were detected using the M2 monoclonal antibody (1-200) and then FITC-conjugated anti-mouse IgG antibody (1-100). ATF-3 was detected using anti-ATF-3 (1-200) and then FITC-conjugated anti-mouse IgG antibody (1-100). Injected neurons were scored for nuclear morphology. Cells with normal nuclei were counted for each of the four injection mixes tested. The data shown represents the average of four independent experiments. Error bars indicate SEM. The increase in normal nuclei observed for cells expressing Δ169, ATF-3, or ATF-3bZIP, was significantly different to that of cells not expressing protein (pcDNA1) [Student's t-test: $*p<0.05$, $**p<0.01$].

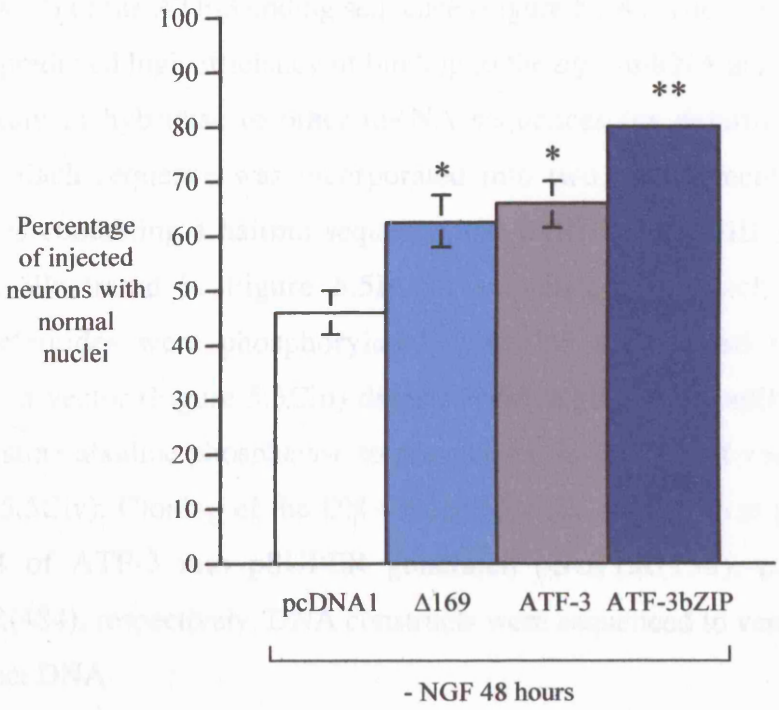
100
90
80
70
60
50
40
30
20
10
0
Percentage of injected neurons with normal nuclei
*
*
**
pcDNA1
Δ169
ATF-3
ATF-3bZIP
- NGF 48 hours

5.2.4 Construction of ATF-3 RNAi expression vectors

To study the role of the endogenous ATF-3 protein in sympathetic neurons deprived of NGF, an ATF-3 RNAi expression vector was constructed to knock down the level of the transcription factor within cells. RNAi sequences were designed using the Oligoengine™ design tool on the website oligoengine.com. Three 19-nucleotide sequences were selected, at positions 158 (5'-CCTTTGCCATCGGATGTCC-3'), 268 (5'-GGAGGCGGCGGGAAAGAAA-3') and 484 (5'-CGCCGGAAGACGAG AGGAA-3') of the ATF-3 coding sequence (Figure 5.5A). These were chosen because of their predicted high efficiency of binding to the *atf-3* mRNA and because they were least likely to hybridise to other mRNA sequences (as determined by a BLAST search). Each sequence was incorporated into two complementary 64-nucleotide sequences containing a hairpin sequence and BglII and HindIII restriction enzyme sites as illustrated in Figure 5.5B for sequence 158. Each pair of 64 base oligonucleotides were phosphorylated, annealed and cloned into the pSUPER expression vector (Figure 5.5Ciii) digested with BglII and HindIII and treated with calf intestine alkaline phosphatase to prevent the re-ligation of vector without insert (Figure 5.5Civ). Cloning of the DNA inserts for the sequences at positions 158, 268 and 484 of ATF-3 into pSUPER generated pSUPER(158), pSUPER(268) and pSUPER(484), respectively. DNA constructs were sequenced to verify the insertion of the correct DNA.

5.2.5 ATF-3 RNAi constructs reduce the level of overexpressed ATF-3 in transfected PC6-3 cells and microinjected sympathetic neurons

To verify that ATF-3 protein levels were knocked down by the RNAi constructs, undifferentiated PC6-3 cells were transfected with pSUPER, pSUPER(158), pSUPER(268) or pSUPER(484) along with the expression vectors pCDFLAGATF-3 or pCDFLAGΔ169. PC6-3 cells (approximately 6 x 10^5 cells) were plated in 6 cm dishes and transfected using Lipofectamine 2000. Protein extracts were prepared after 48 hours and western blot analysis performed with the anti-tubulin antibody and the anti-FLAG M2 antibody to detect expression of FLAG-tagged ATF-3 and Δ169 (Figure 5.6A). FLAGΔ169 was used as a control to measure non-specific effects of the RNAi. Western blots were scanned on a densitometer to quantitate levels of protein. The graph in Figure 5.6B represents the levels of overexpressed

Figure 5.5 Construction of ATF-3 RNAi expression vectors

(A) RNAi sequences were designed using the Oligoengine™ design tool on the website oligoengine.com. Three 19-nucleotide sequences were selected at positions 158 (5'-CCTTTGCCATCGGATGTCC-3'), 268 (5'-GGAGGCGGCGGGAAAGAA A-3') and 484 (5'-CGCCGGAAGACGAGAGGAA-3') of the ATF-3 coding sequence.

(B) The 64-nucleotide oligos containing the RNAi sequence at position 158 of ATF-3. The 19-nucleotide sequence is shown in bold type in the sense and antisense direction, joined together by a hairpin sequence shown in blue. The 5' end corresponds to a BglII site, while the 3' end contains the HindIII restriction site.

(C) The process of generating RNAi using pSUPER. Each pair of 64-nucleotide sequences (500 ng) was phosphorylated, annealed (iii) and inserted into the BglII and HindIII sites of the pSUPER vector (iv). This positions the forward oligo at the correct position downstream from the H1 promoter's TATA box to generate the desired RNAi duplex. In addition the BglII site is destroyed upon ligation to enable more efficient screening of positive clones. The RNA transcript is expressed under the control of the polymerase-III based expression system and forms a short hairpin structure with the 19 base-pair double-stranded region and a hairpin loop formed by the spacer region (ii). The insert is designed such that the first two 5' bases of the spacer region (hairpin loop) are transcribed uridines and includes a specific T5 terminator sequence that incorporates two final uridines at the 3' end of the transcript. When expressed within cells, the hairpin structure is cleaved by the enzyme Dicer to generate a short dsRNA, both strands having a two uridine 3' overhang (i). This generates an efficient effector of RNAi that complies with the design principles established by Tuschl and colleagues (Elbashir *et al.*, 2001).

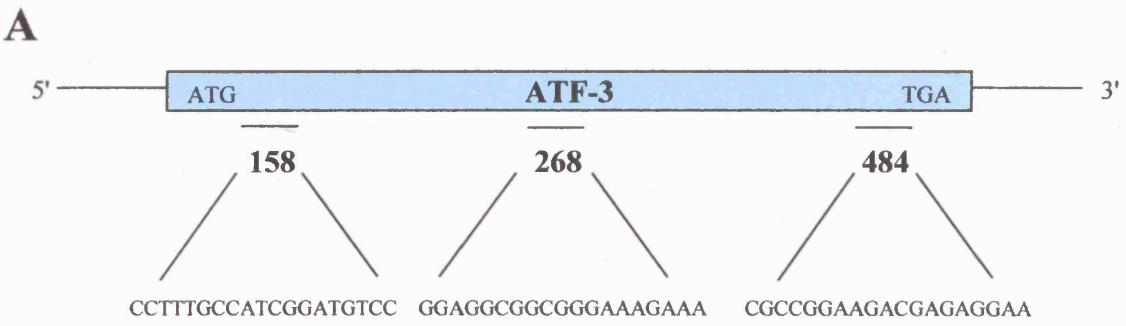
A
5'
ATG
ATF-3
TGA
3'
158
268
484
CCTTTGCCATCGGATGTCC
GGAGGCGGCGGGAAAGAAA
CGCCGGAAGACGAGAGGAA


B
(BglII)
target sequence 158: sense
Hairpin
target sequence158: antisense
5'-GATCCCCCCTTTGCCATCGGATGTCCTTCAAGAGAGGACATCCGATGGCAAAGGTTTTTGGAA-3'
3'-GGGGGAAACGGTAGCCTACAGGAAGTTCTCTCCTGTAGGCTACCGTTTCCAAAAACCTTTTCGA-5'
(HindIII)

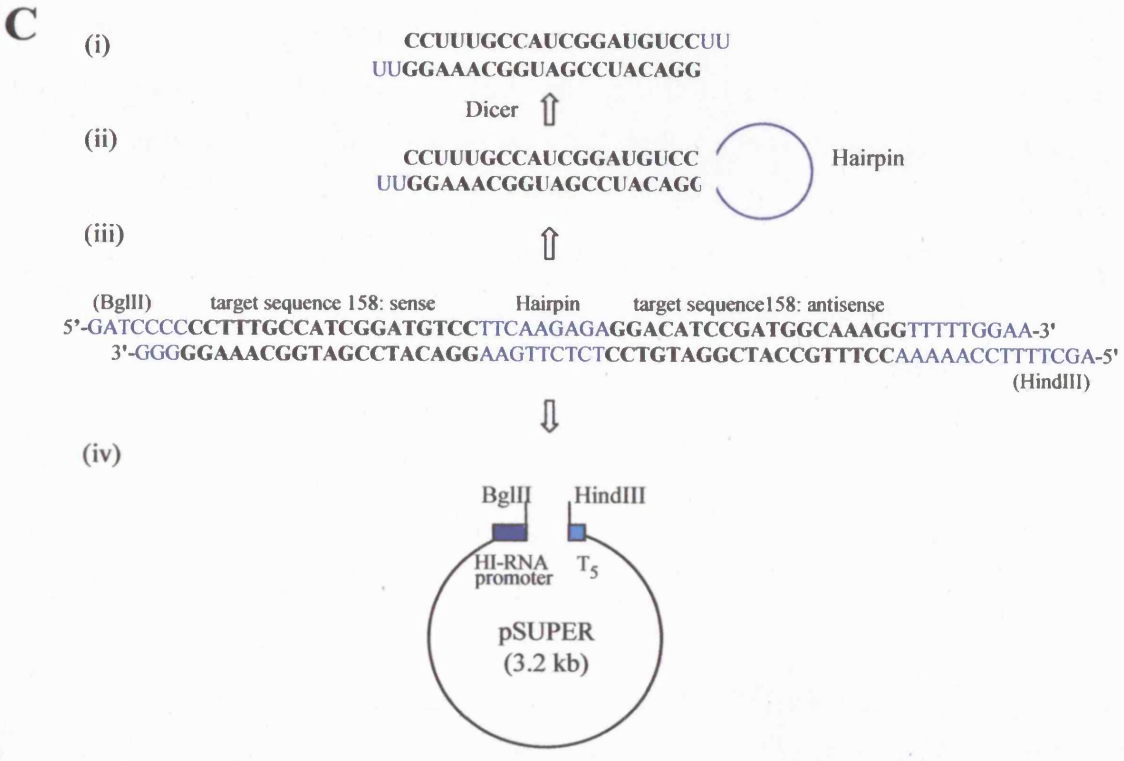
C
(i)
CCUUUGCCAUCGGAUGUCCUU
UUGGAAACGGUAGCCUACAGG
Dicer
(ii)
CCUUUGCCAUCGGAUGUCC
UUGGAAACGGUAGCCUACAGG
Hairpin
(iii)
(BglII)
target sequence 158: sense
Hairpin
target sequence158: antisense
5'-GATCCCCCCTTTGCCATCGGATGTCCTTCAAGAGAGGACATCCGATGGCAAAGGTTTTTGGAA-3'
3'-GGGGGAAACGGTAGCCTACAGGAAGTTCTCTCCTGTAGGCTACCGTTTCCAAAAACCTTTTCGA-5'
(HindIII)
(iv)
BglII
HindIII
HI-RNA promoter
T5
pSUPER
(3.2 kb)

Figure 5.6 ATF-3 RNAi knocks down the level of overexpressed ATF-3 in transfected PC6-3 cells

(A) PC6-3 cells (approximately 6 x 10^5 cells) were plated in 6 cm dishes. DNA mixtures contained 2 μg of pCDFLAGATF-3 or pCDFLAGΔ169 together with 6 μg of pSUPER, pSUPER(158), pSUPER(268) or pSUPER(484). DNA was transfected into PC6-3 cells using Lipofectamine 2000. The DNA (8 μg) and Lipofectamine (20 μl) were both mixed with 273 μl of Opti-MEM® I reduced serum medium as instructed and gently added to the cells. Protein was extracted after 48 hours. Samples were run on a 15% SDS polyacrylamide gel and western blot analysis performed with the anti-tubulin antibody and the anti-FLAG M2 antibody to detect expression of tubulin and FLAG-tagged ATF-3 and Δ169. The transfection experiment was performed more than once to determine the best concentration of RNAi vector to use. A representative experiment is shown.

(B) The blots shown in (A) were scanned on a Bio-Rad GS800 densitometer to quantitate levels of protein expression. Images of bands were captured and quantitated using Bio-Rad Quantity One® software. The graph represents the levels of ATF-3 and Δ169 protein expression relative to that of tubulin to normalise for loadings. All three RNAi constructs strongly reduced FLAGATF-3 levels. In addition, pSUPER(268) had no effect on the level of FLAGΔ169, but pSUPER(158) and pSUPER(484) caused 48% and 77% decreases in the level of FLAGΔ169, respectively.

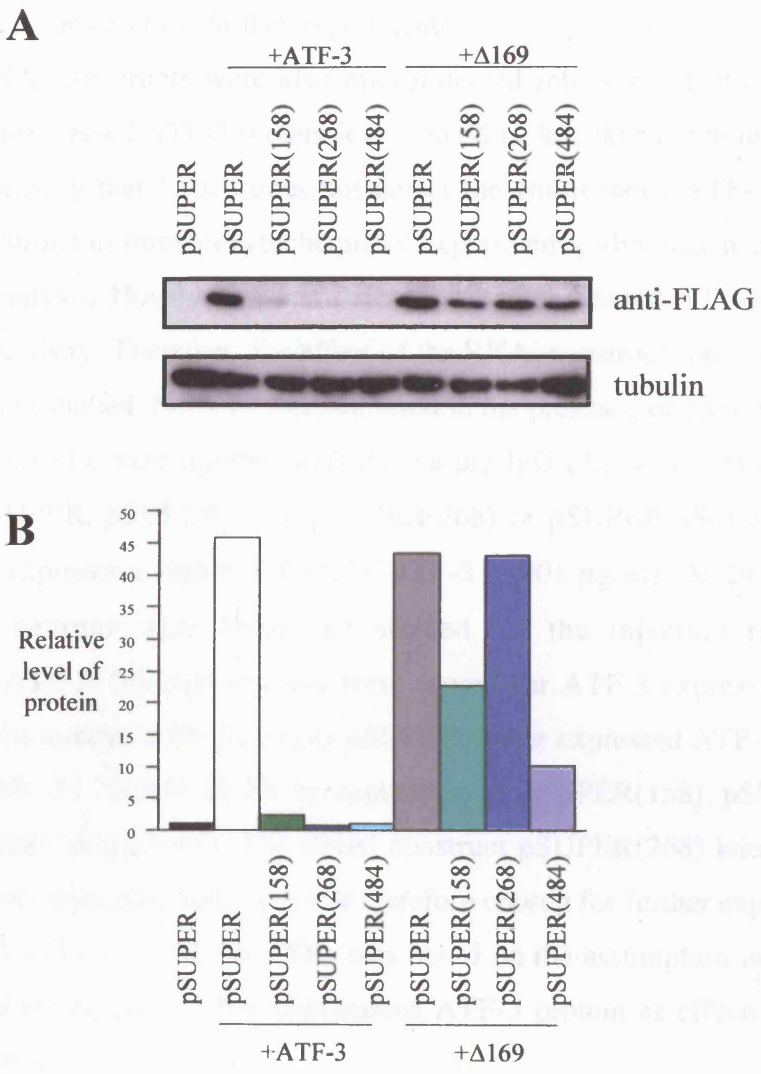
A
+ATF-3
+Δ169
pSUPER
pSUPER
pSUPER(158)
pSUPER(268)
pSUPER(484)
pSUPER
pSUPER(158)
pSUPER(268)
pSUPER(484)
anti-FLAG
tubulin
B
Relative level of protein
50
45
40
35
30
25
20
15
10
5
0
pSUPER
pSUPER
pSUPER(158)
pSUPER(268)
pSUPER(484)
pSUPER
pSUPER(158)
pSUPER(268)
pSUPER(484)
+ATF-3
+Δ169

Δ169 and ATF-3 protein relative to that of tubulin, to normalise for any differences in protein loading. The levels of FLAGATF-3 protein are strongly knocked down by all three RNAi constructs. In addition, the level of Δ169 was not reduced to the same extent. pSUPER(268) did not affect the level of Δ169 expression, suggesting that it might be the best construct for further experiments.

The RNAi constructs were also microinjected into sympathetic neurons to verify that overexpressed ATF-3 protein levels could be knocked down in these cells. The ATF-3 antibody that I used does not detect the endogenous ATF-3 protein in sympathetic neurons in immunocytochemistry experiments, although it can do so in western blot analysis. However, it can detect the overexpressed ATF-3 protein by immunocytochemistry. Therefore, the effect of the RNAi constructs on overexpressed FLAGATF-3 was studied. Neurons were cultured in the presence of NGF for 5-7 days before injection. Cells were injected with guinea pig IgG (2.5 μg/μl) as an injection marker and pSUPER, pSUPER(158), pSUPER(268) or pSUPER(484) at 0.4 μg/μl along with the expression vector pCDFLAGATF-3 (0.001 μg/μl). At 24 hours after injection, the neurons were fixed and stained for the injection marker and overexpressed ATF-3. Injected neurons were scored for ATF-3 expression (Figure 5.7). 61% of cells injected with the empty pSUPER vector expressed ATF-3. This was reduced to 33.3%, 11.7% and 21.7% by expression of pSUPER(158), pSUPER(268) and pSUPER(484), respectively. The RNAi construct pSUPER(268) knocked down ATF-3 expression most efficiently and was therefore chosen for further experiments to study the role of ATF-3 in neurons. This was based on the assumption that it would knock down the expression of the endogenous ATF-3 protein as effectively as the overexpressed protein.

5.2.6 Knocking down ATF-3 in sympathetic neurons increases the rate of cell death after NGF withdrawal

The role of ATF-3 in sympathetic neuron apoptosis was examined in microinjection experiments using the pSUPER(268) RNAi construct. Neurons were cultured in the presence of NGF for 5-7 days before injection. Cells were injected with guinea pig IgG (2.5 μg/μl) as injection marker and 0.2 μg/μl of pSUPER or pSUPER(268). The injected neurons were allowed to recover overnight in medium containing NGF. The following day the neurons were deprived of NGF. After 48

hours, the cells were fixed and stained for the injection marker using a rhodamine-conjugated anti-guinea pig IgG antibody. Injected neurons were scored for nuclear morphology (Figure 5.8). In the case of pSUPER, 59.7% of the neurons had normal nuclei after 48 hours of NGF withdrawal. This was reduced to 42.6% in the case of pSUPER(268). This 17.1% decrease is significant and suggests that the level of ATF-3 regulates the rate of cell death after NGF withdrawal.

Figure 5.7 Expression of ATF-3 RNAi knocks down the level of overexpressed ATF-3 in microinjected sympathetic neurons

Sympathetic neurons were cultured in the presence of NGF for 5-7 days. Neurons were injected with guinea pig IgG (2.5 μg/μl) as an injection marker and the constructs pSUPER, pSUPER(158), pSUPER(268) or pSUPER(484) at 0.4 μg/μl along with the expression vector pCDFLAGATF-3 (0.001 μg/μl). Neurons were left for 24 hours and then immunocytochemistry was performed. Cells were fixed and stained for the injection marker and overexpressed ATF-3. Injected cells were detected using rhodamine-conjugated anti-guinea pig IgG antibody (1-100). ATF-3 was detected using anti-ATF-3 antibody (1-200) and then FITC-conjugated anti-rabbit IgG antibody (1-100). Injected neurons were scored for ATF-3 expression. Injected cells were considered to be expressing ATF-3 if the anti-ATF-3 antibody staining was clearly greater than the background staining observed for uninjected cells. The data shown represents the average of three independent experiments. Error bars indicate SEM.

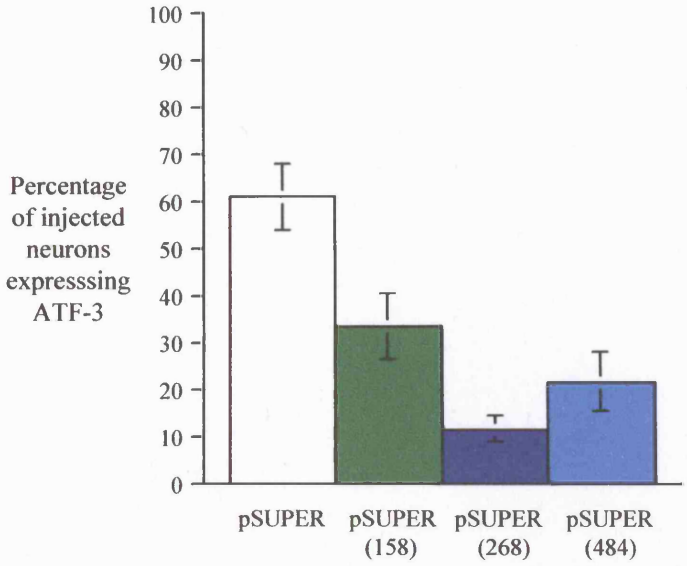
Percentage of injected neurons expresssing ATF-3
100
90
80
70
60
50
40
30
20
10
0
pSUPER
pSUPER (158)
pSUPER (268)
pSUPER (484)

Figure 5.8 Microinjection of pSUPER(268) increases the amount of cell death in sympathetic neurons deprived of NGF

Sympathetic neurons were cultured in the presence of NGF for 5-7 days before injection. Cells were injected with guinea pig IgG (2.5 μg/μl) as injection marker and 0.2 μg/μl of pSUPER or pSUPER(268). The injected neurons were allowed to recover overnight in medium containing NGF. The following day, the neurons were withdrawn from NGF for 48 hours. Cells were fixed and stained for the injection marker using rhodamine-conjugated anti-guinea pig IgG antibody (1-100). Nuclei were stained with Hoechst dye at 10 μg/ml. Injected neurons were scored for nuclear morphology. The data shown represents the average of five independent experiments. Error bars indicate SEM. The percentage of injected neurons with normal nuclei was significantly decreased in the presence of pSUPER(268) [Student's t-test: $*p<0.005$)].

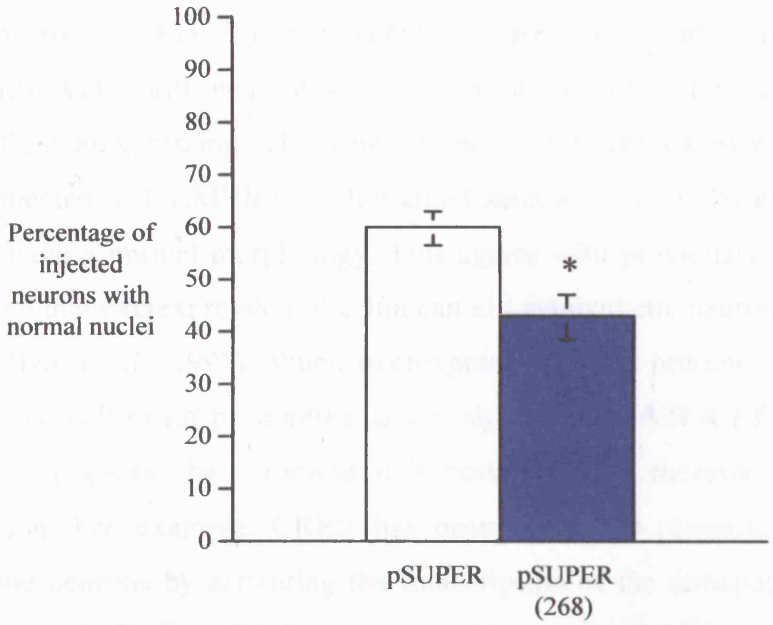
Percentage of injected neurons with normal nuclei
100
90
80
70
60
50
40
30
20
10
0
*
pSUPER
pSUPER (268)

5.3 Discussion

In this chapter, I investigated the function of ATF-3 in sympathetic neurons. Expression vectors encoding full length ATF-3 and the bZIP domain of ATF-3 were constructed and shown to express the proteins in transiently transfected Cos-7 cells and microinjected sympathetic neurons. The bZIP protein was apparently expressed at a lower level in Cos-7 cells than the full length protein, perhaps due to instability/degradation of the shorter peptide.

The role of ATF-3 in sympathetic neurons was studied in microinjection experiments. ATF-3 kills neurons when overexpressed in the presence of NGF. 39.1% of the cells overexpressing ATF-3 had normal nuclei compared with 71.7% of the neurons injected with CMVlacZ. c-Jun killed neurons to a similar extent with 39.3% of nuclei having normal morphology. This agrees with previously published results that showed that overexpression of c-Jun can kill sympathetic neurons in the presence of NGF (Ham *et al.*, 1995). When overexpressed in the presence of NGF, ATF-3 might induce cell death by binding as a homodimer to ATF/CRE elements in the promoters of genes that promote cell survival, and thereby repressing their transcription. For example, CREB has been shown to promote the survival of sympathetic neurons by activating the transcription of the antiapoptotic *bcl-2* gene (Riccio *et al.*, 1999). The CREBm1 mutant, which can bind CRE sites but not activate transcription, kills neurons in the presence of NGF. ATF-3 may bind similar target genes, repressing their transcription, which could lead to apoptosis. A reduction in the number of cells with normal nuclei was also observed when ATF-3 and c-Jun were co-expressed. Expression of both c-Jun and ATF-3 may result in heterodimer formation and therefore the activation of similar gene targets as c-Jun homodimers.

Interestingly, overexpressed ATF-3 did not kill sympathetic neurons in the absence of NGF. In control experiments, 45.8% of sympathetic neurons injected with CMVlacZ had normal nuclei after 48 hours of NGF withdrawal. Overexpression of ATF-3 led to increased survival of neurons after NGF withdrawal (65.55% of injected cells had normal nuclei). This is in agreement with a report that 60% of adenovirus-infected sympathetic neurons overexpressing ATF-3 were viable after 48 hours of NGF withdrawal (Nakagomi *et al.*, 2003). In an organ culture of these neurons, ATF-3 induced neurite outgrowth after NGF withdrawal. Expression of ATF-3 in sympathetic neurons led to a slight increase in expression of Hsp27, but only in cells cultured in the

absence of NGF, suggesting that activation of the JNK/c-Jun pathway is required. ATF-3 is able to bind to the *hsp27* promoter in PC12 cells and transcription of *hsp27* is inhibited by a dominant negative mutant of c-Jun (c-Jun223NLS), again suggesting that the c-Jun/JNK pathway is required.

I also found that expression of the bZIP domain of ATF-3 inhibited cell death to an even greater extent than full length ATF-3. 79.68% of neurons had normal nuclear morphology after 48 hours in the absence of NGF. The ATF-3bZIP protein lacks any transcriptional activation or repression domains. This protein may bind as a homodimer to AP-1 or CRE/ATF sites and prevent endogenous proteins from binding these sites. Alternatively, ATF-3bZIP may form heterodimers with other proteins such as c-Jun, and form complexes with reduced activity. This could imply that overexpressed ATF-3 may be acting as a transcriptional repressor, after NGF withdrawal in sympathetic neurons, since it has the same effect as the bZIP domain alone. This is the opposite of the effect observed by an alternatively spliced form of ATF-3, ATF-3ΔZip. This protein lacks the bZIP domain, and has been shown to stimulate transcription, presumably by sequestering inhibitory cofactors away from the promoter (Chen *et al.*, 1994).

As expected, expression of FLAGΔ169 protected the neurons from NGF withdrawal-induced death. The percentage of injected cells with normal nuclei was significantly higher at 62.45%. This was not as high as the approximately 80% of neurons surviving after 48 hours of NGF withdrawal previously reported (Ham *et al.*, 1995). In those experiments, any neurons that did not have normal nuclei after injection were excluded and survival was scored after 2 days using calcein AM staining, which is converted to fluorescent green calcein in viable cells. This would likely lead to a higher percentage of normal cells compared with my assay, which included all injected cells.

ATF-3 expression was inhibited using the pSUPER RNAi vector system. The RNAi construct pSUPER(268) inhibited FLAGATF-3 expression in Cos-7 cells and sympathetic neurons to the greatest extent and had a minimal effect on the level of overexpressed dominant negative c-Jun (FLAGΔ169). All of the RNAi sequences tested are specific for rat ATF-3 (NCBI blastn search) but may have varying degrees of accessibility to the ATF-3 RNA secondary structure. This would affect their ability to bind the RNA and therefore their ability to lead to the destruction of the double

stranded RNA. The construct pSUPER(268) reduced the percentage of sympathetic neurons with normal nuclei, at 48 hours after NGF withdrawal, to 42.6% compared with the pSUPER control (59.7%). This suggests that the level of ATF-3 regulates the rate of cell death after NGF withdrawal. This agrees with my overexpression results, which found that ATF-3 protected sympathetic neurons against NGF withdrawal-induced death. A reduction in the amount of ATF-3 in sympathetic neurons deprived of NGF could result in increased formation of c-Jun homodimers, which could lead to increased cell death.

The differences in ATF-3 function observed in the presence and absence of NGF may be due to differences in the dimerisation partners present and/or other proteins necessary for NGF withdrawal-induced apoptosis, for example proteins of the c-Jun/JNK pathway. If c-Jun is the dimerisation partner of ATF-3 after NGF withdrawal, the outcome of either cell death or survival will depend on the relative levels of each transcription factor present within dying neurons. c-Jun homodimers could activate transcriptional targets that lead to apoptosis, whereas ATF-3 homodimers could repress the same or different transcriptional targets and cause cell survival. Initially after NGF withdrawal, c-Jun levels and c-Jun activity begin to increase. c-Jun homodimers or c-Jun/X heterodimers may promote apoptosis, since knocking out *c-jun* in sympathetic neurons *in vitro* inhibited NGF withdrawal-induced death (Palmada *et al*, 2002). The delayed induction of ATF-3 may be a compensatory mechanism to rescue neurons from NGF withdrawal-induced death. High levels of ATF-3 could suppress the transcription of gene targets necessary for apoptosis. In sympathetic neurons deprived of NGF, the actual increase in ATF-3 levels may not be high enough to inhibit apoptosis due the presence of high levels of proapoptotic proteins already induced at this time. In addition, the absolute levels of ATF-3 and c-Jun within the dying neurons are unknown and may determine the outcome of cell death or survival. If ATF-3 is much lower than c-Jun at the peak of ATF-3 induction, for example, c-Jun homodimers or c-Jun/X heterodimers might predominate. A hypothetical model of the functional role of these transcription factors is shown in Figure 5.9.

Figure 5.9 Hypothetical model of the function of ATF-3 in sympathetic neurons

(A) In the presence of NGF, the levels of c-Jun and ATF-3 are low and their transcriptional targets are unlikely to be bound by these factors. Genes encoding transcription factors, such as CREB, promote the survival of sympathetic neurons in the presence of NGF. For example, CREB can bind to and activate the *bcl-2* promoter (Riccio *et al.*, 1999).

(B) In the absence of NGF, the levels of c-Jun and then ATF-3 begin to rise. The outcome of either cell death or survival will depend on the relative levels of each transcription factor present within dying neurons.

(i) Initially after NGF withdrawal, c-Jun levels and c-Jun activity begin to increase. c-Jun homodimers or c-Jun/X heterodimers may promote apoptosis by activating cell death genes. Microinjection of sympathetic neurons with a dominant negative c-Jun (FLAGΔ169) or antibodies specific for c-Jun, protects sympathetic neurons from NGF withdrawal-induced death (Ham *et al.*, 1995). Knocking out *c-jun* in sympathetic neurons *in vitro* inhibits NGF withdrawal-induced death (Palmada *et al*, 2002).

(ii) The levels of ATF-3 begin to rise after that of c-Jun. ATF-3 may be induced by the JNK/c-Jun pathway to form c-Jun/ATF-3 heterodimers and ATF-3 homodimers that function in cell survival and neurite outgrowth (Nakagomi *et al.*, 2003). When overexpressed in neurons, ATF-3 decreases the number of dying cells after NGF withdrawal and knocking down ATF-3 in sympathetic neurons *in vitro* increases the rate of cell death. ATF-3 could suppress the transcription of gene targets necessary for apoptosis, as suggested by the protective effect observed when ATF-3bZIP is expressed in neurons. Alternatively c-Jun/ATF-3 heterodimers may activate antiapoptotic genes, such as *hsp27*. The relative levels of ATF-3 and c-Jun within dying neurons may determine whether the outcome is cell death or cell survival.

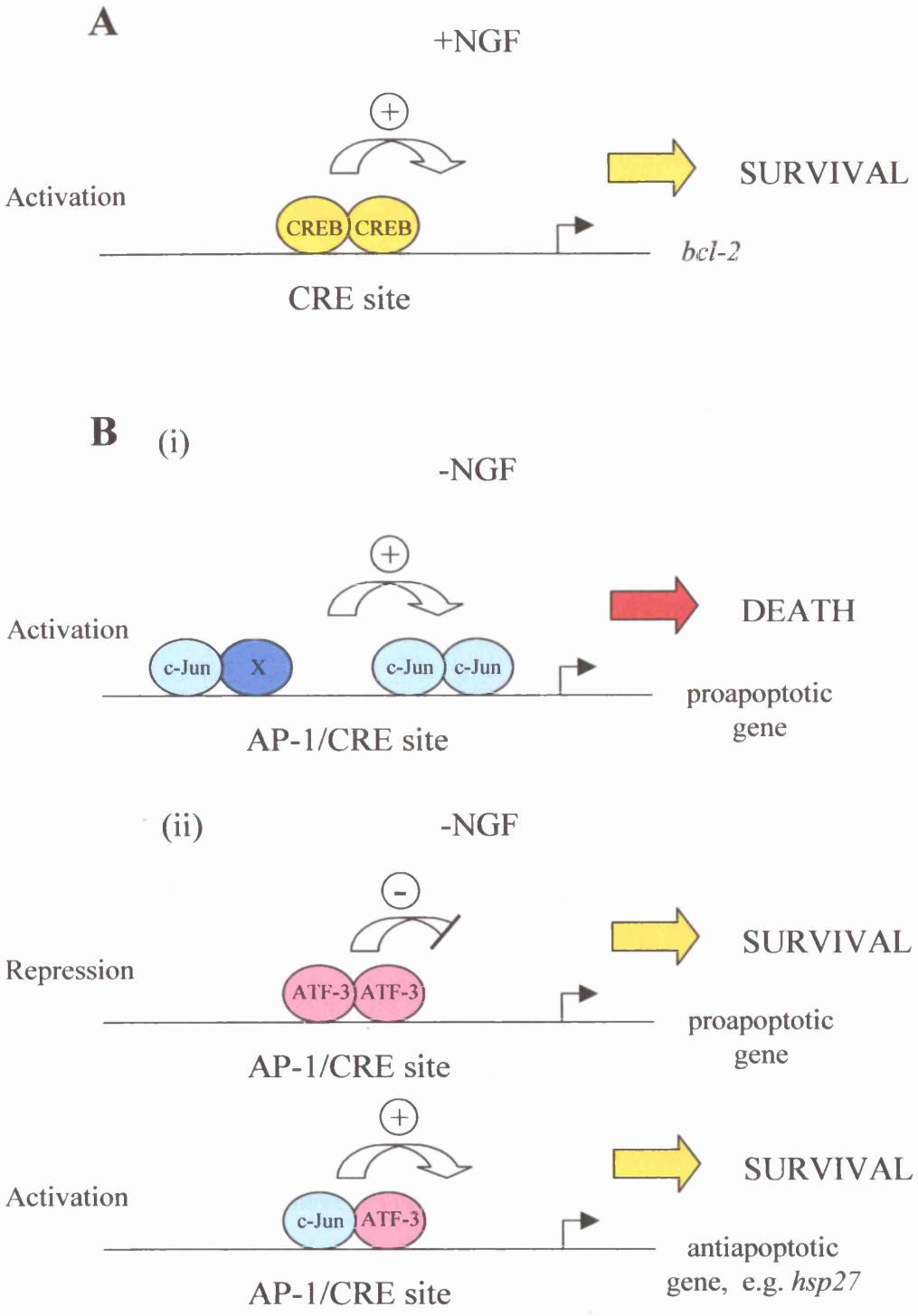
A
+NGF
Activation
CREB
CREB
SURVIVAL
bcl-2
CRE site
B
(i)
-NGF
Activation
c-Jun
X
c-Jun
c-Jun
DEATH
proapoptotic
gene
AP-1/CRE site
(ii)
-NGF
Repression
ATF-3
ATF-3
SURVIVAL
proapoptotic
gene
AP-1/CRE site
Activation
c-Jun
ATF-3
SURVIVAL
antiapoptotic
gene, e.g. hsp27
AP-1/CRE site

Chapter 6: Discussion

Neuronal apoptosis occurs extensively during the normal development of the mammalian nervous system. This death is important for establishing neuronal populations of the correct size and for ensuring that appropriate connections are made between neurons and their target cells (Barde, 1989; Cowan *et al.*, 1984; Levi-Montalcini, 1987). In addition, neuronal apoptosis may contribute to the pathology of human neurodegenerative disorders. Sympathetic neurons and neuronally differentiated PC6-3 cells have proved to be useful *in vitro* models for studying neuronal apoptosis mechanisms. Developing sympathetic neurons and differentiated PC6-3 cells depend on NGF for survival and die by apoptosis in a transcription-dependent manner when this survival factor is removed (Martin *et al.*, 1988; Pittman *et al.*, 1993). The JNK/c-Jun pathway is activated and promotes apoptosis in these cells following NGF withdrawal, but little is known about the transcriptional targets of this pathway.

To study the genes involved in neuronal apoptosis, Affymetrix GeneChip® arrays were used. In three independent experiments, PC6-3 cells were differentiated for 7 days in the presence of NGF, before being deprived of NGF for 16 hours, at which time samples were prepared for microarray experiments. 16 hours was chosen as the time point at which RNA was extracted from PC6-3 cells because this is after the induction and activation of c-Jun and prior to the cell death commitment point. In the case of sympathetic neurons, the cell death commitment point, when 50% of neurons can no longer be rescued from apoptosis by re-addition of NGF, is around 22 hours after NGF withdrawal (Deckwerth and Johnson, 1993). The expression of 78 genes was found to change in level in differentiated PC6-3 cells deprived of NGF for 16 hours. Some of the genes have previously been described as NGF-regulated genes, or as genes induced in neuronal cells undergoing apoptosis, for example c-Jun, ATF-3, GADD153, Txnip and MKP-3. This initial microarray data will be the basis for future experiments. Some of the 78 regulated genes could be characterised further using the approaches described for ATF-3. It would also be informative to perform Affymetrix GeneChip® experiments with RNA isolated from primary sympathetic neurons cultured in the presence and absence of NGF. Methods are now available to amplify the RNA species isolated from small amounts of cells, for use on the arrays. Two cycle

target labelling can be performed using as little as 10 - 100 ng of total RNA. In addition, more comprehensive rat arrays are now available. The GeneChip® Rat Genome 230 Array contains over 28,000 known genes, substantially more than the 7,000 known genes on the U34A array used in this study. This would provide a more detailed analysis of the changes in gene expression in neurons after NGF withdrawal. Another variation would be to perform the NGF withdrawal for different lengths of time, for example 4, 8 and 16 hours, to establish the kinetics of the gene changes observed. To specifically identify targets of the JNK/c-Jun pathway, experiments could be performed using JNK inhibitor compounds such as CEP-11004 or SP600125. RNA isolated from neurons cultured in the presence and absence of NGF and with and without inhibitor, could be used on the GeneChip® Rat Genome 230 Array, to help indicate which genes are regulated by the JNK/c-Jun pathway.

ATF-3 was selected for more detailed analysis because it was the most highly up-regulated gene in the Affymetrix GeneChip® experiments and because it is a potential c-Jun dimerisation partner and c-Jun target gene, whose role in neuronal apoptosis had not been investigated in detail. The increase in ATF-3 expression level detected in the microarray experiments was confirmed at both the RNA and protein level, in agreement with previously published results (Mayumi-Matsuda *et al.*, 1999). The induction of c-Jun occurs prior to the induction of ATF-3 in PC6-3 cells. The expression pattern of ATF-3 in sympathetic neurons undergoing apoptosis was also investigated. There was a 2.1 fold increase in *atf-3* RNA at 16 hours after NGF withdrawal, which agrees with previously published results (Mayumi-Matsuda *et al.*, 1999). This increase in *atf-3* RNA leads to an increase in the amount of ATF-3 protein. The ATF-3 protein started to increase in level between 8 and 16 hours after NGF withdrawal and continued to increase between 16 and 24 hours in the absence of NGF. The level of c-Jun protein and c-Jun N-terminal phosphorylation (manifested as a mobility shift) began to increase between 4 and 8 hours after NGF withdrawal and remained elevated at 16 and 24 hours. It has been shown previously that c-Jun increases in level and is phosphorylated between 8 and 24 hours after NGF withdrawal (Ham *et al*, 1995). The kinetics of induction of these two proteins shows that c-Jun is induced and phosphorylated prior to ATF-3 induction. The *atf-3* promoter contains a number of AP-1 binding sites and can be activated by overexpression of c-Jun and ATF-2 in HeLa cells (Liang *et al.*, 1996) and by MEKK1, an upstream activator of

JNK, in HCT116 colorectal carcinoma cells (Fan *et al.*, 2002). Induction of ATF-3 by ionizing radiation in primary human fibroblasts is mediated by signalling through JNKs and ATF-2 (Kool *et al.*, 2003). ATF-3 therefore has the potential to be a c-Jun and/or ATF-2 target in sympathetic neurons. ATF-2 N-terminal phosphorylation has been shown to increase when sympathetic neurons are deprived of NGF (Eilers *et al.*, 2001). Thus, ATF-2 and c-Jun may activate the transcription of *atf-3* after NGF withdrawal. It would be interesting to investigate whether c-Jun and ATF-2 can bind to the *aft-3* promoter in PC6-3 cells and sympathetic neurons undergoing NGF withdrawal-induced apoptosis. Chromatin immunoprecipitation experiments could be performed with chromatin isolated from differentiated PC6-3 cells cultured in the presence and absence of NGF. Antibodies specific for c-Jun, ATF-2 and ATF-3 and primers specific for the *atf-3* promoter could be used to determine which of these transcription factors are bound to the *atf-3* promoter in PC6-3 cells undergoing apoptosis. Nuclear extracts from PC6-3 cells and possibly sympathetic neurons, cultured in the presence and absence of NGF, could also be used in EMSA experiments. ^{32}P-labelled oligonucleotides containing potential AP-1/ATF binding sites in the *aft-3* promoter could be incubated with the nuclear extracts to determine which transcription factors bind to the promoter during apoptosis.

The involvement of the JNK/c-Jun pathway in ATF-3 induction was investigated using chemical inhibitors. The MLK inhibitor CEP-11004 was added to neurons at the time of NGF withdrawal. This compound is closely related to CEP-1347, which rescues sympathetic neurons from death by NGF deprivation (Maroney *et al.*, 1999), by inhibiting MLKs upstream of JNK in the JNK/c-Jun pathway (Maroney *et al.*, 2001). The induction of ATF-3 after NGF withdrawal was completely inhibited by CEP-11004. However, in contrast to the effect on ATF-3, the increase in c-Jun protein level and phosphorylation observed after NGF withdrawal was reduced but not completely inhibited by addition of CEP-11004. This difference could be due to incomplete inhibition of JNK activity at the concentration of CEP-11004 used (Wang *et al.*, 2005). This reduced JNK activity may be sufficient to induce the expression of some c-Jun protein but not sufficient to induce ATF-3. The JNK inhibitor SP600125 was also used to investigate the involvement of the JNK/c-Jun pathway in ATF-3 protein induction after NGF deprivation. Addition of this compound at the time of NGF withdrawal completely inhibited the increase in c-Jun protein level and

phosphorylation, as expected. ATF-3 induction after NGF deprivation was also completely prevented by SP600125. These results suggest that ATF-3 levels are regulated by the JNK/c-Jun pathway. However, CEP-11004 can also have effects on other signalling pathways. The protective action of CEP-11004 could be mediated through activation of the PI3K survival pathway as well as inhibition of the JNK/c-Jun death pathway (Wang *et al.*, 2005). Therefore it could be argued that the effect of CEP-11004 on ATF-3 protein expression may not be through inhibition of the JNK pathway. However, taken together with the fact that the JNK inhibitor, SP600125, also caused inhibition of ATF-3 induction following NGF-withdrawal, it seems likely that the JNK/c-Jun pathway is involved in ATF-3 regulation. To back up the experiments with chemical inhibitors, it would be interesting to see if direct JNK activation in sympathetic neurons, perhaps using a MLK3 or MEKK1 adenovirus, would lead to induction of ATF-3, and whether ATF-3 induction following NGF withdrawal is inhibited by expressing the JNK binding domain of JIP-1, a direct inhibitor of JNKs.

Having shown that ATF-3 is induced following NGF withdrawal from sympathetic neurons and PC6-3 cells, I next investigated the function of ATF-3 in sympathetic neuron apoptosis. ATF-3 can either act as a transcriptional repressor or activator depending upon whether it is a homodimer or heterodimer, respectively. However, the actual biological function of ATF-3 is not clear, with both protective and detrimental roles proposed. In microinjection experiments, I found that overexpression of ATF-3 kills sympathetic neurons in the presence of NGF. The expression of c-Jun killed neurons to a similar extent and is in agreement with previously published results (Ham *et al.*, 1995). A significant reduction in the percentage of normal neurons was also observed when ATF-3 and c-Jun were expressed together. When overexpressed in the presence of NGF, ATF-3 might induce cell death by binding as a homodimer to ATF/CRE elements in the promoters of genes that promote cell survival, such as *bcl-2*, repressing their transcription. It would be interesting to investigate whether overexpressed ATF-3 homodimers repress such genes. ATF-3/c-Jun heterodimers, however, may act on different target genes to activate transcription of death promoting genes in the presence of NGF. These targets could be the same or different to those targeted by c-Jun homodimers.

Interestingly, overexpressed ATF-3 did not kill sympathetic neurons in the absence of NGF. Injection of an expression vector for ATF-3 lead to increased

survival of neurons after NGF withdrawal. This is in agreement with a report that 60% of adenovirus-infected sympathetic neurons overexpressing ATF-3 were viable after 48 hours of NGF withdrawal (Nakagomi *et al.*, 2003). I have shown that microinjection of an expression vector for dominant negative c-Jun, FLAGΔ169, protected the neurons from NGF withdrawal-induced death, as previously reported (Ham *et al.*, 1995). These results suggest that ATF-3 acts to protect neurons, in contrast to c-Jun, which kills sympathetic neurons after NGF withdrawal. I also found that the bZIP domain of ATF-3 alone inhibited cell death to an even greater extent than full length ATF-3. The ATF-3bZIP protein lacks any transcriptional activation or repression domains. This protein may form heterodimers with other proteins, such as c-Jun, and these complexes may have reduced activity. Alternatively, ATF-3bZIP may bind as a homodimer to AP-1 or CRE/ATF sites and thereby prevent endogenous proteins from binding to these sites. This would imply that overexpressed ATF-3 may be acting as a transcriptional repressor after NGF withdrawal in sympathetic neurons, since it has the same effect as the bZIP domain alone. For example, ATF-3 may repress the transcription of death promoting genes.

To further investigate the function of ATF-3 in sympathetic neurons, the expression of ATF-3 was inhibited using the pSUPER RNAi vector system. A pSUPER vector containing an RNAi sequence specific for ATF-3 reduced the level of overexpressed ATF-3 in Cos-7 cells and sympathetic neurons. This construct reduced the number of normal neurons observed after 48 hours of NGF withdrawal. If the RNAi construct has the same effect on the endogenous ATF-3 as overexpressed ATF-3, then this result would suggest that the level of ATF-3 regulates the rate of cell death after NGF withdrawal. The absence of ATF-3 in sympathetic neurons deprived of NGF could result in increased formation of c-Jun homodimers, which should lead to increased cell death. In addition, if ATF-3 homodimers can repress the transcription of death promoting genes, then a lack of ATF-3 would lead to increased expression of these genes.

The differences in ATF-3 function observed in the presence and absence of NGF may be due to differences in the dimerisation partners present and/or other proteins necessary for NGF withdrawal-induced apoptosis, for example proteins of the JNK/c-Jun pathway. It seems that ATF-3 kills sympathetic neurons in the absence of a factor that becomes available after NGF withdrawal.

The kinetics of ATF-3 and c-Jun induction may play a large part in the effects observed in sympathetic neurons. Initially after NGF withdrawal, c-Jun levels and c-Jun activity begin to increase. c-Jun homodimers or c-Jun/X heterodimers may promote apoptosis, since knocking out *c-jun* in sympathetic neurons *in vitro* inhibited NGF withdrawal-induced death (Palmada *et al*, 2002). Subsequently ATF-3 levels rise and remain elevated at 24 hours after NGF withdrawal. At this time, the levels of c-Jun are also high. My results suggest a protective role for ATF-3 in sympathetic neurons when deprived of NGF. In the ATF-3 overexpression experiments, ATF-3 would be expressed at the time when NGF is removed from the cells and may inhibit c-Jun dimer formation and the activation of cell death genes, thereby promoting survival. However, sympathetic neurons cultured *in vitro* and deprived of NGF die by apoptosis, when both c-Jun and ATF-3 are present in the cell. This would suggest that ATF-3/c-Jun heterodimers could play a role in promoting apoptosis. Perhaps the balance between c-Jun and ATF-3 is critical and each protein regulates the function of the other. High levels of c-Jun promote cell death, whereas high levels of ATF-3 promote survival. Experiments in which both ATF-3 and c-Jun are either overexpressed or knocked down in sympathetic neurons, deprived of NGF, would help establish more precisely their role in apoptosis. I have shown that knocking down ATF-3 protein levels, in the absence of NGF, increased the rate of cell death. Is this due to increased formation of c-Jun homodimers? What happens when c-Jun is also absent? Immunoprecipitation experiments could be performed at different times after NGF withdrawal to determine if and when c-Jun and ATF-3 form homo- or heterodimers after NGF withdrawal from sympathetic neurons, as has been reported in cell lines (Hai and Curran, 1991; Pearson *et al.*, 2003). In addition, identifying the genes that are targeted by these transcription factors, after NGF withdrawal, would help in our understanding of the apoptosis/survival process in neurons.

The targets of ATF-3 within sympathetic neurons are unknown. The *hsp27* gene has been reported as one possible target of c-Jun/ATF-3 heterodimers after NGF withdrawal (Nakagomi *et al.*, 2003). This study suggested that ATF-3 is able to bind to the *hsp27* promoter at an atypical CRE site in PC12 cells but it was not shown whether c-Jun can directly bind the same site. However, this was suggested because transcription of *hsp27* is inhibited by a dominant negative mutant of c-Jun (c-Jun223NLS), in the presence of activated MEKK1. ATF-3 can repress the

transcription of *GADD153* and form a non-functional heterodimer that does not bind to the ATF/CRE element consensus site and does not repress transcription (Chen *et al.*, 1996). My Affymetrix GeneChip® experiment showed that the *GADD153* mRNA increased in level in PC6-3 cells deprived of NGF. GADD153 can induce apoptosis and this is accompanied by a downregulation of *bcl-2* (Matsumoto *et al.*, 1996). Oxidative stress leads to increased binding of Fos and Jun proteins to the AP-1 site in the *GADD153* promoter when transfected into HeLa cells (Guyton *et al.*, 1996). Thus, GADD153 expression may be regulated by the ATF/AP-1 family during apoptosis. It would of interest to examine the kinetics of induction of this protein after NGF deprivation in sympathetic neurons, and whether ATF-3 can regulate GADD153 expression in neurons or PC6-3 cells.

ATF-3 is up-regulated in response to axotomy with a similar expression pattern to c-Jun (Takeda *et al.*, 2000; Tsujino *et al.*, 2000). Expression of ATF-3 enhances c-Jun-mediated neurite sprouting in PC12 cells (Pearson *et al.*, 2003) and infection of sympathetic neurons with an adenovirus expressing ATF-3 was shown to induce nerve elongation (Nakagomi *et al.*, 2003). This suggests that expression of these proteins following axotomy represents an attempt by an injured cell to activate a regeneration response and that they may cooperate to initiate cell survival. A recent study using mice with a conditional knockout of c-Jun in neural cells (*c-Jun*$^{\Delta N}$), showed that CNS-specific inactivation of *c-jun* caused severe defects in the axonal response, leading to impaired target reinnervation (Raivich *et al.*, 2004). In addition, these motoneurons were resistant to axotomy-induced cell death, supporting a role for c-Jun in both neuronal apoptosis and axonal regeneration. If c-Jun is the dimerisation partner of ATF-3 after NGF withdrawal, the outcome of either cell death or survival may depend on the relative levels of each transcription factor present within dying neurons.

In conclusion, I have shown that the transcription factor ATF-3 is induced following NGF deprivation in PC6-3 cells and sympathetic neurons. This increase in expression occurs after the increase in level of c-Jun and the JNK/c-Jun pathway is potentially involved in this up-regulation of ATF-3 after NGF withdrawal. The overexpression of ATF-3 kills sympathetic neurons in the presence of NGF, but increases survival of these cells in the absence of NGF. The bZIP domain of ATF-3 also increases neuronal survival, suggesting that full length ATF-3 may inhibit transcription after NGF withdrawal. Knocking down ATF-3 in sympathetic neurons

increases the rate of cell death, further suggesting that ATF-3 is involved in controlling the extent of neuronal apoptosis after NGF withdrawal. Experiments to knock down c-Jun in cells in which ATF-3 has been knocked down, will confirm whether this increased rate of death is due to increased formation of c-Jun homodimers in the absence of ATF-3. The RNAi results could also be confirmed by culturing neurons from *aft-3*$^{-/-}$ knockout mice (Hartman *et al.*, 2004). The rate of cell death of sympathetic neurons deprived of NGF from these knockout mice could be compared to wild-type and heterozygous littermates. Sympathetic neurons expressing a floxed *c-jun* gene could be used to knock out this gene *in vitro* (following infection with an adenovirus expressing CRE recombinase). These neurons could be used to investigate whether the levels of ATF-3 induction are affected by the absence of c-Jun and thus indicate whether ATF-3 is a c-Jun target gene.

Appendix A

List B Statistically significant gene changes, genes detected in 2 of 3 experiments

List B **Increased genes**

Accession number	Fold Increase	Gene	Gene Symbol	Function	Cellular component
M34253	2.37	interferon regulatory factor 1	Irf1	immune response / regulation of transcription, DNA-dependent	nucleus
J03754	1.9	ATPase, Ca++ transporting, plasma membrane 2	Atp2b2	calcium ion transport / cation transport / metabolism / perception of sound	integral to membrane / membrane / plasma membrane
E04239	1.86	choline kinase alpha	Chka	choline kinase activity / kinase activity / transferase activity	cytoplasm
AF006664	1.81	NK2 transcription factor related, locus 5 (Drosophila)	Nkx2-5	transcription factor activity / cardiac development	nucleus
AI014169	1.78	up-regulated by 1,25-dihydroxyvitamin D-3	Txnip	regulation of cell proliferation	cytoplasm
AI171090	1.61	3-hydroxy-3-methylglutaryl CoA lyase	Hmgcl	catalytic activity / hydroxymethylglutaryl-CoA lyase activity / Cholesterol biosynthesis / Synthesis and degradation of ketone bodies	mitochondrion
Y08138	1.57	dHand protein	Hand2	angiogenesis / development / heart development / positive regulation of transcription, DNA-dependent	nucleus
AF067727	1.54	MAD homolog 1 (Drosophila)	Madh1/ SMAD1	regulation of transcription, DNA-dependent	intracellular cytoplasm / peripheral membrane / nucleus
AF018261	1.54	Epsin 1	Epn1	endocytosis	cytoplasm / peripheral membrane
L26268	1.51	B-cell translocation gene 1, anti-proliferative	Btg1	anti-proliferative / t(8;12)(q24;q22) chromosomal translocation in a case of B-cell chronic lymphocytic leukemia	nucleus / cytoplasm
M26125	1.49	epoxide hydrolase	EPHX	aminopeptidase activity / catalytic activity / epoxide hydrolase activity / proteolysis and peptidolysis / xenobiotic metabolism	endoplasmic reticulum / extracellular space / integral to membrane / microsome

List B **Decreased genes**

Accession number	Fold Decrease	Gene	Gene Symbol	Function	Cellular component
M14775	6.43	cytochrome P450, 2c39	Cyp2c39	monooxygenase	micosomal / mitochondrial / integral membrane
U42627	5.46	dual specificity phosphatase 6 / MAPkinase phosphatase-3	Dusp6 / MKP-3	protein amino acid dephosphorylation / cell differentiation / MAP kinase phosphatase activity	cytoplasm
AI177004 X52625	2.53 2.15	3-hydroxy-3-methylglutaryl-Coenzyme A synthase 1	Hmgcs1	acetyl-CoA metabolism / cholesterol biosynthesis / transferase activity	cytoplasm
E12625	2.1	sterol-C4-methyl oxidase-like	Sc4mol	metabolism / sterol biosynthesis / catalytic activity / oxidoreductase activity	endoplasmic reticulum / integral to membrane
X55286	2.01	3-hydroxy-3-methylglutaryl-Coenzyme A reductase	Hmgcr	biosynthesis / cholesterol biosynthesis / lipid metabolism / hydroxymethylglutaryl-CoA reductase activity / oxidoreductase activity	endoplasmic reticulum / endoplasmic reticulum membrane / integral to membrane
U02316	2	neuregulin 1	Nrg1	embryonic development / growth factor activity / receptor binding	integral to membrane
M89945	1.81 1.62	farensyl diphosphate synthase	Fdps	cholesterol biosynthesis / isoprenoid biosynthesis / transferase activity	cytoplasm
U36895	1.8	putative vomeronasal receptor 3	Vnr3/VN3	olfactory receptor / putative transmembrane receptor	putative membrane protein
S63521	1.78	glucose-regulated protein GRP78	GRP78	Heat shock protein family / antiapoptotic ER chaperone-glucose-regulated protein / inhibit PERK phosphorylation / ER stress	endoplasmic reticulum
AA998446	1.72	phosphatidylinositol transfer protein, beta	Pitpnb	transport / lipid binding / phosphatidylinositol transporter activity	intracellular
AF003835	1.71	isopentenyl-diphosphate delta isomerase	Idi1	carotenoid biosynthesis / cholesterol biosynthesis / isoprenoid biosynthesis / sterol biosynthesis / isomerase activity / magnesium ion binding	peroxisome

Accession number	Fold Decrease	Gene	Gene Symbol	Function	Cellular component
U67995 M15114	1.67 1.45	stearoyl-Coenzyme A desaturase 2	Scd2	fatty acid synthesis	integral to membrane
S69329	1.64 1.5	ISL1 transcription factor, LIM/homeodomain 1	Isl1	development / energy pathways / regulation of transcription, DNA-dependent	nucleus
Y00396	1.62	c-myc / v-myc myelocytomatosis viral oncogene homolog (avian)	Myc	regulation of cell cycle / transcription initiation / regulation of transcription, DNA-dependent / cell growth and/or maintenance / pathogenesis	nucleus
AA963449 U17697	1.59 1.54	cytochrome P450, subfamily 51	Cyp51	electron transport / proteolysis and peptidolysis / cholesterol biosynthesis	extracellular space / integral to membrane
M19651	1.52	fos-like antigen 1	Fosl1	positive regulation of transcription from Pol II promoter, mitotic / regulation of transcription, DNA-dependent / transcriptional activator activity	nucleus
AF061266	1.52	transient receptor protein 1	Trp1	cation channels / receptor-dependent activation / Store-operated calcium entry	membrane
AA891041	1.51	Jun-B oncogene	Junb	regulation of transcription, DNA-dependent / positive regulation of transcription from Pol II promoter, mitotic	nucleus
J02585	1.51	stearoyl-Coenzyme A desaturase 1	Scd1	fatty acid synthesis	integral to membrane
Y09507	1.51	hypoxia inducible factor 1, alpha subunit	Hif1a	regulation of transcription, DNA-dependent / response to hypoxia / signal transduction	nucleus
M81183	1.5	Insulin-like growth factor I	IGF1	growth and development / signal transduction / hormone activity / growth factor activity / regulation of cell proliferation	extracellular

Accession number	Fold Decrease	Gene	Gene Symbol	Function	Cellular component
X02412	1.47	tropomyosin 1, alpha	Tpm1	muscle contraction / muscle development / actin binding / structural constituent of cytoskeleton	cytoskeleton / kinesin complex / muscle thin filament tropomyosin
L35558	1.47	solute carrier family 1 (neuronal/epithelial high affinity glutamate transporter), member 1	Slc1a1	transport / dicarboxylic acid transport	integral to plasma membrane / membrane

Appendix B

List C Statistically significant gene changes, genes detected in 3 of 3 experiments

List C **Increased**

Accession number	Fold Increase	Gene	Gene Symbol	Function	Cellular component
J03754	1.9	ATPase, Ca++ transporting, plasma membrane 2	Atp2b2	cation transport / calcium ion transport / perception of sound / metabolism	plasma membrane / integral to membrane
E04239	1.86	choline kinase alpha	Chka	Acetylcholine synthesis / choline kinase activity / kinase activity / transferase activity / cell growth	cytoplasm
AI014169	1.78	up-regulated by 1,25-dihydroxyvitamin D-3	Txnip	regulation of cell proliferation	cytoplasm
Y08138	1.57	dHand protein	Hand2	angiogenesis / regulation of transcription, DNA-dependent / development / heart development	nucleus
AF018261	1.54	Epsin 1	Epn1	endocytosis	cytoplasm / peripheral membrane
L26268	1.51	B-cell translocation gene 1	Btg1	anti-proliferative / t(8;12)(q24;q22) chromosomal translocation in a B-cell chronic lymphocytic leukemia	nucleus / cytoplasm

List C **Decreased**

Accession number	Fold Decrease	Gene	Gene Symbol	Function	Cellular component
U42627	5.46	dual specificity phosphatase 6 / MAPkinase phosphatase-3	Dusp6 / MKP-3	protein amino acid dephosphorylation / cell differentiation / MAP kinase phosphatase activity	cytoplasm
AI177004 X52625	2.53 2.15	3-hydroxy-3-methylglutaryl-Coenzyme A synthase 1	Hmgcs1	acetyl-CoA metabolism / cholesterol biosynthesis	cytoplasm
E12625	2.1	sterol-C4-methyl oxidase-like	Sc4mol	metabolism / sterol biosynthesis	endoplasmic reticulum / integral to membrane
X55286	2.01	3-hydroxy-3-methylglutaryl-Coenzyme A reductase	Hmgcr	lipid metabolism / cholesterol biosynthesis / biosynthesis	endoplasmic reticulum / endoplasmic reticulum membrane / integral to membrane
M89945	1.81 1.62	farensyl diphosphate synthase	Fdps	cholesterol biosynthesis / isoprenoid biosynthesis / transferase activity	cytoplasm
U36895	1.8	putative vomeronasal receptor 3	Vnr3/VN3	olfactory receptor / putative transmembrane receptor	putative membrane protein
S63521	1.78	glucose-regulated protein GRP78	GRP78	Heat shock protein family / antiapoptotic ER chaperone-glucose-regulated protein / inhibit PERK phosphorylation / ER stress	endoplasmic reticulum
AA998446	1.72	phosphatidylinositol transfer protein, beta	Pitpnb	transport / lipid binding / phosphatidylinositol transporter activity	intracellular
AF003835	1.71	isopentenyl-diphosphate delta isomerase	Idi1	carotenoid biosynthesis / cholesterol biosynthesis / isoprenoid biosynthesis / sterol biosynthesis / isomerase activity / magnesium ion binding	peroxisome
U67995 M15114	1.67 1.45	stearoyl-Coenzyme A desaturase 2	Scd2	fatty acid synthesis	integral to membrane

Accession number	Fold Decrease	Gene	Gene Symbol	Function	Cellular component
S69329	1.64 1.5	ISL1 transcription factor, LIM/homeodomain 1	Isl1	development / energy pathways / regulation of transcription, DNA-dependent	nucleus
Y00396	1.62	c-myc / v-myc myelocytomatosis viral oncogene homolog (avian)	Myc	regulation of cell cycle / transcription initiation / regulation of transcription, DNA-dependent / cell growth and/or maintenance / pathogenesis	nucleus
AA963449 U17697	1.59 1.54	cytochrome P450, subfamily 51	Cyp51	electron transport / proteolysis and peptidolysis / cholesterol biosynthesis	extracellular space / integral to membrane
M19651	1.52	fos-like antigen 1	Fosl1	positive regulation of transcription from Pol II promoter, mitotic / regulation of transcription, DNA-dependent / transcriptional activator activity	nucleus
AF061266	1.52	transient receptor protein 1	Trp1	cation channels / receptor-dependent activation / Store-operated calcium entry	membrane
AA891041	1.51	Jun-B oncogene	Junb	regulation of transcription, DNA-dependent / positive regulation of transcription from Pol II promoter, mitotic	nucleus
J02585	1.51	stearoyl-Coenzyme A desaturase 1	Scd1	fatty acid synthesis	integral to membrane
Y09507	1.51	hypoxia inducible factor 1, alpha subunit	Hif1a	regulation of transcription, DNA-dependent / response to hypoxia / signal transduction	nucleus
X02412	1.47	tropomyosin 1, alpha	Tpm1	muscle contraction / muscle development / actin binding / structural constituent of cytoskeleton	cytoskeleton / kinesin complex / muscle thin filament tropomyosin
L35558	1.47	solute carrier family 1 (neuronal/epithelial high affinity glutamate transporter), member 1	Slc1a1	transport / dicarboxylic acid transport	integral to plasma membrane / membrane

References

Acehan, D., Jiang, X., Morgan, D. G., Heuser, J. E., Wang, X., and Akey, C. W. (2002). Three-dimensional structure of the apoptosome: implications for assembly, procaspase-9 binding, and activation. Mol Cell *9*, 423-432.

Akao, Y., Otsuki, Y., Kataoka, S., Ito, Y., and Tsujimoto, Y. (1994). Multiple subcellular localization of bcl-2: detection in nuclear outer membrane, endoplasmic reticulum membrane, and mitochondrial membranes. Cancer Res *54*, 2468-2471.

Akhtar, R. S., Ness, J. M., and Roth, K. A. (2004). Bcl-2 family regulation of neuronal development and neurodegeneration. Biochim Biophys Acta *1644*, 189-203.

Alberts, A. S., Frost, J. A., and Thorburn, A. M. (1993). Rapid transcriptional assay for the expression of two distinct reporter genes by microinjection. DNA Cell Biol *12*, 935-943.

Allan, L. A., Morrice, N., Brady, S., Magee, G., Pathak, S., and Clarke, P. R. (2003). Inhibition of caspase-9 through phosphorylation at Thr 125 by ERK MAPK. Nat Cell Biol *5*, 647-654.

Alnemri, E. S., Livingston, D. J., Nicholson, D. W., Salvesen, G., Thornberry, N. A., Wong, W. W., and Yuan, J. (1996). Human ICE/CED-3 protease nomenclature. Cell *87*, 171.

Aloyz, R. S., Bamji, S. X., Pozniak, C. D., Toma, J. G., Atwal, J., Kaplan, D. R., and Miller, F. D. (1998). p53 is essential for developmental neuron death as regulated by the TrkA and p75 neurotrophin receptors. J Cell Biol *143*, 1691-1703.

Angel, P., Hattori, K., Smeal, T., and Karin, M. (1988). The jun proto-oncogene is positively autoregulated by its product, Jun/AP-1. Cell *55*, 875-885.

Angel, P., and Karin, M. (1991). The role of Jun, Fos and the AP-1 complex in cell-proliferation and transformation. Biochim Biophys Acta *1072*, 129-157.

Anglade, P., Vyas, S., Javoy-Agid, F., Herrero, M. T., Michel, P. P., Marquez, J., Mouatt-Prigent, A., Ruberg, M., Hirsch, E. C., and Agid, Y. (1997). Apoptosis and autophagy in nigral neurons of patients with Parkinson's disease. Histol Histopathol *12*, 25-31.

Antonsson, B., Montessuit, S., Sanchez, B., and Martinou, J. C. (2001). Bax is present as a high molecular weight oligomer/complex in the mitochondrial membrane of apoptotic cells. J Biol Chem *276*, 11615-11623.

Arrowsmith, J. E., Grocott, H. P., Reves, J. G., and Newman, M. F. (2000). Central nervous system complications of cardiac surgery. Br J Anaesth *84*, 378-393.

Ashkenazi, A., and Dixit, V. M. (1998). Death receptors: signaling and modulation. Science *281*, 1305-1308.

Bain, J., McLauchlan, H., Elliott, M., and Cohen, P. (2003). The specificities of protein kinase inhibitors: an update. Biochem J *371*, 199-204.

Bamji, S. X., Majdan, M., Pozniak, C. D., Belliveau, D. J., Aloyz, R., Kohn, J., Causing, C. G., and Miller, F. D. (1998). The p75 neurotrophin receptor mediates neuronal apoptosis and is essential for naturally occurring sympathetic neuron death. J Cell Biol *140*, 911-923.

Banati, R. B., Daniel, S. E., and Blunt, S. B. (1998). Glial pathology but absence of apoptotic nigral neurons in long-standing Parkinson's disease. Mov Disord *13*, 221-227.

Banda, N. K., Bernier, J., Kurahara, D. K., Kurrle, R., Haigwood, N., Sekaly, R. P., and Finkel, T. H. (1992). Crosslinking CD4 by human immunodeficiency virus gp120 primes T cells for activation-induced apoptosis. J Exp Med *176*, 1099-1106.

Barbacid, M. (1995). Structural and functional properties of the TRK family of neurotrophin receptors. Ann N Y Acad Sci *766*, 442-458.

Barde, Y. A. (1989). Trophic factors and neuronal survival. Neuron *2*, 1525-1534.

Barinaga, M. (1998). Stroke-damaged neurons may commit cellular suicide. Science *281*, 1302-1303.

Basanez, G., Nechushtan, A., Drozhinin, O., Chanturiya, A., Choe, E., Tutt, S., Wood, K. A., Hsu, Y., Zimmerberg, J., and Youle, R. J. (1999). Bax, but not Bcl-xL, decreases the lifetime of planar phospholipid bilayer membranes at subnanomolar concentrations. Proc Natl Acad Sci U S A *96*, 5492-5497.

Basu, A., and Haldar, S. (2003). Identification of a novel Bcl-xL phosphorylation site regulating the sensitivity of taxol- or 2-methoxyestradiol-induced apoptosis. FEBS Lett *538*, 41-47.

Bazenet, C. E., Mota, M. A., and Rubin, L. L. (1998). The small GTP-binding protein Cdc42 is required for nerve growth factor withdrawal-induced neuronal death. Proc Natl Acad Sci U S A *95*, 3984-3989.

Becker, E. B., Howell, J., Kodama, Y., Barker, P. A., and Bonni, A. (2004). Characterization of the c-Jun N-terminal kinase-BimEL signaling pathway in neuronal apoptosis. J Neurosci *24*, 8762-8770.

Behrens, A., Sibilia, M., and Wagner, E. F. (1999). Amino-terminal phosphorylation of c-Jun regulates stress-induced apoptosis and cellular proliferation. Nat Genet *21*, 326-329.

Benedetti, M., Levi, A., and Chao, M. V. (1993). Differential expression of nerve growth factor receptors leads to altered binding affinity and neurotrophin responsiveness. Proc Natl Acad Sci U S A *90*, 7859-7863.

Bennett, B. L., Sasaki, D. T., Murray, B. W., O'Leary, E. C., Sakata, S. T., Xu, W., Leisten, J. C., Motiwala, A., Pierce, S., Satoh, Y., *et al.* (2001). SP600125, an

anthrapyrazolone inhibitor of Jun N-terminal kinase. Proc Natl Acad Sci U S A *98*, 13681-13686.

Bergeron, L., Perez, G. I., Macdonald, G., Shi, L., Sun, Y., Jurisicova, A., Varmuza, S., Latham, K. E., Flaws, J. A., Salter, J. C., *et al.* (1998). Defects in regulation of apoptosis in caspase-2-deficient mice. Genes Dev *12*, 1304-1314.

Berridge, M. J. (2002). The endoplasmic reticulum: a multifunctional signaling organelle. Cell Calcium *32*, 235-249.

Bibel, M., Hoppe, E., and Barde, Y. A. (1999). Biochemical and functional interactions between the neurotrophin receptors trk and p75NTR. Embo J *18*, 616-622.

Biggs, W. H., 3rd, Meisenhelder, J., Hunter, T., Cavenee, W. K., and Arden, K. C. (1999). Protein kinase B/Akt-mediated phosphorylation promotes nuclear exclusion of the winged helix transcription factor FKHR1. Proc Natl Acad Sci U S A *96*, 7421-7426.

Biswas, S. C., and Greene, L. A. (2002). Nerve growth factor (NGF) down-regulates the Bcl-2 homology 3 (BH3) domain-only protein Bim and suppresses its proapoptotic activity by phosphorylation. J Biol Chem *277*, 49511-49516.

Bock, B. C., Vacratsis, P. O., Qamirani, E., and Gallo, K. A. (2000). Cdc42-induced activation of the mixed-lineage kinase SPRK in vivo. Requirement of the Cdc42/Rac interactive binding motif and changes in phosphorylation. J Biol Chem *275*, 14231-14241.

Bogoyevitch, M. A., Boehm, I., Oakley, A., Ketterman, A. J., and Barr, R. K. (2004). Targeting the JNK MAPK cascade for inhibition: basic science and therapeutic potential. Biochim Biophys Acta *1697*, 89-101.

Boise, L. H., Minn, A. J., Noel, P. J., June, C. H., Accavitti, M. A., Lindsten, T., and Thompson, C. B. (1995). CD28 costimulation can promote T cell survival by enhancing the expression of Bcl-XL. Immunity *3*, 87-98.

Boldin, M. P., Varfolomeev, E. E., Pancer, Z., Mett, I. L., Camonis, J. H., and Wallach, D. (1995). A novel protein that interacts with the death domain of Fas/APO1 contains a sequence motif related to the death domain. J Biol Chem *270*, 7795-7798.

Bonni, A., Brunet, A., West, A. E., Datta, S. R., Takasu, M. A., and Greenberg, M. E. (1999). Cell survival promoted by the Ras-MAPK signaling pathway by transcription-dependent and -independent mechanisms. Science *286*, 1358-1362.

Boss, V., Roback, J. D., Young, A. N., Roback, L. J., Weisenhorn, D. M., Medina-Flores, R., and Wainer, B. H. (2001). Nerve growth factor, but not epidermal growth factor, increases Fra-2 expression and alters Fra-2/JunD binding to AP-1 and CREB binding elements in pheochromocytoma (PC12) cells. J Neurosci *21*, 18-26.

Bottjer, S. W., and Arnold, A. P. (1997). Developmental plasticity in neural circuits for a learned behavior. Annu Rev Neurosci *20*, 459-481.

Boudreau, N., Sympson, C. J., Werb, Z., and Bissell, M. J. (1995). Suppression of ICE and apoptosis in mammary epithelial cells by extracellular matrix. Science *267*, 891-893.

Bouillet, P., Metcalf, D., Huang, D. C., Tarlinton, D. M., Kay, T. W., Kontgen, F., Adams, J. M., and Strasser, A. (1999). Proapoptotic Bcl-2 relative Bim required for certain apoptotic responses, leukocyte homeostasis, and to preclude autoimmunity. Science *286*, 1735-1738.

Brichese, L., Cazettes, G., and Valette, A. (2004). JNK is associated with Bcl-2 and PP1 in mitochondria: paclitaxel induces its activation and its association with the phosphorylated form of Bcl-2. Cell Cycle *3*, 1312-1319.

Bronk, S. F., and Gores, G. J. (1993). pH-dependent nonlysosomal proteolysis contributes to lethal anoxic injury of rat hepatocytes. Am J Physiol *264*, G744-751.

Brown, P. H., Chen, T. K., and Birrer, M. J. (1994). Mechanism of action of a dominant-negative mutant of c-Jun. Oncogene *9*, 791-799.

Brown, R. H., Jr. (1995). Superoxide dismutase in familial amyotrophic lateral sclerosis: models for gain of function. Curr Opin Neurobiol *5*, 841-846.

Bruckner, S. R., Tammariello, S. P., Kuan, C. Y., Flavell, R. A., Rakic, P., and Estus, S. (2001). JNK3 contributes to c-Jun activation and apoptosis but not oxidative stress in nerve growth factor-deprived sympathetic neurons. J Neurochem *78*, 298-303.

Brummelkamp, T. R., Bernards, R., and Agami, R. (2002). A system for stable expression of short interfering RNAs in mammalian cells. Science *296*, 550-553.

Brunet, A., Bonni, A., Zigmond, M. J., Lin, M. Z., Juo, P., Hu, L. S., Anderson, M. J., Arden, K. C., Blenis, J., and Greenberg, M. E. (1999). Akt promotes cell survival by phosphorylating and inhibiting a Forkhead transcription factor. Cell *96*, 857-868.

Buendia, B., Santa-Maria, A., and Courvalin, J. C. (1999). Caspase-dependent proteolysis of integral and peripheral proteins of nuclear membranes and nuclear pore complex proteins during apoptosis. J Cell Sci *112 (Pt 11)*, 1743-1753.

Cai, Y., Zhang, C., Nawa, T., Aso, T., Tanaka, M., Oshiro, S., Ichijo, H., and Kitajima, S. (2000). Homocysteine-responsive ATF3 gene expression in human vascular endothelial cells: activation of c-Jun NH(2)-terminal kinase and promoter response element. Blood *96*, 2140-2148.

Cain, K., Bratton, S. B., Langlais, C., Walker, G., Brown, D. G., Sun, X. M., and Cohen, G. M. (2000). Apaf-1 oligomerizes into biologically active approximately 700-kDa and inactive approximately 1.4-MDa apoptosome complexes. J Biol Chem *275*, 6067-6070.

Camps, M., Chabert, C., Muda, M., Boschert, U., Gillieron, C., and Arkinstall, S. (1998). Induction of the mitogen-activated protein kinase phosphatase MKP3 by nerve growth factor in differentiating PC12. FEBS Lett *425*, 271-276.

Carmody, R. J., and Cotter, T. G. (2000). Oxidative stress induces caspase-independent retinal apoptosis in vitro. Cell Death Differ *7*, 282-291.

Casaccia-Bonnefil, P., Carter, B. D., Dobrowsky, R. T., and Chao, M. V. (1996). Death of oligodendrocytes mediated by the interaction of nerve growth factor with its receptor p75. Nature *383*, 716-719.

Castellazzi, M., Spyrou, G., La Vista, N., Dangy, J. P., Piu, F., Yaniv, M., and Brun, G. (1991). Overexpression of c-jun, junB, or junD affects cell growth differently. Proc Natl Acad Sci U S A *88*, 8890-8894.

Castle, V. P., Heidelberger, K. P., Bromberg, J., Ou, X., Dole, M., and Nunez, G. (1993). Expression of the apoptosis-suppressing protein bcl-2, in neuroblastoma is associated with unfavorable histology and N-myc amplification. Am J Pathol *143*, 1543-1550.

Catz, S. D., and Johnson, J. L. (2001). Transcriptional regulation of bcl-2 by nuclear factor kappa B and its significance in prostate cancer. Oncogene *20*, 7342-7351.

Cecconi, F., Alvarez-Bolado, G., Meyer, B. I., Roth, K. A., and Gruss, P. (1998). Apaf1 (CED-4 homolog) regulates programmed cell death in mammalian development. Cell *94*, 727-737.

Cerretti, D. P., Kozlosky, C. J., Mosley, B., Nelson, N., Van Ness, K., Greenstreet, T. A., March, C. J., Kronheim, S. R., Druck, T., Cannizzaro, L. A., and et al. (1992). Molecular cloning of the interleukin-1 beta converting enzyme. Science *256*, 97-100.

Chang, B. S., Minn, A. J., Muchmore, S. W., Fesik, S. W., and Thompson, C. B. (1997). Identification of a novel regulatory domain in Bcl-X(L) and Bcl-2. Embo J *16*, 968-977.

Chang, L., Jones, Y., Ellisman, M. H., Goldstein, L. S., and Karin, M. (2003). JNK1 is required for maintenance of neuronal microtubules and controls phosphorylation of microtubule-associated proteins. Dev Cell *4*, 521-533.

Chao, M. V. (1992). Neurotrophin receptors: a window into neuronal differentiation. Neuron *9*, 583-593.

Chen, B. P., Liang, G., Whelan, J., and Hai, T. (1994). ATF3 and ATF3 delta Zip. Transcriptional repression versus activation by alternatively spliced isoforms. J Biol Chem *269*, 15819-15826.

Chen, B. P., Wolfgang, C. D., and Hai, T. (1996). Analysis of ATF3, a transcription factor induced by physiological stresses and modulated by gadd153/Chop10. Mol Cell Biol *16*, 1157-1168.

Chen, J., Nagayama, T., Jin, K., Stetler, R. A., Zhu, R. L., Graham, S. H., and Simon, R. P. (1998). Induction of caspase-3-like protease may mediate delayed neuronal death in the hippocampus after transient cerebral ischemia. J Neurosci *18*, 4914-4928.

Cheng, E. H., Kirsch, D. G., Clem, R. J., Ravi, R., Kastan, M. B., Bedi, A., Ueno, K., and Hardwick, J. M. (1997). Conversion of Bcl-2 to a Bax-like death effector by caspases. Science *278*, 1966-1968.

Cheng, E. H., Wei, M. C., Weiler, S., Flavell, R. A., Mak, T. W., Lindsten, T., and Korsmeyer, S. J. (2001). BCL-2, BCL-X(L) sequester BH3 domain-only molecules preventing BAX- and BAK-mediated mitochondrial apoptosis. Mol Cell *8*, 705-711.

Cheng, Y., Deshmukh, M., D'Costa, A., Demaro, J. A., Gidday, J. M., Shah, A., Sun, Y., Jacquin, M. F., Johnson, E. M., and Holtzman, D. M. (1998). Caspase inhibitor affords neuroprotection with delayed administration in a rat model of neonatal hypoxic-ischemic brain injury. J Clin Invest *101*, 1992-1999.

Chinnaiyan, A. M., O'Rourke, K., Lane, B. R., and Dixit, V. M. (1997). Interaction of CED-4 with CED-3 and CED-9: a molecular framework for cell death. Science *275*, 1122-1126.

Chinnaiyan, A. M., O'Rourke, K., Tewari, M., and Dixit, V. M. (1995). FADD, a novel death domain-containing protein, interacts with the death domain of Fas and initiates apoptosis. Cell *81*, 505-512.

Chittenden, T., Flemington, C., Houghton, A. B., Ebb, R. G., Gallo, G. J., Elangovan, B., Chinnadurai, G., and Lutz, R. J. (1995). A conserved domain in Bak, distinct from BH1 and BH2, mediates cell death and protein binding functions. Embo J *14*, 5589-5596.

Chiu, R., Angel, P., and Karin, M. (1989). Jun-B differs in its biological properties from, and is a negative regulator of, c-Jun. Cell *59*, 979-986.

Choi, D. W. (1992). Excitotoxic cell death. J Neurobiol *23*, 1261-1276.

Choi, D. W. (1996). Ischemia-induced neuronal apoptosis. Curr Opin Neurobiol *6*, 667-672.

Chu, W. M., Ostertag, D., Li, Z. W., Chang, L., Chen, Y., Hu, Y., Williams, B., Perrault, J., and Karin, M. (1999). JNK2 and IKKbeta are required for activating the innate response to viral infection. Immunity *11*, 721-731.

Chung, S., Gumienny, T. L., Hengartner, M. O., and Driscoll, M. (2000). A common set of engulfment genes mediates removal of both apoptotic and necrotic cell corpses in C. elegans. Nat Cell Biol *2*, 931-937.

Clark, E. A., and Brugge, J. S. (1995). Integrins and signal transduction pathways: the road taken. Science *268*, 233-239.

Clarke, A. R., Purdie, C. A., Harrison, D. J., Morris, R. G., Bird, C. C., Hooper, M. L., and Wyllie, A. H. (1993). Thymocyte apoptosis induced by p53-dependent and independent pathways. Nature *362*, 849-852.

Clarke, P. G., and Clarke, S. (1996). Nineteenth century research on naturally occurring cell death and related phenomena. Anat Embryol (Berl) *193*, 81-99.

Cleary, M. L., and Sklar, J. (1985). Nucleotide sequence of a t(14;18) chromosomal breakpoint in follicular lymphoma and demonstration of a breakpoint-cluster region near a transcriptionally active locus on chromosome 18. Proc Natl Acad Sci U S A *82*, 7439-7443.

Clem, R. J., Cheng, E. H., Karp, C. L., Kirsch, D. G., Ueno, K., Takahashi, A., Kastan, M. B., Griffin, D. E., Earnshaw, W. C., Veliuona, M. A., and Hardwick, J. M. (1998). Modulation of cell death by Bcl-XL through caspase interaction. Proc Natl Acad Sci U S A *95*, 554-559.

Clemens, M. J. (1996). Protein kinases that phosphorylate eIF2 and eIF2B, and their role in eukaryotic cell translational control.

Connor, J. H., Weiser, D. C., Li, S., Hallenbeck, J. M., and Shenolikar, S. (2001). Growth arrest and DNA damage-inducible protein GADD34 assembles a novel signaling complex containing protein phosphatase 1 and inhibitor 1. Mol Cell Biol *21*, 6841-6850.

Conradt, B., and Horvitz, H. R. (1998). The C. elegans protein EGL-1 is required for programmed cell death and interacts with the Bcl-2-like protein CED-9. Cell *93*, 519-529.

Constant, S. L., Dong, C., Yang, D. D., Wysk, M., Davis, R. J., and Flavell, R. A. (2000). JNK1 is required for T cell-mediated immunity against Leishmania major infection. J Immunol *165*, 2671-2676.

Coucouvanis, E., and Martin, G. R. (1995). Signals for death and survival: a two-step mechanism for cavitation in the vertebrate embryo. Cell *83*, 279-287.

Coughlin, M. D., and Collins, M. B. (1985). Nerve growth factor-independent development of embryonic mouse sympathetic neurons in dissociated cell culture. Dev Biol *110*, 392-401.

Cowan, W. M., Fawcett, J. W., O'Leary, D. D., and Stanfield, B. B. (1984). Regressive events in neurogenesis. Science *225*, 1258-1265.

Creedon, D. J., Johnson, E. M., and Lawrence, J. C. (1996). Mitogen-activated protein kinase-independent pathways mediate the effects of nerve growth factor and cAMP on neuronal survival. J Biol Chem *271*, 20713-20718.

Crompton, M., Virji, S., Doyle, V., Johnson, N., and Ward, J. M. (1999). The mitochondrial permeability transition pore. Biochem Soc Symp *66*, 167-179.

Crowder, R. J., and Freeman, R. S. (1998). Phosphatidylinositol 3-kinase and Akt protein kinase are necessary and sufficient for the survival of nerve growth factor-dependent sympathetic neurons. J Neurosci *18*, 2933-2943.

Crowley, C., Spencer, S. D., Nishimura, M. C., Chen, K. S., Pitts-Meek, S., Armanini, M. P., Ling, L. H., MacMahon, S. B., Shelton, D. L., Levinson, A. D., and et al. (1994). Mice lacking nerve growth factor display perinatal loss of sensory and

sympathetic neurons yet develop basal forebrain cholinergic neurons. Cell *76*, 1001-1011.

Csordas, G., and Hajnoczky, G. (2001). Sorting of calcium signals at the junctions of endoplasmic reticulum and mitochondria. Cell Calcium *29*, 249-262.

Cuenda, A., and Dorow, D. S. (1998). Differential activation of stress-activated protein kinase kinases SKK4/MKK7 and SKK1/MKK4 by the mixed-lineage kinase-2 and mitogen-activated protein kinase kinase (MKK) kinase-1. Biochem J *333 (Pt 1)*, 11-15.

Cyster, J. G., Hartley, S. B., and Goodnow, C. C. (1994). Competition for follicular niches excludes self-reactive cells from the recirculating B-cell repertoire. Nature *371*, 389-395.

Datta, S. R., Brunet, A., and Greenberg, M. E. (1999). Cellular survival: a play in three Akts. Genes Dev *13*, 2905-2927.

Datta, S. R., Dudek, H., Tao, X., Masters, S., Fu, H., Gotoh, Y., and Greenberg, M. E. (1997). Akt phosphorylation of BAD couples survival signals to the cell-intrinsic death machinery. Cell *91*, 231-241.

Davey, F., and Davies, A. M. (1998). TrkB signalling inhibits p75-mediated apoptosis induced by nerve growth factor in embryonic proprioceptive neurons. Curr Biol *8*, 915-918.

Davis, R. J. (2000). Signal transduction by the JNK group of MAP kinases. Cell *103*, 239-252.

Dawson, T., Mandir, A., and Lee, M. (2002). Animal models of PD: pieces of the same puzzle? Neuron *35*, 219-222.

de Bilbao, F., Guarin, E., Nef, P., and Dubois-Dauphin, M. (1999). The mouse cpp32 mRNA transcript is early up-regulated in axotomized motoneurons following facial nerve transection. Neurosci Lett *266*, 65-68.

Dechant, G., and Barde, Y. A. (1997). Signalling through the neurotrophin receptor p75NTR. Curr Opin Neurobiol *7*, 413-418.

Deckwerth, T. L., Elliott, J. L., Knudson, C. M., Johnson, E. M., Jr., Snider, W. D., and Korsmeyer, S. J. (1996). BAX is required for neuronal death after trophic factor deprivation and during development. Neuron *17*, 401-411.

Deckwerth, T. L., and Johnson, E. M., Jr. (1993). Temporal analysis of events associated with programmed cell death (apoptosis) of sympathetic neurons deprived of nerve growth factor. J Cell Biol *123*, 1207-1222.

del Peso, L., Gonzalez-Garcia, M., Page, C., Herrera, R., and Nunez, G. (1997). Interleukin-3-induced phosphorylation of BAD through the protein kinase Akt. Science *278*, 687-689.

Deng, H. X., Hentati, A., Tainer, J. A., Iqbal, Z., Cayabyab, A., Hung, W. Y., Getzoff, E. D., Hu, P., Herzfeldt, B., Roos, R. P., and et al. (1993). Amyotrophic lateral sclerosis and structural defects in Cu,Zn superoxide dismutase. Science *261*, 1047-1051.

Deng, T., and Karin, M. (1993). JunB differs from c-Jun in its DNA-binding and dimerization domains, and represses c-Jun by formation of inactive heterodimers. Genes Dev *7*, 479-490.

Derijard, B., Raingeaud, J., Barrett, T., Wu, I. H., Han, J., Ulevitch, R. J., and Davis, R. J. (1995). Independent human MAP-kinase signal transduction pathways defined by MEK and MKK isoforms. Science *267*, 682-685.

Deshmukh, M., Du, C., Wang, X., and Johnson, E. M., Jr. (2002). Exogenous smac induces competence and permits caspase activation in sympathetic neurons. J Neurosci *22*, 8018-8027.

Deshmukh, M., and Johnson, E. M., Jr. (1997). Programmed cell death in neurons: focus on the pathway of nerve growth factor deprivation-induced death of sympathetic neurons. Mol Pharmacol *51*, 897-906.

Deshmukh, M., and Johnson, E. M., Jr. (1998). Evidence of a novel event during neuronal death: development of competence-to-die in response to cytoplasmic cytochrome c. Neuron *21*, 695-705.

Deshmukh, M., Kuida, K., and Johnson, E. M., Jr. (2000). Caspase inhibition extends the commitment to neuronal death beyond cytochrome c release to the point of mitochondrial depolarization. J Cell Biol *150*, 131-143.

Deshmukh, M., Vasilakos, J., Deckwerth, T. L., Lampe, P. A., Shivers, B. D., and Johnson, E. M., Jr. (1996). Genetic and metabolic status of NGF-deprived sympathetic neurons saved by an inhibitor of ICE family proteases. J Cell Biol *135*, 1341-1354.

Deveraux, Q. L., and Reed, J. C. (1999). IAP family proteins--suppressors of apoptosis. Genes Dev *13*, 239-252.

Deveraux, Q. L., Takahashi, R., Salvesen, G. S., and Reed, J. C. (1997). X-linked IAP is a direct inhibitor of cell-death proteases. Nature *388*, 300-304.

Dhein, J., Behrmann, I., Daniel, P. T., Debatin, K. M., Klas, C., Moller, P., Oehm, A., Trauth, B. C., Walczak, H., and Krammer, P. H. (1994). APO-I-mediated apoptosis in normal and malignant lymphocytes. Biochem Soc Trans *22*, 598-600.

Dierlamm, J., Baens, M., Wlodarska, I., Stefanova-Ouzounova, M., Hernandez, J. M., Hossfeld, D. K., De Wolf-Peeters, C., Hagemeijer, A., Van den Berghe, H., and Marynen, P. (1999). The apoptosis inhibitor gene API2 and a novel 18q gene, MLT, are recurrently rearranged in the t(11;18)(q21;q21)p6ssociated with mucosa-associated lymphoid tissue lymphomas. Blood *93*, 3601-3609.

Don, M. M., Ablett, G., Bishop, C. J., Bundesen, P. G., Donald, K. J., Searle, J., and Kerr, J. F. (1977). Death of cells by apoptosis following attachment of specifically allergized lymphocytes in vitro. Aust J Exp Biol Med Sci *55*, 407-417.

Dong, C., Yang, D. D., Tournier, C., Whitmarsh, A. J., Xu, J., Davis, R. J., and Flavell, R. A. (2000). JNK is required for effector T-cell function but not for T-cell activation. Nature *405*, 91-94.

Dong, C., Yang, D. D., Wysk, M., Whitmarsh, A. J., Davis, R. J., and Flavell, R. A. (1998). Defective T cell differentiation in the absence of Jnk1. Science *282*, 2092-2095.

Doutheil, J., Althausen, S., Gissel, C., and Paschen, W. (1999). Activation of MYD116 (gadd34) expression following transient forebrain ischemia of rat: implications for a role of disturbances of endoplasmic reticulum calcium homeostasis. Brain Res Mol Brain Res *63*, 225-232.

Dragunow, M. (1992). Axotomized medial septal-diagonal band neurons express Jun-like immunoreactivity. Brain Res Mol Brain Res *15*, 141-144.

Dragunow, M., Xu, R., Walton, M., Woodgate, A., Lawlor, P., MacGibbon, G. A., Young, D., Gibbons, H., Lipski, J., Muravlev, A., *et al.* (2000). c-Jun promotes neurite outgrowth and survival in PC12 cells. Brain Res Mol Brain Res *83*, 20-33.

Drappa, J., Vaishnaw, A. K., Sullivan, K. E., Chu, J. L., and Elkon, K. B. (1996). Fas gene mutations in the Canale-Smith syndrome, an inherited lymphoproliferative disorder associated with autoimmunity. N Engl J Med *335*, 1643-1649.

Du, C., Fang, M., Li, Y., Li, L., and Wang, X. (2000). Smac, a mitochondrial protein that promotes cytochrome c-dependent caspase activation by eliminating IAP inhibition. Cell *102*, 33-42.

Du, C., Hu, R., Csernansky, C. A., Hsu, C. Y., and Choi, D. W. (1996). Very delayed infarction after mild focal cerebral ischemia: a role for apoptosis? J Cereb Blood Flow Metab *16*, 195-201.

Du, K., and Montminy, M. (1998). CREB is a regulatory target for the protein kinase Akt/PKB. J Biol Chem *273*, 32377-32379.

Duan, H., and Dixit, V. M. (1997). RAIDD is a new 'death' adaptor molecule. Nature *385*, 86-89.

Duan, W., Zhu, X., Ladenheim, B., Yu, Q. S., Guo, Z., Oyler, J., Cutler, R. G., Cadet, J. L., Greig, N. H., and Mattson, M. P. (2002). p53 inhibitors preserve dopamine neurons and motor function in experimental parkinsonism. Ann Neurol *52*, 597-606.

Edwards, S. N., and Tolkovsky, A. M. (1994). Characterization of apoptosis in cultured rat sympathetic neurons after nerve growth factor withdrawal. J Cell Biol *124*, 537-546.

Eilers, A., Whitfield, J., Babij, C., Rubin, L. L., and Ham, J. (1998). Role of the Jun kinase pathway in the regulation of c-Jun expression and apoptosis in sympathetic neurons. J Neurosci *18*, 1713-1724.

Eilers, A., Whitfield, J., Shah, B., Spadoni, C., Desmond, H., and Ham, J. (2001). Direct inhibition of c-Jun N-terminal kinase in sympathetic neurones prevents c-jun promoter activation and NGF withdrawal-induced death. J Neurochem *76*, 1439-1454.

Ekegren, T., Grundstrom, E., Lindholm, D., and Aquilonius, S. M. (1999). Upregulation of Bax protein and increased DNA degradation in ALS spinal cord motor neurons. Acta Neurol Scand *100*, 317-321.

El-Agnaf, O. M., Jakes, R., Curran, M. D., Middleton, D., Ingenito, R., Bianchi, E., Pessi, A., Neill, D., and Wallace, A. (1998). Aggregates from mutant and wild-type alpha-synuclein proteins and NAC peptide induce apoptotic cell death in human neuroblastoma cells by formation of beta-sheet and amyloid-like filaments. FEBS Lett *440*, 71-75.

Elbashir, S. M., Harborth, J., Lendeckel, W., Yalcin, A., Weber, K., and Tuschl, T. (2001). Duplexes of 21-nucleotide RNAs mediate RNA interference in cultured mammalian cells. Nature *411*, 494-498.

Ellis, H. M., and Horvitz, H. R. (1986). Genetic control of programmed cell death in the nematode C. elegans. Cell *44*, 817-829.

Ellis, R. E., and Horvitz, H. R. (1991). Two C. elegans genes control the programmed deaths of specific cells in the pharynx. Development *112*, 591-603.

Ellis, R. E., Jacobson, D. M., and Horvitz, H. R. (1991a). Genes required for the engulfment of cell corpses during programmed cell death in Caenorhabditis elegans. Genetics *129*, 79-94.

Ellis, R. E., Yuan, J. Y., and Horvitz, H. R. (1991b). Mechanisms and functions of cell death. Annu Rev Cell Biol *7*, 663-698.

Estus, S., Tucker, H. M., van Rooyen, C., Wright, S., Brigham, E. F., Wogulis, M., and Rydel, R. E. (1997). Aggregated amyloid-beta protein induces cortical neuronal apoptosis and concomitant "apoptotic" pattern of gene induction. J Neurosci *17*, 7736-7745.

Estus, S., Zaks, W. J., Freeman, R. S., Gruda, M., Bravo, R., and Johnson, E. M., Jr. (1994). Altered gene expression in neurons during programmed cell death: identification of c-jun as necessary for neuronal apoptosis. J Cell Biol *127*, 1717-1727.

Fan, F., Jin, S., Amundson, S. A., Tong, T., Fan, W., Zhao, H., Zhu, X., Mazzacurati, L., Li, X., Petrik, K. L., *et al.* (2002). ATF3 induction following DNA damage is regulated by distinct signaling pathways and over-expression of ATF3 protein suppresses cells growth. Oncogene *21*, 7488-7496.

Fawcett, T. W., Martindale, J. L., Guyton, K. Z., Hai, T., and Holbrook, N. J. (1999). Complexes containing activating transcription factor (ATF)/cAMP-responsive-element-binding protein (CREB) interact with the CCAAT/enhancer-binding protein (C/EBP)-ATF composite site to regulate Gadd153 expression during the stress response. Biochem J *339 (Pt 1)*, 135-141.

Ferri, K. F., and Kroemer, G. (2001). Organelle-specific initiation of cell death pathways. Nat Cell Biol *3*, E255-263.

Finucane, D. M., Bossy-Wetzel, E., Waterhouse, N. J., Cotter, T. G., and Green, D. R. (1999). Bax-induced caspase activation and apoptosis via cytochrome c release from mitochondria is inhibitable by Bcl-xL. J Biol Chem *274*, 2225-2233.

Fisher, G. H., Rosenberg, F. J., Straus, S. E., Dale, J. K., Middleton, L. A., Lin, A. Y., Strober, W., Lenardo, M. J., and Puck, J. M. (1995). Dominant interfering Fas gene mutations impair apoptosis in a human autoimmune lymphoproliferative syndrome. Cell *81*, 935-946.

Fortin, A., Cregan, S. P., MacLaurin, J. G., Kushwaha, N., Hickman, E. S., Thompson, C. S., Hakim, A., Albert, P. R., Cecconi, F., Helin, K., *et al.* (2001). APAF1 is a key transcriptional target for p53 in the regulation of neuronal cell death. J Cell Biol *155*, 207-216.

Foyouzi-Youssefi, R., Arnaudeau, S., Borner, C., Kelley, W. L., Tschopp, J., Lew, D. P., Demaurex, N., and Krause, K. H. (2000). Bcl-2 decreases the free Ca2+ concentration within the endoplasmic reticulum. Proc Natl Acad Sci U S A *97*, 5723-5728.

Frade, J. M., and Barde, Y. A. (1999). Genetic evidence for cell death mediated by nerve growth factor and the neurotrophin receptor p75 in the developing mouse retina and spinal cord. Development *126*, 683-690.

Francis, J. S., Dragunow, M., and During, M. J. (2004). Over expression of ATF-3 protects rat hippocampal neurons from in vivo injection of kainic acid. Brain Res Mol Brain Res *124*, 199-203.

Friedlander, R. M., Gagliardini, V., Hara, H., Fink, K. B., Li, W., MacDonald, G., Fishman, M. C., Greenberg, A. H., Moskowitz, M. A., and Yuan, J. (1997). Expression of a dominant negative mutant of interleukin-1 beta converting enzyme in transgenic mice prevents neuronal cell death induced by trophic factor withdrawal and ischemic brain injury. J Exp Med *185*, 933-940.

Ganiatsas, S., Kwee, L., Fujiwara, Y., Perkins, A., Ikeda, T., Labow, M. A., and Zon, L. I. (1998). SEK1 deficiency reveals mitogen-activated protein kinase cascade crossregulation and leads to abnormal hepatogenesis. Proc Natl Acad Sci U S A *95*, 6881-6886.

Garcia, I., Martinou, I., Tsujimoto, Y., and Martinou, J. C. (1992). Prevention of programmed cell death of sympathetic neurons by the bcl-2 proto-oncogene. Science *258*, 302-304.

Ghadge, G. D., Lee, J. P., Bindokas, V. P., Jordan, J., Ma, L., Miller, R. J., and Roos, R. P. (1997). Mutant superoxide dismutase-1-linked familial amyotrophic lateral sclerosis: molecular mechanisms of neuronal death and protection. J Neurosci *17*, 8756-8766.

Gibson, M. E., Han, B. H., Choi, J., Knudson, C. M., Korsmeyer, S. J., Parsadanian, M., and Holtzman, D. M. (2001). BAX contributes to apoptotic-like death following neonatal hypoxia-ischemia: evidence for distinct apoptosis pathways. Mol Med *7*, 644-655.

Gilley, J., Coffer, P. J., and Ham, J. (2003). FOXO transcription factors directly activate bim gene expression and promote apoptosis in sympathetic neurons. J Cell Biol *162*, 613-622.

Ginham, R., Harrison, D. C., Facci, L., Skaper, S., and Philpott, K. L. (2001). Upregulation of death pathway molecules in rat cerebellar granule neurons undergoing apoptosis. Neurosci Lett *302*, 113-116.

Golstein, P. (1997). Cell death: TRAIL and its receptors. Curr Biol *7*, R750-753.

Gonzalez-Garcia, M., Garcia, I., Ding, L., O'Shea, S., Boise, L. H., Thompson, C. B., and Nunez, G. (1995). bcl-x is expressed in embryonic and postnatal neural tissues and functions to prevent neuronal cell death. Proc Natl Acad Sci U S A *92*, 4304-4308.

Goto, K., Ishige, A., Sekiguchi, K., Iizuka, S., Sugimoto, A., Yuzurihara, M., Aburada, M., Hosoya, E., and Kogure, K. (1990). Effects of cycloheximide on delayed neuronal death in rat hippocampus. Brain Res *534*, 299-302.

Gotoh, T., Oyadomari, S., Mori, K., and Mori, M. (2002). Nitric oxide-induced apoptosis in RAW 264.7 macrophages is mediated by endoplasmic reticulum stress pathway involving ATF6 and CHOP. J Biol Chem *277*, 12343-12350.

Grandgirard, D., Studer, E., Monney, L., Belser, T., Fellay, I., Borner, C., and Michel, M. R. (1998). Alphaviruses induce apoptosis in Bcl-2-overexpressing cells: evidence for a caspase-mediated, proteolytic inactivation of Bcl-2. Embo J *17*, 1268-1278.

Green, D. R. (2000). Apoptotic pathways: paper wraps stone blunts scissors. Cell *102*, 1-4.

Greene, L. A., and Tischler, A. S. (1976). Establishment of a noradrenergic clonal line of rat adrenal pheochromocytoma cells which respond to nerve growth factor. Proc Natl Acad Sci U S A *73*, 2424-2428.

Greenlund, L. J., Korsmeyer, S. J., and Johnson, E. M., Jr. (1995). Role of BCL-2 in the survival and function of developing and mature sympathetic neurons. Neuron *15*, 649-661.

Gross, A., Jockel, J., Wei, M. C., and Korsmeyer, S. J. (1998). Enforced dimerization of BAX results in its translocation, mitochondrial dysfunction and apoptosis. Embo J *17*, 3878-3885.

Gross, A., Yin, X. M., Wang, K., Wei, M. C., Jockel, J., Milliman, C., Erdjument-Bromage, H., Tempst, P., and Korsmeyer, S. J. (1999). Caspase cleaved BID targets mitochondria and is required for cytochrome c release, while BCL-XL prevents this release but not tumor necrosis factor-R1/Fas death. J Biol Chem *274*, 1156-1163.

Guegan, C., Vila, M., Rosoklija, G., Hays, A. P., and Przedborski, S. (2001). Recruitment of the mitochondrial-dependent apoptotic pathway in amyotrophic lateral sclerosis. J Neurosci *21*, 6569-6576.

Gupta, S., Barrett, T., Whitmarsh, A. J., Cavanagh, J., Sluss, H. K., Derijard, B., and Davis, R. J. (1996). Selective interaction of JNK protein kinase isoforms with transcription factors. Embo J *15*, 2760-2770.

Gupta, S., Campbell, D., Derijard, B., and Davis, R. J. (1995). Transcription factor ATF2 regulation by the JNK signal transduction pathway. Science *267*, 389-393.

Gurney, M. E., Pu, H., Chiu, A. Y., Dal Canto, M. C., Polchow, C. Y., Alexander, D. D., Caliendo, J., Hentati, A., Kwon, Y. W., Deng, H. X., and et al. (1994). Motor neuron degeneration in mice that express a human Cu,Zn superoxide dismutase mutation. Science *264*, 1772-1775.

Guyton, K. Z., Xu, Q., and Holbrook, N. J. (1996). Induction of the mammalian stress response gene GADD153 by oxidative stress: role of AP-1 element. Biochem J *314 (Pt 2)*, 547-554.

Hagmeyer, B. M., Duyndam, M. C., Angel, P., de Groot, R. P., Verlaan, M., Elfferich, P., van der Eb, A., and Zantema, A. (1996). Altered AP-1/ATF complexes in adenovirus-E1-transformed cells due to EIA-dependent induction of ATF3. Oncogene *12*, 1025-1032.

Hague, A., Moorghen, M., Hicks, D., Chapman, M., and Paraskeva, C. (1994). BCL-2 expression in human colorectal adenomas and carcinomas. Oncogene *9*, 3367-3370.

Hai, T., and Curran, T. (1991). Cross-family dimerization of transcription factors Fos/Jun and ATF/CREB alters DNA binding specificity. Proc Natl Acad Sci U S A *88*, 3720-3724.

Hai, T., and Hartman, M. G. (2001). The molecular biology and nomenclature of the activating transcription factor/cAMP responsive element binding family of transcription factors: activating transcription factor proteins and homeostasis. Gene *273*, 1-11.

Hai, T., Wolfgang, C. D., Marsee, D. K., Allen, A. E., and Sivaprasad, U. (1999). ATF3 and stress responses. Gene Expr *7*, 321-335.

Hakem, R., Hakem, A., Duncan, G. S., Henderson, J. T., Woo, M., Soengas, M. S., Elia, A., de la Pompa, J. L., Kagi, D., Khoo, W., *et al.* (1998). Differential requirement for caspase 9 in apoptotic pathways in vivo. Cell *94*, 339-352.

Haldar, S., Basu, A., and Croce, C. M. (1997). Bcl2 is the guardian of microtubule integrity. Cancer Res *57*, 229-233.

Ham, J., Babij, C., Whitfield, J., Pfarr, C. M., Lallemand, D., Yaniv, M., and Rubin, L. L. (1995). A c-Jun dominant negative mutant protects sympathetic neurons against programmed cell death. Neuron *14*, 927-939.

Han, Z., Chang, L., Yamanishi, Y., Karin, M., and Firestein, G. S. (2002). Joint damage and inflammation in c-Jun N-terminal kinase 2 knockout mice with passive murine collagen-induced arthritis. Arthritis Rheum *46*, 818-823.

Hara, H., Friedlander, R. M., Gagliardini, V., Ayata, C., Fink, K., Huang, Z., Shimizu-Sasamata, M., Yuan, J., and Moskowitz, M. A. (1997). Inhibition of interleukin 1beta converting enzyme family proteases reduces ischemic and excitotoxic neuronal damage. Proc Natl Acad Sci U S A *94*, 2007-2012.

Harding, H. P., Zhang, Y., and Ron, D. (1999). Protein translation and folding are coupled by an endoplasmic-reticulum-resident kinase. Nature *397*, 271-274.

Harding, T. C., Xue, L., Bienemann, A., Haywood, D., Dickens, M., Tolkovsky, A. M., and Uney, J. B. (2001). Inhibition of JNK by overexpression of the JNL binding domain of JIP-1 prevents apoptosis in sympathetic neurons. J Biol Chem *276*, 4531-4534.

Harris, C. A., Deshmukh, M., Tsui-Pierchala, B., Maroney, A. C., and Johnson, E. M., Jr. (2002). Inhibition of the c-Jun N-terminal kinase signaling pathway by the mixed lineage kinase inhibitor CEP-1347 (KT7515) preserves metabolism and growth of trophic factor-deprived neurons. J Neurosci *22*, 103-113.

Harris, C. A., and Johnson, E. M., Jr. (2001). BH3-only Bcl-2 family members are coordinately regulated by the JNK pathway and require Bax to induce apoptosis in neurons. J Biol Chem *276*, 37754-37760.

Hartman, M. G., Lu, D., Kim, M. L., Kociba, G. J., Shukri, T., Buteau, J., Wang, X., Frankel, W. L., Guttridge, D., Prentki, M., *et al.* (2004). Role for activating transcription factor 3 in stress-induced beta-cell apoptosis. Mol Cell Biol *24*, 5721-5732.

Hashimoto, Y., Zhang, C., Kawauchi, J., Imoto, I., Adachi, M. T., Inazawa, J., Amagasa, T., Hai, T., and Kitajima, S. (2002). An alternatively spliced isoform of transcriptional repressor ATF3 and its induction by stress stimuli. Nucleic Acids Res *30*, 2398-2406.

Hassouna, I., Wickert, H., Zimmermann, M., and Gillardon, F. (1996). Increase in bax expression in substantia nigra following 1-methyl-4-phenyl-1,2,3,6-tetrahydropyridine (MPTP) treatment of mice. Neurosci Lett *204*, 85-88.

Hata, R., Gillardon, F., Michaelidis, T. M., and Hossmann, K. A. (1999). Targeted disruption of the bcl-2 gene in mice exacerbates focal ischemic brain injury. Metab Brain Dis *14*, 117-124.

Haviv, R., Lindenboim, L., Yuan, J., and Stein, R. (1998). Need for caspase-2 in apoptosis of growth-factor-deprived PC12 cells. J Neurosci Res *52*, 491-497.

He, H., Lam, M., McCormick, T. S., and Distelhorst, C. W. (1997). Maintenance of calcium homeostasis in the endoplasmic reticulum by Bcl-2. J Cell Biol *138*, 1219-1228.

He, Y., Lee, T., and Leong, S. K. (2000). 6-Hydroxydopamine induced apoptosis of dopaminergic cells in the rat substantia nigra. Brain Res *858*, 163-166.

Hedgecock, E. M., Sulston, J. E., and Thomson, J. N. (1983). Mutations affecting programmed cell deaths in the nematode Caenorhabditis elegans. Science *220*, 1277-1279.

Hengartner, M. O. (2000). The biochemistry of apoptosis. Nature *407*, 770-776.

Hengartner, M. O., Ellis, R. E., and Horvitz, H. R. (1992). Caenorhabditis elegans gene ced-9 protects cells from programmed cell death. Nature *356*, 494-499.

Hengartner, M. O., and Horvitz, H. R. (1994). C. elegans cell survival gene ced-9 encodes a functional homolog of the mammalian proto-oncogene bcl-2. Cell *76*, 665-676.

Herbeuval, J. P., Boasso, A., Grivel, J. C., Hardy, A. W., Anderson, S. A., Dolan, M. J., Chougnet, C., Lifson, J. D., and Shearer, G. M. (2004). TNF-related apoptosis-inducing ligand (TRAIL) in HIV-1-infected patients and its in vitro production by antigen-presenting cells. Blood.

Herdegen, T., Claret, F. X., Kallunki, T., Martin-Villalba, A., Winter, C., Hunter, T., and Karin, M. (1998). Lasting N-terminal phosphorylation of c-Jun and activation of c-Jun N-terminal kinases after neuronal injury. J Neurosci *18*, 5124-5135.

Herdegen, T., and Waetzig, V. (2001). The JNK and p38 signal transduction following axotomy. Restor Neurol Neurosci *19*, 29-39.

Hibi, M., Lin, A., Smeal, T., Minden, A., and Karin, M. (1993). Identification of an oncoprotein- and UV-responsive protein kinase that binds and potentiates the c-Jun activation domain. Genes Dev *7*, 2135-2148.

Hilberg, F., Aguzzi, A., Howells, N., and Wagner, E. F. (1993). c-jun is essential for normal mouse development and hepatogenesis. Nature *365*, 179-181.

Hirai, S., Katoh, M., Terada, M., Kyriakis, J. M., Zon, L. I., Rana, A., Avruch, J., and Ohno, S. (1997). MST/MLK2, a member of the mixed lineage kinase family, directly phosphorylates and activates SEK1, an activator of c-Jun N-terminal kinase/stress-activated protein kinase. J Biol Chem *272*, 15167-15173.

Hirai, S. I., Ryseck, R. P., Mechta, F., Bravo, R., and Yaniv, M. (1989). Characterization of junD: a new member of the jun proto-oncogene family. Embo J *8*, 1433-1439.

Hirosumi, J., Tuncman, G., Chang, L., Gorgun, C. Z., Uysal, K. T., Maeda, K., Karin, M., and Hotamisligil, G. S. (2002). A central role for JNK in obesity and insulin resistance. Nature *420*, 333-336.

Hirsch, T., Dallaporta, B., Zamzami, N., Susin, S. A., Ravagnan, L., Marzo, I., Brenner, C., and Kroemer, G. (1998). Proteasome activation occurs at an early, premitochondrial step of thymocyte apoptosis. J Immunol *161*, 35-40.

Hockenbery, D., Nunez, G., Milliman, C., Schreiber, R. D., and Korsmeyer, S. J. (1990). Bcl-2 is an inner mitochondrial membrane protein that blocks programmed cell death. Nature *348*, 334-336.

Hockenbery, D. M., Oltvai, Z. N., Yin, X. M., Milliman, C. L., and Korsmeyer, S. J. (1993). Bcl-2 functions in an antioxidant pathway to prevent apoptosis. Cell *75*, 241-251.

Hoffman, B., and Liebermann, D. A. (1994). Molecular controls of apoptosis: differentiation/growth arrest primary response genes, proto-oncogenes, and tumor suppressor genes as positive & negative modulators. Oncogene *9*, 1807-1812.

Hollander, M. C., Zhan, Q., Bae, I., and Fornace, A. J., Jr. (1997). Mammalian GADD34, an apoptosis- and DNA damage-inducible gene. J Biol Chem *272*, 13731-13737.

Horvitz, H. R., Sternberg, P. W., Greenwald, I. S., Fixsen, W., and Ellis, H. M. (1983). Mutations that affect neural cell lineages and cell fates during the development of the nematode Caenorhabditis elegans. Cold Spring Harb Symp Quant Biol *48 Pt 2*, 453-463.

Hossmann, K. A. (2001). [Neuronal apoptosis. A new means of treatment for cerebral ischemia?]. Anaesthesist *50*, 903-904.

Howard, S., Bottino, C., Brooke, S., Cheng, E., Giffard, R. G., and Sapolsky, R. (2002). Neuroprotective effects of bcl-2 overexpression in hippocampal cultures: interactions with pathways of oxidative damage. J Neurochem *83*, 914-923.

Hsu, H., Xiong, J., and Goeddel, D. V. (1995). The TNF receptor 1-associated protein TRADD signals cell death and NF-kappa B activation. Cell *81*, 495-504.

Hsu, J. C., Bravo, R., and Taub, R. (1992). Interactions among LRF-1, JunB, c-Jun, and c-Fos define a regulatory program in the G1 phase of liver regeneration. Mol Cell Biol *12*, 4654-4665.

Hu, S., Vincenz, C., Ni, J., Gentz, R., and Dixit, V. M. (1997). I-FLICE, a novel inhibitor of tumor necrosis factor receptor-1- and CD-95-induced apoptosis. J Biol Chem *272*, 17255-17257.

Huang, D. C., Adams, J. M., and Cory, S. (1998). The conserved N-terminal BH4 domain of Bcl-2 homologues is essential for inhibition of apoptosis and interaction with CED-4. Embo J *17*, 1029-1039.

Huang, H., Joazeiro, C. A., Bonfoco, E., Kamada, S., Leverson, J. D., and Hunter, T. (2000). The inhibitor of apoptosis, cIAP2, functions as a ubiquitin-protein ligase and promotes in vitro monoubiquitination of caspases 3 and 7. J Biol Chem *275*, 26661-26664.

Hughes, F. M., Jr., Evans-Storms, R. B., and Cidlowski, J. A. (1998). Evidence that non-caspase proteases are required for chromatin degradation during apoptosis. Cell Death Differ *5*, 1017-1027.

Hunter, J. J., and Parslow, T. G. (1996). A peptide sequence from Bax that converts Bcl-2 into an activator of apoptosis. J Biol Chem *271*, 8521-8524.

Imaizumi, K., Benito, A., Kiryu-Seo, S., Gonzalez, V., Inohara, N., Lieberman, A. P., Kiyama, H., and Nunez, G. (2004). Critical role for DP5/Harakiri, a Bcl-2 homology domain 3-only Bcl-2 family member, in axotomy-induced neuronal cell death. J Neurosci *24*, 3721-3725.

Imaizumi, K., Morihara, T., Mori, Y., Katayama, T., Tsuda, M., Furuyama, T., Wanaka, A., Takeda, M., and Tohyama, M. (1999). The cell death-promoting gene DP5, which interacts with the BCL2 family, is induced during neuronal apoptosis following exposure to amyloid beta protein. J Biol Chem *274*, 7975-7981.

Imaizumi, K., Tsuda, M., Imai, Y., Wanaka, A., Takagi, T., and Tohyama, M. (1997). Molecular cloning of a novel polypeptide, DP5, induced during programmed neuronal death. J Biol Chem *272*, 18842-18848.

Imoto, I., Yang, Z. Q., Pimkhaokham, A., Tsuda, H., Shimada, Y., Imamura, M., Ohki, M., and Inazawa, J. (2001). Identification of cIAP1 as a candidate target gene within an amplicon at 11q22 in esophageal squamous cell carcinomas. Cancer Res *61*, 6629-6634.

Inohara, N., Koseki, T., Hu, Y., Chen, S., and Nunez, G. (1997). CLARP, a death effector domain-containing protein interacts with caspase-8 and regulates apoptosis. Proc Natl Acad Sci U S A *94*, 10717-10722.

Ip, Y. T., and Davis, R. J. (1998). Signal transduction by the c-Jun N-terminal kinase (JNK)--from inflammation to development. Curr Opin Cell Biol *10*, 205-219.

Irmler, M., Thome, M., Hahne, M., Schneider, P., Hofmann, K., Steiner, V., Bodmer, J. L., Schroter, M., Burns, K., Mattmann, C., *et al.* (1997). Inhibition of death receptor signals by cellular FLIP. Nature *388*, 190-195.

Irving, E. A., and Bamford, M. (2002). Role of mitogen- and stress-activated kinases in ischemic injury. J Cereb Blood Flow Metab *22*, 631-647.

Ishizaki, Y., Cheng, L., Mudge, A. W., and Raff, M. C. (1995). Programmed cell death by default in embryonic cells, fibroblasts, and cancer cells. Mol Biol Cell *6*, 1443-1458.

Ito, T., Deng, X., Carr, B., and May, W. S. (1997). Bcl-2 phosphorylation required for anti-apoptosis function. J Biol Chem *272*, 11671-11673.

Jacobsen, M. D., Weil, M., and Raff, M. C. (1996). Role of Ced-3/ICE-family proteases in staurosporine-induced programmed cell death. J Cell Biol *133*, 1041-1051.

Jacobson, M. D., Burne, J. F., and Raff, M. C. (1994). Programmed cell death and Bcl-2 protection in the absence of a nucleus. Embo J *13*, 1899-1910.

Jacobson, M. D., Weil, M., and Raff, M. C. (1997). Programmed cell death in animal development. Cell *88*, 347-354.

Jiang, H. Y., Wek, S. A., McGrath, B. C., Lu, D., Hai, T., Harding, H. P., Wang, X., Ron, D., Cavener, D. R., and Wek, R. C. (2004). Activating transcription factor 3 is integral to the eukaryotic initiation factor 2 kinase stress response. Mol Cell Biol *24*, 1365-1377.

Jiang, X., and Wang, X. (2000). Cytochrome c promotes caspase-9 activation by inducing nucleotide binding to Apaf-1. J Biol Chem *275*, 31199-31203.

Jiang, Y., Woronicz, J. D., Liu, W., and Goeddel, D. V. (1999). Prevention of constitutive TNF receptor 1 signaling by silencer of death domains. Science *283*, 543-546.

Jin, K., Mao, X. O., Eshoo, M. W., del Rio, G., Rao, R., Chen, D., Simon, R. P., and Greenberg, D. A. (2002). cDNA microarray analysis of changes in gene expression induced by neuronal hypoxia in vitro. Neurochem Res *27*, 1105-1112.

Jin, S., Kalkum, M., Overholtzer, M., Stoffel, A., Chait, B. T., and Levine, A. J. (2003). CIAP1 and the serine protease HTRA2 are involved in a novel p53-dependent apoptosis pathway in mammals. Genes Dev *17*, 359-367.

Joza, N., Susin, S. A., Daugas, E., Stanford, W. L., Cho, S. K., Li, C. Y., Sasaki, T., Elia, A. J., Cheng, H. Y., Ravagnan, L., *et al.* (2001). Essential role of the mitochondrial apoptosis-inducing factor in programmed cell death. Nature *410*, 549-554.

Junn, E., and Mouradian, M. M. (2001). Apoptotic signaling in dopamine-induced cell death: the role of oxidative stress, p38 mitogen-activated protein kinase, cytochrome c and caspases. J Neurochem *78*, 374-383.

Jurgensmeier, J. M., Xie, Z., Deveraux, Q., Ellerby, L., Bredesen, D., and Reed, J. C. (1998). Bax directly induces release of cytochrome c from isolated mitochondria. Proc Natl Acad Sci U S A *95*, 4997-5002.

Kakimura, J., Kitamura, Y., Takata, K., Kohno, Y., Nomura, Y., and Taniguchi, T. (2001). Release and aggregation of cytochrome c and alpha-synuclein are inhibited by the antiparkinsonian drugs, talipexole and pramipexole. Eur J Pharmacol *417*, 59-67.

Kanamoto, T., Mota, M., Takeda, K., Rubin, L. L., Miyazono, K., Ichijo, H., and Bazenet, C. E. (2000). Role of apoptosis signal-regulating kinase in regulation of the c-Jun N-terminal kinase pathway and apoptosis in sympathetic neurons. Mol Cell Biol *20*, 196-204.

Kane, L. P., Shapiro, V. S., Stokoe, D., and Weiss, A. (1999). Induction of NF-kappaB by the Akt/PKB kinase. Curr Biol *9*, 601-604.

Kaplan, D. R., and Miller, F. D. (1997). Signal transduction by the neurotrophin receptors. Curr Opin Cell Biol *9*, 213-221.

Karin, M. (1995). The regulation of AP-1 activity by mitogen-activated protein kinases. J Biol Chem *270*, 16483-16486.

Karin, M., Liu, Z., and Zandi, E. (1997). AP-1 function and regulation. Curr Opin Cell Biol *9*, 240-246.

Karlsson, R., Engstrom, M., Jonsson, M., Karlberg, P., Pronk, C. J., Richter, J., and Jonsson, J. I. (2003). Phosphatidylinositol 3-kinase is essential for kit ligand-mediated survival, whereas interleukin-3 and flt3 ligand induce expression of antiapoptotic Bcl-2 family genes. J Leukoc Biol *74*, 923-931.

Katz, S., and Aronheim, A. (2002). Differential targeting of the stress mitogen-activated protein kinases to the c-Jun dimerization protein 2. Biochem J *368*, 939-945.

Kaufman, R. J. (1999). Stress signaling from the lumen of the endoplasmic reticulum: coordination of gene transcriptional and translational controls. Genes Dev *13*, 1211-1233.

Kaufmann, S. H., and Hengartner, M. O. (2001). Programmed cell death: alive and well in the new millennium. Trends Cell Biol *11*, 526-534.

Kelekar, A., Chang, B. S., Harlan, J. E., Fesik, S. W., and Thompson, C. B. (1997). Bad is a BH3 domain-containing protein that forms an inactivating dimer with Bcl-XL. Mol Cell Biol *17*, 7040-7046.

Kerr, J. F., Harmon, B., and Searle, J. (1974). An electron-microscope study of cell deletion in the anuran tadpole tail during spontaneous metamorphosis with special reference to apoptosis of striated muscle fibers. J Cell Sci *14*, 571-585.

Kerr, J. F., Wyllie, A. H., and Currie, A. R. (1972). Apoptosis: a basic biological phenomenon with wide-ranging implications in tissue kinetics. Br J Cancer *26*, 239-257.

Kitamura, Y., Kosaka, T., Kakimura, J. I., Matsuoka, Y., Kohno, Y., Nomura, Y., and Taniguchi, T. (1998). Protective effects of the antiparkinsonian drugs talipexole and pramipexole against 1-methyl-4-phenylpyridinium-induced apoptotic death in human neuroblastoma SH-SY5Y cells. Mol Pharmacol *54*, 1046-1054.

Knudson, C. M., and Korsmeyer, S. J. (1997). Bcl-2 and Bax function independently to regulate cell death. Nat Genet *16*, 358-363.

Knudson, C. M., Tung, K. S., Tourtellotte, W. G., Brown, G. A., and Korsmeyer, S. J. (1995). Bax-deficient mice with lymphoid hyperplasia and male germ cell death. Science *270*, 96-99.

Komiyama, T., Ray, C. A., Pickup, D. J., Howard, A. D., Thornberry, N. A., Peterson, E. P., and Salvesen, G. (1994). Inhibition of interleukin-1 beta converting enzyme by the cowpox virus serpin CrmA. An example of cross-class inhibition. J Biol Chem *269*, 19331-19337.

Kool, J., Hamdi, M., Cornelissen-Steijger, P., van der Eb, A. J., Terleth, C., and van Dam, H. (2003). Induction of ATF3 by ionizing radiation is mediated via a signaling pathway that includes ATM, Nibrin1, stress-induced MAPkinases and ATF-2. Oncogene *22*, 4235-4242.

Kops, G. J., de Ruiter, N. D., De Vries-Smits, A. M., Powell, D. R., Bos, J. L., and Burgering, B. M. (1999). Direct control of the Forkhead transcription factor AFX by protein kinase B. Nature *398*, 630-634.

Korsmeyer, S. J., Wei, M. C., Saito, M., Weiler, S., Oh, K. J., and Schlesinger, P. H. (2000). Pro-apoptotic cascade activates BID, which oligomerizes BAK or BAX into pores that result in the release of cytochrome c. Cell Death Differ *7*, 1166-1173.

Kosel, S., Egensperger, R., von Eitzen, U., Mehraein, P., and Graeber, M. B. (1997). On the question of apoptosis in the parkinsonian substantia nigra. Acta Neuropathol (Berl) *93*, 105-108.

Kothakota, S., Azuma, T., Reinhard, C., Klippel, A., Tang, J., Chu, K., McGarry, T. J., Kirschner, M. W., Koths, K., Kwiatkowski, D. J., and Williams, L. T. (1997). Caspase-3-generated fragment of gelsolin: effector of morphological change in apoptosis. Science *278*, 294-298.

Kouhara, H., Hadari, Y. R., Spivak-Kroizman, T., Schilling, J., Bar-Sagi, D., Lax, I., and Schlessinger, J. (1997). A lipid-anchored Grb2-binding protein that links FGF-receptor activation to the Ras/MAPK signaling pathway. Cell *89*, 693-702.

Krajewska, M., Wang, H. G., Krajewski, S., Zapata, J. M., Shabaik, A., Gascoyne, R., and Reed, J. C. (1997). Immunohistochemical analysis of in vivo patterns of expression of CPP32 (Caspase-3), a cell death protease. Cancer Res *57*, 1605-1613.

Krammer, P. H., Dhein, J., Walczak, H., Behrmann, I., Mariani, S., Matiba, B., Fath, M., Daniel, P. T., Knipping, E., Westendorp, M. O., and et al. (1994). The role of APO-1-mediated apoptosis in the immune system. Immunol Rev *142*, 175-191.

Kroemer, G. (1997). The proto-oncogene Bcl-2 and its role in regulating apoptosis. Nat Med *3*, 614-620.

Kuan, C. Y., Whitmarsh, A. J., Yang, D. D., Liao, G., Schloemer, A. J., Dong, C., Bao, J., Banasiak, K. J., Haddad, G. G., Flavell, R. A., *et al.* (2003). A critical role of neural-specific JNK3 for ischemic apoptosis. Proc Natl Acad Sci U S A *100*, 15184-15189.

Kuan, C. Y., Yang, D. D., Samanta Roy, D. R., Davis, R. J., Rakic, P., and Flavell, R. A. (1999). The Jnk1 and Jnk2 protein kinases are required for regional specific apoptosis during early brain development. Neuron *22*, 667-676.

Kudla, G., Montessuit, S., Eskes, R., Berrier, C., Martinou, J. C., Ghazi, A., and Antonsson, B. (2000). The destabilization of lipid membranes induced by the C-terminal fragment of caspase 8-cleaved bid is inhibited by the N-terminal fragment. J Biol Chem *275*, 22713-22718.

Kuida, K., Haydar, T. F., Kuan, C. Y., Gu, Y., Taya, C., Karasuyama, H., Su, M. S., Rakic, P., and Flavell, R. A. (1998). Reduced apoptosis and cytochrome c-mediated caspase activation in mice lacking caspase 9. Cell *94*, 325-337.

Kuida, K., Lippke, J. A., Ku, G., Harding, M. W., Livingston, D. J., Su, M. S., and Flavell, R. A. (1995). Altered cytokine export and apoptosis in mice deficient in interleukin-1 beta converting enzyme. Science *267*, 2000-2003.

Kuida, K., Zheng, T. S., Na, S., Kuan, C., Yang, D., Karasuyama, H., Rakic, P., and Flavell, R. A. (1996). Decreased apoptosis in the brain and premature lethality in CPP32-deficient mice. Nature *384*, 368-372.

Kyriakis, J. M., and Avruch, J. (1996). Protein kinase cascades activated by stress and inflammatory cytokines. Bioessays *18*, 567-577.

Lang, A. E., and Lozano, A. M. (1998a). Parkinson's disease. First of two parts. N Engl J Med *339*, 1044-1053.

Lang, A. E., and Lozano, A. M. (1998b). Parkinson's disease. Second of two parts. N Engl J Med *339*, 1130-1143.

Lawler, S., Fleming, Y., Goedert, M., and Cohen, P. (1998). Synergistic activation of SAPK1/JNK1 by two MAP kinase kinases in vitro. Curr Biol *8*, 1387-1390.

Lawrence, M. S., McLaughlin, J. R., Sun, G. H., Ho, D. Y., McIntosh, L., Kunis, D. M., Sapolsky, R. M., and Steinberg, G. K. (1997). Herpes simplex viral vectors expressing Bcl-2 are neuroprotective when delivered after a stroke. J Cereb Blood Flow Metab *17*, 740-744.

Lee, J. M., and Bernstein, A. (1993). p53 mutations increase resistance to ionizing radiation. Proc Natl Acad Sci U S A *90*, 5742-5746.

Lee, K. F., Davies, A. M., and Jaenisch, R. (1994). p75-deficient embryonic dorsal root sensory and neonatal sympathetic neurons display a decreased sensitivity to NGF. Development *120*, 1027-1033.

Levi-Montalcini, R. (1987). The nerve growth factor 35 years later. Science *237*, 1154-1162.

Levine, A. J. (1993). The tumor suppressor genes. Annu Rev Biochem *62*, 623-651.

Lewin, G. R., and Barde, Y. A. (1996). Physiology of the neurotrophins. Annu Rev Neurosci *19*, 289-317.

Ley, R., Balmanno, K., Hadfield, K., Weston, C., and Cook, S. J. (2003). Activation of the ERK1/2 signaling pathway promotes phosphorylation and proteasome-dependent degradation of the BH3-only protein, Bim. J Biol Chem *278*, 18811-18816.

Ley, R., Ewings, K. E., Hadfield, K., Howes, E., Balmanno, K., and Cook, S. J. (2004). Extracellular signal-regulated kinases 1/2 are serum-stimulated "Bim(EL) kinases" that bind to the BH3-only protein Bim(EL) causing its phosphorylation and turnover. J Biol Chem *279*, 8837-8847.

Li, H., Zhu, H., Xu, C. J., and Yuan, J. (1998). Cleavage of BID by caspase 8 mediates the mitochondrial damage in the Fas pathway of apoptosis. Cell *94*, 491-501.

Li, L. Y., Luo, X., and Wang, X. (2001). Endonuclease G is an apoptotic DNase when released from mitochondria. Nature *412*, 95-99.

Li, P., Allen, H., Banerjee, S., Franklin, S., Herzog, L., Johnston, C., McDowell, J., Paskind, M., Rodman, L., Salfeld, J., and et al. (1995a). Mice deficient in IL-1 beta-converting enzyme are defective in production of mature IL-1 beta and resistant to endotoxic shock. Cell *80*, 401-411.

Li, P., Nijhawan, D., Budihardjo, I., Srinivasula, S. M., Ahmad, M., Alnemri, E. S., and Wang, X. (1997a). Cytochrome c and dATP-dependent formation of Apaf-1/caspase-9 complex initiates an apoptotic protease cascade. Cell *91*, 479-489.

Li, Y., Chopp, M., Jiang, N., Zhang, Z. G., and Zaloga, C. (1995b). Induction of DNA fragmentation after 10 to 120 minutes of focal cerebral ischemia in rats. Stroke *26*, 1252-1257; discussion 1257-1258.

Li, Y., Chopp, M., Powers, C., and Jiang, N. (1997b). Apoptosis and protein expression after focal cerebral ischemia in rat. Brain Res *765*, 301-312.

Liang, G., Wolfgang, C. D., Chen, B. P., Chen, T. H., and Hai, T. (1996). ATF3 gene. Genomic organization, promoter, and regulation. J Biol Chem *271*, 1695-1701.

Lin, A., Minden, A., Martinetto, H., Claret, F. X., Lange-Carter, C., Mercurio, F., Johnson, G. L., and Karin, M. (1995). Identification of a dual specificity kinase that activates the Jun kinases and p38-Mpk2. Science *268*, 286-290.

Lin, E. Y., Orlofsky, A., Berger, M. S., and Prystowsky, M. B. (1993). Characterization of A1, a novel hemopoietic-specific early-response gene with sequence similarity to bcl-2. J Immunol *151*, 1979-1988.

Linden, R. (1994). The survival of developing neurons: a review of afferent control. Neuroscience *58*, 671-682.

Lindsay, R. M. (1979). Adult rat brain astrocytes support survival of both NGF-dependent and NGF-insensitive neurones. Nature *282*, 80-82.

Lindsten, T., Ross, A. J., King, A., Zong, W. X., Rathmell, J. C., Shiels, H. A., Ulrich, E., Waymire, K. G., Mahar, P., Frauwirth, K., *et al.* (2000). The combined functions of proapoptotic Bcl-2 family members bak and bax are essential for normal development of multiple tissues. Mol Cell *6*, 1389-1399.

Lithgow, T., van Driel, R., Bertram, J. F., and Strasser, A. (1994). The protein product of the oncogene bcl-2 is a component of the nuclear envelope, the endoplasmic reticulum, and the outer mitochondrial membrane. Cell Growth Differ *5*, 411-417.

Liu, X., Kim, C. N., Yang, J., Jemmerson, R., and Wang, X. (1996). Induction of apoptotic program in cell-free extracts: requirement for dATP and cytochrome c. Cell *86*, 147-157.

Lockshin, R. A. (1969). Programmed cell death. Activation of lysis by a mechanism involving the synthesis of protein. J Insect Physiol *15*, 1505-1516.

Lockshin, R. A., and Williams, C. M. (1965). Programmed Cell Death--I. Cytology of Degeneration in the Intersegmental Muscles of the Pernyi Silkmoth. J Insect Physiol *11*, 123-133.

Loddick, S. A., MacKenzie, A., and Rothwell, N. J. (1996). An ICE inhibitor, z-VAD-DCB attenuates ischaemic brain damage in the rat. Neuroreport *7*, 1465-1468.

Lorenzo, H. K., Susin, S. A., Penninger, J., and Kroemer, G. (1999). Apoptosis inducing factor (AIF): a phylogenetically old, caspase-independent effector of cell death. Cell Death Differ *6*, 516-524.

Love, S. (2003). Apoptosis and brain ischaemia. Prog Neuropsychopharmacol Biol Psychiatry *27*, 267-282.

Lowe, S. W., Schmitt, E. M., Smith, S. W., Osborne, B. A., and Jacks, T. (1993). p53 is required for radiation-induced apoptosis in mouse thymocytes. Nature *362*, 847-849.

Luo, X., Budihardjo, I., Zou, H., Slaughter, C., and Wang, X. (1998a). Bid, a Bcl2 interacting protein, mediates cytochrome c release from mitochondria in response to activation of cell surface death receptors. Cell *94*, 481-490.

Luo, Y., Umegaki, H., Wang, X., Abe, R., and Roth, G. S. (1998b). Dopamine induces apoptosis through an oxidation-involved SAPK/JNK activation pathway. J Biol Chem *273*, 3756-3764.

Ma, K., Vattem, K. M., and Wek, R. C. (2002). Dimerization and release of molecular chaperone inhibition facilitate activation of eukaryotic initiation factor-2 kinase in response to endoplasmic reticulum stress. J Biol Chem *277*, 18728-18735.

Maki, Y., Bos, T. J., Davis, C., Starbuck, M., and Vogt, P. K. (1987). Avian sarcoma virus 17 carries the jun oncogene. Proc Natl Acad Sci U S A *84*, 2848-2852.

Mann, C. L., Hughes, F. M., Jr., and Cidlowski, J. A. (2000). Delineation of the signaling pathways involved in glucocorticoid-induced and spontaneous apoptosis of rat thymocytes. Endocrinology *141*, 528-538.

Maroney, A. C., Finn, J. P., Bozyczko-Coyne, D., O'Kane, T. M., Neff, N. T., Tolkovsky, A. M., Park, D. S., Yan, C. Y., Troy, C. M., and Greene, L. A. (1999). CEP-1347 (KT7515), an inhibitor of JNK activation, rescues sympathetic neurons and neuronally differentiated PC12 cells from death evoked by three distinct insults. J Neurochem *73*, 1901-1912.

Maroney, A. C., Finn, J. P., Connors, T. J., Durkin, J. T., Angeles, T., Gessner, G., Xu, Z., Meyer, S. L., Savage, M. J., Greene, L. A., *et al.* (2001). Cep-1347 (KT7515), a semisynthetic inhibitor of the mixed lineage kinase family. J Biol Chem *276*, 25302-25308.

Marsters, S. A., Sheridan, J. P., Pitti, R. M., Huang, A., Skubatch, M., Baldwin, D., Yuan, J., Gurney, A., Goddard, A. D., Godowski, P., and Ashkenazi, A. (1997). A novel receptor for Apo2L/TRAIL contains a truncated death domain. Curr Biol *7*, 1003-1006.

Martin, D. P., Schmidt, R. E., DiStefano, P. S., Lowry, O. H., Carter, J. G., and Johnson, E. M., Jr. (1988). Inhibitors of protein synthesis and RNA synthesis prevent neuronal death caused by nerve growth factor deprivation. J Cell Biol *106*, 829-844.

Martin, J. H., Mohit, A. A., and Miller, C. A. (1996). Developmental expression in the mouse nervous system of the p493F12 SAP kinase. Brain Res Mol Brain Res *35*, 47-57.

Martin, L. J. (1999). Neuronal death in amyotrophic lateral sclerosis is apoptosis: possible contribution of a programmed cell death mechanism. J Neuropathol Exp Neurol *58*, 459-471.

Martinou, I., Fernandez, P. A., Missotten, M., White, E., Allet, B., Sadoul, R., and Martinou, J. C. (1995). Viral proteins E1B19K and p35 protect sympathetic neurons from cell death induced by NGF deprivation. J Cell Biol *128*, 201-208.

Martinou, J. C., Dubois-Dauphin, M., Staple, J. K., Rodriguez, I., Frankowski, H., Missotten, M., Albertini, P., Talabot, D., Catsicas, S., Pietra, C., and et al. (1994). Overexpression of BCL-2 in transgenic mice protects neurons from naturally occurring cell death and experimental ischemia. Neuron *13*, 1017-1030.

Marzo, I., Brenner, C., and Kroemer, G. (1998a). The central role of the mitochondrial megachannel in apoptosis: evidence obtained with intact cells, isolated mitochondria, and purified protein complexes. Biomed Pharmacother *52*, 248-251.

Marzo, I., Brenner, C., Zamzami, N., Susin, S. A., Beutner, G., Brdiczka, D., Remy, R., Xie, Z. H., Reed, J. C., and Kroemer, G. (1998b). The permeability transition pore complex: a target for apoptosis regulation by caspases and bcl-2-related proteins. J Exp Med *187*, 1261-1271.

Mashima, T., Udagawa, S., and Tsuruo, T. (2001). Involvement of transcriptional repressor ATF3 in acceleration of caspase protease activation during DNA damaging agent-induced apoptosis. J Cell Physiol *188*, 352-358.

Masserano, J. M., Gong, L., Kulaga, H., Baker, I., and Wyatt, R. J. (1996). Dopamine induces apoptotic cell death of a catecholaminergic cell line derived from the central nervous system. Mol Pharmacol *50*, 1309-1315.

Mathiasen, I. S., Lademann, U., and Jaattela, M. (1999). Apoptosis induced by vitamin D compounds in breast cancer cells is inhibited by Bcl-2 but does not involve known caspases or p53. Cancer Res *59*, 4848-4856.

Matsumoto, M., Minami, M., Takeda, K., Sakao, Y., and Akira, S. (1996). Ectopic expression of CHOP (GADD153) induces apoptosis in M1 myeloblastic leukemia cells. FEBS Lett *395*, 143-147.

Matsuyama, T., Hata, R., Yamamoto, Y., Tagaya, M., Akita, H., Uno, H., Wanaka, A., Furuyama, J., and Sugita, M. (1995). Localization of Fas antigen mRNA induced in postischemic murine forebrain by in situ hybridization. Brain Res Mol Brain Res *34*, 166-172.

Maundrell, K., Antonsson, B., Magnenat, E., Camps, M., Muda, M., Chabert, C., Gillieron, C., Boschert, U., Vial-Knecht, E., Martinou, J. C., and Arkinstall, S. (1997). Bcl-2 undergoes phosphorylation by c-Jun N-terminal kinase/stress-activated protein kinases in the presence of the constitutively active GTP-binding protein Rac1. J Biol Chem *272*, 25238-25242.

Mayumi-Matsuda, K., Kojima, S., Nakayama, T., Suzuki, H., and Sakata, T. (1999). Scanning gene expression during neuronal cell death evoked by nerve growth factor depletion. Biochim Biophys Acta *1489*, 293-302.

McCarthy, M. J., Rubin, L. L., and Philpott, K. L. (1997a). Involvement of caspases in sympathetic neuron apoptosis. J Cell Sci *110 (Pt 18)*, 2165-2173.

McCarthy, N. J., Whyte, M. K., Gilbert, C. S., and Evan, G. I. (1997b). Inhibition of Ced-3/ICE-related proteases does not prevent cell death induced by oncogenes, DNA damage, or the Bcl-2 homologue Bak. J Cell Biol *136*, 215-227.

McConkey, D. J., and Orrenius, S. (1997). The role of calcium in the regulation of apoptosis. Biochem Biophys Res Commun *239*, 357-366.

McDonnell, T. J., Troncoso, P., Brisbay, S. M., Logothetis, C., Chung, L. W., Hsieh, J. T., Tu, S. M., and Campbell, M. L. (1992). Expression of the protooncogene bcl-2 in the prostate and its association with emergence of androgen-independent prostate cancer. Cancer Res *52*, 6940-6944.

Mena, M. A., Khan, U., Togasaki, D. M., Sulzer, D., Epstein, C. J., and Przedborski, S. (1997). Effects of wild-type and mutated copper/zinc superoxide dismutase on neuronal survival and L-DOPA-induced toxicity in postnatal midbrain culture. J Neurochem *69*, 21-33.

Merry, D. E., Veis, D. J., Hickey, W. F., and Korsmeyer, S. J. (1994). bcl-2 protein expression is widespread in the developing nervous system and retained in the adult PNS. Development *120*, 301-311.

Mesner, P. W., Epting, C. L., Hegarty, J. L., and Green, S. H. (1995). A timetable of events during programmed cell death induced by trophic factor withdrawal from neuronal PC12 cells. J Neurosci *15*, 7357-7366.

Mesner, P. W., Winters, T. R., and Green, S. H. (1992). Nerve growth factor withdrawal-induced cell death in neuronal PC12 cells resembles that in sympathetic neurons. J Cell Biol *119*, 1669-1680.

Metz, R., Bannister, A. J., Sutherland, J. A., Hagemeier, C., O'Rourke, E. C., Cook, A., Bravo, R., and Kouzarides, T. (1994). c-Fos-induced activation of a TATA-box-containing promoter involves direct contact with TATA-box-binding protein. Mol Cell Biol *14*, 6021-6029.

Metzstein, M. M., Hengartner, M. O., Tsung, N., Ellis, R. E., and Horvitz, H. R. (1996). Transcriptional regulator of programmed cell death encoded by Caenorhabditis elegans gene ces-2. Nature *382*, 545-547.

Metzstein, M. M., Stanfield, G. M., and Horvitz, H. R. (1998). Genetics of programmed cell death in C. elegans: past, present and future. Trends Genet *14*, 410-416.

Meyaard, L., Otto, S. A., Jonker, R. R., Mijnster, M. J., Keet, R. P., and Miedema, F. (1992). Programmed death of T cells in HIV-1 infection. Science *257*, 217-219.

Miller, L. K. (1999). An exegesis of IAPs: salvation and surprises from BIR motifs. Trends Cell Biol *9*, 323-328.

Miller, T. M., Tansey, M. G., Johnson, E. M., Jr., and Creedon, D. J. (1997). Inhibition of phosphatidylinositol 3-kinase activity blocks depolarization- and insulin-like growth factor I-mediated survival of cerebellar granule cells. J Biol Chem *272*, 9847-9853.

Mizuno, Y., Hattori, N., Mori, H., Suzuki, T., and Tanaka, K. (2001). Parkin and Parkinson's disease. Curr Opin Neurol *14*, 477-482.

Mochizuki, H., Goto, K., Mori, H., and Mizuno, Y. (1996). Histochemical detection of apoptosis in Parkinson's disease. J Neurol Sci *137*, 120-123.

Morishima, N., Nakanishi, K., Takenouchi, H., Shibata, T., and Yasuhiko, Y. (2002). An endoplasmic reticulum stress-specific caspase cascade in apoptosis. Cytochrome c-independent activation of caspase-9 by caspase-12. J Biol Chem *277*, 34287-34294.

Morishima, N., Nakanishi, K., Tsuchiya, K., Shibata, T., and Seiwa, E. (2004). Translocation of Bim to the endoplasmic reticulum (ER) mediates ER stress signaling for activation of caspase-12 during ER stress-induced apoptosis. J Biol Chem *279*, 50375-50381.

Motoyama, N., Wang, F., Roth, K. A., Sawa, H., Nakayama, K., Negishi, I., Senju, S., Zhang, Q., Fujii, S., and et al. (1995). Massive cell death of immature hematopoietic cells and neurons in Bcl-x-deficient mice. Science *267*, 1506-1510.

Muchmore, S. W., Sattler, M., Liang, H., Meadows, R. P., Harlan, J. E., Yoon, H. S., Nettesheim, D., Chang, B. S., Thompson, C. B., Wong, S. L., *et al.* (1996). X-ray and NMR structure of human Bcl-xL, an inhibitor of programmed cell death. Nature *381*, 335-341.

Muzio, M., Stockwell, B. R., Stennicke, H. R., Salvesen, G. S., and Dixit, V. M. (1998). An induced proximity model for caspase-8 activation. J Biol Chem *273*, 2926-2930.

Nagai, M., Aoki, M., Miyoshi, I., Kato, M., Pasinelli, P., Kasai, N., Brown, R. H., Jr., and Itoyama, Y. (2001). Rats expressing human cytosolic copper-zinc superoxide dismutase transgenes with amyotrophic lateral sclerosis: associated mutations develop motor neuron disease. J Neurosci *21*, 9246-9254.

Nagata, S. (2000). Apoptotic DNA fragmentation. Exp Cell Res *256*, 12-18.

Nakagawa, T., Zhu, H., Morishima, N., Li, E., Xu, J., Yankner, B. A., and Yuan, J. (2000). Caspase-12 mediates endoplasmic-reticulum-specific apoptosis and cytotoxicity by amyloid-beta. Nature *403*, 98-103.

Nakagomi, S., Suzuki, Y., Namikawa, K., Kiryu-Seo, S., and Kiyama, H. (2003). Expression of the activating transcription factor 3 prevents c-Jun N-terminal kinase-induced neuronal death by promoting heat shock protein 27 expression and Akt activation. J Neurosci *23*, 5187-5196.

Nakano, K., and Vousden, K. H. (2001). PUMA, a novel proapoptotic gene, is induced by p53. Mol Cell *7*, 683-694.

Nakayama, K., Negishi, I., Kuida, K., Shinkai, Y., Louie, M. C., Fields, L. E., Lucas, P. J., Stewart, V., Alt, F. W., and et al. (1993). Disappearance of the lymphoid system in Bcl-2 homozygous mutant chimeric mice. Science *261*, 1584-1588.

Namura, S., Zhu, J., Fink, K., Endres, M., Srinivasan, A., Tomaselli, K. J., Yuan, J., and Moskowitz, M. A. (1998). Activation and cleavage of caspase-3 in apoptosis induced by experimental cerebral ischemia. J Neurosci *18*, 3659-3668.

Narita, M., Shimizu, S., Ito, T., Chittenden, T., Lutz, R. J., Matsuda, H., and Tsujimoto, Y. (1998). Bax interacts with the permeability transition pore to induce permeability transition and cytochrome c release in isolated mitochondria. Proc Natl Acad Sci U S A *95*, 14681-14686.

Nawa, T., Nawa, M. T., Cai, Y., Zhang, C., Uchimura, I., Narumi, S., Numano, F., and Kitajima, S. (2000). Repression of TNF-alpha-induced E-selectin expression by PPAR activators: involvement of transcriptional repressor LRF-1/ATF3. Biochem Biophys Res Commun *275*, 406-411.

Neame, S. J., Rubin, L. L., and Philpott, K. L. (1998). Blocking cytochrome c activity within intact neurons inhibits apoptosis. J Cell Biol *142*, 1583-1593.

Ni, B., Wu, X., Su, Y., Stephenson, D., Smalstig, E. B., Clemens, J., and Paul, S. M. (1998). Transient global forebrain ischemia induces a prolonged expression of the caspase-3 mRNA in rat hippocampal CA1 pyramidal neurons. J Cereb Blood Flow Metab *18*, 248-256.

Nicholson, D. W. (1999). Caspase structure, proteolytic substrates, and function during apoptotic cell death. Cell Death Differ *6*, 1028-1042.

Nishi, K. (1997). Expression of c-Jun in dopaminergic neurons of the substantia nigra in 1-methyl-4-phenyl-1,2,3,6-tetrahydropyridine (MPTP)-treated mice. Brain Res *771*, 133-141.

Nishina, H., Vaz, C., Billia, P., Nghiem, M., Sasaki, T., De la Pompa, J. L., Furlonger, K., Paige, C., Hui, C., Fischer, K. D., *et al.* (1999). Defective liver formation and liver cell apoptosis in mice lacking the stress signaling kinase SEK1/MKK4. Development *126*, 505-516.

Nobori, K., Ito, H., Tamamori-Adachi, M., Adachi, S., Ono, Y., Kawauchi, J., Kitajima, S., Marumo, F., and Isobe, M. (2002). ATF3 inhibits doxorubicin-induced apoptosis in cardiac myocytes: a novel cardioprotective role of ATF3. J Mol Cell Cardiol *34*, 1387-1397.

Nordeen, E. J., Nordeen, K. W., Sengelaub, D. R., and Arnold, A. P. (1985). Androgens prevent normally occurring cell death in a sexually dimorphic spinal nucleus. Science *229*, 671-673.

Novack, D. V., and Korsmeyer, S. J. (1994). Bcl-2 protein expression during murine development. Am J Pathol *145*, 61-73.

Novoa, I., Zeng, H., Harding, H. P., and Ron, D. (2001). Feedback inhibition of the unfolded protein response by GADD34-mediated dephosphorylation of eIF2alpha. J Cell Biol *153*, 1011-1022.

Nunez, G., London, L., Hockenbery, D., Alexander, M., McKearn, J. P., and Korsmeyer, S. J. (1990). Deregulated Bcl-2 gene expression selectively prolongs survival of growth factor-deprived hemopoietic cell lines. J Immunol *144*, 3602-3610.

O'Connor, L., Strasser, A., O'Reilly, L. A., Hausmann, G., Adams, J. M., Cory, S., and Huang, D. C. (1998). Bim: a novel member of the Bcl-2 family that promotes apoptosis. Embo J *17*, 384-395.

O'Reilly, L. A., Cullen, L., Visvader, J., Lindeman, G. J., Print, C., Bath, M. L., Huang, D. C., and Strasser, A. (2000). The proapoptotic BH3-only protein bim is expressed in hematopoietic, epithelial, neuronal, and germ cells. Am J Pathol *157*, 449-461.

Oberhammer, F., Fritsch, G., Pavelka, M., Froschl, G., Tiefenbacher, R., Purchio, T., and Schulte-Hermann, R. (1992). Induction of apoptosis in cultured hepatocytes and in the regressing liver by transforming growth factor-beta 1 occurs without activation of an endonuclease. Toxicol Lett *64-65 Spec No*, 701-704.

Oda, E., Ohki, R., Murasawa, H., Nemoto, J., Shibue, T., Yamashita, T., Tokino, T., Taniguchi, T., and Tanaka, N. (2000). Noxa, a BH3-only member of the Bcl-2 family and candidate mediator of p53-induced apoptosis. Science *288*, 1053-1058.

Offen, D., Ziv, I., Panet, H., Wasserman, L., Stein, R., Melamed, E., and Barzilai, A. (1997). Dopamine-induced apoptosis is inhibited in PC12 cells expressing Bcl-2. Cell Mol Neurobiol *17*, 289-304.

Okado, N., and Oppenheim, R. W. (1984). Cell death of motoneurons in the chick embryo spinal cord. IX. The loss of motoneurons following removal of afferent inputs. J Neurosci *4*, 1639-1652.

Olanow, C. W., and Tatton, W. G. (1999). Etiology and pathogenesis of Parkinson's disease. Annu Rev Neurosci *22*, 123-144.

Oltvai, Z. N., Milliman, C. L., and Korsmeyer, S. J. (1993). Bcl-2 heterodimerizes in vivo with a conserved homolog, Bax, that accelerates programmed cell death. Cell *74*, 609-619.

Opferman, J. T., and Korsmeyer, S. J. (2003). Apoptosis in the development and maintenance of the immune system. Nat Immunol *4*, 410-415.

Oppenheim, R. W. (1991). Cell death during development of the nervous system. Annu Rev Neurosci *14*, 453-501.

Ottilie, S., Diaz, J. L., Horne, W., Chang, J., Wang, Y., Wilson, G., Chang, S., Weeks, S., Fritz, L. C., and Oltersdorf, T. (1997). Dimerization properties of human BAD. Identification of a BH-3 domain and analysis of its binding to mutant BCL-2 and BCL-XL proteins. J Biol Chem *272*, 30866-30872.

Palmada, M., Kanwal, S., Rutkoski, N. J., Gustafson-Brown, C., Johnson, R. S., Wisdom, R., and Carter, B. D. (2002). c-jun is essential for sympathetic neuronal death induced by NGF withdrawal but not by p75 activation. J Cell Biol *158*, 453-461.

Pan, Y., Chen, H., Siu, F., and Kilberg, M. S. (2003). Amino acid deprivation and endoplasmic reticulum stress induce expression of multiple activating transcription factor-3 mRNA species that, when overexpressed in HepG2 cells, modulate transcription by the human asparagine synthetase promoter. J Biol Chem *278*, 38402-38412.

Parrish, J., Li, L., Klotz, K., Ledwich, D., Wang, X., and Xue, D. (2001). Mitochondrial endonuclease G is important for apoptosis in C. elegans. Nature *412*, 90-94.

Pastorino, J. G., Chen, S. T., Tafani, M., Snyder, J. W., and Farber, J. L. (1998). The overexpression of Bax produces cell death upon induction of the mitochondrial permeability transition. J Biol Chem *273*, 7770-7775.

Pearson, A. G., Gray, C. W., Pearson, J. F., Greenwood, J. M., During, M. J., and Dragunow, M. (2003). ATF3 enhances c-Jun-mediated neurite sprouting. Brain Res Mol Brain Res *120*, 38-45.

Petroske, E., Meredith, G. E., Callen, S., Totterdell, S., and Lau, Y. S. (2001). Mouse model of Parkinsonism: a comparison between subacute MPTP and chronic MPTP/probenecid treatment. Neuroscience *106*, 589-601.

Philpott, K. L., McCarthy, M. J., Klippel, A., and Rubin, L. L. (1997). Activated phosphatidylinositol 3-kinase and Akt kinase promote survival of superior cervical neurons. J Cell Biol *139*, 809-815.

Piana, S., Sulpizi, M., and Rothlisberger, U. (2003). Structure-based thermodynamic analysis of caspases reveals key residues for dimerization and activity. Biochemistry *42*, 8720-8728.

Pinton, P., Ferrari, D., Magalhaes, P., Schulze-Osthoff, K., Di Virgilio, F., Pozzan, T., and Rizzuto, R. (2000). Reduced loading of intracellular Ca(2+) stores and downregulation of capacitative Ca(2+) influx in Bcl-2-overexpressing cells. J Cell Biol *148*, 857-862.

Pitti, R. M., Marsters, S. A., Lawrence, D. A., Roy, M., Kischkel, F. C., Dowd, P., Huang, A., Donahue, C. J., Sherwood, S. W., Baldwin, D. T., *et al.* (1998). Genomic amplification of a decoy receptor for Fas ligand in lung and colon cancer. Nature *396*, 699-703.

Pittman, R. N., Wang, S., DiBenedetto, A. J., and Mills, J. C. (1993). A system for characterizing cellular and molecular events in programmed neuronal cell death. J Neurosci *13*, 3669-3680.

Polymeropoulos, M. H. (2000). Genetics of Parkinson's disease. Ann N Y Acad Sci *920*, 28-32.

Polymeropoulos, M. H., Lavedan, C., Leroy, E., Ide, S. E., Dehejia, A., Dutra, A., Pike, B., Root, H., Rubenstein, J., Boyer, R., *et al.* (1997). Mutation in the alpha-synuclein gene identified in families with Parkinson's disease. Science *276*, 2045-2047.

Potts, P. R., Singh, S., Knezek, M., Thompson, C. B., and Deshmukh, M. (2003). Critical function of endogenous XIAP in regulating caspase activation during sympathetic neuronal apoptosis. J Cell Biol *163*, 789-799.

Price, J. M., Donahoe, P. K., Ito, Y., and Hendren, W. H., 3rd (1977). Programmed cell death in the Mullerian duct induced by Mullerian inhibiting substance. Am J Anat *149*, 353-375.

Przedborski, S., Donaldson, D. M., Murphy, P. L., Hirsch, O., Lange, D., Naini, A. B., McKenna-Yasek, D., and Brown, R. H., Jr. (1996). Blood superoxide dismutase, catalase and glutathione peroxidase activities in familial and sporadic amyotrophic lateral sclerosis. Neurodegeneration *5*, 57-64.

Przedborski, S., and Jackson-Lewis, V. (1998). Mechanisms of MPTP toxicity. Mov Disord *13 Suppl 1*, 35-38.

Pulsinelli, W. A., Brierley, J. B., and Plum, F. (1982). Temporal profile of neuronal damage in a model of transient forebrain ischemia. Ann Neurol *11*, 491-498.

Putcha, G. V., Deshmukh, M., and Johnson, E. M., Jr. (1999). BAX translocation is a critical event in neuronal apoptosis: regulation by neuroprotectants, BCL-2, and caspases. J Neurosci *19*, 7476-7485.

Putcha, G. V., Harris, C. A., Moulder, K. L., Easton, R. M., Thompson, C. B., and Johnson, E. M., Jr. (2002). Intrinsic and extrinsic pathway signaling during neuronal apoptosis: lessons from the analysis of mutant mice. J Cell Biol *157*, 441-453.

Putcha, G. V., Le, S., Frank, S., Besirli, C. G., Clark, K., Chu, B., Alix, S., Youle, R. J., LaMarche, A., Maroney, A. C., and Johnson, E. M., Jr. (2003). JNK-mediated BIM phosphorylation potentiates BAX-dependent apoptosis. Neuron *38*, 899-914.

Putcha, G. V., Moulder, K. L., Golden, J. P., Bouillet, P., Adams, J. A., Strasser, A., and Johnson, E. M. (2001). Induction of BIM, a proapoptotic BH3-only BCL-2 family member, is critical for neuronal apoptosis. Neuron *29*, 615-628.

Qian, X., Riccio, A., Zhang, Y., and Ginty, D. D. (1998). Identification and characterization of novel substrates of Trk receptors in developing neurons. Neuron *21*, 1017-1029.

Rabizadeh, S., Gralla, E. B., Borchelt, D. R., Gwinn, R., Valentine, J. S., Sisodia, S., Wong, P., Lee, M., Hahn, H., and Bredesen, D. E. (1995). Mutations associated with amyotrophic lateral sclerosis convert superoxide dismutase from an antiapoptotic gene to a proapoptotic gene: studies in yeast and neural cells. Proc Natl Acad Sci U S A *92*, 3024-3028.

Raff, M. C. (1992). Social controls on cell survival and cell death. Nature *356*, 397-400.

Raingeaud, J., Gupta, S., Rogers, J. S., Dickens, M., Han, J., Ulevitch, R. J., and Davis, R. J. (1995). Pro-inflammatory cytokines and environmental stress cause p38 mitogen-activated protein kinase activation by dual phosphorylation on tyrosine and threonine. J Biol Chem *270*, 7420-7426.

Raivich, G., Bohatschek, M., Da Costa, C., Iwata, O., Galiano, M., Hristova, M., Nateri, A. S., Makwana, M., Riera-Sans, L., Wolfer, D. P., *et al.* (2004). The AP-1 transcription factor c-Jun is required for efficient axonal regeneration. Neuron *43*, 57-67.

Rao, L., Perez, D., and White, E. (1996). Lamin proteolysis facilitates nuclear events during apoptosis. J Cell Biol *135*, 1441-1455.

Rasola, A., Gramaglia, D., Boccaccio, C., and Comoglio, P. M. (2001). Apoptosis enhancement by the HIV-1 Nef protein. J Immunol *166*, 81-88.

Ray, C. A., Black, R. A., Kronheim, S. R., Greenstreet, T. A., Sleath, P. R., Salvesen, G. S., and Pickup, D. J. (1992). Viral inhibition of inflammation: cowpox virus encodes an inhibitor of the interleukin-1 beta converting enzyme. Cell *69*, 597-604.

Reaume, A. G., Elliott, J. L., Hoffman, E. K., Kowall, N. W., Ferrante, R. J., Siwek, D. F., Wilcox, H. M., Flood, D. G., Beal, M. F., Brown, R. H., Jr., *et al.* (1996). Motor neurons in Cu/Zn superoxide dismutase-deficient mice develop normally but exhibit enhanced cell death after axonal injury. Nat Genet *13*, 43-47.

Riccio, A., Ahn, S., Davenport, C. M., Blendy, J. A., and Ginty, D. D. (1999). Mediation by a CREB family transcription factor of NGF-dependent survival of sympathetic neurons. Science *286*, 2358-2361.

Rieux-Laucat, F., Le Deist, F., Hivroz, C., Roberts, I. A., Debatin, K. M., Fischer, A., and de Villartay, J. P. (1995). Mutations in Fas associated with human lymphoproliferative syndrome and autoimmunity. Science *268*, 1347-1349.

Rizzuto, R., Pinton, P., Carrington, W., Fay, F. S., Fogarty, K. E., Lifshitz, L. M., Tuft, R. A., and Pozzan, T. (1998). Close contacts with the endoplasmic reticulum as determinants of mitochondrial Ca2+ responses. Science *280*, 1763-1766.

Robles, A. I., Bemmels, N. A., Foraker, A. B., and Harris, C. C. (2001). APAF-1 is a transcriptional target of p53 in DNA damage-induced apoptosis. Cancer Res *61*, 6660-6664.

Rodriguez, J., and Lazebnik, Y. (1999). Caspase-9 and APAF-1 form an active holoenzyme. Genes Dev *13*, 3179-3184.

Ron, D. (2002). Translational control in the endoplasmic reticulum stress response. J Clin Invest *110*, 1383-1388.

Roux, P. P., Dorval, G., Boudreau, M., Angers-Loustau, A., Morris, S. J., Makkerh, J., and Barker, P. A. (2002). K252a and CEP1347 are neuroprotective compounds that inhibit mixed-lineage kinase-3 and induce activation of Akt and ERK. J Biol Chem *277*, 49473-49480.

Rozengurt, E. (1992). Growth factors and cell proliferation. Curr Opin Cell Biol *4*, 161-165.

Rukenstein, A., Rydel, R. E., and Greene, L. A. (1991). Multiple agents rescue PC12 cells from serum-free cell death by translation- and transcription-independent mechanisms. J Neurosci *11*, 2552-2563.

Ryden, M., Hempstead, B., and Ibanez, C. F. (1997). Differential modulation of neuron survival during development by nerve growth factor binding to the p75 neurotrophin receptor. J Biol Chem *272*, 16322-16328.

Saito, K., Elce, J. S., Hamos, J. E., and Nixon, R. A. (1993). Widespread activation of calcium-activated neutral proteinase (calpain) in the brain in Alzheimer disease: a potential molecular basis for neuronal degeneration. Proc Natl Acad Sci U S A *90*, 2628-2632.

Saitoh, T., Tanaka, S., and Koike, T. (2001). Rapid induction and Ca(2+) influx-mediated suppression of vitamin D3 up-regulated protein 1 (VDUP1) mRNA in cerebellar granule neurons undergoing apoptosis. J Neurochem *78*, 1267-1276.

Salvesen, G. S., and Dixit, V. M. (1999). Caspase activation: the induced-proximity model. Proc Natl Acad Sci U S A *96*, 10964-10967.

Salvesen, G. S., and Duckett, C. S. (2002). IAP proteins: blocking the road to death's door. Nat Rev Mol Cell Biol *3*, 401-410.

Sambrook, J., Fritsch, E. F., and Maniatis, T. (1989). Molecular Cloning, A laboratory Manual. Second Edition. Cold Spring Harbor Laboratory Press.

Saporito, M. S., Brown, E. M., Miller, M. S., and Carswell, S. (1999). CEP-1347/KT-7515, an inhibitor of c-jun N-terminal kinase activation, attenuates the 1-methyl-4-phenyl tetrahydropyridine-mediated loss of nigrostriatal dopaminergic neurons In vivo. J Pharmacol Exp Ther *288*, 421-427.

Saunders, J. W., Jr. (1966). Death in embryonic systems. Science *154*, 604-612.

Saxen, L., and Sariola, H. (1987). Early organogenesis of the kidney. Pediatr Nephrol *1*, 385-392.

Schievella, A. R., Chen, J. H., Graham, J. R., and Lin, L. L. (1997). MADD, a novel death domain protein that interacts with the type 1 tumor necrosis factor receptor and activates mitogen-activated protein kinase. J Biol Chem *272*, 12069-12075.

Schlingensiepen, K. H., Schlingensiepen, R., Kunst, M., Klinger, I., Gerdes, W., Seifert, W., and Brysch, W. (1993). Opposite functions of jun-B and c-jun in growth regulation and neuronal differentiation. Dev Genet *14*, 305-312.

Schreiber, M., Kolbus, A., Piu, F., Szabowski, A., Mohle-Steinlein, U., Tian, J., Karin, M., Angel, P., and Wagner, E. F. (1999). Control of cell cycle progression by c-Jun is p53 dependent. Genes Dev *13*, 607-619.

Scorrano, L., Oakes, S. A., Opferman, J. T., Cheng, E. H., Sorcinelli, M. D., Pozzan, T., and Korsmeyer, S. J. (2003). BAX and BAK regulation of endoplasmic reticulum Ca2+: a control point for apoptosis. Science *300*, 135-139.

Searle, J., Lawson, T. A., Abbott, P. J., Harmon, B., and Kerr, J. F. (1975). An electron-microscope study of the mode of cell death induced by cancer-chemotherapeutic agents in populations of proliferating normal and neoplastic cells. J Pathol *116*, 129-138.

Segal, R. A., and Greenberg, M. E. (1996). Intracellular signaling pathways activated by neurotrophic factors. Annu Rev Neurosci *19*, 463-489.

Shaham, S., and Horvitz, H. R. (1996). Developing Caenorhabditis elegans neurons may contain both cell-death protective and killer activities. Genes Dev *10*, 578-591.

Shaulian, E., and Karin, M. (2001). AP-1 in cell proliferation and survival. Oncogene *20*, 2390-2400.

Shi, Y. (2004). Caspase activation: revisiting the induced proximity model. Cell *117*, 855-858.

Shigeno, T., Yamasaki, Y., Kato, G., Kusaka, K., Mima, T., Takakura, K., Graham, D. I., and Furukawa, S. (1990). Reduction of delayed neuronal death by inhibition of protein synthesis. Neurosci Lett *120*, 117-119.

Shimizu, S., Eguchi, Y., Kamiike, W., Funahashi, Y., Mignon, A., Lacronique, V., Matsuda, H., and Tsujimoto, Y. (1998). Bcl-2 prevents apoptotic mitochondrial dysfunction by regulating proton flux. Proc Natl Acad Sci U S A *95*, 1455-1459.

Shimizu, S., Narita, M., and Tsujimoto, Y. (1999). Bcl-2 family proteins regulate the release of apoptogenic cytochrome c by the mitochondrial channel VDAC. Nature *399*, 483-487.

Shinagawa, T., Yoshioka, K., Kakumu, S., Wakita, T., Ishikawa, T., Itoh, Y., and Takayanagi, M. (1991). Apoptosis in cultured rat hepatocytes: the effects of tumour necrosis factor alpha and interferon gamma. J Pathol *165*, 247-253.

Shindler, K. S., Latham, C. B., and Roth, K. A. (1997). Bax deficiency prevents the increased cell death of immature neurons in bcl-x-deficient mice. J Neurosci *17*, 3112-3119.

Shinoe, T., Wanaka, A., Nikaido, T., Kanazawa, K., Shimizu, J., Imaizumi, K., and Kanazawa, I. (2001). Upregulation of the pro-apoptotic BH3-only peptide harakiri in spinal neurons of amyotrophic lateral sclerosis patients. Neurosci Lett *313*, 153-157.

Smeyne, R. J., Klein, R., Schnapp, A., Long, L. K., Bryant, S., Lewin, A., Lira, S. A., and Barbacid, M. (1994). Severe sensory and sympathetic neuropathies in mice carrying a disrupted Trk/NGF receptor gene. Nature *368*, 246-249.

Smith, C., and Mackay, S. (1991). Morphological development and fate of the mouse mesonephros. J Anat *174*, 171-184.

Snider, W. D. (1994). Functions of the neurotrophins during nervous system development: what the knockouts are teaching us. Cell *77*, 627-638.

Squier, M. K., Miller, A. C., Malkinson, A. M., and Cohen, J. J. (1994). Calpain activation in apoptosis. J Cell Physiol *159*, 229-237.

Stanger, B. Z., Leder, P., Lee, T. H., Kim, E., and Seed, B. (1995). RIP: a novel protein containing a death domain that interacts with Fas/APO-1 (CD95) in yeast and causes cell death. Cell *81*, 513-523.

Stefanis, L., Park, D. S., Yan, C. Y., Farinelli, S. E., Troy, C. M., Shelanski, M. L., and Greene, L. A. (1996). Induction of CPP32-like activity in PC12 cells by withdrawal of trophic support. Dissociation from apoptosis. J Biol Chem *271*, 30663-30671.

Stefanis, L., Troy, C. M., Qi, H., and Greene, L. A. (1997). Inhibitors of trypsin-like serine proteases inhibit processing of the caspase Nedd-2 and protect PC12 cells and sympathetic neurons from death evoked by withdrawal of trophic support. J Neurochem *69*, 1425-1437.

Steller, H. (1995). Mechanisms and genes of cellular suicide. Science *267*, 1445-1449.

Stennicke, H. R., Deveraux, Q. L., Humke, E. W., Reed, J. C., Dixit, V. M., and Salvesen, G. S. (1999). Caspase-9 can be activated without proteolytic processing. J Biol Chem *274*, 8359-8362.

Sugioka, R., Shimizu, S., Funatsu, T., Tamagawa, H., Sawa, Y., Kawakami, T., and Tsujimoto, Y. (2003). BH4-domain peptide from Bcl-xL exerts anti-apoptotic activity in vivo. Oncogene *22*, 8432-8440.

Sulston, J. E., and Horvitz, H. R. (1977). Post-embryonic cell lineages of the nematode, Caenorhabditis elegans. Dev Biol *56*, 110-156.

Susin, S. A., Lorenzo, H. K., Zamzami, N., Marzo, I., Snow, B. E., Brothers, G. M., Mangion, J., Jacotot, E., Costantini, P., Loeffler, M., *et al.* (1999). Molecular characterization of mitochondrial apoptosis-inducing factor. Nature *397*, 441-446.

Swat, W., Fujikawa, K., Ganiatsas, S., Yang, D., Xavier, R. J., Harris, N. L., Davidson, L., Ferrini, R., Davis, R. J., Labow, M. A., *et al.* (1998). SEK1/MKK4 is required for maintenance of a normal peripheral lymphoid compartment but not for lymphocyte development. Immunity *8*, 625-634.

Takahashi, R., Deveraux, Q., Tamm, I., Welsh, K., Assa-Munt, N., Salvesen, G. S., and Reed, J. C. (1998). A single BIR domain of XIAP sufficient for inhibiting caspases. J Biol Chem *273*, 7787-7790.

Takeda, M., Kato, H., Takamiya, A., Yoshida, A., and Kiyama, H. (2000). Injury-specific expression of activating transcription factor-3 in retinal ganglion cells and its colocalized expression with phosphorylated c-Jun. Invest Ophthalmol Vis Sci *41*, 2412-2421.

Tata, J. R. (1966). Requirement for RNA and protein synthesis for induced regression of the tadpole tail in organ culture. Dev Biol *13*, 77-94.

Tatton, N. A., and Kish, S. J. (1997). In situ detection of apoptotic nuclei in the substantia nigra compacta of 1-methyl-4-phenyl-1,2,3,6-tetrahydropyridine-treated mice using terminal deoxynucleotidyl transferase labelling and acridine orange staining. Neuroscience *77*, 1037-1048.

Tatton, N. A., Maclean-Fraser, A., Tatton, W. G., Perl, D. P., and Olanow, C. W. (1998). A fluorescent double-labeling method to detect and confirm apoptotic nuclei in Parkinson's disease. Ann Neurol *44*, S142-148.

Testa, U. (2004). Apoptotic mechanisms in the control of erythropoiesis. Leukemia *18*, 1176-1199.

Thellmann, M., Hatzold, J., and Conradt, B. (2003). The Snail-like CES-1 protein of C. elegans can block the expression of the BH3-only cell-death activator gene egl-1 by antagonizing the function of bHLH proteins. Development *130*, 4057-4071.

Thompson, C. B. (1995). Apoptosis in the pathogenesis and treatment of disease. Science *267*, 1456-1462.

Thornberry, N. A., Bull, H. G., Calaycay, J. R., Chapman, K. T., Howard, A. D., Kostura, M. J., Miller, D. K., Molineaux, S. M., Weidner, J. R., Aunins, J., and et al. (1992). A novel heterodimeric cysteine protease is required for interleukin-1 beta processing in monocytes. Nature *356*, 768-774.

Thornberry, N. A., and Lazebnik, Y. (1998). Caspases: enemies within. Science *281*, 1312-1316.

Thornberry, N. A., Rano, T. A., Peterson, E. P., Rasper, D. M., Timkey, T., Garcia-Calvo, M., Houtzager, V. M., Nordstrom, P. A., Roy, S., Vaillancourt, J. P., *et al.* (1997). A combinatorial approach defines specificities of members of the caspase family and granzyme B. Functional relationships established for key mediators of apoptosis. J Biol Chem *272*, 17907-17911.

Tibbles, L. A., Ing, Y. L., Kiefer, F., Chan, J., Iscove, N., Woodgett, J. R., and Lassam, N. J. (1996). MLK-3 activates the SAPK/JNK and p38/RK pathways via SEK1 and MKK3/6. Embo J *15*, 7026-7035.

Tischler, A. S., and Greene, L. A. (1975). Nerve growth factor-induced process formation by cultured rat pheochromocytoma cells. Nature *258*, 341-342.

Tompkins, M. M., Basgall, E. J., Zamrini, E., and Hill, W. D. (1997). Apoptotic-like changes in Lewy-body-associated disorders and normal aging in substantia nigral neurons. Am J Pathol *150*, 119-131.

Torriglia, A., Chaudun, E., Chany-Fournier, F., Courtois, Y., and Counis, M. F. (2001). Involvement of L-DNase II in nuclear degeneration during chick retina development. Exp Eye Res *72*, 443-453.

Tournier, C., Hess, P., Yang, D. D., Xu, J., Turner, T. K., Nimnual, A., Bar-Sagi, D., Jones, S. N., Flavell, R. A., and Davis, R. J. (2000). Requirement of JNK for stress-induced activation of the cytochrome c-mediated death pathway. Science *288*, 870-874.

Tournier, C., Whitmarsh, A. J., Cavanagh, J., Barrett, T., and Davis, R. J. (1997). Mitogen-activated protein kinase kinase 7 is an activator of the c-Jun NH2-terminal kinase. Proc Natl Acad Sci U S A *94*, 7337-7342.

Trauth, B. C., Klas, C., Peters, A. M., Matzku, S., Moller, P., Falk, W., Debatin, K. M., and Krammer, P. H. (1989). Monoclonal antibody-mediated tumor regression by induction of apoptosis. Science *245*, 301-305.

Trimmer, P. A., Smith, T. S., Jung, A. B., and Bennett, J. P., Jr. (1996). Dopamine neurons from transgenic mice with a knockout of the p53 gene resist MPTP neurotoxicity. Neurodegeneration *5*, 233-239.

Troy, C. M., Rabacchi, S. A., Hohl, J. B., Angelastro, J. M., Greene, L. A., and Shelanski, M. L. (2001). Death in the balance: alternative participation of the caspase-2 and -9 pathways in neuronal death induced by nerve growth factor deprivation. J Neurosci *21*, 5007-5016.

Troy, C. M., Stefanis, L., Greene, L. A., and Shelanski, M. L. (1997). Nedd2 is required for apoptosis after trophic factor withdrawal, but not superoxide dismutase (SOD1) downregulation, in sympathetic neurons and PC12 cells. J Neurosci *17*, 1911-1918.

Tsujimoto, Y., Jaffe, E., Cossman, J., Gorham, J., Nowell, P. C., and Croce, C. M. (1985). Clustering of breakpoints on chromosome 11 in human B-cell neoplasms with the t(11;14) chromosome translocation. Nature *315*, 340-343.

Tsujino, H., Kondo, E., Fukuoka, T., Dai, Y., Tokunaga, A., Miki, K., Yonenobu, K., Ochi, T., and Noguchi, K. (2000). Activating transcription factor 3 (ATF3) induction by axotomy in sensory and motoneurons: A novel neuronal marker of nerve injury. Mol Cell Neurosci *15*, 170-182.

van Dam, H., Wilhelm, D., Herr, I., Steffen, A., Herrlich, P., and Angel, P. (1995). ATF-2 is preferentially activated by stress-activated protein kinases to mediate c-jun induction in response to genotoxic agents. Embo J *14*, 1798-1811.

van Loo, G., van Gurp, M., Depuydt, B., Srinivasula, S. M., Rodriguez, I., Alnemri, E. S., Gevaert, K., Vandekerckhove, J., Declercq, W., and Vandenabeele, P. (2002). The serine protease Omi/HtrA2 is released from mitochondria during apoptosis. Omi interacts with caspase-inhibitor XIAP and induces enhanced caspase activity. Cell Death Differ *9*, 20-26.

Varfolomeev, E. E., Schuchmann, M., Luria, V., Chiannilkulchai, N., Beckmann, J. S., Mett, I. L., Rebrikov, D., Brodianski, V. M., Kemper, O. C., Kollet, O., *et al.* (1998). Targeted disruption of the mouse Caspase 8 gene ablates cell death induction by the TNF receptors, Fas/Apo1, and DR3 and is lethal prenatally. Immunity *9*, 267-276.

Vaux, D. L., Cory, S., and Adams, J. M. (1988). Bcl-2 gene promotes haemopoietic cell survival and cooperates with c-myc to immortalize pre-B cells. Nature *335*, 440-442.

Veis, D. J., Sorenson, C. M., Shutter, J. R., and Korsmeyer, S. J. (1993). Bcl-2-deficient mice demonstrate fulminant lymphoid apoptosis, polycystic kidneys, and hypopigmented hair. Cell *75*, 229-240.

Vekrellis, K., McCarthy, M. J., Watson, A., Whitfield, J., Rubin, L. L., and Ham, J. (1997). Bax promotes neuronal cell death and is downregulated during the development of the nervous system. Development *124*, 1239-1249.

Verhagen, A. M., Ekert, P. G., Pakusch, M., Silke, J., Connolly, L. M., Reid, G. E., Moritz, R. L., Simpson, R. J., and Vaux, D. L. (2000). Identification of DIABLO, a mammalian protein that promotes apoptosis by binding to and antagonizing IAP proteins. Cell *102*, 43-53.

Vila, M., Jackson-Lewis, V., Vukosavic, S., Djaldetti, R., Liberatore, G., Offen, D., Korsmeyer, S. J., and Przedborski, S. (2001). Bax ablation prevents dopaminergic neurodegeneration in the 1-methyl- 4-phenyl-1,2,3,6-tetrahydropyridine mouse model of Parkinson's disease. Proc Natl Acad Sci U S A *98*, 2837-2842.

Vila, M., and Przedborski, S. (2003). Targeting programmed cell death in neurodegenerative diseases. Nat Rev Neurosci *4*, 365-375.

Vila, M., Vukosavic, S., Jackson-Lewis, V., Neystat, M., Jakowec, M., and Przedborski, S. (2000). Alpha-synuclein up-regulation in substantia nigra dopaminergic neurons following administration of the parkinsonian toxin MPTP. J Neurochem *74*, 721-729.

Virdee, K., Bannister, A. J., Hunt, S. P., and Tolkovsky, A. M. (1997). Comparison between the timing of JNK activation, c-Jun phosphorylation, and onset of death commitment in sympathetic neurones. J Neurochem *69*, 550-561.

Vivanco, I., and Sawyers, C. L. (2002). The phosphatidylinositol 3-Kinase AKT pathway in human cancer. Nat Rev Cancer *2*, 489-501.

Vogelstein, B., Lane, D., and Levine, A. J. (2000). Surfing the p53 network. Nature *408*, 307-310.

Vogt, P. K., and Bos, T. J. (1990). jun: oncogene and transcription factor. Adv Cancer Res *55*, 1-35.

Vucic, D., Stennicke, H. R., Pisabarro, M. T., Salvesen, G. S., and Dixit, V. M. (2000). ML-IAP, a novel inhibitor of apoptosis that is preferentially expressed in human melanomas. Curr Biol *10*, 1359-1366.

Vukosavic, S., Dubois-Dauphin, M., Romero, N., and Przedborski, S. (1999). Bax and Bcl-2 interaction in a transgenic mouse model of familial amyotrophic lateral sclerosis. J Neurochem *73*, 2460-2468.

Waldmeier, P. C. (2003). Prospects for antiapoptotic drug therapy of neurodegenerative diseases. Prog Neuropsychopharmacol Biol Psychiatry *27*, 303-321.

Wang, J., Cao, Y., and Steiner, D. F. (2003). Regulation of proglucagon transcription by activated transcription factor (ATF) 3 and a novel isoform, ATF3b, through the cAMP-response element/ATF site of the proglucagon gene promoter. J Biol Chem *278*, 32899-32904.

Wang, K., Gross, A., Waksman, G., and Korsmeyer, S. J. (1998a). Mutagenesis of the BH3 domain of BAX identifies residues critical for dimerization and killing. Mol Cell Biol *18*, 6083-6089.

Wang, L. H., Paden, A. J., and Johnson, E. M., Jr. (2005). Mixed-lineage kinase inhibitors require the activation of trk receptors to maintain long-term neuronal trophism and survival. J Pharmacol Exp Ther *312*, 1007-1019.

Wang, S., Miura, M., Jung, Y. K., Zhu, H., Li, E., and Yuan, J. (1998b). Murine caspase-11, an ICE-interacting protease, is essential for the activation of ICE. Cell *92*, 501-509.

Waterhouse, N. J., Finucane, D. M., Green, D. R., Elce, J. S., Kumar, S., Alnemri, E. S., Litwack, G., Khanna, K., Lavin, M. F., and Watters, D. J. (1998). Calpain activation is upstream of caspases in radiation-induced apoptosis. Cell Death Differ *5*, 1051-1061.

Watson, A., Eilers, A., Lallemand, D., Kyriakis, J., Rubin, L. L., and Ham, J. (1998). Phosphorylation of c-Jun is necessary for apoptosis induced by survival signal withdrawal in cerebellar granule neurons. J Neurosci *18*, 751-762.

Wei, M. C., Lindsten, T., Mootha, V. K., Weiler, S., Gross, A., Ashiya, M., Thompson, C. B., and Korsmeyer, S. J. (2000). tBID, a membrane-targeted death ligand, oligomerizes BAK to release cytochrome c. Genes Dev *14*, 2060-2071.

Wei, M. C., Zong, W. X., Cheng, E. H., Lindsten, T., Panoutsakopoulou, V., Ross, A. J., Roth, K. A., MacGregor, G. R., Thompson, C. B., and Korsmeyer, S. J. (2001). Proapoptotic BAX and BAK: a requisite gateway to mitochondrial dysfunction and death. Science *292*, 727-730.

Weil, M., Jacobson, M. D., Coles, H. S., Davies, T. J., Gardner, R. L., Raff, K. D., and Raff, M. C. (1996). Constitutive expression of the machinery for programmed cell death. J Cell Biol *133*, 1053-1059.

Weil, M., Jacobson, M. D., and Raff, M. C. (1997). Is programmed cell death required for neural tube closure? Curr Biol *7*, 281-284.

Weil, M., Raff, M. C., and Braga, V. M. (1999). Caspase activation in the terminal differentiation of human epidermal keratinocytes. Curr Biol *9*, 361-364.

Weiner, J. A., and Chun, J. (1999). Schwann cell survival mediated by the signaling phospholipid lysophosphatidic acid. Proc Natl Acad Sci U S A *96*, 5233-5238.

White, F. A., Keller-Peck, C. R., Knudson, C. M., Korsmeyer, S. J., and Snider, W. D. (1998). Widespread elimination of naturally occurring neuronal death in Bax-deficient mice. J Neurosci *18*, 1428-1439.

Whitfield, J., Neame, S. J., and Ham, J. (2004). Methods for culturing primary sympathetic neurons and for determining neuronal viability. Methods Mol Biol *282*, 157-168.

Whitfield, J., Neame, S. J., Paquet, L., Bernard, O., and Ham, J. (2001). Dominant-negative c-Jun promotes neuronal survival by reducing BIM expression and inhibiting mitochondrial cytochrome c release. Neuron *29*, 629-643.

Wiese, S., Digby, M. R., Gunnersen, J. M., Gotz, R., Pei, G., Holtmann, B., Lowenthal, J., and Sendtner, M. (1999). The anti-apoptotic protein ITA is essential for NGF-mediated survival of embryonic chick neurons. Nat Neurosci *2*, 978-983.

Williams, G. T., Smith, C. A., Spooncer, E., Dexter, T. M., and Taylor, D. R. (1990). Haemopoietic colony stimulating factors promote cell survival by suppressing apoptosis. Nature *343*, 76-79.

Wolfgang, C. D., Chen, B. P., Martindale, J. L., Holbrook, N. J., and Hai, T. (1997). gadd153/Chop10, a potential target gene of the transcriptional repressor ATF3. Mol Cell Biol *17*, 6700-6707.

Wolfgang, C. D., Liang, G., Okamoto, Y., Allen, A. E., and Hai, T. (2000). Transcriptional autorepression of the stress-inducible gene ATF3. J Biol Chem *275*, 16865-16870.

Wolter, K. G., Hsu, Y. T., Smith, C. L., Nechushtan, A., Xi, X. G., and Youle, R. J. (1997). Movement of Bax from the cytosol to mitochondria during apoptosis. J Cell Biol *139*, 1281-1292.

Wong, P. C., Pardo, C. A., Borchelt, D. R., Lee, M. K., Copeland, N. G., Jenkins, N. A., Sisodia, S. S., Cleveland, D. W., and Price, D. L. (1995). An adverse property of a familial ALS-linked SOD1 mutation causes motor neuron disease characterized by vacuolar degeneration of mitochondria. Neuron *14*, 1105-1116.

Wright, L. L., Cunningham, T. J., and Smolen, A. J. (1983). Developmental neuron death in the rat superior cervical sympathetic ganglion: cell counts and ultrastructure. J Neurocytol *12*, 727-738.

Wullner, U., Kornhuber, J., Weller, M., Schulz, J. B., Loschmann, P. A., Riederer, P., and Klockgether, T. (1999). Cell death and apoptosis regulating proteins in Parkinson's disease--a cautionary note. Acta Neuropathol (Berl) *97*, 408-412.

Wyllie, A. H. (1980). Glucocorticoid-induced thymocyte apoptosis is associated with endogenous endonuclease activation. Nature *284*, 555-556.

Wyllie, A. H., Morris, R. G., Smith, A. L., and Dunlop, D. (1984). Chromatin cleavage in apoptosis: association with condensed chromatin morphology and dependence on macromolecular synthesis. J Pathol *142*, 67-77.

Xia, X. G., Harding, T., Weller, M., Bieneman, A., Uney, J. B., and Schulz, J. B. (2001). Gene transfer of the JNK interacting protein-1 protects dopaminergic neurons in the MPTP model of Parkinson's disease. Proc Natl Acad Sci U S A *98*, 10433-10438.

Xia, Z., Dickens, M., Raingeaud, J., Davis, R. J., and Greenberg, M. E. (1995). Opposing effects of ERK and JNK-p38 MAP kinases on apoptosis. Science *270*, 1326-1331.

Xiang, J., Chao, D. T., and Korsmeyer, S. J. (1996). BAX-induced cell death may not require interleukin 1 beta-converting enzyme-like proteases. Proc Natl Acad Sci U S A *93*, 14559-14563.

Xu, Z., Maroney, A. C., Dobrzanski, P., Kukekov, N. V., and Greene, L. A. (2001). The MLK family mediates c-Jun N-terminal kinase activation in neuronal apoptosis. Mol Cell Biol *21*, 4713-4724.

Xue, D., Shaham, S., and Horvitz, H. R. (1996). The Caenorhabditis elegans cell-death protein CED-3 is a cysteine protease with substrate specificities similar to those of the human CPP32 protease. Genes Dev *10*, 1073-1083.

Yamada, M., Oligino, T., Mata, M., Goss, J. R., Glorioso, J. C., and Fink, D. J. (1999). Herpes simplex virus vector-mediated expression of Bcl-2 prevents 6-

hydroxydopamine-induced degeneration of neurons in the substantia nigra in vivo. Proc Natl Acad Sci U S A *96*, 4078-4083.

Yamada, T., Ohyama, H., Kinjo, Y., and Watanabe, M. (1981). Evidence for the internucleosomal breakage of chromatin in rat thymocytes irradiated in vitro. Radiat Res *85*, 544-553.

Yan, M., Dai, T., Deak, J. C., Kyriakis, J. M., Zon, L. I., Woodgett, J. R., and Templeton, D. J. (1994). Activation of stress-activated protein kinase by MEKK1 phosphorylation of its activator SEK1. Nature *372*, 798-800.

Yang, D., Tournier, C., Wysk, M., Lu, H. T., Xu, J., Davis, R. J., and Flavell, R. A. (1997a). Targeted disruption of the MKK4 gene causes embryonic death, inhibition of c-Jun NH2-terminal kinase activation, and defects in AP-1 transcriptional activity. Proc Natl Acad Sci U S A *94*, 3004-3009.

Yang, D. D., Conze, D., Whitmarsh, A. J., Barrett, T., Davis, R. J., Rincon, M., and Flavell, R. A. (1998a). Differentiation of CD4+ T cells to Th1 cells requires MAP kinase JNK2. Immunity *9*, 575-585.

Yang, D. D., Kuan, C. Y., Whitmarsh, A. J., Rincon, M., Zheng, T. S., Davis, R. J., Rakic, P., and Flavell, R. A. (1997b). Absence of excitotoxicity-induced apoptosis in the hippocampus of mice lacking the Jnk3 gene. Nature *389*, 865-870.

Yang, E., Zha, J., Jockel, J., Boise, L. H., Thompson, C. B., and Korsmeyer, S. J. (1995). Bad, a heterodimeric partner for Bcl-XL and Bcl-2, displaces Bax and promotes cell death. Cell *80*, 285-291.

Yang, J., Liu, X., Bhalla, K., Kim, C. N., Ibrado, A. M., Cai, J., Peng, T. I., Jones, D. P., and Wang, X. (1997c). Prevention of apoptosis by Bcl-2: release of cytochrome c from mitochondria blocked. Science *275*, 1129-1132.

Yang, Q. H., Church-Hajduk, R., Ren, J., Newton, M. L., and Du, C. (2003). Omi/HtrA2 catalytic cleavage of inhibitor of apoptosis (IAP) irreversibly inactivates IAPs and facilitates caspase activity in apoptosis. Genes Dev *17*, 1487-1496.

Yang, T., Buchan, H. L., Townsend, K. J., and Craig, R. W. (1996). MCL-1, a member of the BLC-2 family, is induced rapidly in response to signals for cell differentiation or death, but not to signals for cell proliferation. J Cell Physiol *166*, 523-536.

Yang, X., Chang, H. Y., and Baltimore, D. (1998b). Essential role of CED-4 oligomerization in CED-3 activation and apoptosis. Science *281*, 1355-1357.

Yang, Y., Fang, S., Jensen, J. P., Weissman, A. M., and Ashwell, J. D. (2000). Ubiquitin protein ligase activity of IAPs and their degradation in proteasomes in response to apoptotic stimuli. Science *288*, 874-877.

Yao, R., and Cooper, G. M. (1995). Requirement for phosphatidylinositol-3 kinase in the prevention of apoptosis by nerve growth factor. Science *267*, 2003-2006.

Yeh, W. C., Pompa, J. L., McCurrach, M. E., Shu, H. B., Elia, A. J., Shahinian, A., Ng, M., Wakeham, A., Khoo, W., Mitchell, K., *et al.* (1998). FADD: essential for embryo development and signaling from some, but not all, inducers of apoptosis. Science *279*, 1954-1958.

Yin, X. M., Wang, K., Gross, A., Zhao, Y., Zinkel, S., Klocke, B., Roth, K. A., and Korsmeyer, S. J. (1999). Bid-deficient mice are resistant to Fas-induced hepatocellular apoptosis. Nature *400*, 886-891.

Yoshida, H., Kong, Y. Y., Yoshida, R., Elia, A. J., Hakem, A., Hakem, R., Penninger, J. M., and Mak, T. W. (1998). Apaf1 is required for mitochondrial pathways of apoptosis and brain development. Cell *94*, 739-750.

Yu, J., Zhang, L., Hwang, P. M., Kinzler, K. W., and Vogelstein, B. (2001). PUMA induces the rapid apoptosis of colorectal cancer cells. Mol Cell *7*, 673-682.

Yu, L. Y., Korhonen, L., Martinez, R., Jokitalo, E., Chen, Y., Arumae, U., and Lindholm, D. (2003). Regulation of sympathetic neuron and neuroblastoma cell death by XIAP and its association with proteasomes in neural cells. Mol Cell Neurosci *22*, 308-318.

Yuan, J., Shaham, S., Ledoux, S., Ellis, H. M., and Horvitz, H. R. (1993). The C. elegans cell death gene ced-3 encodes a protein similar to mammalian interleukin-1 beta-converting enzyme. Cell *75*, 641-652.

Yuan, J. Y., and Horvitz, H. R. (1990). The Caenorhabditis elegans genes ced-3 and ced-4 act cell autonomously to cause programmed cell death. Dev Biol *138*, 33-41.

Zha, J., Harada, H., Osipov, K., Jockel, J., Waksman, G., and Korsmeyer, S. J. (1997). BH3 domain of BAD is required for heterodimerization with BCL-XL and pro-apoptotic activity. J Biol Chem *272*, 24101-24104.

Zha, J., Harada, H., Yang, E., Jockel, J., and Korsmeyer, S. J. (1996). Serine phosphorylation of death agonist BAD in response to survival factor results in binding to 14-3-3 not BCL-X(L). Cell *87*, 619-628.

Zheng, T. S., Schlosser, S. F., Dao, T., Hingorani, R., Crispe, I. N., Boyer, J. L., and Flavell, R. A. (1998). Caspase-3 controls both cytoplasmic and nuclear events associated with Fas-mediated apoptosis in vivo. Proc Natl Acad Sci U S A *95*, 13618-13623.

Zhu, S., Stavrovskaya, I. G., Drozda, M., Kim, B. Y., Ona, V., Li, M., Sarang, S., Liu, A. S., Hartley, D. M., Wu du, C., *et al.* (2002). Minocycline inhibits cytochrome c release and delays progression of amyotrophic lateral sclerosis in mice. Nature *417*, 74-78.

Zimmermann, K. C., Bonzon, C., and Green, D. R. (2001). The machinery of programmed cell death. Pharmacol Ther *92*, 57-70.

Ziv, I., Melamed, E., Nardi, N., Luria, D., Achiron, A., Offen, D., and Barzilai, A. (1994). Dopamine induces apoptosis-like cell death in cultured chick sympathetic

neurons--a possible novel pathogenetic mechanism in Parkinson's disease. Neurosci Lett *170*, 136-140.

Ziv, I., Offen, D., Haviv, R., Stein, R., Panet, H., Zilkha-Falb, R., Shirvan, A., Barzilai, A., and Melamed, E. (1997). The proto-oncogene Bcl-2 inhibits cellular toxicity of dopamine: possible implications for Parkinson's disease. Apoptosis *2*, 149-155.

Zong, W. X., Li, C., Hatzivassiliou, G., Lindsten, T., Yu, Q. C., Yuan, J., and Thompson, C. B. (2003). Bax and Bak can localize to the endoplasmic reticulum to initiate apoptosis. J Cell Biol *162*, 59-69.

Zong, W. X., Lindsten, T., Ross, A. J., MacGregor, G. R., and Thompson, C. B. (2001). BH3-only proteins that bind pro-survival Bcl-2 family members fail to induce apoptosis in the absence of Bax and Bak. Genes Dev *15*, 1481-1486.

Zou, H., Henzel, W. J., Liu, X., Lutschg, A., and Wang, X. (1997). Apaf-1, a human protein homologous to C. elegans CED-4, participates in cytochrome c-dependent activation of caspase-3. Cell *90*, 405-413.

Zuch, C. L., Nordstroem, V. K., Briedrick, L. A., Hoernig, G. R., Granholm, A. C., and Bickford, P. C. (2000). Time course of degenerative alterations in nigral dopaminergic neurons following a 6-hydroxydopamine lesion. J Comp Neurol *427*, 440-454.